MODULATION OF APOLIPOPROTEIN B-100 DEGRADATION AND SECRETION BY HEPATIC PROTEIN QUALITY CONTROL COMPONENTS

by

Eric Alexander Fisher

Submitted in partial fulfilment of the requirements
for the degree of Doctor of Philosophy.

at

Dalhousie University
Halifax, Nova Scotia
March 2013

DALHOUSIE UNIVERSITY

DEPARTMENT OF BIOCHEMISTRY & MOLECULAR BIOLOGY

The undersigned hereby certify that they have read and recommend to the Faculty of Graduate Studies for acceptance a thesis entitled "Modulation of Apolipoprotein B-100 Degradation and Secretion by Hepatic Protein Quality Control Components" by Eric Alexander Fisher in partial fulfilment of the requirements for the degree of Doctor of Philosophy.

Dated: March 28th, 2013

External Examiner: _____

Research Supervisor: _____

Examining Committee: _____

_____

_____

Departmental Representative: _____

DALHOUSIE UNIVERSITY

DATE: March 28th, 2013

AUTHOR: Eric Alexander Fisher

TITLE: Modulation of Apolipoprotein B-100 Degradation and Secretion by
Hepatic Protein Quality Control Components

DEPARTMENT OR SCHOOL: Department of Biochemistry & Molecular Biology

DEGREE: PhD   CONVOCATION: May   YEAR: 2013

Permission is herewith granted to Dalhousie University to circulate and to have copied for non-commercial purposes, at its discretion, the above title upon the request of individuals or institutions. I understand that my thesis will be electronically available to the public.

The author reserves other publication rights, and neither the thesis nor extensive extracts from it may be printed or otherwise reproduced without the author's written permission.

The author attests that permission has been obtained for the use of any copyrighted material appearing in the thesis (other than the brief excerpts requiring only proper acknowledgement in scholarly writing), and that all such use is clearly acknowledged.

_____
Signature of Author

DEDICATION PAGE

Dedicated to my mother and father, Jane and David.

TABLE OF CONTENTS

LIST OF TABLES

LIST OF FIGURES

ABSTRACT

The central protein component of hepatic very low density lipoproteins (VLDL), apolipoprotein B-100 (apoB-100), is unique in that it is removed via endoplasmic reticulum-associated degradation (ERAD) when poorly lipidated. Protein quality control processes that govern apoB-100 production can impact the secretion rate of VLDL. The human hepatoma cell line HepG2 was used to characterize the functional role of several proteins in the apoB-100 ERAD pathway. A network of cellular protein components serves as the machinery to identify ERAD substrates, remove them from the ER and deliver them to the cytosolic proteasome. Here, the retrotranslocation of apoB-100 out of the ER was found to require p97, as the siRNA-mediated knockdown of p97 impaired the release of apoB-100 and polyubiquitinated apoB into the cytosol. Blocking p97-dependent retrotranslocation did not increase apoB-100 secretion, suggesting that apoB-100 was committed to degradation by the time it associated with p97. In contrast, knockdown of the ER-resident ubiquitin ligase gp78 decreased apoB-100 ubiquitination and increased apoB-100 secretion. Depletion of gp78 reversed the p97-dependent accumulation of apoB-100, suggesting that gp78 acted upstream of p97 during ERAD. Surprisingly, blocking gp78-dependent ubiquitination of apoB-100 allowed the assembly of more buoyant, lipid-rich VLDL. The cytosolic chaperone "holdase" Bag6 was identified by mass spectrometry and immunoblot to associate with apoB-100 following proteasome inhibition. Bag6 associated with newly synthesized, cytosolic apoB-100. Intriguingly, the depletion of Bag6 protein by siRNA reduced apoB-100 secretion efficiency by as much as 50%. Furthermore, the synthesis of apoB-100 was not affected, suggesting that the loss of Bag6 function increased the degradation of apoB-100. This degradation occured at a post-translational step of assembly by an unidentified mechanism. Taken together, these data suggest that ubiquitination is the committing step in the apoB-100 ERAD pathway and that ubiquitination may play a regulatory role in VLDL assembly. Elements of cellular quality control act as modulators of VLDL output, and may be dysregulated in several human diseases which are characterized by increased VLDL production.

LIST OF ABBREVIATIONS USED

AMFR	autocrine motility factor receptor
apoB	apolipoprotein B-100
ATF6	activating transcription factor 6
ATP	adenosine triphosphate
Bag6	Bcl2-associated athanogene 6
BAT3	human leukocyte antigen B (HLA-B)-associated transcript 3
BSA	bovine serum albumin
CCT	CTP:phosphocholine cytidylyltransferase
CHOP	C/EBP homologous protein
CLD	cytosolic lipid droplet
DAG	diacylglycerol
DMEM	Dulbecco's modified Eagles medium
DRiPs	Defective ribosomal products
DTT	dithiothreitol
DUB	deubiquitinating enzyme
ER	Endoplasmic Reticulum
ERAD	Endoplasmic Reticulum-Associated Degradation
ERK	Extracellular signal-regulated kinases
FBS	fetal bovine serum
FFA	free fatty acid
Grp78	Glucose-related protein 78
HDL	High Density Lipoprotein
HSF	Heat Shock Factor
Hsp	Heat Shock Protein
HSR	Heat Shock Response
KD	knockdown
KO	knockout
IP	immunoprecipitation
IRE1α	Inositol-requiring enzyme-1 α
LD	lipid droplet
LLD	luminal lipid droplet
LDL	Low Density Lipoprotein
MALD	microsome-associated lipid droplets
MEK	Mitogen-activated protein kinase kinase
MTP	microsomal triglyceride transfer protein
OA	Oleic Acid
PAGE	polyacrylamide gel electrophoresis
PBS	phosphate-buffered saline
PERK	PKR-like ER kinase
PERPP	Pre-secretory, Post-ER Proteolysis
PUFA	polyunsaturated fatty acid
QPCR	quantitative polymerase chain reaction
RNAi	Ribonucleic Acid Interference

ROS	reactive oxygen species
SDS	sodium dodecyl sulfate
siRNA	small interfering ribonucleic acid
TG	triglyceride
UPR	unfolded protein response
VLDL	Very Low Density Lipoprotein
XBP1	X-box-binding protein 1

ACKNOWLEDGEMENTS

I would like to thank all the wonderful people I have gotten to know during my time at Dalhousie and in Halifax in general. Graduate school has turned into a major chapter in my life. My lab group, department and colleagues have been amazingly supportive over the entire course of my degree. I could not have asked for a better supervisor in Roger, who somehow manages to allow his trainees significant creative freedom and independence, while also being readily available with advice and support. I recognize this balance is not to be taken for granted. I would also like to thank my committee members, Drs. Ridgway, Duncan and Byers, for all of their feedback and encouragement over the years.

My time at Dalhousie and in Halifax has not always been straightforward, as I have had to cope with and adapt to a lengthy recovery from post-concussion syndrome. It behooves me to say that I benefited tremendously from the compassion and support of those around me, both professionally and personally. I would not have achieved as much success in the lab as I have without being surrounded by such positive influences. It has been wonderful to be around people as dedicated to helping others as they are to their own work. I have come a long way during this trying time period, learned a lot about myself and now look forward to new challenges.

Finally I would like to thank my parents, Jane and David. They have been there for me every step of the way. They raised me well and gave me a supportive environment within which to grow and suceed. They have an unflappable faith in my abilities, but also have shown a healthy dose of loving parental concern from afar during my challenges in Halifax. Together we have helped Porter enjoy a profitable Halifax-Ottawa flight schedule over the years. I look forward tremendously to my parents being able to witness my becoming a PhD graduate.

CHAPTER 1 – INTRODUCTION

1.1 Very Low Density Lipoproteins

Despite significant progress in recent decades in both our understanding and treatment of heart disease (Fox et al., 2004), adverse coronary events remain a significant medical problem in our society. Lifestyle and pharmaceutical interventions have helped to lower the incidence of disease, yet for many people current therapies remain inadequate. Plasma low density lipoproteins (LDL) cholesterol (LDL-C) has long been considered a major risk factor for cardiovascular disease (CVD), and is measured in the clinic in parallel with high density lipoproteins (HDL) cholesterol (HDL-C). Lowering of the LDL/HDL ratio, plasma triglycerides (TG) and blood pressure encapsulates the therapeutic approach for individuals at risk for CVD. LDL particles originate in the liver as VLDL, which is converted in circulation into the smaller, more dense LDL through the transfer of its core neutral lipid cargo (predominantly TG) to HDL or peripheral tissues. However, the pool of TG and LDL-C is associated with a heterogeneous mixture of lipoprotein particles of differing size, composition and atherogenicity. In recent years measurements of the protein content of plasma LDL has emerged as a valuable clinical tool.

Apolipoprotein B-100 (apoB-100, or apoB) is the essential, structure- and function-defining protein of VLDL and LDL (and all plasma lipoprotein remnant species derived from VLDL). There is exactly one apoB-100 protein per VLDL particle, whereas each particle can contain varying levels of TG, cholesterol and cholesterol esters (Sniderman et al., 2009). As such, plasma apoB-100 protein measurements provide an accurate estimate of particle number (Sniderman et al., 2010). In addition, VLDL

overproduction is prevalent among patients with type 2 diabetes (T2D) (Adiels et al., 2008). This increased output of VLDL, referred to as diabetic dyslipidemia, represents an additional risk of cardiovascular disease for T2D patients who are already burdened with the insulin-resistant state (Verges, 2010). The emergence of plasma apoB-100 levels as a primary target to lower risk for heart disease and as an indicator of T2D renews the onus on basic researchers to expand our knowledge of hepatic apoB-100 protein production: in particular, how is this process regulated?

The apoB-100 protein is constitutively synthesized in hepatocytes and requires a continuous supply of lipid ligands to support the assembly of VLDL. A robust quality control network monitors protein folding in the secretory pathway. To identify new components that specifically affect apoB-100 metabolism, I have used a human hepatoma cell line (HepG2) which is widely employed to study apoB-containing lipoprotein (LpB) assembly. The hepatic endoplasmic reticulum (ER) is of particular importance to this story, as it is not only the organelle where VLDL assembly is initiated, but is also a regulatory hub for protein and lipid metabolism. This thesis focuses directly on the intracellular environment in which apoB-100 is produced. The chapters herein present data pertaining to the interplay between proteasomal degradation of apoB-100 and secretion of apoB-containing lipoproteins. This introduction will provide context for my studies, including an overview of the sources of requisite apoB-100 lipid ligands, apoB-100 structure/function and components of the protein folding and degradation pathways.

1.2 The Lipid Ligands of ApoB-100

Dietary fatty acids and cholesterol are known to influence plasma LDL cholesterol levels (Dietschy, 1998). Some of these effects exert widespread metabolic changes, as these nutrients can elicit strong systemic signalling responses. Additionally, the structure of certain fatty acids can affect VLDL assembly directly when they are esterified into TG or CE for lipidation of apoB-100. One study demonstrated in primary hepatocytes from chickens that medium-chain fatty acids, of 8, 10, and 12 carbons in length decreased VLDL secretion when compared to C16 palmitate (Sato et al., 2005). Notably, octanoate (8:0) suppressed VLDL output at the transcriptional and translational level while not altering apoB degradation (Tachibana et al., 2005). In contrast to increased VLDL secretion caused by oleic acid (18:1 n-9), hepatocytes supplemented with polyunsaturated fatty acids such as docosahexaenoic acid (22:6 n-3) or eicosapentaenoic acid (20:5 n-3) display decreased VLDL secretion (Pan et al., 2008; Tran et al., 2006). In mice, an essential fatty acid-deficient diet stimulated the production of larger VLDL particles with faster catabolic rates, resulting in hypotriglyceridemia (Werner et al., 2005). As well as being directly incorporated into VLDL, many fatty acid species have bio-active properties, thus making the effects of dietary fatty acids an intriguing and difficult area of research when probing the cause and effect mechanisms at play in human metabolism.

1.2.1 Diacylglycerol & Triglycerides

Fatty acids are the most energy-dense form of nutrients by mass, compared to carbohydrate and amino acids. In healthy mammals, excess nutrients are safely stored in

adipose tissue as TG. Triglycerides are synthesized by the stepwise addition of three fatty acid moieties to a glycerol backbone (glycerol-3-phosphate). Triglyceride storage, typically in the lipid droplets of adipocytes, represents an inert or "safe" way for the human body to sequester excess energy. Triglycerides, along with cholesterol esters, also comprise the lipid core of VLDL particles. Triglycerides utilized for VLDL assembly can be derived from re-esterification of exogenous fatty acids or from fatty acids synthesized *de novo* in hepatocytes. Diacylglycerol (DAG) is the major precursor to triglyceride, but is also a substrate in the production of phospholipids. Triglyceride storage protects the cell from the detergent properties of fatty acids, but high levels of DAG species are also suggested to cause insulin resistance (Erion and Shulman, 2010).

Phosphatidate phosphohydrolase-1 (PAP-1) converts phosphatidate into diacylglycerol and is the rate-limiting step in *de novo* synthesis of TG and PL (including PC and PE) (Carman and Han, 2006). PAP-1 is encoded by several members of the lipin gene family, which includes lipin-1, -2 and -3. The *Lpn1* gene is suppressed by insulin and induced by glucocorticoids (Manmontri et al., 2008). When transiently expressed in McA-RH7777 cells, both forms of lipin-1, lipin-1α and β (which are alternatively spliced isoforms), increased synthesis and secretion of glycerolipids (Bou Khalil et al., 2009). Interestingly, TG synthesis was unchanged in lipin-1 knockout mice, and reintroduction of lipin-1 using an adenovirus suppressed VLDL-TG secretion (Chen et al., 2008). The effect of lipin-1 on VLDL secretion was dependent on its nuclear localization (Bou Khalil et al., 2009). Lipin-1 is an activator of hepatic lipid metabolism via induction of the peroxisome proliferator-activated receptor γ (PPARγ) coactivator 1 α (PGC-1α) and PPARα transcription factors (Finck et al., 2006). Results from the transient expression

and knockout studies are not consistent and further studies may reveal the manner in which lipin-1 modulates TG secretion.

Both the availability and the structure of the fatty acid moieties of TG can have profound effects on the production of VLDL. Some fatty acids are more readily incorporated into VLDL than others. Triglycerides with oleic acid moieties may more effectively support VLDL production, in part because this TG is efficiently mobilized to the ER. In contrast, TG rich in EPA was poorly secreted and stored in the cytosol of McA-RH7777 cells (Tran et al., 2006). Lipotoxicity in hepatocytes, rather than the excess of TG storage in the cytosol, is associated with decreased ability to convert free fatty acids into TG (Mantzaris et al., 2011).

The triglycerides that comprise the bulk of nascent VLDL particles (~70% of the mass) are those that have entered the cytosolic TG pool, and are then hydrolysed and re-esterified for luminal availability (Wiggins and Gibbons, 1992). Triglyceride synthesis is catalysed by diacylglycerol acyltransferases (DGATs), of which there are two forms: DGAT1 and DGAT2 (Yen et al., 2008). DGAT2 is essential for life, as DGAT2-deficient mice are lipopenic and die shortly after birth (Stone et al., 2004). In contrast, DGAT-1 deficiency in the mouse is a viable phenotype. DGAT2 expression in humans is particularly abundant in tissues producing a lot of TG, including the liver (Cases et al., 2001).

Studies of DGAT activity have provided insight into their structure and function, but the functional roles of the individual DGAT forms in VLDL assembly are not yet clear. In mice, short term overexpression of DGAT1 or DGAT2 increased hepatic TG content, but did not enhance VLDL output (Millar et al., 2006). In contrast,

overexpression of human DGAT1 in McArdle cells (rat hepatoma) increased TG synthesis, cellular TG and VLDL secretion (Liang et al., 2004). Permeabilization of the microsomal membrane revealed that TG synthesis occurs on both sides of the membrane, demonstrating distinctly separate DGAT activities in both the cytosol and microsomal lumen (termed overt and latent, respectively) (Owen et al., 1997; Yen et al., 2008). In mice, short-term overexpression of DGAT1, but not DGAT2, increased latent ER luminal DGAT activity and VLDL secretion (Yamazaki et al., 2005). Curiously, DGAT1 possesses a dual membrane topology in HepG2 cells, which could partially account for discrepancies in past DGAT literature (Wurie et al., 2011).

Knockdown of murine DGAT2 expression *in vivo* using antisense oligonucleotide (ASO) technology lowered fasting TG levels and decreased VLDL secretion (Liu et al., 2008; Yu et al., 2005). The hepatic steatosis that results from reduced MTP (microsomal triglyceride transfer protein) expression (and subsequently impaired VLDL output), was rescued by also silencing DGAT2 (Tep et al., 2012). This implies that when the lipid-transfer action of MTP is reduced, hepatocytes experience deleterious levels of microsomal TG, mobilized by DGAT2. Stable isotope-labelled glycerol and oleic acid has revealed a difference in substrate preference of DGAT1 and 2, in both HepG2 cells and mice (Qi et al., 2012). DGAT1, not DGAT2, esterified exogenous, labelled oleic acid into TG, while DGAT2 synthesized TG from primarily endogenous fatty acids and the labelled glycerol. Despite inconsistencies in the literature, it is clear that hepatic DGAT activity in the liver contributes to the TG pool that is available for VLDL assembly, from both fatty acids synthesized *de novo* and dietary fatty acyl groups.

1.2.2 Cholesterol and Cholesterol Esters

Esterified cholesterol composes 5% - 15% of VLDL-associated lipids and this proportion increases in rats on a high-cholesterol diet (Davis et al., 1982). The cholesterol ester content of apoB-containing lipoproteins can influence their atherogenic properties. Cholesterol synthesis is governed by the rate-limiting conversion of HMG CoA into mevalonate, which is catalyzed by the enzyme HMG CoA reductase (Goldstein and Brown, 1990). The many products of mevalonate metabolism, both sterols and non-sterols, have long been known to participate in a feedback mechanism that directly targets the rate-limiting reductase enzyme (Brown and Goldstein, 1980). Cholesterol and cholesterol esters (CE) are present on the surface of, and inside, newly formed VLDL particles, respectively. VLDL assembly is dependent on the availability of cholesterol, such that inhibition of cholesterol synthesis in the liver will decrease VLDL output. Inhibitors of HMG CoA reductase reduce cholesterol synthesis in the liver, but also increase the level of LDL receptors that clear LDL and VLDL remnants from circulation (Khan et al., 1990). Thus, since HMG CoA reductase inhibition can both decrease production and increase removal of plasma lipoproteins, it is unclear to what extent the decreased availability of cholesterol during VLDL assembly is responsible for the improved plasma lipid profiles. Statins have helped millions of patients lower their LDL-cholesterol levels. Unfortunately, however, a large portion of "high and very high risk" patients do not achieve the desired reductions in plasma cholesterol in response to statin therapy alone (Yan et al., 2006). Therefore, there is a need for novel interventions that will improve the plasma lipid profile for those that are refractory to statin therapy.

Acyl CoA:cholesterol transferase (ACAT) catalyzes the esterification of cholesterol with a fatty acyl chain at the ER membrane. Results vary regarding the impact of ACAT isoforms 1 and 2 on VLDL output. Humans mainly express ACAT1 in the liver, whereas mice express ACAT2. The active site of ACAT2 faces the ER lumen, while that of ACAT1 faces the cytosol, lending support to the hypothesis that ACAT2 supplies VLDL assembly with CE, while ACAT1 may maintain the intracellular balance between CE and free cholesterol (Joyce et al., 2000). Co-expression of truncated apoB, MTP and ACAT2 in COS cells demonstrated the ability of ACAT2 to stimulate an increase in CE content and secretion of apoB-containing lipoproteins (Temel et al., 2007). On the other hand, inhibiting ACAT activity with the flavanone naringenin reduced CE in the microsomal lumen without diminishing apoB-100 secretion from HepG2 cells (Borradaile et al., 2002). High ACAT activity may be stimulatory toward VLDL assembly, but reduced luminal CE supply does not appear to limit apoB-100 secretion.

1.2.3 Phospholipids

VLDL assembly also depends on synthesis of phospholipids via *de novo* lipogenesis. Phosphatidylcholine (PC) is synthesized by two distinct pathways in the liver: the CDP-choline pathway which provides about 70% of PC, and by methylation of phosphatidylethanolamine (PE) which provides the remaining 30% (Cole et al., 2012). Mice lacking the gene encoding PE *N*-methyltransferase (PEMT) had a normal plasma lipid profile as well as normal liver PC levels, which was attributed to compensation by the CCT (CTP:phosphocholine cytidylyltransferase) pathway (Walkey et al., 1997). In

contrast, VLDL levels are greatly reduced in mice possessing a liver-specific CCTα knockout (Jacobs et al., 2004). Notably, adenovirus-mediated re-introduction of CCTα back into the knockout mice returned plasma VLDL to normal (Jacobs et al., 2008). These data suggest that the PC generated by CCTα is necessary to support VLDL assembly *in vivo*.

1.3 Structure, Function and Metabolism of ApoB-100

1.3.1 Structural Regions of ApoB-100

Hepatic apoB-100 has a mass of approximately 550 kDa and is composed of 4536 amino acids. Intestinally-derived apoB-48 is the protein component of chylomicrons and originates from an mRNA editing mechanism that generates an in-frame stop codon, limiting translation to the N-terminal 48% of apoB-100 (Tennyson et al., 1989). The apoB-100 protein is very large and is particularly hydrophobic in several regions, making structural analysis of apoB-containing lipoproteins technically challenging. Much of our initial understanding of apoB-100 structure originates from linking abnormal plasma lipid profile with apoB mutations. Familial combined hypobetalipoproteinemia (FHBL) is an autosomal dominant trait where mutations in *APOB* cause homozygotes to have almost undetectable levels of plasma apoB-100, consequently giving them a reduced risk of CVD (Schonfeld et al., 2005). Unfortunately, the inability to export lipids from the liver often leads to ectopic fat storage in hepatocytes and hepatic steatosis (Zhong et al., 2010). Summarized below are some of the pertinent findings that have shaped the current understanding of apoB-100 structure/function, gleaned from a variety of techniques.

1.3.2 The Pentapartite Model

The distinct regions within the apoB-100 protein are described by the pentapartite model, which divides apoB-100 into five major regions consisting of α-helices and β-strands (Segrest et al., 2001) (Figure 1.1). The globular N-terminal domain of apoB translocates into the ER lumen through the Sec61 translocon (Chen et al., 1998). Elements of the latter half of the βα1 domain recruit phospholipids into a lipid-binding pocket. There exists significant sequence homology between the βα1 domain of apoB and lipovitellin, which is an egg yolk lipoprotein (Mann et al., 1999). The defining structural characteristic of lipovitellin is a large lipid-binding pocket composed of anti-parallel β-sheets (Anderson et al., 1998). The lipid pocket formed from β-sheets is believed to be the site on apoB where lipoprotein assembly initiates (Richardson et al., 2005). Interestingly, there appears to be a common ancestral lipid transfer protein between apoB-100, MTP, insect apolipophorin, and several forms of vitellogenin. (Babin et al., 1999).

MTP is the major protein involved in apoB lipidation and begins to associate with apoB sequences 10 to 13% from the N-terminus (Hussain et al., 1998; Segrest et al., 1999). MTP recruitment to the βα1 domain may be to prepare for lipid recruitment as apoB synthesis continues, since MTP activity seems dispensable for production and secretion of a truncated βα1 domain (Dashti et al., 2007). The βα1 domain of apoB contains several essential post-translational modifications that are important for VLDL assembly (Sundaram and Yao, 2010). Two disulfide bridges within the βα1 domain are essential for apoB-100 secretion (Huang and Shelness, 1997; Tran et al., 1998). N-linked glycosylation is prominent on the apoB-100 protein, with 16 asparigine residues reported
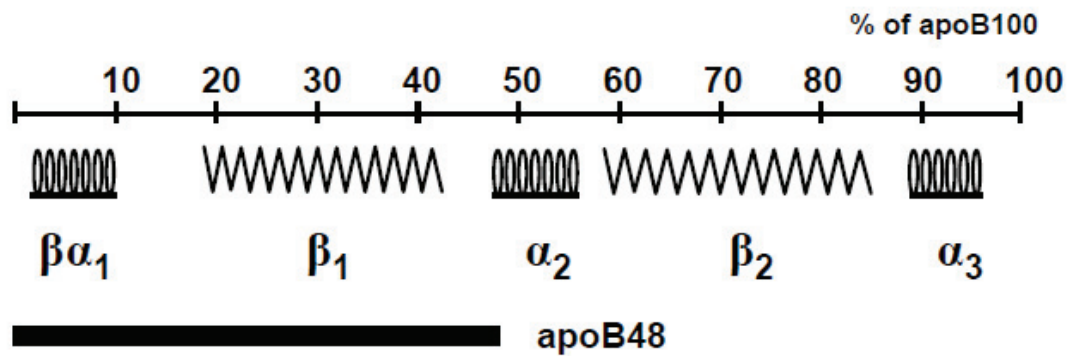
Figure 1.1. Schematic of the apoB100 protein sequence. Regions of the apoB100 protein are presented relative to the % of the full-length, starting at the N-terminus. The globular βα1 domain lies at the N-terminus. The β1 and β2 regions are densely hydrophobic regions thought to consist mainly of amphipathic, anti-parallel β sheets. The α2 and α3 regions flanking β2 are amphipathic and alpha helical. In the human intestine, cells edit apoB mRNA to yield apoB48, while the liver expresses the full-length protein. This figure was originally published in the Journal of Lipid Research. Segrest et al. Structure of apolipoprotein B-100 in low density lipoproteins. *J. Lipid Res*. 2001; 42: 1346-1367. © the American Society for Biochemistry and Molecular Biology.

to possess oligosaccharides (Taniguchi et al., 1989). Notably, five of the asparagine residues lie within the βα1 domain of apoB-100 and are necessary for apoB-100 stability and secretion, in particular Asn[1496] (Vukmirica et al., 2002). Indeed, apoB-100 stability and VLDL secretion are drastically impaired in the presence of compounds that block disulfide bond formation (Dithiothreitol (DTT)) (Ingram and Shelness, 1996) or N-linked glycosylation (Macri and Adeli, 1997; Vukmirica et al., 2002) (tunicamycin). Proper folding of the βα1 domain at the N-terminus of apoB-100 is paramount for assembly of a "secretion-competent" VLDL particle. Recombinant apoB proteins that lack the 1000 amino acids of N terminus are either barely secreted, or not at all (Gretch et al., 1996; McLeod et al., 1996).

The β1 region contains the sequence of apoB that begins to co-translationally form a nascent lipoprotein (Shelness et al., 2003). Using truncated apoB constructs, it was shown that the apoB-37-42 portion of the β1 region conferred instability to the protein, evident through increased cytosolic exposure and proteasomal degradation (Lapierre et al., 2004). This same B37-42 region was shown to irreversibly bind neutral lipids (Wang et al., 2009), suggesting that if neutral lipid ligands are not incorporated into the growing, nascent lipoprotein, the poorly lipidated B37-42 motif triggers the degradation of apoB, likely provoked by inefficient translocation and cytosolic exposure of the polypeptide. Constructs containing segments of the β1 region were delayed in translocation across the ER membrane, displayed cytosolic exposure and were degraded by the proteasome following MTP inhibition (Liang et al., 1998). COS cells were able to secrete multiple apoB constructs in the absence of MTP expression, except those that contained elements from the β1 domain (Wang et al., 1996). Fusion of β1 domain

12

segments with apoAI (B29-34, B34-37, B37-42) resulted in secretion of VLDL-sized particles from McArdle cells, demonstrating that recruitment of TG does not depend solely on apoB peptide length but also specific sequence requirements (McLeod et al., 1996). These data suggest that sequences within the β1 region confer to apoB the ability to assemble VLDL while also rendering apoB susceptible to degradation.

The β2 region lies at the C-terminal end of apoB-100 and contains the LDL receptor binding site, making apoB-100 functionally distinct from the intestinally-derived apoB-48 protein (Sundaram and Yao, 2010). The two amphipathic α-helical regions, α1 and α2, are thought to confer a certain flexibility to the structure of apoB-100, allowing a stable conformation to be achieved at a variety of lipid cargo volumes (Wang et al., 2006a).

ApoB polypeptide length was shown to dictate the volume, or diameter, of the primordial lipoprotein core (McLeod et al., 1996; Spring et al., 1992). C-terminal truncated apoB constructs demonstrated that the length of apoB governs the diameter of secreted apoB-containing lipoproteins. Lipid recruitment increased linearly with apoB60, 72, 80, 88, 94 and 100 (McLeod et al., 1994). Conversely, the intracellular stability and translocation efficiency were found to be inversely proportional to the length of truncated apoB polypeptides, with full-length apoB-100 being the least stable among the group (apoB15, B29, B48, B100) (Cavallo et al., 1998).

The structure of lipidated apoB-100 (i.e. a mature VLDL particle) is poorly defined. Some structural inferences have been made based on other lipid-binding proteins such as fatty acid binding proteins (FABP). Cytosolic FABP can bind noncovalently to cholesterol, bile salts, lysophospholipids and fatty acids (Glatz and van der Vusse, 1996).

The anti-parallel beta-strands of FABP form 2 sheets that create a ligand binding cavity (Scapin et al., 1992). Structural analyses demonstrate a "clam shell"-shaped structure within which lipid ligands are found (Sacchettini and Gordon, 1993). ApoB-100 was initially proposed to adopt a "belt"-like conformation, referring to how it may wrap around the neutral lipid core and be flexible in the amount of cargo it carries (Schumaker et al., 1994). However, more recently a model has suggested that the apoB-100 protein creates a central cavity by adopting a curved shape (Johs et al., 2006) (Figure 1.2). The β-sheet regions of apoB-100 are non-exchangeable once lipid-bound, suggesting they confer stability to the particle once formed. In contrast, the amphipathic alpha-helices absorb and desorb rapidly from a triolein:water surface, implying that they may create the flexibility needed to accommodate variable amounts of lipid ligands (Wang et al., 2006a; Wang et al., 2009). These studies have revealed novel characteristics of apoB-100, but there has yet to be an atomic view of apoB-100 structure.

1.3.3 Mechanism of VLDL Assembly

Patients with abetalipoproteinemia, a condition characterized by the absence of circulating VLDL or chylomicrons, were found to lack detectable MTP in liver or intestinal biopsies, suggesting that MTP is required for apoB-containing lipoprotein production (Wetterau et al., 1992). MTP performs lipid binding and lipid transfer (Jamil et al., 1995) while in the form of a heterodimer with protein disulfide isomerase (PDI) (Wetterau et al., 1990). While PDI is not required for the lipid-transfer activity of MTP (Wang et al., 1997), MTP activity is increased when PDI is upregulated by the Unfolded Protein Response (UPR) *in vivo* (Wang et al., 2012). The broad specificity of MTP lipid
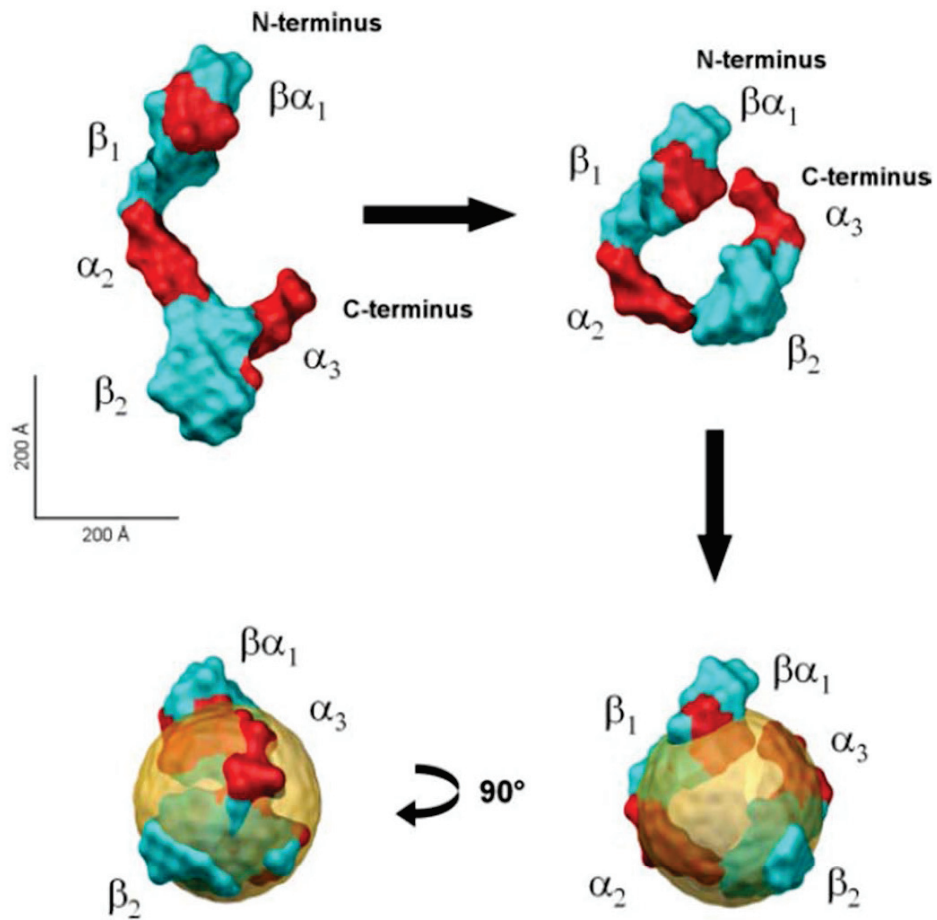
Figure 1.2. Three-dimensional model of apoB-100 domains on hepatic VLDL. This research was originally published in the Journal of Biological Chemistry. Johs et al. Modular structure of solubilized human apolipoprotein B-100. Low resolution model revealed by small angle neutron scattering. *J. Biol. Chem.* 2006; 281: 19732-19739. © the American Society for Biochemistry and Molecular Biology.

transfer activity has made the essential mechanism of MTP-facilitated VLDL assembly remains elusive. MTP has been shown to facilitate transfer of TG, CE, DAG and PC between liposomes *in vitro*. With the exception of DAG, the rest of these species are found in VLDL particles. *In vitro* data suggests that CE and TG are the preferred substrates of MTP lipid transfer (Jamil et al., 1995). Interestingly, MTP from Drosophila has only the ability to transfer phospholipids, not CE and TG, but can still stimulate secretion of apoB from COS cells (Rava et al., 2006). This suggests that although TG and CE may be preferred MTP substrates in other species, transfer of phospholipids to apoB by MTP may stimulate apoB secretion.

1.3.4 The Two-step Model

The two-step model for VLDL assembly arose partly from the observation that apoB48 can be secreted as either a lipid-rich or a lipid-poor lipoprotein particle (Boren et al., 1994; Swift, 1995). The two steps are: (1) initiation of assembly by the formation of a primordial lipoprotein in an MTP-dependent manner in the ER and (2) expansion of the neutral lipid core by additional lipid recruitment sometime after translocation has completed (depicted in Figure 1.3). MTP activity is able to prevent the co-translational proteasomal degradation of apoB-100 (Benoist and Grand-Perret, 1997; Wang et al., 1996), thereby implicating MTP in the first step of assembly. MTP activity is essential for transfer of TG into the ER lumen for VLDL assembly (Raabe et al., 1999), which in turn reduces the degradation of apoB-100 (that is no longer poorly lipidated). Importantly, MTP inhibition impairs the recruitment of TG from the ER and Golgi
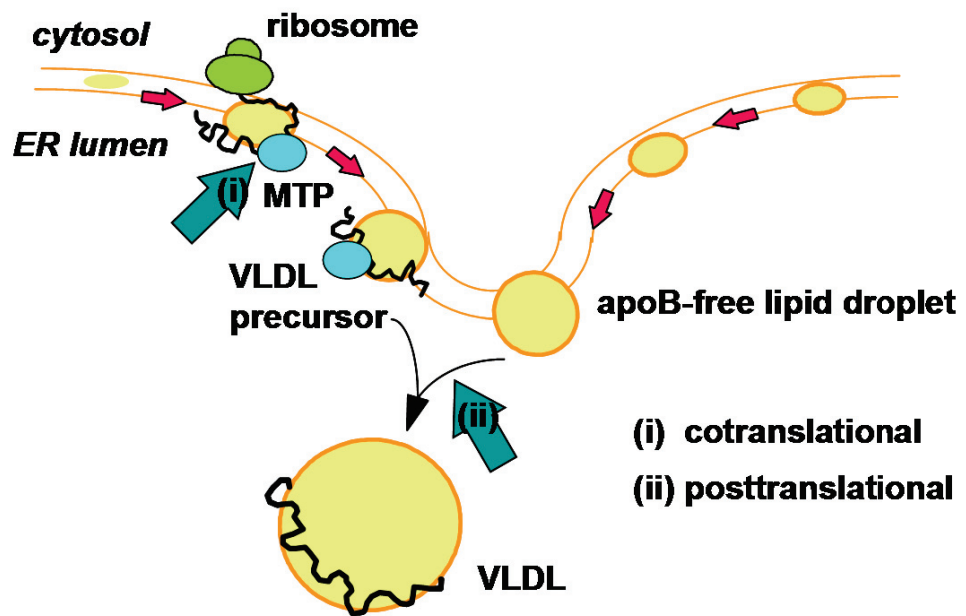
16

Figure 1.3 Two-step model of VLDL assembly. ApoB-100 translocates into the ER lumen through the Sec61 translocon. The first step of assembly begins here, where nascent apoB is lipidated co-translationally in an MTP-dependent process. Following the completion of apoB-100 synthesis, the primordial VLDL particle remains membrane-associated. Step two of assembly occurs when apoB-100 acquires bulk neutral lipid from an apoB-free luminal lipid droplet. Following particle expansion to full-sized VLDL, the particle is released into the lumen.

membrane for VLDL assembly without affecting TG synthesis (Hebbachi and Gibbons, 1999; Wang et al., 1999).

The ER-retention KDEL signal on the PDI subunit of MTP suggests that post-ER particle maturation is MTP-independent; however, MTP has been detected in the Golgi (Swift et al., 2003). Treatment with inhibitors of TG synthesis or MTP activity during the chase period of an apoB metabolic labelling study did not alter the density of the secreted radiolabelled apoB-100, suggesting that the post-translational expansion of pre-VLDL particles is MTP-independent (Pan et al., 2002). Brefeldin A (BFA) blocks anterograde vesicular trafficking from the ER to Golgi (De Lemos-Chiarandini et al., 1992). BFA treatment inhibits formation of only mature VLDL, not pre-VLDL (Tran et al., 2002). McA-RH7777 cell studies revealed that VLDL secretion is very rapid following core expansion, which likely occurs in the distal Golgi (Tran et al., 2002). On the other hand, one group reported the formation of VLDL explicitly in the ER, and not the Golgi, in McA-RH7777 cells (Yamaguchi et al., 2003). Mature VLDL particles have been found in the ER of rat hepatocytes (Rusinol et al., 1993). It has also been reported, however, that only pre-VLDL particles are found within the ER, which supports the notion that further lipid recruitment occurs in a post-ER compartment (Pan et al., 2002). These discrepancies in the literature could be dependent on the sub-cellular fractionation techniques or differences between the model systems.

Multiple studies using different models have demonstrated that MTP is needed during the initial steps of VLDL assembly, but is not essential for the "late-stage" addition of TG to form fully mature VLDL (Gordon and Jamil, 2000; Rustaeus et al., 1998; Wang et al., 1997). Studies of truncated apoB mutants revealed that sequences

between apoB-51 and apoB-53 (within the α1 region) had the highest requirement for MTP activity (Nicodeme et al., 1999). This amphipathic α-helical portion of apoB-100 is predicted to bind lipid reversibly and is proposed to help propel stable, lipid-poor apoB48 into the lipid-rich conformation of VLDL-sized apoB-100 (Nicodeme et al., 1999).

The direct source of neutral lipid for nascent particle expansion is believed to be luminal lipid droplets (LLD), also known as microsome-associated lipid droplets (MALD). These lipid droplets are formed in the presence of MTP (Raabe et al., 1999), likely at the microsomal membrane where lipid biosynthetic enzymes reside, and then are incorporated into the apoB-containing lipoprotein. Proteomic analysis of "apoB-free" lipid droplets revealed many associated proteins including apoE, MTP, TG hydrolase (TGH) and carboxylesterase 1 (Ces 1) (Wang et al., 2007), none of which are found on cytosolic lipid droplets. The pool of apoB-free particles is heterogeneous in size and TG composition and it is suggested that this is the bulk lipid source that is transferred to apoB-100 post-translationally during the final stage of VLDL particle maturation. The mechanism of core expansion remains enigmatic.

Although levels and activity of MTP may change modestly in conjunction with whole body metabolism in humans, prolonged impairment of VLDL secretion by disrupting MTP activity invariably leads to steatosis, except perhaps when combined with additional interventions (Rizzo and Wierzbicki, 2011). Similarly, siRNA-induced apoB knockdown resulted in steatosis in mice (Ason et al., 2011). However, an ASO-mediated inhibition of apoB mRNA in LDL receptor-knockout mice demonstrated that modest reduction of apoB may allow for a therapeutic window of improved plasma lipid profile without liver TG accumulation (Mullick et al., 2011).

ApoE and apoC-III have been shown to promote lipid recruitment during later stages of VLDL assembly (Yao and Wang, 2012) and a loss-of-function apoC-III mutation caused impaired MALD formation (Qin et al., 2011). A different apoC-III mutation prevented the incorporation of MALD-derived lipids into nascent VLDL, but still allowed the formation of MALD (Sundaram et al., 2010). Palmitate-induced phosphorylation of eIF2α was decreased by expression of normal human apoC-III, but not the mutants (Yao et al., 2012), suggesting that a short-term increased output of $VLDL_1$ mediated by apoC-III may serve to reduce fatty acid-induced ER stress. Export of $VLDL_1$ particles has been suggested to be a protective mechanism through which the liver can dispense with a large amount of TG in the short term.

1.3.5 Cytosolic and Microsome-associated Lipid Droplets

CideB is an ER- and cytosolic lipid droplet-associated protein that appears to be involved in TG mobilization and VLDL assembly in hepatocytes. Knockout of CideB led to increased hepatic TG storage and reduced VLDL secretion. Interestingly, restoring VLDL output in CideB-null mice required expression of CideB containing both its ER- and LD-associating domains. Combined with its direct interaction with apoB, this observation suggests an integral role for CideB in provision of lipids for VLDL assembly (Ye et al., 2009). Recently, it was reported that CideB-null mice possessed marked upregulation of hepatic perilipin 2/ADRP, which is known to promote storage of TG in CLD rather than mobilization for VLDL assembly (Li et al., 2012). The authors reported that knockdown of perilipin 2 enhanced VLDL production and reduced TG accumulation,

which suggested opposing roles for CideB and perilipin 2 in controlling lipid availability for VLDL assembly (Li et al., 2012).

The manner in which CLD and MALD are formed may differ since the function of the two TG pools are distinct: namely, lipid storage versus assembly into lipoproteins for secretion. Also, it is unknown whether MALD are mobile within the microsome lumen or are associated with the membrane bilayer. Causing the collapse of the Golgi back into the ER by blocking anterograde vesicular movement with Brefeldin A reportedly does not impair TG deposition or cytosolic LD formation (Fei et al., 2009). This would indicate that the neutral supply for LD creation can move directly from the ER into the LD.

1.3.6 Intracellular Trafficking of ApoB-containing Lipoproteins

The trafficking of nascent, pre-VLDL particles from the ER to Golgi is a COPII-dependent process, since apoB transport was reduced when a dominant negative version of COPII component Sar1 was expressed (Gusarova et al., 2003). In the human hepatoma Huh7 cell line, the oxysterol binding protein family member ORP10/OSBPL10 associates with microtubules and the Golgi via independent domains and negatively regulates apoB-100 secretion (Nissila et al., 2012). This suggests that COPII-dependent vesicular transport facilitates secretion of mature VLDL from hepatocytes. Paradoxically, the diameters of VLDL (containing apoB-100) and chylomicrons (containing apoB-48) both exceed the maximum diameter of any known intracellular transport vesicles. It is currently unknown exactly how VLDL are transported in the secretory pathway or how they exit from the cell.

1.3.7 Regulation of Hepatic ApoB-100 Metabolism

Under physiological conditions, the rate of VLDL secretion is tightly coordinated with whole body metabolism. Output of VLDL is increased during fasting and decreased during feeding. The insulin released from the pancreas in the fed state reduces hepatic VLDL production by several mechanisms that occur in parallel, including reduced lipid availability for assembly, post-translational removal of apoB-100 from the secretory pathway and suppression of apoB-100 translation (Sparks et al., 2012). Diabetic dyslipidemia is in large part driven by VLDL overproduction (Adiels et al., 2008). Interestingly, the ability of insulin to suppress VLDL production appears to become compromised prior to systemic insulin resistance, as suggested by genetic animal models and studies of obese human males (Sorensen et al., 2011; Sparks and Sparks, 1994; Wiegman et al., 2003). Physiologically, VLDL output represents an elegant balance of lipid, protein and carbohydrate metabolism, which is unfortunately disrupted by insulin resistance.

There is evidence that apoB-100 is regulated at the transcriptional, translational and post-translational level (Rutledge et al., 2010). ApoB mRNA appears to be sequestered away from polysomes in HepG2 cells in response to insulin, thereby reducing translation (Karimian Pour and Adeli, 2011). Insulin can reduce synthesis of apoB even while global protein production is enhanced (Sparks and Sparks, 1990). Interestingly, apoB translation is reduced in a protein kinase C-dependent manner during which the protein complex at the 5' untranslated region of apoB mRNA is altered (Sidiropoulos et al., 2005; Sidiropoulos et al., 2007). VLDL secretion is suppressed via activation of insulin-mediated phosphoinositide 3-kinase (PI3-kinase) signalling (Phung

et al., 1997; Sparks et al., 1996). The resulting downstream effect is that insulin-dependent degradation of VLDL precursors by the autophagy machinery is enhanced, resulting in the eventual delivery of apoB-100 to the lysosome (Sparks et al., 1996). This clearance of apoB-100 is disrupted by the intracellular blunting of the insulin signaling cascade, possibly through the increased activity of PTP1B (protein tyrosine phosphatase 1B) and PTEN (phophatase and tensin homolog) (Sparks et al., 2012). During hepatic insulin resistance, Forkhead box O1 (FoxO1) increases MTP and apoC-III expression, providing a lipid-rich environment to support excessive VLDL assembly. In addition, hepatic lipogenesis remains insulin sensitive during systemic insulin resistance via mTORC1-dependent activation of SREBP-1c (Li et al., 2010), providing additional lipid substrates for VLDL assembly.

These diverse yet insulin-mediated effects on apoB-100 metabolism underscore the importance of studying the factors or "inputs" that determine net hepatic VLDL output. The relative contribution of these mechanisms to disease pathology in humans will no doubt emerge with future studies. The cellular fate of apoB-100 can be dictated by signalling events and also by protein quality control surveillance. The "decision" to destroy a nascent apoB-containing lipoprotein rather than to secrete it is a poorly defined process. Yet, it is becoming clear that functional ER homeostasis, lipid droplet metabolism and multiple degradation pathways are required to dispose of unwanted apoB. Dysregulation of apoB degradation may indeed contribute to overproduction of VLDL.

1.3.8 Regulation of ApoB-100 by Hepatic Degradation Pathways

The production of hepatic apoB-100 is largely governed by the rate of its intracellular turnover, rather than its rate of transcription or translation (Sakata et al., 1993). Multiple degradation mechanisms exist in hepatocytes that can target apoB-100 and remove it from the secretory pool (Brodsky and Fisher, 2008). VLDL assembly occurs in multiple compartments and is dependent on both the appropriate quantity and composition of lipids available during the window of time when each particle has to successfully assemble into a secretion-competent lipoprotein. The 26S proteasome, located in the cytosol, is known to carry out the ER-associated degradation (ERAD) of apoB (Benoist and Grand-Perret, 1997). The ER-luminal protease ER-60 has also been implicated in apoB-100 degradation (Qiu et al., 2004). Low MTP activity or a lack of lipid supply can stimulate the proteasomal degradation of apoB-100 and prevent its secretion (Benoist and Grand-Perret, 1997; Dixon et al., 1991). Ritonavir is an inhibitor of the chymotrypsin-like activity in the 20S core of the proteasome and is part of the anti-retroviral therapy for human immunodeficiency virus (Parker et al., 2005). Ritonavir has been suggested to cause hyperlipidemia in these patients by blocking apoB degradation (Riddle et al., 2002). Although this is suggestive of the relevance of the proteasome pathway in human VLDL production, further studies are required to elucidate the role of apoB ERAD *in vivo*.

A novel quality control mechanism has been recently characterized, centred around a ribosome-bound complex (Brandman et al., 2012). Ribosome-associated ubiquitin ligases have been reported to help trigger the co-translational degradation of nascent proteins (Bengtson and Joazeiro, 2010). It is conceivable that hepatic apoB

turnover could be influenced by this manner of quality control decision, thus warranting the investigation of ribosome-associated quality control in the co-translational degradation of apoB.

Lipid perodixation and oxidative stress cause the non-proteasomal degradation of apoB-100 (Pan et al., 2004). More recently it was reported that polyunsaturated fatty acids provoke this type of degradation via stimulation of autophagy in a process termed pre-secretory, post-ER proteolysis (PERPP) (Pan et al., 2008). The necessary and sufficient cellular components for PERPP remain to be elucidated. Especially interesting is the question of how cytosolic autophagosome formation might selectively sequester apoB-100 for degradation out of the secretory pathway without engulfing additional luminal components.

The degradation of apoB-100 by the proteasome and by autophagy are reported to converge at cytosolic lipid droplets (Ohsaki et al., 2006; Ohsaki et al., 2008; Suzuki et al., 2012). It appears that the cumbersome process of assembling or destroying a bulky, hydrophobic assemblage of lipid and protein is intimately related to the lipid droplet system. Notably, production and release of infectious Hepatitis C virus particles from hepatocytes requires the successful hijacking of the VLDL assembly machinery (Gastaminza et al., 2008; Nahmias et al., 2008) as well as subversion of the ER-lipid droplet microenvironment (Miyanari et al., 2007).

1.4 Overview of the ERAD Pathway

The concept of ER-associated degradation in a non-ER compartment arose from studies in the late 1980's and early 1990's that began to reveal how the degradation of ER

proteins did not in fact take place inside the ER and required elements of the cytosolic ubiquitin proteasome system. Studies of the biogenesis of the T-cell receptor (TCR) complex showed that subunits of the TCR complex were degraded in a pre-Golgi, non-lysosomal compartment (Lippincott-Schwartz et al., 1988). These systems proved useful for characterizing proteolysis because the disproportionate overexpression of receptor complex subunits yielded supra-physiological levels of degradation. In 1993, Sommer and Jentsch demonstrated that a loss-of-function mutation in an ubiquitin conjugation protein was able to suppress the defect in protein translocation into the ER caused by mutant SEC61, which forms the translocation channel (Sommer and Jentsch, 1993). This provided a novel connection between the production of ER proteins and the cytosolic ubiquitin proteasome system. Similar discoveries followed involving the CFTR (cystic fibrosis transmembrane conductance regulator) protein (Jensen et al., 1995; Ward et al., 1995) and carboxypeptidase Y (CPY*) (Hiller et al., 1996). An explosion of subsequent studies centred on these and other degradation substrates would create the framework for the ERAD pathway.

Over the last twenty years, our understanding of the ER has evolved dramatically. Many components of the ERAD system were revealed using the power of yeast genetics, which then allowed the extrapolation of the findings into studies of the mammalian orthologs. In addition to mutant proteins, engineered fusion proteins and endogenous substrates, it was found that numerous bacterial pathogens exploit the ERAD machinery to gain entry to the cytosol via the ER including cholera toxin, Shiga toxin and ricin (Lord et al., 2005).

A handful of canonical or "model" substrates came to define our understanding of ERAD and the entirety of the components required for the process. An underlying trait of these substrates was that they were often overexpressed mutants, or genetically engineered to misfold in the ER. The proteins were degraded at high rates and were therefore ideal for characterizing ERAD. Over time, many substrates have broken the initial rules of ERAD, to the point that the notion of a "canonical" ERAD substrate has gradually dissolved (Vembar and Brodsky, 2008). While many substrates rely on the same ERAD machinery, there exist examples of "customized" degradation pathways that adopt ERAD machinery for regulatory purposes. HMG CoA reductase (Jo and De Bose-Boyd, 2010) and the inositol-3-phosphate receptor (IP$_3$R) (Wojcikiewicz et al., 2009) are examples of substrates where elegantly evolved mechanisms employ ERAD machinery to selectively target functional proteins for destruction. The cellular level of these ERAD substrates help to maintain cholesterol and calcium homeostasis, respectively. Recently, the expression of an enzyme involved in synthesis of galactosylceramides (utilized to produce glycosphingolipids) was shown to be regulated by ERAD in a sterol-sensitive manner (Hayashi et al., 2012). As illustrated by these and other examples, ERAD is responsible for more than simply sending unwanted ER proteins on a one-way trip to the 26S proteasome, or "taking out the trash," if you will. Given that the ERAD capacity of a cell is intimately linked to ER homeostasis, it is perhaps not surprising that ER stress is associated with dysregulation of many other seemingly unrelated processes.

For any given ERAD substrate there are a minimum of four steps in the pathway: (1) substrate recognition (Maattanen et al., 2010), (2) ubiquitination, (3) removal from the ER or "retrotranslocation" (Hampton and Sommer, 2012) and finally, (4) proteasomal

degradation. Over the next few sections I will describe the ubiquitin proteasome system and provide a stepwise overview of the ERAD machinery, including components which have been implicated in the ERAD pathway specific to apoB-100.

1.4.1 The Ubiquitin Proteasome System

A functional ubiquitin proteasome system is crucial to the ongoing survival of living organisms. Proteins of all kinds inevitably become damaged or misfolded and must be detected and removed to ensure that normal biological processes are not impaired. In addition to the removal of long-lived proteins, a surprisingly large amount (up to 30%) of newly synthesized proteins are destroyed by proteasomes before they reach a functional conformation (Schubert et al., 2000). While there are many mysteries still surrounding the ubiquitin proteasome system, intensive research has revealed a dynamic, subtly regulated network of dozens of subunits and associated proteins.

Ubiquitin is a widely conserved, 76 amino acid protein that is covalently attached to target substrates by ubiquitination machinery (pictured in Figure 1.4). The E1 enzyme is considered "ubiquitin-activating," which then passes the ubiquitin moiety to an E2 ubiquitin-conjugating enzyme. The next step involves an E3 ubiquitin ligase facilitating either the direct transfer of ubiquitin from the E2 onto the target substrate, or transfer of the ubiquitin from the E2 to the E3 and then onto the target. There exist several families of E3 ligases that perform the same task but in a structurally and mechanistically distinct manner. There exists a handful of E1 enzymes, several dozen E2 enzymes and hundreds of E3 ligases. The ligases are distributed among cellular compartments, including the nucleus, cytosol and within organelle membranes. Thus, it has been assumed that E3
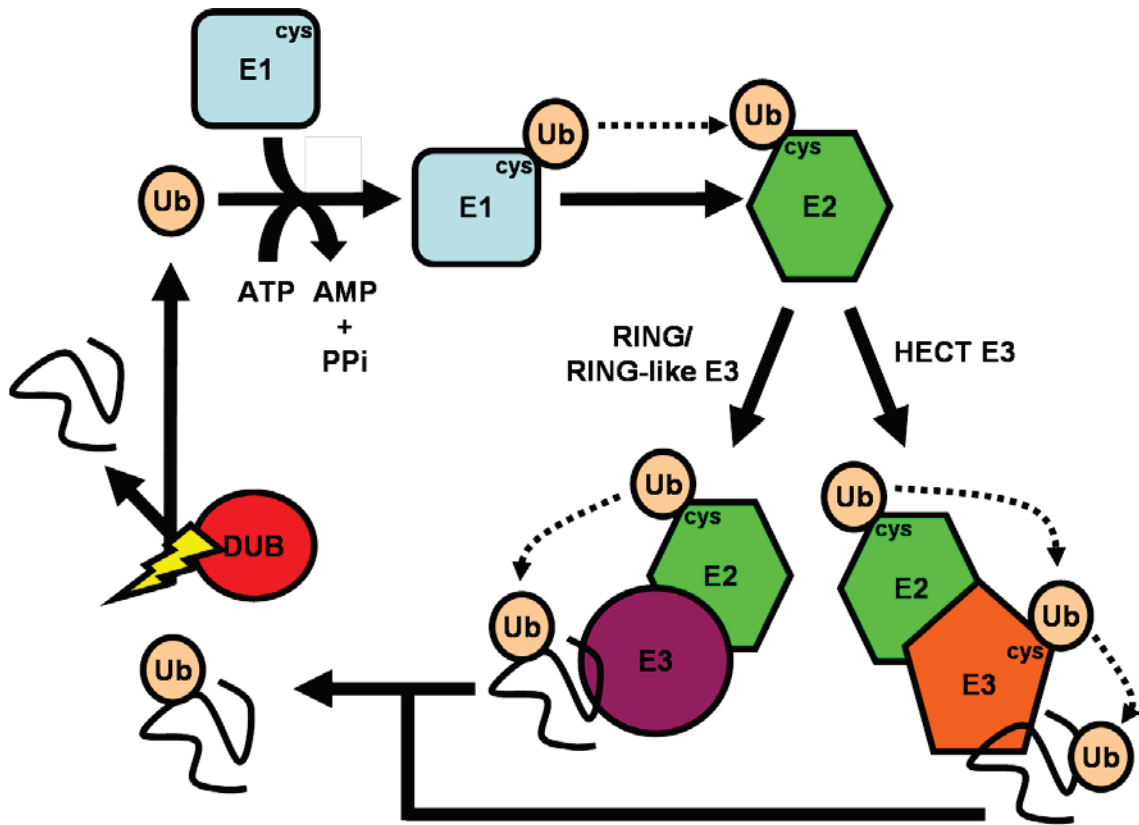
Figure 1.4. Cartoon representation of the ubiquitin-conjugation pathway. Free ubiquitin is "activated" by an E1 enzyme. The ubiquitin is attached covalently to an E1 cysteine residue in an ATP-dependent reaction. The ubiquitin monomer is then transferred from the E1 to an E2 ubiquitin-conjugating enzyme. Depending on the family of E3 ubiquitin ligase, the ubiquitin moiety is transferred directly to the substrate (curved black line) from the E2, with the E3 mediating substrate specificity (RING, RING-like E3s), or the ubiquitin is sequentially transferred from the E2 to the E3 to the substrate (HECT E3s). Repeated ubiquitination reactions can add to the monoubiquitinated substrate, resulting in a polyubiquitinated substrate. Conversely, a de-ubiquitinating (DUB) enzyme can break the bond between ubiquitin and the substrate, thus allowing the ubiquitin monomer to be recycled and modulating the function/fate of the target substrate.

ligases and proteins that modulate their function/localization are important in determining substrate specificity.

Proteasome-associated ubiquitin ligases and deubiquitinase enzymes (DUBs) have the ability to extend and disassemble ubiquitin chains, respectively, such that proteasomes are thought to actively control a substrate's commitment to degradation (Crosas et al., 2006). Furthermore, some DUBs that associate with the proteasome can either remove entire ubiquitin chains at their base or "trim" back the terminus of the chain (Lee et al., 2011). Needless to say, the outcome of such DUB reactions will have effects on the turnover of the target substrate.

1.4.2 Deubiquitinating Enzymes

For every ubiquitination event in living cells there is almost invariably a deubiquitination reaction that must occur. This must be true given that ubiquitin chains are seldom degraded alongside the target substrate to which they were attached. Instead, the ubiquitin is removed and recycled as the substrate enters the core proteasome. Compared to the ubiquitination machinery, the widespread study of deubiquitinating enzymes (DUBs) has only occurred relatively recently. DUBs have emerged rapidly as a potentially "druggable" set of new targets (Colland, 2010). USP19 was the first ER-membrane resident DUB to be associated with the ERAD pathway via its ability to rescue the canonical substrates CFTRΔF508 and TCRα (Hassink et al., 2009). A comprehensive proteomic analysis of 75 DUB enzymes has yielded hundreds of possible interacting proteins and placed DUBs into many previously unrelated arenas of cell biology (Sowa et al., 2009). This will no doubt be an exciting field and hopefully one that provides novel

therapeutics related to some of these very diverse, now DUB-associated processes. Proteasome-associated DUBs are discussed in the proteasome section below.

1.4.3 Ubiquitination as a Dynamic, Multi-faceted, Post-translational Signal

Ubiquitination of a target substrate can elicit an array of effects including proteasomal degradation, endocytosis of target receptors, altered transcriptional expression, etc. [reviewed in (Hochstrasser, 2009)]. Ubiquitin proteins can be linked together via covalent isopeptide bonds between the amino-terminus of ubiquitin and any of the seven distinct lysine residues on the incoming "next link" of the ubiquitin chain. Linkages through lysine-48 (K48) are devoted to demarcating proteasome substrates. Meanwhile, K63 linkages are predominantly associated with regulatory "switches," which has placed ubiquitin (and ubiquitin-like proteins) onto the list of other post-translational modifications (PTM) that elicit a functional change in the target substrate. The other chain linkages, while reported to occur in nature, are less well defined [reviewed in (Behrends and Harper, 2011)].The unconventional chain linkage through lysine K11 appears to function in some ERAD pathways (Xu et al., 2009). Interestingly, the IP$_3$ receptor has been found to possess ubiquitin chains linked through both K48 and K63 (Sliter et al., 2011). However, only the K48 chains induce degradation of the receptor, suggesting that the K63 ubiquitin chains may play a non-degradative regulatory role when attached to this ERAD substrate.

Polyubiquitin chains of at least 4 ubiquitin monomers are needed to demark a protein as a proteasome substrate (Pickart, 2000). An additional requirement of an "unstructured region" on the substrate itself may be necessary to trigger degradation

(Prakash et al., 2004). Further, when a substrate is presented to the proteasome it may allosterically participate in its own degradation by causing the gate to open and increase proteolytic activity (Bech-Otschir et al., 2009).

Proteins are targeted most often by ubiquitination at lysine residues. Target lysines have been a contentious area of research mostly because mutagenesis of *bonafide* target lysines often results in compensatory ubiquitination of alternative lysines, serine/threonine residues and even amino termini (Shimizu et al., 2010). The required ubiquitin signal for proteasomal degradation appears to depend in part on the size of the substrate. Monoubiquitination, rather than polyubiquitination, is sufficient for degradation of proteins smaller than around 150 residues in size (Shabek et al., 2012). Ubiquitin (and ubiquitin-like modifiers) create an enormously complicated network of post-translational modifications that contain a rich volume of regulatory information in living cells. The evolution of this field will be fascinating as techniques and technologies improve in the post-proteome era.

1.4.4 The 26S Proteasome

The 26S proteasome is very large multimeric complex that performs the majority of proteolysis in living cells. Some of the fundamental processes that depend on proteasome function are the cell cycle, signal transduction, cell death, immune responses, metabolism, quality control and development. Generally speaking, the regulated turnover of cellular proteins is paramount to the long-term health and survival of living organisms. Not surprisingly, dysfunction of the proteasome has emerged as a factor in many diseases.

The mammalian 26S proteasome is divided into two functionally and structurally distinct components: the 20S Catalytic Particle (CP), inside the core of which substrates are destroyed, and the 19S Regulatory Particle (RP), which processes substrates prior to their entry into the core. Processing can include accepting substrates from proteasome-related substrate binding proteins, deubiquitinating the substrates and unfolding/stabilizing the already unfolded polypeptides such that they can enter into the narrow pore of the core particle. The careful arrangement of the over thirty subunits during proteasome assembly is a remarkably complex and elegant process in itself and is beyond the scope of this Introduction [reviewed in (Bedford et al., 2010)].

The 26S proteasome (named 26S based on its sedimentation coefficient during density gradient ultracentrifugation) has an approximate mass of 1.66 MDa. However, this refers to a CP plus an RP at only one end. The "elongated" fully assembled proteasome is actually 30S with a mass of ~2.59 MDa (pictured in Figure 1.5). Generally, an RP binds to one or both ends of the inactive CP and creates an active proteasome complex. The RP has two components, named by their structural appearance: the base and the cap. Nomenclature for the RP subunits is as follows: Regulatory particle of triple-ATPases (Rpt1-6) and Regulatory particle of non-ATPase subunits (Rpn1-15). The mammalian catalytic 20S core of the proteasome (and that of all eukaryotes) consists of two outer alpha rings and two inner beta rings, formed by "axial stacking".

The β1, β2 and β5 subunits cleave substrates at the C-terminal side of acidic, basic and hydrophobic residues, respectively. The interior of the barrel-shaped CP contains the central catalytic core, flanked by two "antechambers," which serve to maintain substrates in an unfolded state as they are threaded through the gate on their
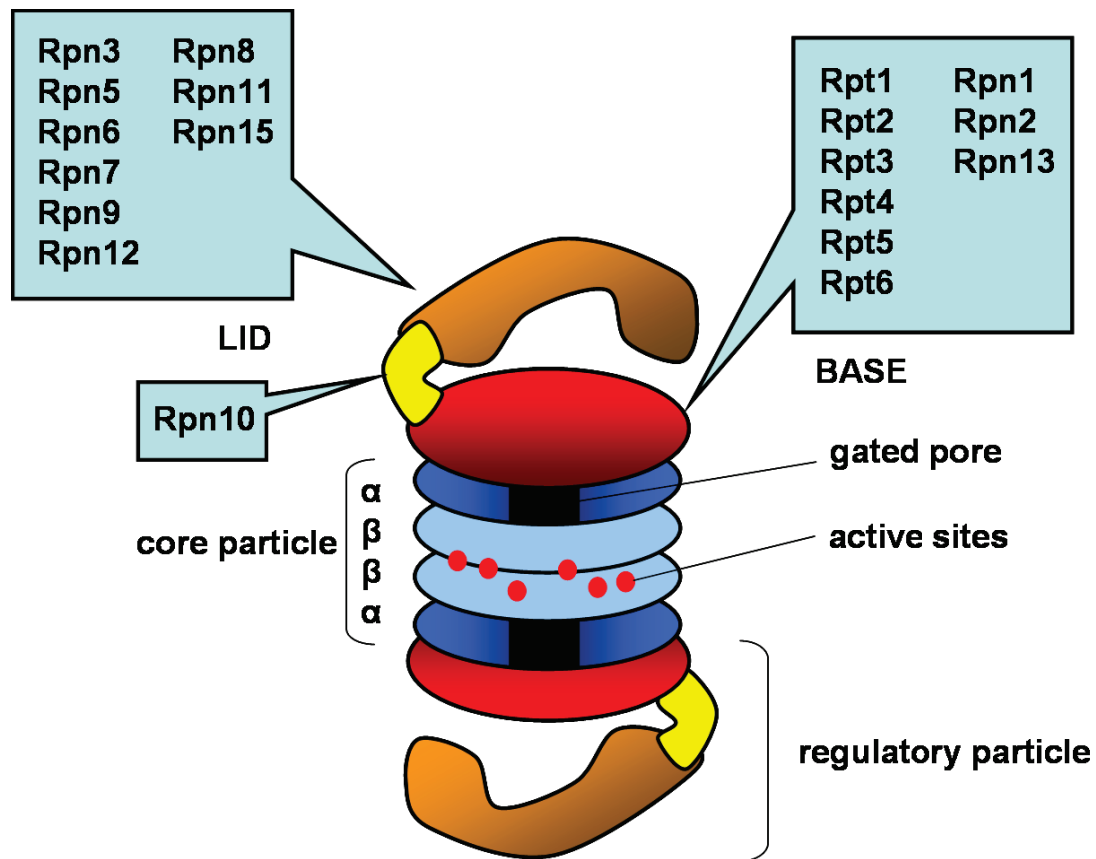
Figure 1.5. Schematic of the 26S proteasome. The proteasome consists of a catalytic core particle and regulatory particle(s). The active sites of six proteases lie within the β-rings of the core. The base of the regulatory particle is in contact with the gated pore, which opens and closes in response to specific substrate binding events at the regulatory particle. Names of the lid and base components are shown in coloured text boxes. (Used with permission (Hanna and Finley, 2007)).

way to the core (Ruschak et al., 2010). The opening to the CP is a narrow 13 Å, with the ordered structure of the "closed gate" consisting of an asymmetric arrangement of the α2, α3 and α4 subunits (Groll et al., 1997).

Proteasome function is ATP dependent, and the ATPase subunits of the ring/base are believed to carry out the bulk of the energy dependent tasks during degradation. Specifically, substrates must be unfolded and the gate must be opened before substrate translocation into the core. As a whole, the RP ATPase ring that sits against the top/bottom of the CP cooperates to perform substrate binding, unfolding and translocation (Saeki and Tanaka, 2012). EM studies of the proteasome from yeast have demonstrated a large degree of structural variability, mostly at the lid/base interface (Bohn et al., 2010). Interestingly, experimental evidence supports a model for ATPase-driven gate opening involving the "wobbling" of the base along the axis of the core particle. The hexameric base is observed to be both tilted and off centre with respect to the CP. ATP binding, but not hydrolysis, appears to drive this process.

The first proteasome subunit known to bind a ubiquitin chain was Rpn10, through what became known as an ubiquitin-interacting motif (UIM) (Deveraux et al., 1995). Rpn13 has since been found to also "grab" ubiquitin chains, but through a "plekstrin-like receptor for the ubiquitin" (Pru) domain. Several protein-protein interactions that are also integral in the proteasome system are mediated by Ubiquitin-like-UBA (ubiquitin-associated) (UBL) ubiquitin receptors. Included in this group are Rad23 and Dsk2, which shuttle ERAD substrates in the cytosol. The UBA domain carries the ubiquitinated substrates while the UBL region can interact directly with Rpn1, Rpn10 and Rpn13 (Hartmann-Petersen and Gordon, 2004). A plethora of proteins are transiently associated

with the proteasome. Given the highly-conserved structure, yet extremely diverse function of the proteasome, these factors likely tailor proteasome activity to meet the needs of the particular cell-type. An arsenal of ubiquitin receptors, ubiquitin ligases and deubiquitinases was revealed by mass spectrometry to reversibly associate with the proteasome (Guerrero et al., 2008).

1.4.5 Proteasome-associated Deubiquitinases

As indicated above, polyubiquitinated proteasome substrates typically have their ubiquitin chains removed immediately prior to their insertion into the 20S core. There are three DUB enzymes associated with the human 26S proteasome: Rpn11, Usp14 and Uch37 (Lee et al., 2011). The striking difference in activity between these is that Rpn11 supports substrate degradation while Usp14 and Uch37 delay or prevent degradation. Though Rpn11 is a DUB enzyme, it cannot hydrolyze ATP. Rpn11 cross-links with the Rpt3 ATPase of the base structure (Bohn et al., 2010), suggesting that Rpn11 depends on the ATPase activity of Rpt3. Rpn11-mediated DUB reactions might occur even after the substrate has been engaged by the ATPases in the central pore (Lee et al., 2011). To allow for the recycling of ubiquitin, Rpn11 cleaves at the base of the chain.

While the activities above are involved in substrate recognition and ubiquitin recovery, other DUB activities are involved in modulating the rate of protein degradation. Usp14 and Uch37 DUB activity targets substrates immediately on arrival at the proteasome, much earlier than Rpn11. Also unlike Rpn11, Uch37 removes ubiquitin moieties from the end of the ubiquitin chain, as does Ubp6, the yeast ortholog of Usp14 (Hanna et al., 2006; Lam et al., 1997). It appears that Usp14 and Uch37 activity are able

to modulate rates of proteasomal degradation and influence the outcome for ubiquitinated substrates. Rpn13 is a proteasome subunit capable of accepting substrates and activating Uch37, but not Usp14. Thus, there may be a network of interactions that govern the net fate of various substrates, depending on which factors they engage. Clearly, many intriguing questions remain regarding proteasome DUB function.

A small molecule inhibitor of Usp14 was found to disrupt the replication of the Dengue virus (Nag and Finley, 2012). Inhibition of the DUB activity of Usp14, enhanced proteasome activity and the degradation of oxidized proteins was accelerated (Lee et al., 2010a). Increased proteasome activity may have benefits in certain disease states afflicting humans, especially neurodegeneration.

1.4.6 Proteasome and Disease

The proteasome inhibitor bortezomib (known as Velcade) has been used clinically since 2003 for treatment of multiple myeloma (MM), and has since become a first line treatment for the disease. Initially it was thought that MM cells were vulnerable to apoptosis by proteasome inhibition due to impaired NF-κB activation (Adams, 2004). It later emerged that the actual mechanism of action was via an unfolded protein response (UPR). MM cells secrete large amounts of proteins compared to other cells and experience chronic ER stress activation (Meister et al., 2007). This large burden for protein secretion renders the MM cells particularly sensitive to the accumulation of proteasome substrates, via an apoptopic UPR (Obeng et al., 2006). Thus, the proteasome inhibitor treatment was effective was because the cells were overwhelmed by accumulation of unfolded proteins and were eliminated by apoptosis.

Several natural proteasome inhibitors have been discovered since Bortezomib and are at various stages of development. In addition, more subunits in both the CP and RP of the proteasome may be "druggable" targets, for which there are no specific compounds yet. These include proteases, ATPases and deubiquitinases. Understanding the complete proteasome structure and function will further our knowledge of protein turnover with relation to human disease.

1.5 ER Resident Chaperones – Friends and Foes of Nascent Proteins

1.5.1 Grp78/BiP

The ER contains a complex array of mechanisms for folding nascent proteins into their functional, mature conformation. The demands of each specific substrate can vary depending on whether they are glycoproteins, contain disulfide bridges, require assembly into larger oligomeric structures or, in the case of apoB-100, require lipid ligands to attain stability. Many components of the ER chaperone system are well characterized; however, the manner in which they interact and determine substrate fate during quality control processes is continuously being discovered.

BiP/Grp78 is the ER-resident cousin of the Heat shock protein 70 (Hsp70) chaperone system in the cytosol, and both perform diverse functions in their respective environment (Otero et al., 2010). BiP interacts with substrates through its C-terminal substrate binding domain (SBD) and is regulated by its N-terminal nucleotide binding domain (NBD). ATP binding in the NBD cleft leaves the SBD in an open form, while hydrolysis of the ATP to ADP causes closure of the cleft on the SBD and stabilizes the interaction with the substrate protein. When the ADP is exchanged for ATP, the substrate

is released and given the opportunity to fold. BiP cofactors can control the ATPase cycle and stimulate tight binding. For example, BiP-associated protein (BAP) is a nucleotide exchange factor (NEF) strongly expressed in secretory tissues and is capable of modulating BiP activity (Chung et al., 2002). When overexpressed, BAP causes excessive substrate release from BiP. BAP is not upregulated by the UPR; thus, ER stress greatly increases the ratio of BiP/BAP. Notably, neurodegeneration can ensue with mutations in BAP, providing one of the few examples of a mutational defect in secretory chaperone capacity compared to the many known disease-associated mutations found in client substrates of ER chaperones (Otero et al., 2010).

BiP function can also be modulated by ER resident proteins called ERdjs via J domains. ERdj proteins can bind target substrates, recruit BiP and release the target before protein folding is completed (Otero et al., 2010). Some ERdj proteins are upregulated by the UPR transcriptional program while others are not. In this regard, it appears that BiP specific functions are largely governed by where and when it is recruited to substrates by its co-factors. ERdj5 is a disulfide reductase that breaks disulfide bonds and enables the cell to efficiently degrade ERAD substrates (Ushioda et al., 2008). ERdj4/Mdg1 is upregulated by the UPR (Otero et al., 2010) and, together with ERdj5, was shown to coordinate ERAD of misfolded surfactant protein SP-C (Dong et al., 2008). These data suggest that BiP function is highly flexible based on its co-factor associations and where in the ER it is performing its substrate bind-and-release cycle. Much like Hsc70 (Matsumura et al., 2011), the cytosolic cousin of BiP, it appears BiP activity can be pro- or anti-degradative depending many outside factors.

1.5.2 The Protein Disulfide Isomerase Family

A balanced redox capacity is important for maintaining ER homeostasis. Many newly made proteins require disulfide bridges in order to obtain a stable, native folding state. On the other hand, misfolded and unfolded proteins that must be removed from ER and degraded first require that their disulfide bridges be broken. The perpetual demand for efficient disulfide bond formation is illustrated by the immediate disruption of protein folding and ER homeostasis by DTT treatment, a potent reducing agent (Jamsa et al., 1994).

An array of enzymes, proteins and molecules monitor and maintain the redox balance within the ER. The ER contains glutathione, a redox buffer initially synthesized in the cytosol. What distinguishes the ER from the cytosol is the lower ratio of glutathione (GSH) to its oxidized equivalent glutathione sulphide (GSSG) in the ER (1:1, compared to 3:1 in the cytosol) (Hwang et al., 1992). While the lower GSH:GSSG ratio helps in part to maintain the oxidizing environment of the ER, the luminal protein Ero1 (Endoplasmic reticulum oxidoreductin 1) appears to be the principal acceptor of electrons during disulfide bond formation (Cabibbo et al., 2000). Ero1 and the protein disulfide isomerases are crucial in controlling the redox potential in the ER (Sevier and Kaiser, 2008). To form a disulfide bond, the oxidized form of Ero1 transfers electrons from PDI to oxygen (producing hydrogen peroxide) and then PDI facilitates bridge formation on the target substrate. Of the two human Ero1 isoforms, one is constitutively expressed (Ero1-L) while the other is upregulated by the UPR (Ero1-Lβ) (Pagani et al., 2000).

There are over 20 members in the human protein disulfide isomerase family (Higa and Chevet, 2012). Many PDI family members have diverse redox potentials, suggesting

that within the same compartment some are dedicated reductases while others can serve as oxidases. ERp44 interacts with the inositol-3-phosphate receptor 1 (IP3R1) and affects the calcium channel activity (Higo et al., 2005). The association between IP3R and ERp44 is itself sensitive to the redox environment, luminal pH and calcium levels, suggesting that this process may represent a molecular monitoring system for the ER redox status (Higa and Chevet, 2012).

1.5.3 The Calnexin/calreticulin Cycle and the N-glycan Glucose Timer Pathway

Hydrophilic, pre-assembled carbohydrate moieties are attached to many newly synthesized proteins, which increases their solubility and decreases the likelihood of aggregation during folding (Helenius and Aebi, 2004). In addition, these sugar moieties are a component of an elegantly evolved system of molecular timers governing the fate of newly made glycoproteins (Maattanen et al., 2010).

1.6 ERAD Machinery: Substrate Movement from the ER to the Proteasome

1.6.1 The Retrotranslocation Channel(s)

Out of all the ERAD components needed to facilitate substrate degradation, the elements required for moving substrates from the ER lumen/membrane into the cytosol remain the least understood. The pursuit of a bonafide "retrotranslocation channel" has yielded a lot of evidence, much of which is compelling but inconclusive in proving the "necessary and sufficient" protein components. It appears that, much like substrate recognition, there are multiple means by which a protein can be sent to the cytosol. The

diversity among ERAD substrates and their pathway(s) to destruction support the notion that there is no one true "retrotranslocon" to serve all of the ER.

When ER proteins were first observed to be degraded in the cytosol rather than by luminal proteases, the putative Sec61 translocon was the first primary candidate to be the retrotranslocation channel (Wiertz et al., 1996). Glycan-containing ERAD substrates are removed to the cytosol first before their sugar moieties are removed by the Png1 *N*-glycanase (Mehnert et al., 2010). An X-ray crystallography structure of the Sec61 channel shows that the core of the translocon is only wide enough to contain linear, unfolded peptides (Van den Berg et al., 2004). This suggests that the Sec61 channel may not be directly involved in retrotranslocation. On the other hand, the Sec61 hetero-trimeric channel displays flexibility during the membrane integration of transmembrane domains (Devaraneni et al., 2011), translation-independent pore opening (Wonderlin, 2009) and a requirement for BiP to mediate channel closure (Alder et al., 2005). Further, crystallography provides no information about dynamic conformational changes. Together these data do not rule out retrograde movement of proteins through the Sec61 translocon. However, since all nascent proteins must enter the ER through Sec61, it is understandably difficult to design an experimental system such that this issue can be resolved conclusively.

Studies by two independent groups in 2004 in mammalian cells and *C. Elegans* suggested that Derlin-1 proteins served as components in a retro-translocation channel (Lilley and Ploegh, 2004; Ye et al., 2004). However, as recently as 2010, this suggestion was challenged (Mehnert et al., 2010), perhaps because the evidence was, to a large degree, circumstantial. Simply because a protein is required for efficient

retrotranslocation of substrates does not confirm that it forms the channel. The ER bilayer consists of supra-molecular complexes, the organization (and stability) of which is only partly understood. Nonetheless, more substrates for Derlin-dependent retrotranslocation have since emerged, lending support to this route out of the ER (Dougan et al., 2011; Greenblatt et al., 2011; Moore et al., 2010).

More recently, a "tour de force" photocrosslinking technique was used to show that amino acids of the Hrd1 protein within the transmembrane domain come into direct contact with ERAD substrates (Carvalho et al., 2010; Stanley et al., 2011). The protein Usa1 (known as HERP in mammals) supports the interaction of multiple Hrd1 proteins, which may in turn facilitate the formation of relatively large, dynamic retrotranslocation channels capable of moving partially folded protein cargo through to the cytosol (Horn et al., 2009). The Sec61 translocon is also associated with the Hrd1 complex (Schafer and Wolf, 2009). Together, these data suggest that perhaps several mechanisms of protein-mediated retrotranslocation exist and that differing hypotheses have arisen from substrate and model-specific ERAD pathways.

A fascinating alternative hypothesis to protein channel-mediated retrotranslocation was suggested by Hidde Ploegh, who speculated that a lipid-based "escape hatch" could explain the observed retrograde movement of large protein cargo and mostly-assembled virions into the cytosol from the ER (Ploegh, 2007). The formation or "blebbing" of lipid droplets from within ER membrane into the cytosol may allow the escape of large, non-linearized cargo during the brief breach in membrane integrity. It has been shown that complete protein unfolding is not necessarily required for retrotranslocation (Tirosh et al., 2003). Furthermore, the movement of partially

assembled virus particles into the cytosol is unlikely to occur via narrow protein channels. An *in vitro* assay of HMG CoA reductase retrotranslocation showed that the whole protein was removed intact (Garza et al., 2009). Another observation has been made during sterol-induced HMG CoA reductase degradation: it requires retrotranslocation into the cytosol through an ER subdomain "closely associated" with lipid droplets (Hartman et al., 2010). This hypothesis would in no way exclude the involvement of proteins in this process, but the budding process for lipid droplet formation is proposed to be adapted (or co-opted) for efficient and stable transfer of large, possibly hydrophobic cargo between compartments. The mechanism(s) of retrotranslocation remains a technically challenging and an intriguing open question.

1.6.2 E3 Ubiquitin Ligases Enzymes of the ERAD Pathway

There are several E3 ligases associated with the ERAD pathway. Of these, Hrd1 and gp78 are by far the best characterized and have the longest lists of known substrates, with others such as RNF5/RMA1, Trc8, Teb4, Rfp2 and Kf-1 remaining relatively mysterious (Mehnert et al., 2010). A common observation of many groups is the overlap between E3 ligase target proteins and the sharing of co-factors. Initially, because E3 ligases numbered in the hundreds, it was thought that these governed substrate specificity. It has come to light that ubiquitin ligases are rather promiscuous in their substrate selection and that specificity likely occurs via subtly regulated supra-molecular complexes containing a ligase and multiple ERAD components.

It is worth noting that soluble, freely cytosolic E3 ligases have been shown to ubiquitinate glycoproteins and secretory proteins, including the well-studied, Hsp70-

associated E3 ligase CHIP (Imai et al., 2002; Yoshida et al., 2002). In hindsight, the recent model featuring the deubiquitination of p97 clients by YOD1 during their retrotranslocation (Ernst et al., 2009) may leave room for re-ubiquitination of ER-derived substrates by soluble E3 ligases that are not readily found associated with the ER membrane.

The sterol-sensitive ubiquitination of the HMG CoA reductase enzyme has been shown to be gp78-dependent (Song et al., 2005). The model was later updated to include another ligase, Trc8, and also to involve Insig-1 and Insig-2 (Jo et al., 2011). Another group recently reported that they found no evidence for either gp78 or Trc8-dependent, sterol-accelerated degradation of the reductase (Tsai et al., 2012). In their model, gp78 appears to ubiquitinate Insig-1 and not the reductase. Several explanations for the discrepancy are offered, including different model systems and issues with knockdown technologies. This is both an unfinished story and perhaps a cautionary tale of how diverse and malleable quality control processes are from one experimental model to another.

1.6.3 The Gp78/AMFR E3 Ubiquitin Ligase

Gp78, also known as autocrine motility factor receptor (AMFR), was the first identified ER membrane-resident E3 ubiquitin ligase in mammals (Fang et al., 2001). Aside from ERAD, gp78 is known to participate in glycolysis, matrix remodelling and receptor endocytosis (Fairbank et al., 2009). Gp78 is a RING domain ubiquitin ligase. The active site of gp78 is situated in the cytosol, as there are no elements of ubiquitin machinery or ubiquitin itself in the ER lumen. The cytosolic tail of gp78 displays diverse

functionality in addition to the E3 active site: it contains a polyubiquitination binding site (Cue domain), an E2 binding site and a p97-interacting VCP-interacting motif (VIM) domain (Fairbank et al., 2009). Together these regions are thought to coordinate events during ERAD at the ER membrane.

Gp78 displays the ability to ubiquitinate substrates that possess luminal, transmembrane or cytosolic folding lesions (i.e. all three possible locations for ERAD substrates to misfold). Target substrates of gp78 include, but are not limited to, CD3δ and TCRα (unassembled subunits of TCR), the Z variant of α1-antitrypsin and the mutant CFTRΔF508 protein that causes cystic fibrosis (Ballar and Fang, 2008). Notably, gp78 was also the first E3 ligase to be associated with the hyperactive ERAD of the KAI1 tumour suppressor, and is implicated in the metastases of certain cancers (Tsai et al., 2007).

Gp78 and p97 are known to interact and coordinate the processes of ubiquitination and retrotranslocation, along with other ERAD machinery components (Zhong et al., 2004) via the VIM domain of gp78 (Ballar et al., 2006; Ballar et al., 2007). Ufd1 is a co-factor of gp78 during ERAD, independent of its role in the p97-Ufd1-Npl4 retrotranslocation complex (Cao et al., 2007). The Ufd1 cofactor contains two ubiquitin binding domains: one binds monoubiquitin and the other associates with polyubiquitin. Gp78 activity is enhanced when Ufd1 is bound by monoubiquitin (Cao et al., 2007), while the Ufd1.p97 association increases the affinity of Ufd1 for polyubiquitin chains (Park et al., 2005; Ye et al., 2003). During the ERAD of CTFRΔF508, gp78 displays "E4" activity, referring to multiubiquitin chain assembly factors, which are capable of recognizing and extending existing polyubiquitin chains (Morito et al., 2008). Another

unique feature of gp78 is the ability to transfer pre-assembled ubiquitin chains from an E2 protein onto its target substrate (Li et al., 2007).

These and other data demonstrate the subtle complexity of gp78 function with respect to its diverse, transient binding partners at the ER and E3 ligase activity. New studies of gp78 biology continue to appear in the literature. I will discuss my own findings about gp78 and apoB metabolism (Chapter 4, (Fisher et al., 2011)) in the context of recently published data in the Discussion found in Chapter 7.

1.6.4 Retrotranslocation by the AAA ATPase p97

ERAD substrates can be either luminal or transmembrane, with the latter being able to present folding lesions on either side of the ER bilayer or directly within it. The inherent diversity of these peptides demands an equally diverse system of detection, as illustrated above. The common requirement for these ERAD substrates is to be efficiently removed from the locale in which they are poorly folded and delivered to the cytosolic proteasome. The proteasome itself has been implicated in directly removing substrates from the ER (Mayer et al., 1998). However, the majority of known ERAD substrates share the same cytosolic retrotranslocation (or dislocation) machinery, the AAA ATPase called Cdc 48 in yeast and p97/VCP (Valosin-Containing Protein) in mammals.

In 2001, it was reported that Cdc48/p97/VCP had the ability to transport proteins from the ER into the cytosol (Ye et al., 2001). p97 is described as having a "segregase" ability, referring to the ATP-dependent extraction of proteins from both membranes and supra-molecular protein complexes (Braun et al., 2002). The force needed to "pull" proteins out of the ER is provided by ATP hydrolysis, which causes conformational

changes in the p97 hexamer. The ATPase-driven abilities of the highly-conserved p97 complex have been employed for a variety of energy-dependent tasks in mammalian cells. The processes p97 participates in are ER and Golgi membrane fusion, DNA repair, DNA replication, activation of membrane-bound transcription factors and ERAD (Madsen et al., 2009).

Seven groups of p97-interacting proteins exist, separated based on the p97 region they interact with: the UBX domain, PUB domain, BS1/Shp box, VBM domain, UBX-like domain, PUL-domain and the VIM domain (Madsen et al., 2009). Ubiquitin Regulatory X or UBX domain-containing proteins are the largest group of co-factors of p97 (Schuberth and Buchberger, 2008), and are also considered p97 "adaptors." All human UBX-containing proteins are known to interact with p97 (Alexandru et al., 2008) and have a similar structure to the ubiquitin protein itself (Schuberth and Buchberger, 2008).

During ERAD, a heterodimer composed of the cytosolic proteins Ufd1 and Npl4 regulate the retrotranslocation function of p97 (Ye et al., 2003). VIMP (VCP-interacting membrane protein) is a single-pass ER membrane protein that helps mediate the interaction between the p97-Ufd1-Npl4 complex and Derlin-1 (Ye et al., 2004). The promiscuity of the p97-Ufd1-Npl4 complex allows it to target many classes of substrates, drawing on complexes with more specificity than the p97 complex itself (Ballar et al., 2011).

Substrate binding by p97 appears to be twofold: the ATPase domain of p97 is able to recognize non-ubiquitinated peptide segments, while the poly-ubiquitin chain on the substrate interacts with both p97 and a ubiquitin-binding site on Ufd1 (Ye et al., 2003).

Substrates require ubiquitin chains linked through lysine 48 for retrotranslocation to occur (Flierman et al., 2003).

Ubiquitinated proteins are extracted from the ER by p97, but they can also have their ubiquitin chains remodelled while in association with p97. Ufd2 is an ubiquitin-chain elongation factor (or "E4" protein in the ubiquitin pathway nomenclature) (Koegl et al., 1999). Once p97-Ufd1-Npl4 is bound to a substrate, Ufd2 can then associate with p97 and extend the polyubiquitin chain. Interestingly, Ufd2 can associate with proteasome-associated substrate "shuttle" proteins Rad23 and Dsk2, providing a possible means by which some substrates are sent to the proteasome following retrotranslocation (Richly et al., 2005). One way that cells can fine-tune rates of protein degradation is to inhibit steps within the ERAD. Ufd3 disrupts the p97-Ufd2 interaction by competing for the same binding site, thus negatively regulating substrate processing (Rumpf and Jentsch, 2006).

Several DUB enzymes contain UBX domains. The deubiquitinase YOD1 associates with p97 by its UBX domain in a complex that includes Derlin-1 and Ubxd8 (Ernst et al., 2009). A catalytic-inactive YOD1 mutant stabilized both membrane and luminal ERAD substrates, suggesting a role for YOD1 at or beyond the convergence of these distinct pathways, likely between engaging a particular retrotranslocon and proteasomal delivery. Intriguingly, the authors proposed a model where YOD1 removes some of the ubiquitin moieties from the substrate (while already in association with p97) such that the peptide can be threaded into the central pore of the p97 hexamer (Ernst et al., 2009). There are Ufd2-like E4 activities associated with p97 which may then re-extend the ubiquitin chain such that either a shuttling protein like Rad23 or perhaps the proteasome cap itself may retrieve the retrotranslocated substrate for further processing.

In addition, a ubiquitin shuttle protein named ataxin-3 has also been implicated in p97 regulation (Wang et al., 2006b), perhaps indicating a homeostatic regulation of retrotranslocation by ubiquitin-dependent events in the cytosol. In the years since our initial p97 study (Chapter 3, (Fisher et al., 2008)), the understanding of p97 and the ERAD pathway has evolved significantly. Chapter 7 includes an update and commentary on the ramifications of these new data.

1.6.5 Cytosolic Chaperones & ERAD Substrate Trafficking

Proteasomes can localize to the cytosolic surface of the ER bilayer (Tcherpakov et al., 2008), suggesting that the extraction of proteins from the ER membrane/lumen is tightly coupled to their processing at the 19S cap and subsequent insertion into the 20S catalytic core. The delivery of some ubiquitinated substrates to the proteasome can occur via shuttling proteins such as Rad23 and ataxin3. Cytosolic protein Rad23 coordinates the deglycosylation of ERAD substrates (Kim et al., 2006) and is also a reversibly bound proteasome accessory serving as an ubiquitin receptor (elsasser) while targeting substrates to the proteasome (Chen and Madura, 2002). Another cytosolic ubiquitin receptor, ataxin-3, associates with p97, Rad23 and the proteasome (Doss-Pepe et al., 2003). Interestingly, ataxin-3 possesses deubiquitinating activity, binds polyubiquitinated proteins (Burnett et al., 2003), modulates p97-dependent retrotranslocation of ERAD substrates (Wang et al., 2006b), and in turn, is activated by p97 (Laco et al., 2012). Mutations in ataxin-3 are implicated in Machado-Joseph disease (MJD), or Spinocerebellar Ataxia type 3, an inherited disease characterized by polyglutamine expansions of CAG in the ATXN3 gene (Riess et al., 2008). The data suggests that

together these proteins, among other functions, facilitate the efficient, regulated processing and delivery of polyubiquitinated ERAD substrates to the proteasome. As usual, additional co-factors and accessory proteins are proposed to mediate substrate specificity.

1.7 ERAD of ApoB-100

Conditions that limit the assembly of VLDL such as low levels of lipid ligands (Dixon et al., 1991) or MTP inhibition (Benoist and Grand-Perret, 1997) can trigger the degradation of apoB-100 by ERAD. The translocation efficiency of apoB is tied to its co-translational acquisition of lipid ligands. When lipidation is inadequate, apoB can undergo "translocation arrest," resulting in a prolonged presence in the translocon and exposure to the cytosol (Chuck and Lingappa, 1992; Du et al., 1994; Mitchell et al., 1998). If translation proceeds during temporary translocation arrest, a loop of newly synthesized apoB experiences prolonged exposure to the cytosol side of the ER membrane. Three "lesions" likely occur all at once: (1) exposure of poorly lipidated apoB regions in the ER lumen (B37-42, in particular), (2) prolonged presence in the translocon and (3) exposure of apoB motifs to the cytosol (pictured in Figure 1.6). With regard to apoB, it is of no consolation that the nature of substrate recognition and processing by the ERAD machinery appears to be subdivided along the lines of lesion site. Translocation-arrested apoB might present lesions in all three of these microenvironments at once. Given its prolonged bitopic topology, translocation arrested apoB may even behave as an ERAD substrate that is membrane-integrated, despite the final product of VLDL being a luminal, secreted lipoprotein (Baker and Tortorella, 2007).
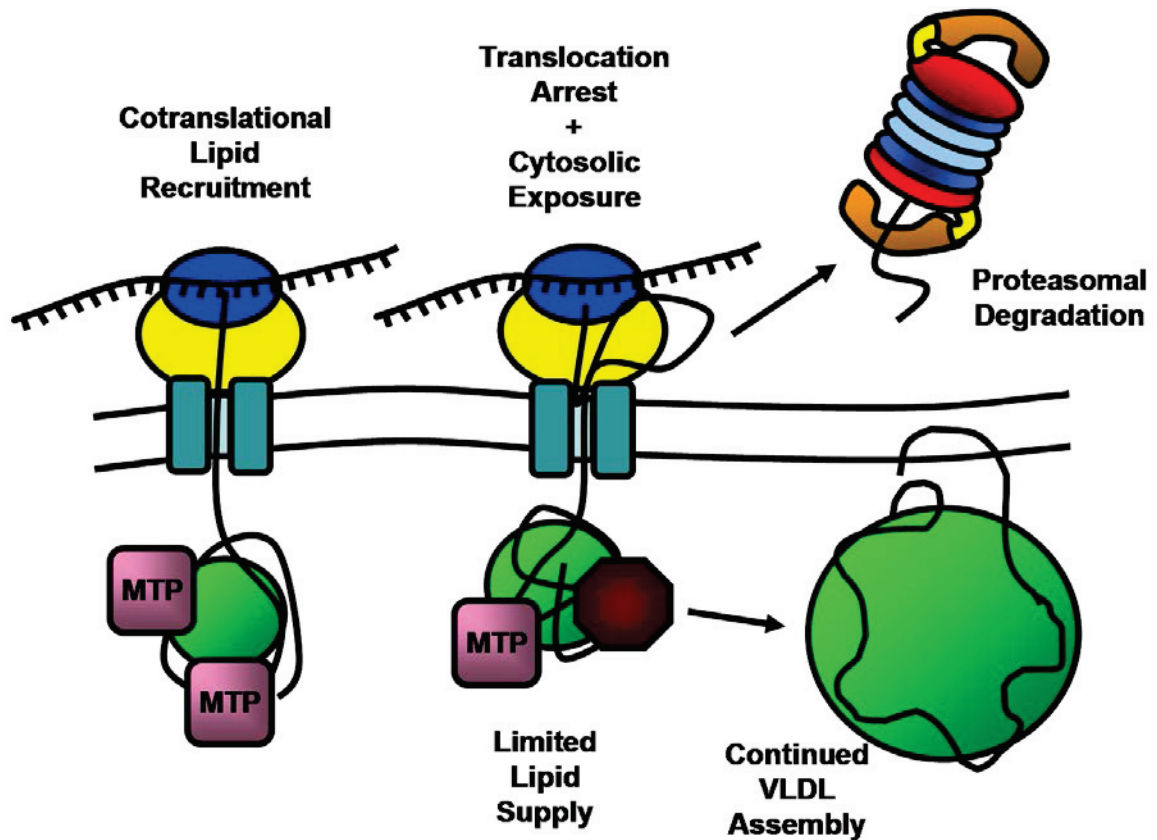
Figure 1.6. Cotranslational translocation arrest of poorly lipidated apoB-100. Lipid transfer onto apoB begins in a cotranslational, MTP-dependent manner. When lipid supply is inadequate, or MTP activity is decreased/inhibited, apoB can undergo translocation arrest. This refers to a scenario where translation continues, translocation temporarily stalls and newly-made apoB is exposed to the cytosol. Limited lipidation of apoB, translocation arrest and cytosolic exposure happen simultaneously, such that apoB assumes a "bitopic topology," relative to the ER membrane. The nascent apoB may either complete translation and continue VLDL assembly or be detected and degraded by the proteasome-dependent ERAD pathway. This quality control decision could be based on to what extent the translocation arrest is prolonged.

52

The ER chaperones BiP, calreticulin, PDI and Grp94 were found to interact with apoB regardless of apoB lipidation status (Linnik and Herscovitz, 1998). However, the ER-resident chaperone BiP was reported to increase binding to apoB when the interaction between nascent apoB and MTP is disrupted (Rutledge et al., 2009). Grp78 is considered by many to be the principal indicator of ER stress induction, as its levels increase incrementally via transcriptional upregulation. This occurs during the Unfolded Protein Response (UPR) in conjunction with increases in the severity and duration of stress. Mild to moderate levels of fatty acid-induced ER stress increase both Grp78 levels and VLDL assembly (Ota et al., 2008). Therefore, it seems that Grp78 levels may not regulate apoB ERAD but more likely that they contribute to stabilizing poorly lipidated apoB motifs prior to their removal from the ER. However, it appears that prolonged apoB-BiP binding may facilitate the ERAD of apoB (Rutledge et al., 2009). It is currently unclear whether apoB is a client of the *N*-glycan sugar timing system that governs glycoprotein quality control. While apoB does associate with calnexin and calreticulin, under "normal" conditions the difference between secretion and degradation of apoB is primarily decided by lipid availability. This does not preclude, however, the possibility that lipid-dependent folding events of the apoB protein might be connected to the glucose-trimming mechanism of quality control.

Overexpression of the ubiquitin ligase gp78 in HepG2 cells causes increased ubiquitination and degradation of apoB combined with a requisite decrease in secretion (Liang et al., 2003). ApoB has also been found to associate with Hrd1, as well as the purported retrotranslocation mediator Derlin-1 (Rutledge et al., 2009). Partially translated apoB was associated with both the Sec61 translocon and proteasome (Pariyarath et al.,

2001), suggesting that retrotranslocation of arrested apoB could occur through the translocon itself. Studies in HepG2 cells revealed that the apoB N-terminal region may not be retrotranslocated to the cytosol (Liang et al., 2000). Instead, the N-terminus could be cleaved and then either degraded or secreted (Du et al., 1994). An ER luminal protease named ER-60 was implicated in apoB ERAD (Qiu et al., 2004) and may participate in this process. Intriguingly, intra-membrane cleavage of ERAD substrates has emerged as a novel proteolytic mechanism, and may yet have relevance in apoB metabolism (Fleig et al., 2012).

It may be that apoB is targeted to ERAD by multiple ligases and by more than one means of escape from the ER. The possibility of E3 overlap and/or cooperativity is perhaps not surprising when considering the heterogeneity of apoB ERAD substrates. Full length apoB-100 is degraded by the proteasome, as are co-translational truncated apoB polypeptides of many different sizes. Thus, the cell may employ different machinery to detect and target these distinct apoB pools to ERAD. The specifics of apoB ubiquitination are poorly understood and warrant further investigation.

Inefficiently translocated apoB is associated with the cytosolic chaperones Hsp70 (Zhou et al., 1995) and Hsp90 (Gusarova et al., 2001). It appears that cytosolic heat shock proteins are necessary to support secretion and degradation. The fact that increased Hsp70 expression enhances apoB ubiquitination when the lipid supply is unaltered suggests a dependence of apoB on cytosolic stability during stages where it is subject to quality control mechanisms. Primary mouse hepatocytes deficient in the DNAj protein p58^{IPK} displayed very slow apoB degradation kinetics in response to an MTP inhibitor (Oyadomari et al., 2006). p58^{IPK} was suggested to recruit Hsp70 to the cytosolic side of

the Sec61 translocon to facilitate co-translational degradation of proteins, thus explaining the increase in substrates and marked sensitivity to ER stress in the p58^{IPK}-/- mice. However, another group reported that p58^{IPK}-/- related-ER stress resulted from the impairment of protein maturation capacity by losing the putative cochaperone function of p58^{IPK} within the ER lumen, and that p58^{IPK}-/- had no discernable role in protein translocation or degradation (Rutkowski et al., 2007). The exact requirement for p58^{IPK} during apoB-100 production is still unclear.

1.8 Statement of Hypotheses

Nascent apoB protein must pass through a loosely defined cellular quality control system in order to be secreted, or face intracellular degradation. I hypothesize that:

1) Hepatic cellular components of the ERAD system are required for the efficient disposal of apoB. Further, I propose that quality control components which mediate apoB-100 degradation can also regulate the assembly and secretion of VLDL.

2) If p97 facilitates the retrotranslocation of apoB during ERAD, then depletion of p97 in HepG2 cells will delay apoB turnover by the proteasome.

3) Knockdown of the ubiquitin ligase gp78 in HepG2 cells will impair the ubiquitination of apoB and allow the secretion of apoB previously targeted for the proteasome by ERAD.

4) Proteomic analysis of apoB-associating proteins following proteasome inhibition may reveal novel protein candidates with specific roles in apoB ERAD.

5)	Identification of target lysines for ubiquitination as well as ubiquitin chain linkages on apoB polypeptides will reveal novel details about apoB quality control in HepG2 cells.

CHAPTER 2 – MATERIALS AND METHODS

2.1 Materials and Methods

2.1.1 Cell Culture – Maintenance of Human Hepatoma HepG2 Cells

HepG2 cells were obtained from the American Type Culture Collection (ATCC, Manassis, VA; HB-8065). Cells were grown in 10 cm culture dishes (BD Biosciences, San Jose, CA) in Dulbecco's modified Eagle's medium (DMEM, Invitrogen Corp. Burlington, ON) supplemented with 2 mM glutamine and either 10% (v/v) FBS. Cells were subcultured by trypsinization (usually at 70-80% confluence) at a ratio of 1:2 or 1:3. For experiments, cells were either plated onto 10 cm dishes, 35 mm Primaria dishes, and 6 or 12 well tissue culture plates (for siRNA transfection). Unless indicated otherwise, cells were maintained in a 37°C humidified incubator with 5% CO_2 atmosphere.

2.1.2 Immunoblot Analysis

For analysis of protein expression, HepG2 cells were harvested in RIPA buffer [50 mM Tris-HCl, pH 8.0, 150 mM NaCl, 1 mM EDTA, 1% Triton X-100] containing 1% SDS. Total cell lysate, ranging from 1 μg to 25 μg was mixed with at least two volumes of 2x sample buffer [125 mM Tris-HCl pH, 4% (w/v) SDS, 20% (v/v) glycerol, 0.02% (w/v) Bromophenol blue] containing 10% (v/v) β-mercaptoethanol. Proteins were resolved on a 5% or 10% acrylamide gel by electrophoresis at 100 V for approximately 1.5 h or at a constant current of 6 mA per gel overnight (for Hoeffer SE600 gel units). Proteins were transferred to nitrocellulose membranes at 100V. For proteins > 200 kDa transfer was for 45 min, 30-200 kDa for 30 min and 20 min for < 30 kDa. For SE600 gels, transfer was for 5-6 h. Primary antibodies specifics are listed in Table 2.1. All secondary antibodies

were mouse- (AP308P) or rabbit-specific (AP132P) horse-radish peroxidase conjugates purchased from Chemicon Inc. (Temecula, CA). Immunoblots were developed using BM chemiluminescence from (11 500 694 001, Roche) , or with the super-sensitive ECL named Illumina Forte (WBLUF0100, Millipore) as needed.

2.1.3   RNA Interference-mediated Reduction of HepG2 Proteins

Non-targeting siRNA #1 (Dharmacon, Inc.), p97/VCP siRNA (si-p97, ID:119276, Ambion, Inc., Austin, TX), one of two different gp78-targeting duplexes (si-gp78, ID:9537, Ambion) or (si-gp78-A, HSS100448, Invitrogen). The Bag6 studies in Chapter 6 used a non-targeting duplex from Dharmacon (siGENOME Non-targeting siRNA #1 D-001210-01-20) along with a validated Bag6-targeting sequence (si-Bag6, ID:15018, Ambion). For each well of a 12-well plate, transfection medium was prepared containing either and siPORT NeoFX transfection reagent (Ambion) adjusted to a final volume of 100 μl using Opti-MEM I medium (Invitrogen). HepG2 cells, at 70-80% confluence, were trypsinized and resuspended in low serum growth medium (2% FBS in DMEM). Resuspended cells were added to the 100 μl transfection medium in each well to a final volume of 1 ml. The optimized final concentration of siRNA were the following: 50 nM for si-p97, 50 nM for si-gp78, 50 nM for si-gp78-A and 100 nM for si-Bag6. The transfection medium was removed and replaced with growth medium 24 hours after transfection and treatments/analyses were performed 72 hours following transfection. The efficiency of the siRNA knockdown was determined by immunoblotting of cell lysates for p97 or Bag6 protein and by quantitative polymerase chain reaction (qPCR) for the gp78 mRNA levels (see section 2.1.6).

Table 2.1. Summary of antibodies employed during this project. Abbreviations: Ms mono (mouse monoclonal), Rb poly (rabbit polyclonal), N/A (not applicable). All antibodies listed react with the human protein, but may also be applicable to other species.

Antibody	1° type	Dilution	Mg/lane	Company	Product Code	Storage (°C)
actin	Ms mono	1:2000	1-2	Millipore	MAB1501	-20
apoB	Ms mono	1:1000	~10	N/A	1D1	-80
Bag6	Ms poly	1:1000	5	Abcam	Ab 88292	-20
BiP/Grp78	Rb poly		2	Sigma	G 8918	-20
Calnexin	Rb poly	1:2000	2	Stressgen	SPA-865	-20
P97	Ms mono	1:500	1-2	Research Diagnostics	10R-P104A	+4
Hsp70	Ms mono	1:1000	2	Enzo	ADI-SPA-820	-20
PDI	Ms mono	1:1000	2	Millipore	SPA-891	-20
MTP	Rb poly	1:200-500	20	Novus	NBP1 26393	-20
HMGCoA Reductase	Rb poly	1:1000	20	Upstate	07-457	-20
PPARgam	Ms mono	N/A	N/A	Santa Cruz	Sc-7273	+4
PPARalpha	Ms mono	1:1000	N/A	Millipore	MAB3890	-20
SREBP1a	Ms mono	1:1000	N/A	Millipore	04-469	-20
apoAI	Ms mono	1:1000	2	N/A	N/A	+4
Phospho-ERK1/2	Rb poly	1:1000	20	Cell Signalling	9101	-20
Total ERK1/2	Rb poly	1:1000	20	Cell Signalling	9102	-20
Ubiquitin	Ms mono	1:1000	varies	Enzo	ADI-SPA-203	-20
HSF1	Rb poly	N/A	N/A	Enzo	ADI-SPA-901	-20

2.1.4 Metabolic Labelling

HepG2 cells were grown in 12 well plates to approximately 70-80% confluence. Cells were incubated in cysteine/methionine-free DMEM for 1 hour and then incubated for 1 to 3 hours, depending on the experiment, in cysteine/methionine-free DMEM containing 100 μCi of [^{35}S] cysteine/methionine (Express Protein Labeling Mix, Perkin-Elmer, Boston, MA). Where indicated, cells were supplemented with 360 μM oleic acid during the depletion, pulse and chase periods. U0126 or MG132 treatments (or DMSO vehicle) were carried through all incubations unless indicated otherwise. For pulse-chase analysis of apoB stability and secretion, the labeling medium was removed after a 1 h pulse and the monolayers were incubated with DMEM containing 2 mM methionine and 0.6 mM cysteine, plus any indicated supplements. Cells were harvested in 200 μl radioimmunoprecipitation assay (RIPA) buffer (50 mM Tris-HCl pH 8.0, 150 mM NaCl, 1 mM EDTA, 1% Triton X-100) containing 1% SDS. All buffers contain fresh PMSF and DTT [0.015% and 1 mM, respectively]. Cell lysates were then heated at approximately 85ºC for 15 minutes and subjected to rapid freeze-thaw cycle to improve solubility. One hundred μl of the cell lysate was removed into a new 1.5 ml tube and diluted to 0.1% SDS-RIPA with 900 μl 0% SDS-RIPA. Nine hundred μl of media was collected into tubes containing 100 μl 10x 0.1% SDS-RIPA buffer.

2.1.5 Immunoprecipitation of ApoB and ApoAI

One hundred μl of cell lysates in 1% SDS-RIPA buffer and medium samples were adjusted to 0.1% SDS-RIPA buffer (all solutions contained freshly added 0.015% PMSF and 1 mM DTT). ApoB protein was collected by overnight immunoprecipitation at 4ºC

with a goat polyclonal antibody to human apoB (AB742; Chemicon International, Inc., Temecula, CA) and the apoAI protein was collected with a polyclonal anti-apoAI antibody (AB740; Chemicon International, Inc., Temecula, CA). Proteins were recovered with Protein A Sepharose beads (Amersham Biosciences, Inc., Baie d'Urfé, QC). The bead/antibody complexes were collected by a 2 min spin at 13 K rpm in a benchtop microcentrifuge. The supernatant from the apoB IP was saved for additional analysis (ie- a control apoAI IP). Beads were washed 5 times in 1 ml 0.1% SDS-RIPA buffer followed by elution into 2X sample loading buffer containing β-mercaptoethanol. by heating at > 90ºC for 5 min. ApoB-100 was resolved by 5% SDS-PAGE (10% gels for apoAI) and visualized by autoradiography. Radioactivity was quantified from excised gel bands by liquid scintillation counting.

2.1.6 Quantitative PCR

RNA was isolated from HepG2 cells with the RNeasy Plus Mini Kit (#74134; Qiagen). Reverse transcription for each RNA was performed as follows: 2 μg RNA, 0.2 mM of each dNTP and 500 ng Oligo dT were brought to 12 μl with water and heated for 5 min at 65ºC and then cooled to 4ºC for 5 min. Added to this mixture were 10 mM DTT, 5x 1st strand buffer and 200 U Superscript II enzyme (18064-014, Invitrogen) for a final volume of 20 μl per tube. Samples were incubated at 42ºC for 50 min, 94ºC for 15 min and cooled to 4ºC. Each PCR reaction contained the following: 4 μl of the reverse transcriptase reaction, 10 μl Platinum SYBR Green Supermix-UDG (11733, Invitrogen), 250-300 nM of each the forward and reverse primers, and brought to 20 μl total volume with water. Reactions were heated at 50ºC for 2 min, 95ºC for 2 min and then subjected

to 40 cycles of: 95ºC 15 s, 65ºC 30 s, 72ºC 30 s. Knockdown efficiency (%) was determined by comparing the ΔCt values between treatments, normalized to cyclophilin as a housekeeping gene.

2.1.7 Digitonin Permeabilization of HepG2 Cells

HepG2 cells cultured in 12-well plates were washed twice with room temperature PBS and then incubated in 500 µl CSK buffer (10 mM PIPES pH 6.8, 0.3 M sucrose, 0.1 M KCl, 2.5 mM $MgCl_2$, 1 mM sodium-free EDTA) with or without digitonin (75 µg/ml) for 10 minutes on ice (Adeli et al., 1997b). The supernatant (containing the cytosol contents) was collected into a 1.5 ml tube. The monolayer was washed once with 500 µl CSK buffer which was removed and added to the first supernatant to complete the cytosol collection. The remaining monolayer was collected by lysis in 1% SDS-RIPA buffer.

2.1.8 Puromycin-synchronized Metabolic Labeling

Transfected HepG2 cells grown in a 12-well culture plate were incubated in depletion (cysteine/methionine free) media for 10 minutes and then treated with 10 µM puromycin (Sigma Aldrich, Saint Louis, MO) in depletion media for 10 minutes at 37ºC (Benoist and Grand-Perret, 1997). Cells were washed in depletion media three times on ice (30 minutes total) to remove the puromycin. Cells were incubated in pre-warmed [^{35}S]cysteine/methionine containing media (with or without 25 µM MG132, where indicated) at 37ºC, by floatation in a shallow water bath, for 5 minutes. Pulse media was discarded, followed by the addition of chase media containing an excess of freshly made cysteine and methionine (also with or without MG132 where indicated) for 5 minute time

points up to 20 minutes. Cell lysis and analysis of apoB-100 was performed as described in 2.1.5.

2.1.9   Sucrose Density Gradient Ultracentrifugation

Medium collected from HepG2 cells pulse-labelled with [^{35}S]cysteine/methionine was mixed with 1 µl/ml each of EDTA (pH 8.0) and 15% (w/v) PMSF for oxidation/protease. Medium samples were brought to 12.5% sucrose content. To prepare the gradients, PBS was added to the centrifuge tube, following by underlaying the sample in 12.5% sucrose, 25% sucrose and finally 47% sucrose. The ultracentrifugation was performed in an SW-60 rotor at 12ºC for 20 hours at 55000 rpm with the slow acceleration and no brake settings chosen. 13 fractions of 330 µl were collected. Immunoprecipitation, resolution and quantification of labeled apoB-100 was performed as described in sections 2.1.4 and 2.1.5.

2.1.10 Protease Protection Assay in Permeabilized HepG2 Cells

Trypsin was added from 5 mg/ml stock solution into CSK buffer and pre-chilled on ice. Transfected HepG2 cells were subjected to digitonin permeabilization (described above) to remove cytosol contents. The permeabilized cells were placed on ice and incubated for 30 minutes with the indicated concentrations of trypsin (Boehringer Mannheim, QC) in CSK buffer. An equal volume of CSK buffer containing 1 mg/ml soybean trypsin inhibitor (Boehringer Mannheim, QC) was then added to a final concentration of 500 µg/ml and incubated on ice for 10 min. Supernatant was collected and subjected to centrifugation for 3 minutes at 13,000 rpm on a benchtop microcentrifuge to collect cells

that were released from the plate during trypsinization. The remaining monolayer was harvested in 1% SDS-RIPA and combined with the cell pellet. Immunoprecipitation of apoB-100 and apoAI were performed as described in 2.2.7. Immunoblot analysis with an antibody specific to the N-terminus of calnexin (SPA-865; Stressgen Bioreagents, Ann Arbor, MI), situated inside the ER lumen, verified both trypsin activity (cleavage of the C-terminus decreases the MW of calnexin) and integrity of the microsomal membrane (the luminal N-terminus of calnexin is detectable and therefore was protected from trypsin).

2.1.11 Metabolic Labelling of Glycerolipids

HepG2 cells were pre-treated (16 hours) with 10 μM U0126 or were transfected with siRNA 72 prior to radiolabelling. Cells were labeled for two hours with 10 μCi/mL [2-^{3}H] glycerol (3.00 Ci/mmol; Amersham GE Healthcare) and incubated with 360 μM OA and/or 10 μM U0126 as indicated. Medium samples were collected and cell monolayers were harvested in PBS. Lipid extraction was performed using chloroform/methanol (2:1, by volume) and lipids were separated by thin-layer chromatography (TLC) on Silica Gel 60 pre-coated plates for TLC (20 x 20 cm, 250 μm thickness) using L-α-phosphatidylcholine (PC), cholesterol oleate and triolein as lipid standards (Wang et al., 1997). Plates were visualized with iodine, TG and PC bands were collected, and radioactivity was quantified by liquid scintillation counting.

2.1.12 Analysis of ApoB Ubiquitination

HepG2 cells were incubated in the absence or presence of 25 μM MG132 for the indicated time. Where indicated, cells were then permeabilized with digitonin and cytosol and cell fractions were collected. Cell lysates were adjusted to 0.1% SDS and apoB was collected by immunoprecipitation with polyclonal antibody to human apoB and protein A Sepharose, as described above. After several washes in RIPA buffer containing 0.1% SDS, the immunoprecipitant apoB was resolved by SDS-PAGE (5%), transferred to nitrocellulose and immunoblotted with monoclonal antibodies to apoB (1D1; Ottawa Heart Institute Research Corp., Ottawa, ON) or ubiquitin (SPA-203; Stressgen Bioreagents, Ann Arbor, MI).

2.1.13 Non-denaturing Immunoprecipitation (NDIP)

Near-confluent (70–80%) monolayers of HepG2 cells, grown on 10 cm dishes, were treated with or without 25 μM MG132 for 1 h and washed twice with PBS. Cells harvested in 1 ml of non-denaturing immunoprecipation (NDIP) buffer [50 mM Tris-HCl, pH 8.0, 50 mM NaCl, 5 mM EDTA, 20% sucrose, 1% Nonidet P40 (Roche Diagnostics)] containing freshly dissolved Complete® (Roche Diagnostics) protease inhibitor cocktail (1 pill per 40 ml NDIP buffer). Cells were scraped into 1.5 ml tubes and rocked for 1 h at 4°C for lysis and solubilization. Lysates were briefly centrifuged at 4°C to remove insoluble debris. The soluble cell lysate was transferred to a new tube. Pre-clearing of the lysate, 1 h incubation at 4°C with 20 μl non-immune goat serum and 40 μl protein A Sepharose was performed in some samples. Supernatants were transferred to a new tube containing 40 μl protein A Sepharose and 20 μl of either the anti-apoB, anti-apoAI or

non-immune goat serum. Immunoprecipitations were completed as described in section 2.1.5, but with NDIP buffer to wash the beads, followed by SDS-PAGE and either gel staining for LC-MS/MS (sections 2.1.15-17) and/or immunoblot analysis (section 2.1.2).

2.1.14 2-dimensional Gel Electrophoresis

Anti-apoB IPs were eluted into 1.5X isoelectric focusing (IEF) buffer, giving a final 1X IEF buffer content [7 M urea, 2 M thiourea, 4% (v/v) CHAPS, 0.5% (v/v) Pharmalyte]. The usual sample buffer for SDS-PAGE is incompatible with IEF, thus proteins were eluted from the beads by adding 1.5x IEF buffer. Final sample volume was 250 μl. Each sample contained 11 μl of 33% DTT (freshly prepared by dissolved approx. 10 mg DTT into the appropriate, calculated volume of IEF buffer). Samples were cleared by centrifugation for 5 min at 12K rpm in a benchtop microcentrifuge and distributed into the strip holder. 13 cm IPG strips (pH 3-10) were placed gel side down onto the sample, followed by the addition of 800 μl of mineral oil over the strip. The rehydration of the IEF was for 16 h at 20ºC on the Ettan IPGphor instrument (Amersham). IEF was performed at 50 uA/strip. Step 1 was performed at 500 V for 1 h, step 2 at 1000 V for 1 h and step 3 at 8000 V for 2.5 h. The final amperage for the IEF should be approximately 21,500 Vh. The reduction buffer [6 M urea, 2% (w/v) SDS, 0.375 M Tris-HCl pH 8.8 (from 1.5 M stock), 20% (v/v) glycerol, 130 mM DTT] and alkylation buffer [6 M urea, 2% (w/v) SDS, 0.375 M Tris-HCl pH 8.8 (from 1.5 M stock), 20% (v/v) glycerol, 135 mM iodoacetamide] were prepared fresh in 6 ml aliquots. Upon completion of the IEF, the excess mineral oil was gently drained from the gel strips. Strips were then incubated in reduction buffer at RT for 15 min. Strips were drained gel side up on paper towel and

then incubated with alkylation buffer for 15 min at RT. The strips were drained of the buffer and then rinsed with SDS-PAGE running buffer, carefully placed between the glass plates of a Hoeffer SE600 gel apparatus in direct contact with the lower (separating) gel. A small Teflon spacer was used to create a well for the protein ladder. A 2% agarose solution containing Bromophenol Blue in running buffer was heated and rapidly added around the strip and spacer and the agarose allowed to solidify. The spacer was removed, protein ladder added to the well and more agarose was overlaid. Proteins were resolved overnight at a constant current of 6 mA per gel. Subsequent steps include either immunoblotting or gel staining (sections 2.1.2 and 2.1.15, respectively).

2.1.15 Gel Staining

Gels were placed immediately in fixing solution [50% (v/v) anhydrous ethanol, 2% (v/v) phosphoric acid] for at least 3 h, then washed for 1 h in distilled water. Proteins were then stained for 3 days in staining solution [34% (v/v) methanol, 2% (v/v) phosphoric acid, 17% (w/v) ammonium sulphate] with Coomassie Brilliant Blue G250 added directly to staining container right before use (a scoop no larger than the top of a pen lid in size). Gels were stored at 4ºC in storage solution [0.375 M Tris-HCl pH 8.8 (from 1.5 M stock), 1% SDS (from 10% SDS stock)].

2.1.16 Identification of ApoB-associated Proteins by Functional Proteomics

HepG2 cells were treated for one hour with either DMSO (vehicle) or MG132 and then harvested in non-denaturing immunoprecipitation buffer (see section 2.1.13 for details). Samples of the IP eluates were resolved by large-scale SDS-PAGE (Hoeffer SE600) with

polyacrylamide ranging from 5% to 15%. Gels were stained (section 2.2.15) and bands of interest were determined by visual assessment of the differential staining patterns between -/+ MG132 samples. Bands were excised inside a sterile culture hood with a clean "kit" (disposable scalpels, Petri dishes, plastic squeeze-bulbs, bottle of MilliQ, forceps and Eppendorf tubes). The use of clean equipment along with multiple MilliQ water rinses of the excised gel slices inside the final sample tube greatly reduce contamination with unwanted peptides such as β-keratin.

2.1.17 Protein Identification by Mass Spectrometry

Identification of unknown protein bands by mass spectrometry was performed by Elden Rowland at the DalGen Proteomics Facility in the Atlantic Research Centre. LC-MS/MS was performed with a nanoflow Ultimate system (LC Packings) interfaced with the nanoflow electrospray ionization (ESI) of a hybrid triple quadrupole linear ion trap (Qtrap) mass spectrometer (Applied Biosystems). Samples were sprayed through a distal coated fused silica needle which had a 75 μM ID with a 15 μM ID tip (New Objectives). Solvent A was 0.1% (v/v) formic acid in water/acetonitrile (98:2) and solvent B was 0.1% (v/v) formic acid in acetonitrile/water (98:2). Excised protein bands were digested with sequencing-grade trypsin (Promega) for 7.5 h at 37ºC. Tryptic peptides were resuspended in 30 μl of 5% acetonitrile and 0.5% formic acid and then injected onto an Onyx monolithic C18 capillary column (0.1 x 150 mm, Phenomenex). The proteolytic fragments were eluted by 3-30% solvent B gradient over a 35 minute period at a 1 μl/minute flow rate. Spectra were obtained utilizing the Information Dependent

Acquisition mode. Peptides were identified using Mascot and search of the SwissProt database (http://web.expasy.org/docs/swiss-prot_guideline.html).

CHAPTER 3 – THE AAA-ATPASE P97 FACILITATES DEGRADATION OF APOLIPOPROTEIN B BY THE UBIQUITIN-PROTEASOME PATHWAY

3.1 Introduction

3.1.1 Statement About Published Works

This research was originally published in Journal of Lipid Research. Fisher, EA, Lapierre, LR, Junkins, RD and McLeod, RS. The AAA-ATPase p97 facilitates degradation of apolipoprotein B by the ubiquitin-proteasome pathway. *J. Lipid Res*. 2008; 49:2149-2160. © the American Society for Biochemistry and Molecular Biology. This Chapter contains the abstract, results and discussion of the published manuscript. Louis Lapierre, a previous PhD student in the McLeod group, performed experiments presented in Fig 3.1, 3.2, 3.3A and B. I performed all other published experiments and revised the existing manuscript to include new data and writing. Rob Junkins also performed several p97 knockdown experiments during his Honours project.

3.1.2 Abstract

The ATPase associated with various cellular activities (AAA-ATPase) p97 (p97) has been implicated in the retrotranslocation of target proteins for delivery to the cytosolic proteasome during endoplasmic reticulum-associated degradation (ERAD). Apolipoprotein B-100 (apoB-100) is an ERAD substrate in liver cells, including the human hepatoma, HepG2. We studied the potential role of p97 in the ERAD of apoB-100 in HepG2 cells using cell permeabilization, coimmunoprecipitation, and gene silencing. Degradation was abolished when HepG2 cytosol was removed by digitonin permeabilization, and treatment of intact cells with the proteasome inhibitor MG132

caused accumulation of ubiquitinated apoB protein in the cytosol. Cross-linking of intact cells with the thiol-cleavable agent dithiobis(succinimidylpropionate) (DSP), as well as nondenaturing immunoprecipitation, demonstrated an interaction between p97 and intracellular apoB. Small interfering ribonucleic acid (siRNA)-mediated reduction of p97 protein increased the intracellular levels of newly synthesized apoB-100, predominantly because of a decrease in the turnover of newly synthesized apoB-100 protein. However, although the posttranslational degradation of newly synthesized apoB-100 was delayed by p97 knockdown, secretion of apoB-100 was not affected. Knockdown of p97 also impaired the release of apoB-100 and polyubiquitinated apoB into the cytosol. In summary, our results suggest that retrotranslocation and proteasomal degradation of apoB-100 can be dissociated in HepG2 cells, and that the AAA-ATPase p97 is involved in the removal of full-length apoB from the biosynthetic pathway to the cytosolic proteasome.

3.2 Results

3.2.1 Intracellular Degradation of ApoB-100 is Markedly Reduced in Permeabilized HepG2 cells

To evaluate the role of cytosolic components in apoB degradation, we compared the effect of MG132 and digitonin permeabilization on the stability of intracellular apoB. In pulse-chase experiments (Figure 3.1A and B, Intact), apoB-100 radiolabel was degraded with a half-life of approximately 2 h. When the proteasome inhibitor MG132 (25 μM) was included in the chase medium, apoB-100 half-life was extended to approximately 4 h (Figure 3.1A and B, Intact/MG132) although most of the effect of
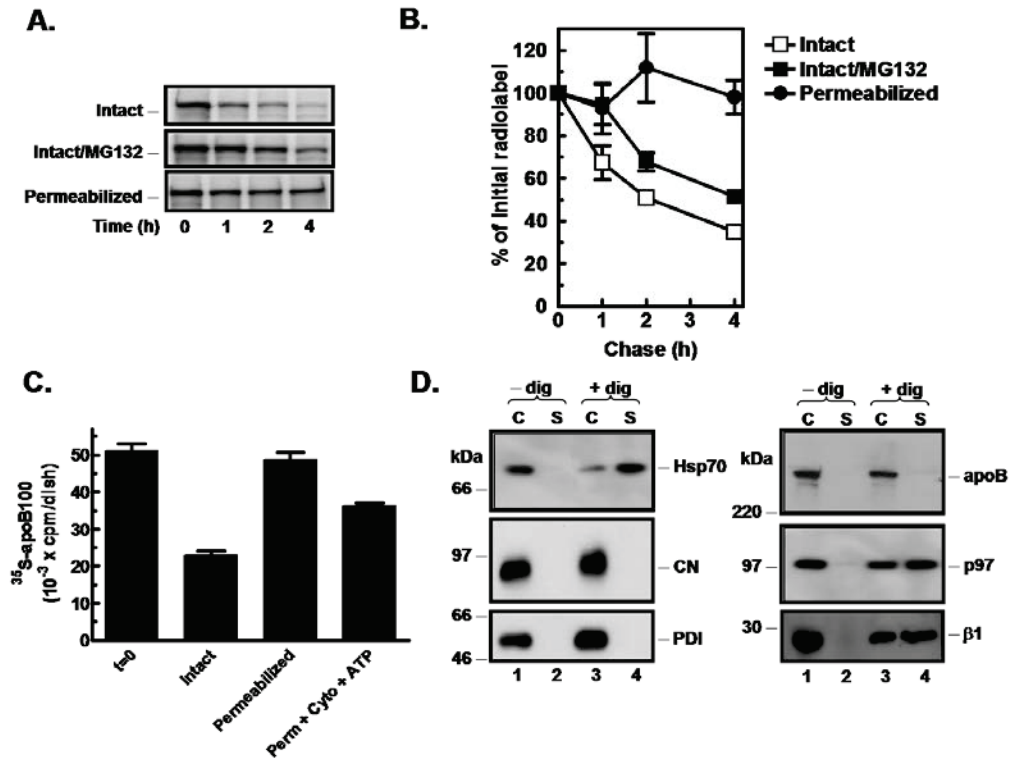
Figure 3.1. Permeabilization of HepG2 cells markedly decreases the degradation of apoB-100. HepG2 monolayers were pretreated for 1 h with or without the proteasome inhibitor MG132 (25 µM) and pulse-labeled for 1 h with [^{35}S]methionine/cysteine (200 µCi/ml). After labeling, one set of dishes was permeabilized with digitonin while the remaining dishes were left intact. The supernatant was removed and replaced with medium with or without MG132 for chase of up to 4 h. At each time point, cells were collected by lysis into 1% SDS-RIPA and apoB-100 was immunoprecipitated and visualized by SDS-PAGE with autoradiography. **A**, Autoradiographs of digitonin-permeabilized cells (*Permeabilized*) and intact cells treated with (*Intact/MG132*) or without (*Intact*) proteasome inhibitor. **B**, Radioactivity in apoB-100 was determined by liquid scintillation counting of the excised band, expressed as percent of the radiolabel at the initiation of the chase. Data points represent the mean (± S.D.) of three independent experiments. □, intact; ■, intact/MG132; ●, permeabilized. **C**, Replicate dishes of HepG2 cells were pulse-labeled as described above. During the 2 h chase, intact or permeabilized cells were incubated with DMEM or DMEM containing HepG2 cytosol (0.7 mg/ml) and an ATP-generating cocktail (1 mM ATP, 5 mM creatine phosphate, 5 mM MgCl$_2$ and 100 µg/ml creatine kinase). ApoB-100 radioactivity was determined as described for **B**. Each bar represents the mean ± S.D. (n=3). **D**, Western blot analysis of cell (*C*) and supernatant (*S*, cytosol) fractions of HepG2 cells following digitonin permeabilization. Cells were treated with or without digitonin and the cell and supernatant fractions were collected. Aliquots of cell and supernatant protein were resolved by 3-15% gradient SDS-PAGE and transferred to nitrocellulose. Membranes were incubated with the indicated antibody and visualized by enhanced chemiluminescence. *dig*, digitonin; *p97*, AAA-ATPase p97; *β1*, 20S proteasome β1 subunit, *Hsp70*, cytosolic heat shock protein 70 kDa; *CN*, calnexin; *PDI*, protein disulfide isomerase.

MG132 was evident only during the first hour of chase. In contrast, permeabilization of the HepG2 cells following the pulse essentially abolished the post-translational degradation of apoB-100 (Figure 3.1A and B, Permeabilized). These results are consistent with the role of the cytosolic proteasome in the early post-translational degradation of apoB-100 in the HepG2 cell. Indeed, degradation could be partially reconstituted by addition of freshly prepared HepG2 cytosol (0.7 mg/ml in DMEM) and an ATP generating system (Gusarova et al., 2001) to the permeabilized cells (Figure 3.1C). Nevertheless, non-proteasomal mechanisms of degradation are also involved, since proteasome inhibition with MG132 was not sufficient to reduce apoB-100 degradation beyond 1 h of chase.

3.2.3 Distribution of Proteins Involved in ER-associated Degradation

We then examined the distribution of known ERAD factors in the membranes and cytosol of HepG2 cells, to identify candidate proteins that may be involved in the retro-translocation and delivery of apoB to the cytosol for degradation. When HepG2 cells were permeabilized with digitonin, essentially all of the cytosolic Hsp70 was released (Figure 3.1D), whereas the ER-resident protein disulfide isomerase (PDI) and calnexin (CN) remained associated with the cell membranes. Similarly, apoB-100 was found almost exclusively with the cell membrane fraction although a small amount of apoB-100 could be detected in the cytosol in longer exposures. In contrast, we found that the AAA-ATPase p97 (p97) and components of the 20S subunit of the proteasome (β1, Figure 3.1D) were equally distributed in the cell and cytosol fractions. Since an interaction between p97 and other ERAD substrates has been implicated in retrotranslocation to the

cytosol (Ye et al., 2003) we examined this possibility for apoB-100 using crosslinking and non-denaturing immunoprecipitation.

3.2.4 Intracellular ApoB-100 is in Complex with AAA-ATPase p97

Potential interacting partners of apoB-100 were captured using a membrane permeable, thiol-cleavable crosslinking agent, DSP. When intact HepG2 cells were incubated with DSP, p97 was found in complex with apoB by immunoprecipitation. ApoB immunoprecipitates from cells treated with DSP were resolved on reducing gels (Figure 3.2A) and contained both apoB-100 (lane 4) and p97 (lane 8). We observed p97 as both monomer and a higher molecular weight form (~300 kDa) despite the reducing conditions. Neither apoB nor p97 was found in immunocomplexes prepared using non-immune serum (lanes 1, 2, 5, and 6). In addition, non-denaturing immunoprecipitation (Figure 3.2B) was able to capture p97 in association with apoB (lanes 5 and 6) but not with apoAI (lanes 3 and 4). The interaction with apoB was also increased with proteasome inhibition (compare lane 6 to lane 5). These studies suggested that apoB may be a substrate for p97-mediated retro-translocation.

3.2.5 Ubiquitinated ApoB Accumulates in the Cytosol of MG132-Treated HepG2 Cells

We next sought to dissociate proteasomal degradation from retro-translocation of apoB-100 as a first step towards the identification of cytosolic components involved in apoB retro-translocation. HepG2 cells were treated with MG132 (25 μM) to inhibit proteasomal proteolysis and ubiquitinated apoB-100 in the cytosol and organelle-
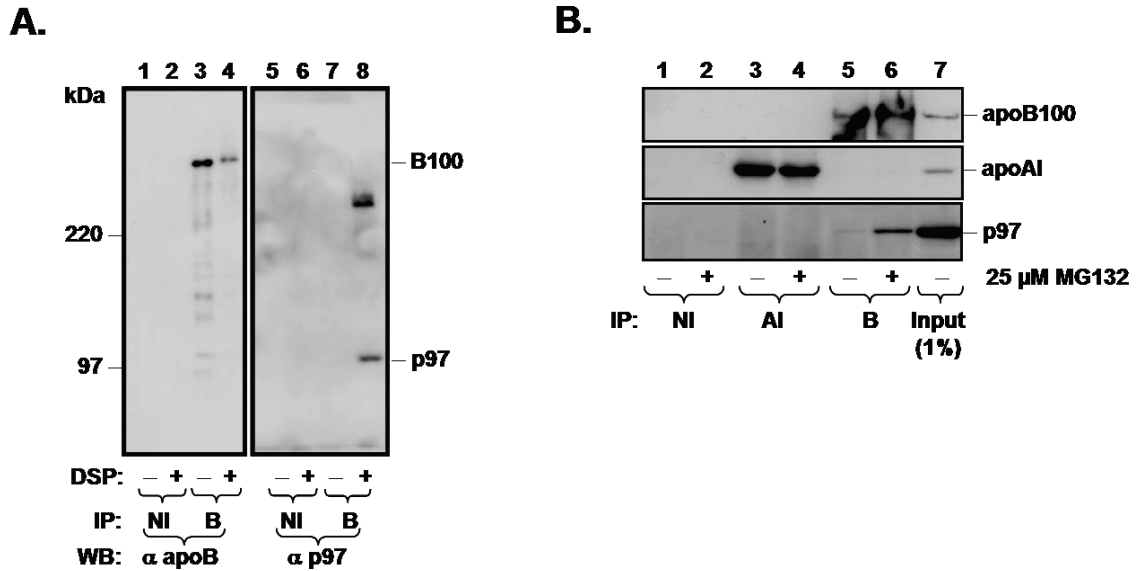
Figure 3.2. AAA-ATPase p97 is associated with apoB-100 in intact HepG2 cells. *A*, HepG2 cells were incubated with or without 2.5 mM of the membrane-permeable, thiol-cleavable crosslinking agent DSP (dithiobis[sulfosuccinimidylpropionate]) for 1 h at room temperature. Tris-HCl, pH 7.4 was added to 50 mM and the incubation was continued for an additional 15 min. The cells were then lysed in 1% SDS buffer and subjected to immunoprecipitation (**IP**) with polyclonal anti-apoB serum (**B**) or with non-immune serum (**NI**). Immunocomplexes were then released into reducing (100 mM DTT) sample buffer and separated on 5% SDS-PAGE gels. Resolved proteins were transferred to nitrocellulose and visualized using monoclonal antibodies to apoB (*left panel*) or p97 (*right panel*) with chemiluminescence detection. *B*, HepG2 cells were incubated with or without 25 μM MG132 for 1 h and then lysed with 1% Nonidet P40. Lysates were cleared by centrifugation and aliquots were subjected to immunoprecipitation with non-immune serum (**NI**), anti-apoAI (**AI**) or anti-apoB (**B**) antiserum. Immunoprecipitates or input lysate were resolved by SDS-PAGE, transferred to nitrocellulose and visualized by immunoblotting with the indicated antibodies and chemiluminescence detection.

associated fraction (*i.e.* that remaining with the monolayer following permeabilization) were recovered by immunoprecipitation and visualized by immunoblotting. In order to visualize cell and cytosol fractions on the same blots, all of the cytosol (S) and approximately 10% of the cell lysate (C) was loaded onto the gel. A small amount of cytosolic apoB-100 could be detected in cells without MG132 treatment (Figure 3.3A, lane 7) and treatment with MG132 increased cytosolic apoB-100 (Figure 3.3A, lane 8). We estimate that the amount of apoB-100 in the cytosolic fraction is ~1% of the total cellular apoB without MG132 and perhaps as high as ~5% of cellular apoB in the presence of MG132. This is consistent with the observations of Liao and colleagues (Liao et al., 2003). Cytosolic and organelle-associated apoB were both polyubiquitinated in MG132-treated cells (Figure 3.3B, lanes 8 and 6, respectively) but polyubiquitinated species were not detectable in cells without MG132 because of the very active proteasomal degradation of apoB-100 in HepG2 cells (Figure 3.3B, lanes 5 and 7). Most of the polyubiquitinated apoB species in MG132-treated cells were in the cytosol, even though this is a much smaller portion of the total apoB. Polyubiquitinated species of various sizes were observed as a smear on the gel because of the presence of partial apoB chains, possibly representing co-translational degradation products (Fisher and Ginsberg, 2002; Liang et al., 2003). Control immunoprecipitations were used to rule out the possibility that the ubiquitin-reactive material could be due to non-specific precipitation of unrelated ubiquitinated proteins (Figure 3.3A and 3.3B, lanes 1 to 4). The presence of full length apoB-100 in the cytosol suggested that, in the absence of proteolysis by the proteasome, some apoB can be extracted from the endomembrane system into the cytosol.
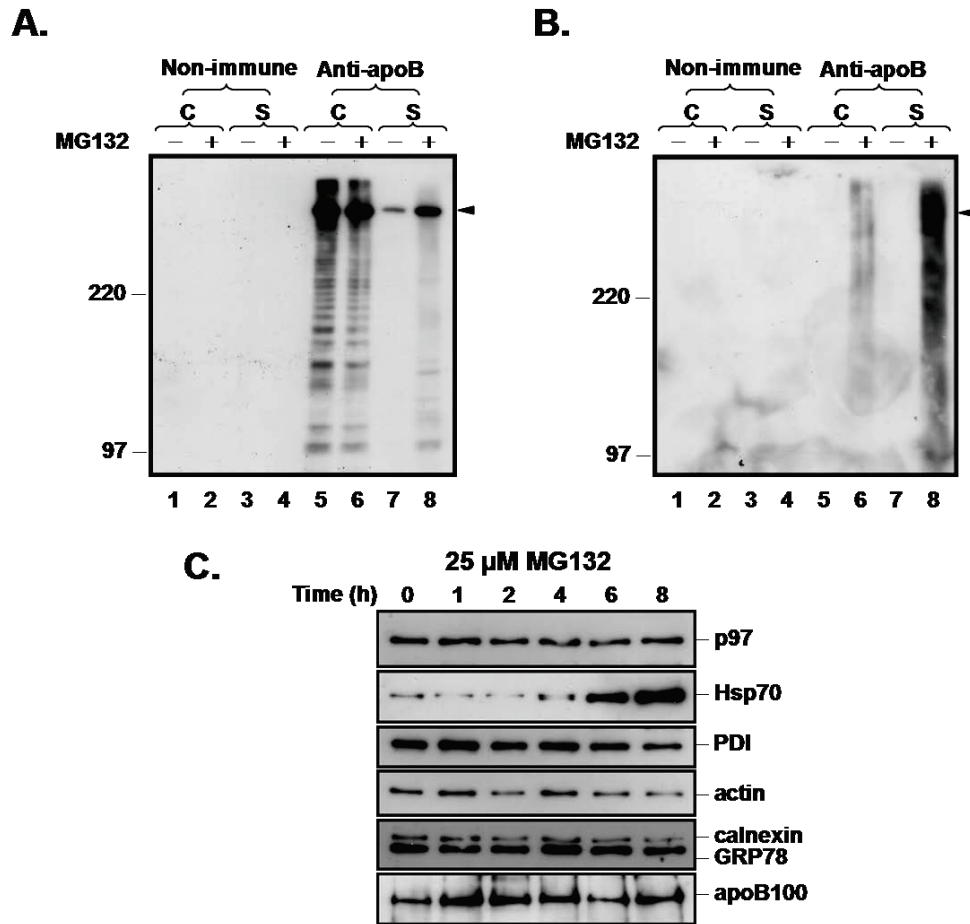
Figure 3.3. Ubiquitinated apoB-100 accumulates in the cytosol of cells treated with MG132. *A,* HepG2 cells were incubated with or without MG132 (25 μM) for 1 h and the monolayers were then permeabilized with digitonin as described in Chapter 2. The resulting permeabilized cell (**C**) and supernatant (**S**, cytosol) fractions were collected and immunoprecipitates were prepared with either polyclonal anti-apoB or non-immune goat serum. Aliquots of each immunocomplex were resolved by 5% SDS-PAGE and, following transfer of the proteins to nitrocellulose, human apoB was revealed by western blot analysis. *Arrowhead* indicates the mobility of full-length apoB-100. *B,* Aliquots of immunoprecipitates prepared as in *A* were visualized with monoclonal anti-ubiquitin antibody. *C,* HepG2 monolayers were treated with 25 μM MG132 for up to 8 h and cells were collected by lysis. Equal amounts of total cell protein were fractionated on SDS-PAGE gels and probed for the indicated protein. *GRP78,* glucose regulated protein.

To assess the lipid content of cytosolic apoB, we characterized the secreted and cytosolic apoB proteins by density gradient ultracentrifugation (Figure 3.4). Secreted apoB from HepG2 cells was found primarily in the low density lipoprotein fractions of the gradient, as shown previously (Boren et al., 1993). Cytosolic apoB-100 was found only near the bottom of the density gradient, in fractions that also contain proteins associated with little or no lipid such as Hsp70. This observation suggested that cytosolic apoB is lipid-poor, lipid-free or associated with other proteins that increase its density by decreasing the lipid:protein ratio.

To explore the changes in the expression of ERAD-associated proteins caused by proteasome inhibition, we used a time course of MG132 treatment and monitored the levels of proteins of the unfolded protein response (UPR) and cytosolic heat shock response. HepG2 cells were incubated with 25 μM MG132 for up to 8 hours and proteins were revealed by western blotting (Figure 3.3C). Substantial accumulation of apoB-100 was observed after 1-2 h, and large increases in Hsp70 were observed after 6-8 h. No changes in p97, actin, calnexin or PDI were observed during the 8 h experiment, while GRP78 increased modestly beginning at about 4 h. Thus, the most profound changes were in the cytosolic stress marker protein and this is consistent with previous observations in this cell model (Liao et al., 2006). However, after 1 h there were no profound changes in any protein except apoB, suggesting that apoB accumulation resulted from a block in its normal rate of turnover, rather than a generalized stress response to the MG132.
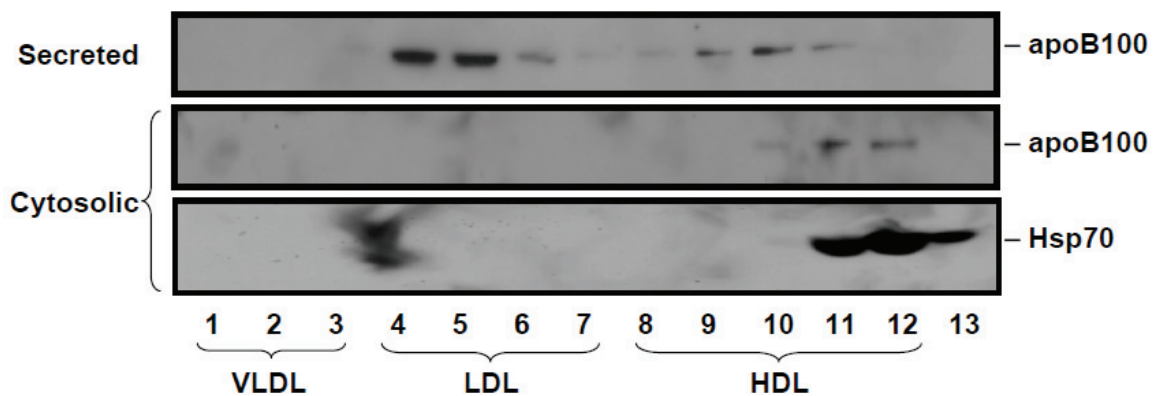
Figure 3.4. Cytosolic apoB100 is lipid-poor. HepG2 cells were incubated with 25 μM MG132 for 1 h. The medium was collected and the cells were permeabilized with digitonin. Medium was collected during the MG132 treatment (*Secreted*) and during the permeabilization (*Cytosolic*) and subjected to sucrose density gradient ultracentrifugation. Gradients were fractionated and apoB-100 in the individual fractions was visualized by western blot analysis.

3.2.6 Reduction of Cellular p97 Increases Cellular ApoB-100

If p97 is necessary, or is part of a complex that is necessary, for retro-translocation of apoB, a reduction of HepG2 p97 would be expected to impair the retro-translocation process and decrease proteasomal degradation of apoB-100. A knockdown approach was used to reduce the level of p97, using double stranded siRNA targeting the p97 transcript. HepG2 cells were transfected with non-targeting siRNA (NT) or siRNA targeting p97 (si-p97), each at a concentration of 50 nM. As shown in Figure 3.5A, 72 h after transfection there was a decrease in cellular p97 in cells transfected with the targeting siRNA (24 ± 9% of mock, n=8) but not in cells transfected with the non-targeting siRNA (99 ± 16 % of mock, n=6). In contrast to the observations in cells treated with MG132 (Figure 3.3C), there were no increases in Hsp70 with p97 knockdown (Figure 3.5A), and PDI and calnexin were also unaffected. In fact, the levels of Hsp70 were decreased compared to the non-targeting siRNA. GRP78 was increased by approximately 35%, suggesting that the effects of p97 knockdown modestly affected this luminal chaperone.

To evaluate the effect of reduced levels of p97 on apoB metabolism, transfected HepG2 cells were analysed by metabolic radiolabeling. In cells transfected with siRNA for p97 (Figure 3.5B), accumulation of radiolabeled apoB-100 increased approximately 2-fold, compared to the non-targeting control siRNA (NT), while the apoAI was not affected. These studies suggested that reduction of cellular p97 decreased the turnover of newly synthesized apoB-100.

Pulse-chase experiments were then performed to directly assess the effect of reduced p97 on the post-translational stability of apoB-100. Compared to non-targeting
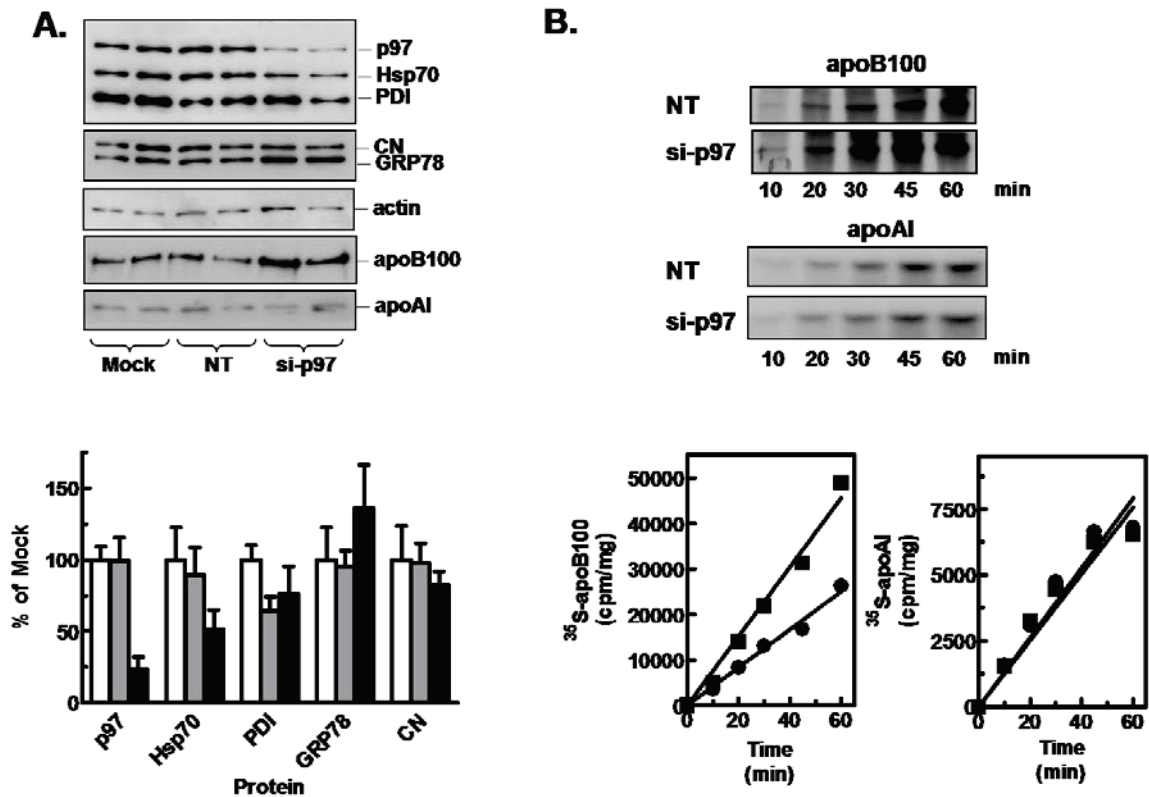
Figure 3.5. siRNA-mediated reduction of cellular p97 increases HepG2 apoB-100 biosynthesis. *A*, Monolayers of HepG2 cells were transfected with non-targeting (**NT, *grey bars***), p97-targeted siRNA (**si-p97,** *black bars*), or mock transfected (**Mock,** *white bars*). Seventy-two hours post-transfection, cells were collected and p97 and proteins indicated were visualized by western blot analysis. Duplicate wells are shown from a representative experiment, repeated three times. Individual proteins were quantified by scanning densitometry and are presented as percentage of the mock-transfected control. Each bar represents mean ± S.D. (n = 6). *B*, Biosynthesis of apoB-100 and apoAI in siRNA-transfected HepG2 cells. Seventy-two hours following transfection with either non-targeting (**NT, ●**) or p97-targeting (**si-p97, ■**) siRNA, cells were pulse-labeled with 100 μCi of [^{35}S] methionine/cysteine for up to 60 minutes. ApoB and apoAI proteins were immunoprecipitated from cell lysates, resolved by SDS-PAGE and visualized by autoradiography (*top panels*). Radioactivity in each protein band was quantified by scintillation counting and normalized for cell protein (*lower panels*). The figure shows a representative experiment, which was repeated three times. There were no differences in cell protein between the NT and si-p97 treated cells.

81

siRNA (NT), treatment with p97 siRNA (si-p97) decreased the post-translational degradation of apoB-100 during the first hour of chase (Figure 3.6A) but had no effect on either stability or secretion of apoA-I (Figure 3.6B). In spite of the decrease in degradation, there was no effect on apoB-100 secretion.

The effects of p97 knockdown on apoB-100 metabolism were not the same as those observed for a UPR resulting from ER stress. The pattern of chaperone protein expression was clearly different with p97 knockdown (Figure 3.5A) and MG132 treatment (Figure 3.3C). Furthermore, since the levels of apoB increased with p97 knockdown but decreased when ER stress was induced using DTT (Figure 3.7A) or tunicamycin (Figure 3.7B), the accumulation of apoB was not likely to be the result of a classical UPR.

3.2.7 Reduction of Cellular p97 Reduces Cytosolic ApoB Accumulation and Diminishes the Protective Effect of MG132

To further characterize the role of p97 in apoB degradation, we examined the effect of p97 reduction on the accumulation of polyubiquitinated cytosolic apoB. HepG2 cells were transfected with NT or si-p97 siRNA and permeabilized 72 h thereafter with digitonin. Immunoblotting of cell lysate (C) and cytosolic (S) fractions for calnexin (CN) and GRP78 (Figure 3.8A, lower panel) indicated that the cytosol fractions were free of ER contents. Immunoprecipitation of apoB and immunoblotting showed that MG132 treatment of cells transfected with the NT siRNA caused the expected increase in cell-associated (Figure 3.8A, lane 2 vs lane 1) and cytosolic apoB-100 (Figure 3.8A, lane 4 vs lane 3). In contrast, the cells transfected with si-p97 siRNA were resistant to the effects
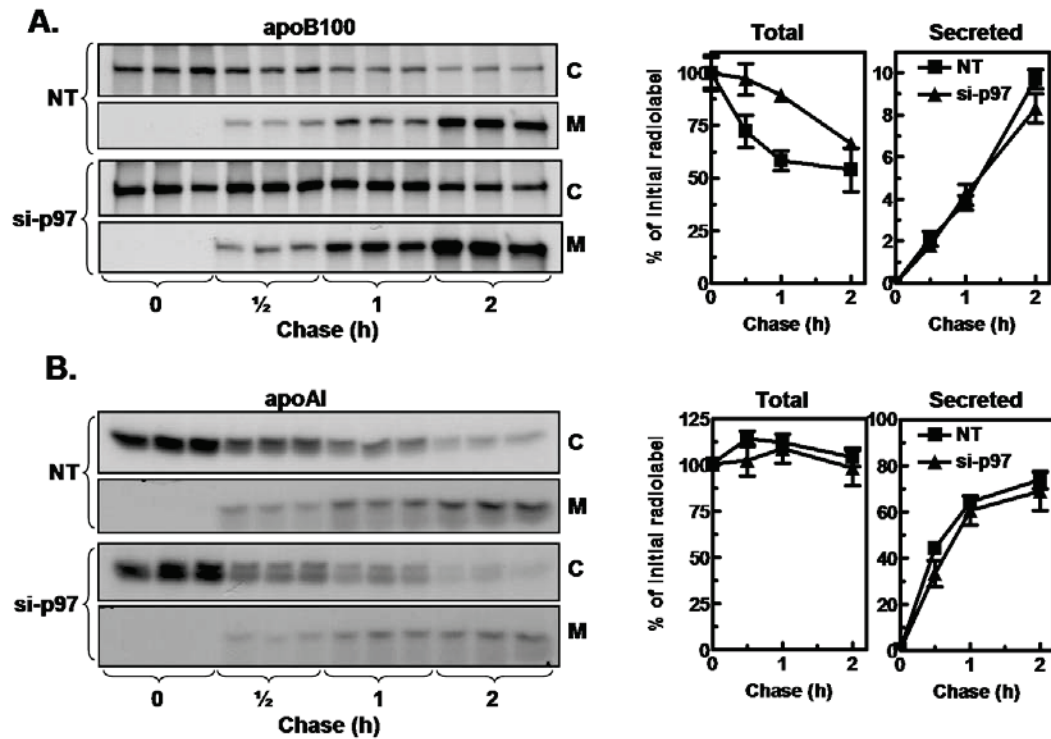
Figure 3.6. siRNA-mediated reduction of cellular p97 increases HepG2 apoB-100 stability but not its secretion efficiency. Autoradiographs and quantitation of apoB-100 (*A*) or apoA-I (*B*) in cells and medium by pulse-chase analysis. Seventy-two hours following transfection, HepG2 monolayers were labeled with [^{35}S]methionine/cysteine for 1 h and then chased for up to 2 h as described in Chapter 2. At each time point apoB or apoAI was recovered from cells and medium by immunoprecipitation and visualized by autoradiography. Cellular decay (*Total* = cells plus medium) and secretion of apolipoprotein radioactivity are expressed as percent of initial radiolabel. Autoradiographs and curves depict triplicate wells from a representative experiment which was repeated three times.
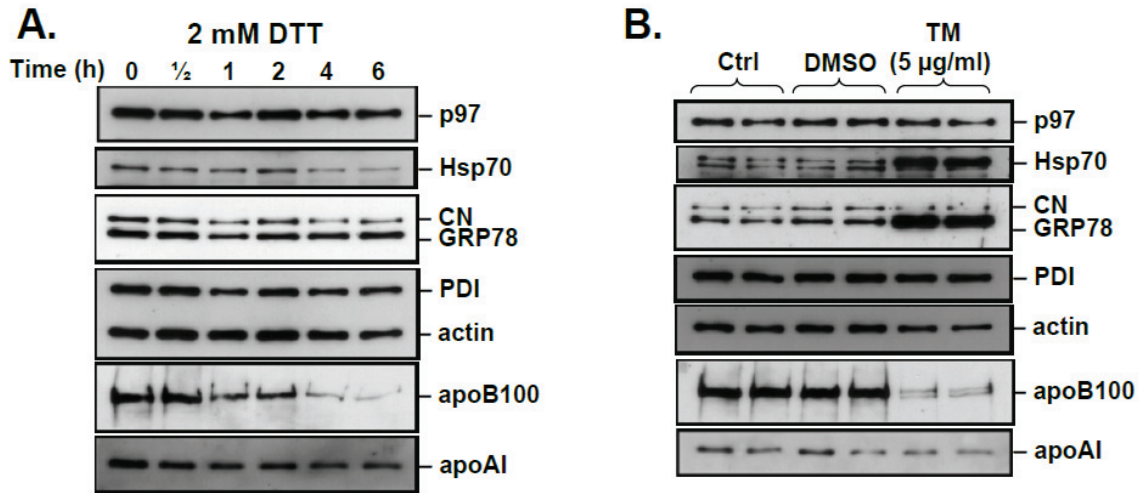
Figure 3.7. Tunicamycin and DTT effects on apoB100 and ER stress marker proteins in HepG2 cells. HepG2 cells were grown to 70-80% confluence in 12 well plates and changed to medium containing 2 mM DTT or 5 µg/ml tunicamycin (*TM*). **A,** Following DTT addition, the cell monolayers were collected after 0 to 6 h in lysis buffer. The total protein was quantified and equal amounts of protein were loaded in each lane of SDS-PAGE gels for western blot analysis for the indicated proteins. **B,** After addition of tunicamycin (*TM*) or vehicle control (*DMSO*), cells were incubated for 16 h, collected by lysis and analysed by western blotting.

of MG132 on apoB-100 levels in the lysate (Figure 3.8A, lane 6 vs lane 5) and in the cytosol (Figure 3.8A, lane 8 vs lane 7). Cell lysate apoB-100 mass was not markedly increased after reduction of p97 (Figure 3.8A), even though newly synthesized apoB-100 was increased (Figure 3.5B), and in some immunoblotting experiments apoB-100 mass increases were evident (Figure 3.5A). Nevertheless, treatment with si-p97 siRNA consistently prevented the accumulation of polyubiquitinated apoB species in the cytosol with MG132 treatment (Figure 3.8B, lane 8 vs lane 4), reflecting the decrease in cytosolic apoB-100. However, polyubiquitinated apoB species were detectable in the cell lysate fractions of si-p97 cells with MG132 treatment (Figure 3.8B, lane 2 vs lane 6). Taken together, these results suggest that p97 knockdown and MG132 treatment affect the same degradation pathway and that p97 is required for the movement of apoB from the organelle fraction into the cytosol for proteasomal degradation.

3.3 Discussion

The present work has evaluated the role of p97 in the delivery of apoB-100 to the cytosolic proteasome for degradation. Digitonin-permeabilization of HepG2 cells indicated that degradation of newly synthesized apoB-100 was minimal if cytosolic components were removed, an observation that confirms a previous report (Sakata et al., 1999). This suggests that cytosolic proteasomal proteolysis is the dominant form of apoB degradation in this cell line. ApoB-100 degradation was partially reconstituted by adding back HepG2 cytosol, indicating that cytosolic components are central to this degradation, even though some elements of the degradation pathway (p97, proteasome core components) remain associated with the cellular membrane fraction. Nevertheless,
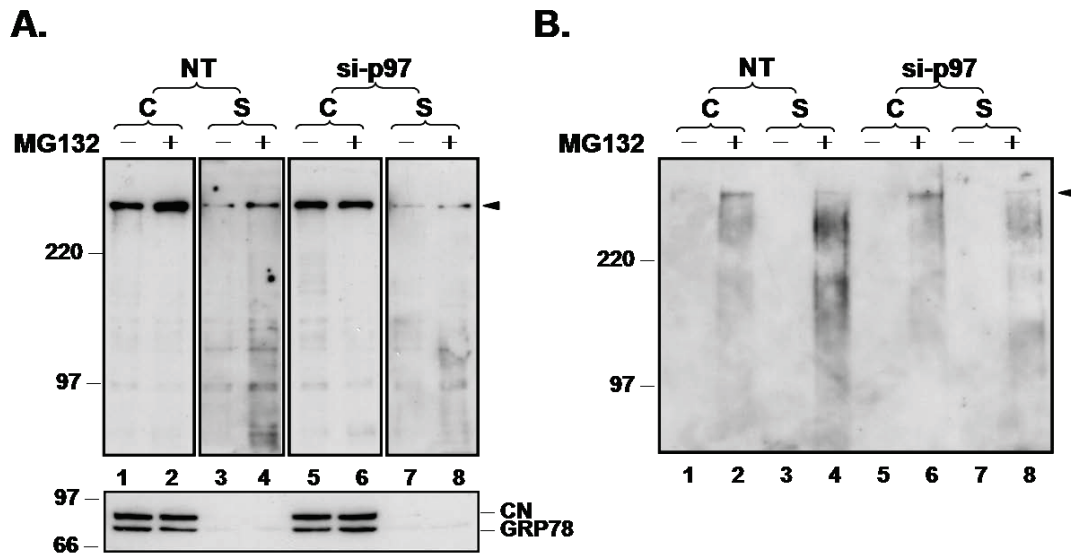
Figure 3.8. siRNA-mediated reduction of cellular p97 affects apoB proteasomal degradation by decreasing the release of apoB into the cytosol. *A*, Western blot analysis of cytosolic apoB-100 after siRNA transfection. HepG2 cells were transfected with non-targeting (lanes 1-4) or p97-targeting siRNAs (lanes 5-8). Seventy-two hours following transfection, cells were incubated with MG132 (25 μM) for 1 h, permeabilized with digitonin and cellular (**C**) and cytosolic (**S**) proteins were collected. Immunoprecipitates were prepared with polyclonal anti-apoB serum. Equal amounts of each immunocomplex were resolved by 5% SDS-PAGE and, following transfer of the proteins to nitrocellulose, human apoB was revealed by western blot analysis. Cellular panels are 1 second exposures, cytosol panels are 60 second exposures of the same membrane. *Arrowhead* indicates the mobility of full-length apoB-100. In the lower panel, equivalent volumes of cellular and cytosolic proteins were resolved by 10% SDS-PAGE and probed for calnexin (CN) and GRP78 by western blot analysis. *B*, Aliquots of immunoprecipitates prepared as in *A* were visualized with monoclonal anti-ubiquitin antibody. The figure shows a representative experiment which was repeated three times.

digitonin-permeabilized HepG2 cells have been shown to have additional post-translational degradation pathways, such as the lumenal ER protease ER-60 (Qiu et al., 2004).

In this study we have shown that two steps involved in apoB ERAD, retro-translocation and degradation, can be uncoupled. Inhibitors of the proteolytic activity of the 20S subunit of the proteasome have been used to demonstrate the accumulation of other ERAD substrates in the cytosol (Oberdorf et al., 2006; VanSlyke and Musil, 2002; Wiertz et al., 1996; Yu et al., 1997) suggesting that for many substrates the proteolytic activities of the proteasome and retro-translocation are separable. Similarly, proteasome inhibition in HepG2 cells resulted in the accumulation of polyubiquitinated apoB proteins in the cytosol. This finding extends previous observations of cytosolic apoB demonstrated biochemically (Liao et al., 2003) and by immunofluorescence microscopy (Ohsaki et al., 2006; Pariyarath et al., 2001). However, experiments with agents that inhibit the proteolytic activity of β-subunits of the 20S proteasome do not exclude the possibility that activities of the 19S subunit may be involved in the retro-translocation of ERAD substrates. Mitchell et al (Mitchell et al., 1998) reported that retrotranslocation and proteasomal degradation of apoB in HepG2 cells are tightly coupled and that apoB does not accumulate to any extent in the cytosol. A recent *in vitro* study of the cystic fibrosis transmembrane-conductance regulator (CFTR) degradation has suggested that the accumulation of full length ERAD substrates in the cytosol during proteasome inhibition may be the result of the uncoupling of peptidase activities of the 20S core from the unfolding and delivery by ATPase activities of the 19S subunit (Oberdorf et al., 2006) as established in the yeast ERAD system (Lee et al., 2004). Our studies with p97

knockdown and proteasome inhibition suggest that apoB-100 is an ERAD substrate for which retro-translocation and proteasome-mediated degradation can be dissociated.

The present work has provided additional evidence for the role of the AAA-ATPase p97 in the retro-translocation of ERAD substrates [reviewed in (Bays and Hampton, 2002; Ye et al., 2001)]. The presence of p97 in association with the endomembrane system after permeabilization is consistent with the existence of a retro-translocation complex containing p97 on the ER membrane (Ye et al., 2004). Crosslinking and non-denaturing immunoprecitipation demonstrated that p97 was in association with apoB-100, suggesting that p97 may be involved in recognition of apoB for ERAD. In addition, reducing the level of p97 in HepG2 cells decreased apoB-100 turnover and reduced its accumulation in the cytosol, suggesting that p97 is involved in one step that is necessary for proteasomal degradation of apoB-100.

p97-mediated retro-translocation has been suggested to require the polyubiquitination of ERAD substrates (Flierman et al., 2003) and, for apoB, this probably occurs while the protein is partially in the ER and spanning the translocation channel. Since the majority of the polyubiquitinated species that accumulate in the presence of MG132 are found in the cytosol (Fig. 3.3B), and are associated with the full-length apoB-100, our results suggest that apoB becomes polyubiquitinated as, or immediately before, it is released into the cytosol. Thus, we suggest that polyubiquitination precedes and may signal the release of apoB-100 into the cytosol. Although our study has examined primarily the full-length apoB-100, the presence of a spectrum of polyubiquitinated apoB proteins in the cytosol is consistent with co-translational polyubiquitination of apoB-100 in HepG2 cells (Zhou et al., 1998) and

suggests that targets for p97-mediated retro-translocation may include partially translated apoB-100 polypeptides. By reducing the level of p97 or by treating the cells with MG132, we decreased apoB-100 turnover and enhanced the early post-translational stability of the full-length protein. However, the stabilization of apoB, in itself, did not enhance apoB secretion. Lipid availability is likely more important in determining the level of apoB-100 secretion (Sakata et al., 1993), as even those apoB proteins that escape ERAD can be degraded by other mechanisms.

Knockdown of p97 to 25% of control level in HepG2 cells did not elicit a profound unfolded protein response (UPR). Ota and colleagues (Ota et al., 2008) recently demonstrated that apoB secretion is compromised by moderate ER stress levels in response to fatty acids. Our observation that apoB-100 secretion is unchanged following p97 knockdown suggests that this experiment did not cause sufficient ER stress to affect cell function globally. This is further supported by the lack of an effect on apoAI metabolism. Tunicamycin and DTT, both known to cause ER stress, reduced HepG2 apoB levels while p97 knockdown decreased apoB-100 turnover and increased cellular apoB-100 mass. The lack of ER stress could be because a portion of functional p97 remains under the conditions of our siRNA experiment, retaining some protection against ER dysfunction. In HeLa cells (Wojcik et al., 2006), reduction of p97 by more than 85% with RNAi caused an ER stress response and swelling of the organelle. In Rat-1 fibroblasts, 62% reduction in p97 was insufficient to cause the accumulation of polyubiquitinated proteins, but did have a specific effect on the ubiquitination and half-life of the inositol-1,4,5-trisphosphate receptor, a known endogenous ERAD substrate (Alzayady et al., 2005). The discrepancies between studies may be related to cell type or

level of p97 reduction. Given the abundance of p97 and its multiple cellular functions, specific cell types may have different requirements. The reasons for the absence of a substantial stress response in our system is not clear, although since HepG2 cells secrete many proteins, they may have an inherently high protein folding capacity and could be relatively resistant to the increased burden of misfolded ERAD substrates caused by reductions in p97. Therefore, the siRNA knockdown of p97 seems to affect apoB-100 metabolism, even though a generalized stress response is not observed.

In the light of our findings, we propose that the proteasomal degradation of apoB-100 occurs in a similar manner to other ERAD substrates. When translocation of apoB is arrested and the polypeptide is exposed to the cytosol, the bitopic topology is comparable to that of other ERAD substrates that are membrane integrated (Baker and Tortorella, 2007). p97 may initiate ERAD by interaction with polyubiquitinated apoB as it is generated by the E3 ligase gp78 (Liang et al., 2003), since it has been suggested that gp78 and p97 and may couple polyubiquitination to retro-translocation for other substrates (Zhong et al., 2004). Recently, it has been shown that Ufd1 binding to gp78 or p97 is a mutually exclusive event and that binding of polyubiquitin chains of substrate proteins by Ufd1 is critical for ERAD (Cao et al., 2007). The p97-mediated retro-translocation of polyubiquitinated apoB may also be guided by Hsp70 and Hsp90, chaperones that have been suggested to facilitate the delivery of polyubiquitinated targets to the 19S subunit of the proteasome (Gusarova et al., 2001). During retro-translocation, continuous delivery of apoB to the 20S core may require the combined ATPase activities of both p97 and proteins in the 19S lid. Hence, the proximity of p97 and the 26S proteasome at the site of apoB-100 translocation may explain how apoB-100 is rapidly

directed for co-translational degradation (Mitchell et al., 1998; Zhou et al., 1998). More work is required to examine the details and sequence of these events.

Cytosolic apoB-100 was found in the high density lipoprotein range, a density similar to apoB-containing lipoproteins found in the lumen of the ER in digitonin-permeabilized HepG2 cells (Adeli et al., 1997a). Since the initiation of lipoprotein assembly begins during the translation of apoB, it is conceivable that disassembly of the lipid-protein complex must occur to allow the polypeptide to transit back through the translocation channel toward the cytosol. The density of the apoB-100 in the cytosol fraction, apparently associated with little or no lipid, supports this hypothesis. However, it is also possible that the cytosolic apoB-100 may exist in complex with additional cytosolic factors, as the density of apoB-100 has been previously suggested to increase when chaperones are bound to the particle (Zhang and Herscovitz, 2003). Immunofluorescence microscopy studies have shown that cytosolic apoB associates with lipid droplets forming crescent-shaped structures (Ohsaki et al., 2006) representing the convergence between proteasomal and other degradation pathways.

Some aspects of the retro-translocation of apoB-100 remain to be clarified. Investigations of relative contributions of the chaperone proteins GRP78 (Qiu et al., 2005), Hsp70 and Hsp90 (Gusarova et al., 2001) to the selection and retro-translocation of apoB-100 are required. This may be particularly relevant since we observed a decrease in Hsp70 with si-p97 treatment. Furthermore, recently characterized components of the retro-translocation machinery such as Derlin-1, SVIP (Ballar et al., 2007), VIMP (Ye et al., 2004) and UBX2 (Neuber et al., 2005; Schuberth and Buchberger, 2005) may also play regulatory roles in apoB degradation. We did not observe an effect of p97

knockdown on post-translational stability beyond 1 h or on the secretion of apoB-100 from HepG2 cells. We also did not find a consistent increase in the mass of apoB-100 in the si-p97 cell membrane fraction after three days at reduced levels of p97. These observations may indicate that, in the absence of p97, additional degradation mechanisms within the cell can still prevent the accumulation or secretion of incompletely assembled lipoprotein when ERAD is compromised.

In conclusion, evidence presented in this work suggests that p97 is a central component in retro-translocation of apoB-100 for its delivery to the proteasome. Therefore, p97 may function at an early stage in apoB-100 biosynthesis where the pre-secretory fate of apoB is determined.

CHAPTER 4 – UBIQUITINATION REGULATES THE ASSEMBLY OF VERY LOW DENSITY LIPOPROTEIN IN HEPG2 CELLS AND IS THE COMMITTING STEP OF THE APOB100 ERAD PATHWAY

4.1 Introduction

4.1.1 Statement About Published Works

This research was originally published in Journal of Lipid Research. Fisher EA, Khanna NA and McLeod RS. Ubiquitination regulates the assembly of very low density lipoprotein in HepG2 cells and is the committing step of the apoB100 ERAD pathway. *J. Lipid Res*. 2011; 52:1170-1180. © the American Society for Biochemistry and Molecular Biology. The following chapter is the abstract, results and discussion section of the published manuscript. I wrote the manuscript with the editing and guidance from Roger. Neeraj Khanna performed the experiments shown in Figure 4.4C and D, and all of Figure 4.7 during his Honours project.

4.1.2 Abstract

Apolipoprotein B-100 (apoB-100) is degraded by endoplasmic reticulum-associated degradation (ERAD) when lipid availability limits assembly of VLDLs. The ubiquitin ligase gp78 and the AAA-ATPase p97 have been implicated in the proteasomal degradation of apoB-100. To study the relationship between ERAD and VLDL assembly, we used small interfering RNA (siRNA) to reduce gp78 expression in HepG2 cells. Reduction of gp78 decreased apoB-100 ubiquitination and cytosolic apoB-ubiquitin conjugates. Radiolabeling studies revealed that gp78 knockdown increased secretion of newly synthesized apoB-100 and, unexpectedly, enhanced VLDL assembly, as the shift

in apoB-100 density in gp78-reduced cells was accompanied by increased triacylglycerol (TG) secretion. To explore the mechanisms by which gp78 reduction might enhance VLDL assembly, we compared the effects of gp78 knockdown with those of U0126, a mitogen-activated protein kinase/ERK kinase1/2 inhibitor that enhances apoB-100 secretion in HepG2 cells. U0126 treatment increased secretion of both apoB100 and TG and decreased the ubiquitination and cellular accumu-lation of apoB-100. Furthermore, p97 knockdown caused apoB-100 to accumulate in the cell, but if gp78 was concomitantly reduced or assembly was enhanced by U0126 treatment, cellular apoB-100 returned toward baseline. This indicates that ubiquitination commits apoB-100 to p97-mediated retrotranslocation during ERAD. Thus, decreasing ubiquitination of apoB-100 enhances VLDL assembly, whereas improving apoB-100 lipidation decreases its ubiquitination, suggesting that ubiquitination has a regulatory role in VLDL assembly.

4.2 Results

4.2.1 Gp78 siRNA Reduces ApoB-100 Ubiquitination and Co-translational Accumulation During Proteasome Inhibition

To examine the functional relationship between gp78 and apoB-100 metabolism we used an RNA interference strategy to reduce gp78 expression in HepG2 cells. It has been previously reported that overexpression of gp78 in HepG2 cells enhances apoB-100 ubiquitination and decreases apoB-100 secretion (Liang et al., 2003). Cells transfected with either a non-targeting (NT) control siRNA duplex or gp78-targeting siRNA (si-gp78) were harvested 72 hours post-transfection for mRNA and protein analysis. To establish the efficiency of the si-gp78 knockdown, total RNA was isolated from the cells
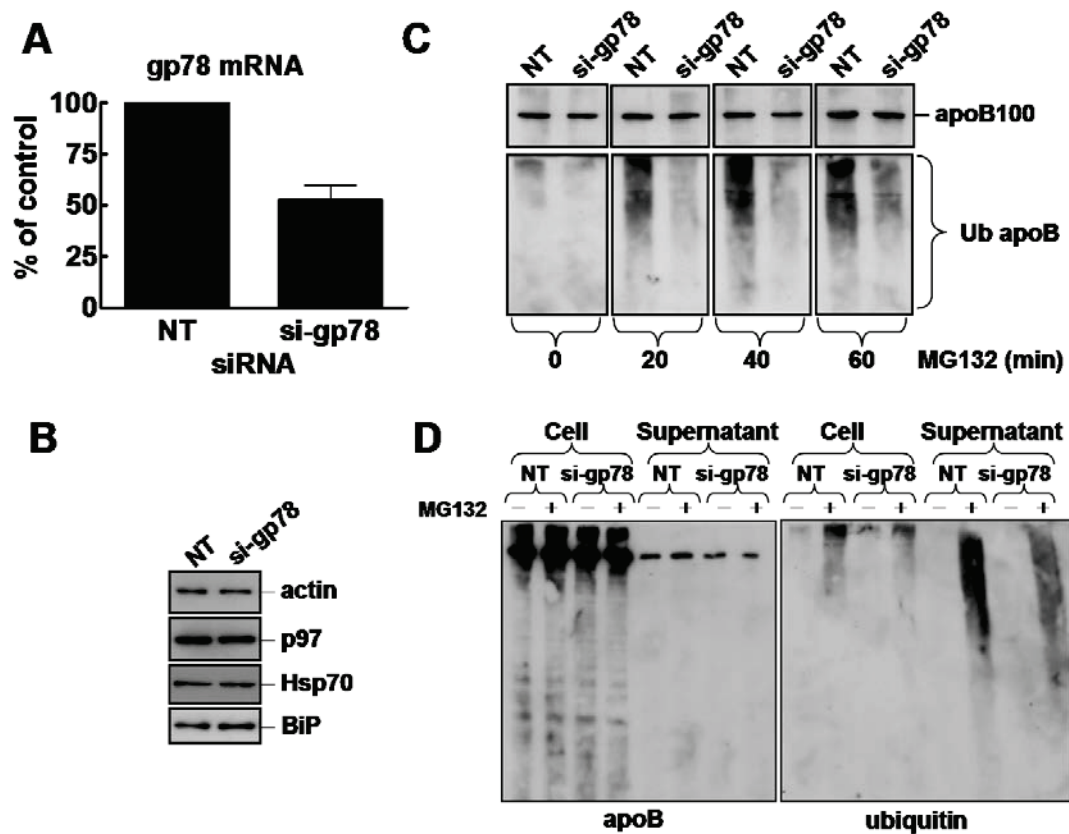
Figure 4.1. siRNA-mediated reduction of gp78 decreases the accumulation of ubiquitinated apoB-100. HepG2 cells were transfected with non-targeting (NT) or gp78-targeting siRNA (si-gp78). **A.** Quantitative PCR analysis of gp78 mRNA at 72 hours post-transfection, normalized to cyclophilin mRNA. Mean ± S.D., n=3. **B.** Seventy-two hours post-transfection total cell lysates were collected, resolved by SDS-PAGE and transferred to nitrocellulose. Cellular proteins in NT and si-gp78 cells were detected by immunoblot analysis. **C.** Seventy-two hours post-transfection, cells were treated with 25 μM of the proteasome inhibitor MG132 for up to one hour. ApoB-100 was immunoprecipitated from cell lysates and apoB-100 and ubiquitin were detected by immunoblot analysis. **D.** Cells were transfected, and then treated for 30 minutes with or without 25 μM MG132. Cells were then permeabilized with digitonin and separated into the membrane (*Cell*) and cytosol (*Supernatant*) fractions. ApoB was recovered by immunoprecipitation and apoB (*left panel*) and ubiquitin (*right panel*) revealed by immunoblotting.

for real-time PCR (RT-PCR) analysis. Gp78 mRNA in the cells was reduced by 54 ± 13% (n=3) compared to NT when normalized to cyclophilin mRNA (Figure 4.1A).

Because gp78 is an ERAD-associated protein, reducing its expression might compromise normal protein turnover in the ER. If this were the case, ER stress caused by impaired protein turnover might trigger an unfolded protein response (UPR), the hallmark of which is increased BiP expression (Zhang and Kaufman, 2008). BiP mass was not changed by the gp78 knockdown (Figure 4.1B) suggesting that ER function was not compromised. Additionally, the cytosolic stress marker Hsp70 was not changed, indicating that no cytosolic heat shock response (HSR) (Tower, 2009) was provoked by the gp78 knockdown, nor was p97 expression altered (Figure 4.1B). Notably, the knockdown of gp78 did not alter the level of apoB-100 in HepG2 cells as detected by immunoblot (Figure 4.1C, *top panels*).

To examine the role of gp78 in apoB degradation, cells transfected with NT or gp78 siRNA were treated with the proteasome inhibitor MG132 for up to one hour. Cells transfected with NT siRNA accumulated ubiquitinated apoB polypeptides (Figure 4.1C, *lower panels*), visible in the apoB immunoprecipitates as a characteristic smear detected with an anti-ubiquitin antibody. In contrast, the cells transfected with gp78 siRNA accumulated far less ubiquitinated apoB protein, suggesting that gp78 expression is responsible for the generation of apoB-ubiquitin conjugates. These data complement previous observations (Liang et al., 2003) where gp78 overexpression increased the ubiquitination of apoB in HepG2 cells.

Digitonin permeabilization was used to examine cytosolic apoB with or without gp78 knockdown. As indicated in the left panel of Figure 4.1D, the majority of apoB was

found in the membrane fraction (*Memb*, deliberately overexposed to reveal the cytosolic apoB). Upon treatment of NT cells with MG132, apoB-ubiquitin conjugates accumulated in both the membrane and cytosol fractions (*right panel*), with the lower molecular weight poly-ubiquitinated species found only in the cytosol fraction. In contrast to NT-transfected cells, the gp78-reduced cells contained less apoB-ubiquitin conjugates in the cytosol and fewer ubiquitin-positive apoB-100 proteins in the membrane fraction (Figure 4.1D). This suggested that gp78 mediates efficient ubiquitination and contributes to the production of lower molecular weight (LMW) apoB-ubiquitin conjugates in the cytosol.

In MG132 treated cells, the LMW apoB-ubiquitin pool detected by immunoblotting could be generated co-translationally (ubiquitinated, incompletely translated apoB-100 protein). To explore this, we monitored apoB-100 synthesis using metabolic labeling (0-20 min) of puromycin synchronized cells (Figure 4.2). Inclusion of MG132 caused the accumulation of incomplete apoB polypeptides in NT cells (*left panel*, +MG132 compared to –MG132 at 5, 10, 20 min). In contrast, in gp78-reduced cells the pattern of incomplete apoB polypeptides was not markedly different with or without MG132 (*right panel*). This suggested that efficient co-translational targeting of apoB to ERAD requires gp78 expression.

4.2.2 Gp78 Knockdown Increases ApoB and Triglyceride Secretion and Shifts the Secreted ApoB-100 Particle Density to VLDL From LDL

To examine the effect of reduced gp78 expression on newly synthesized apoB-100, we monitored intracellular turnover and secretion using pulse-chase radiolabelling. Cells were pulse-labeled for one hour with [^{35}S]cysteine/methionine, and cells and media
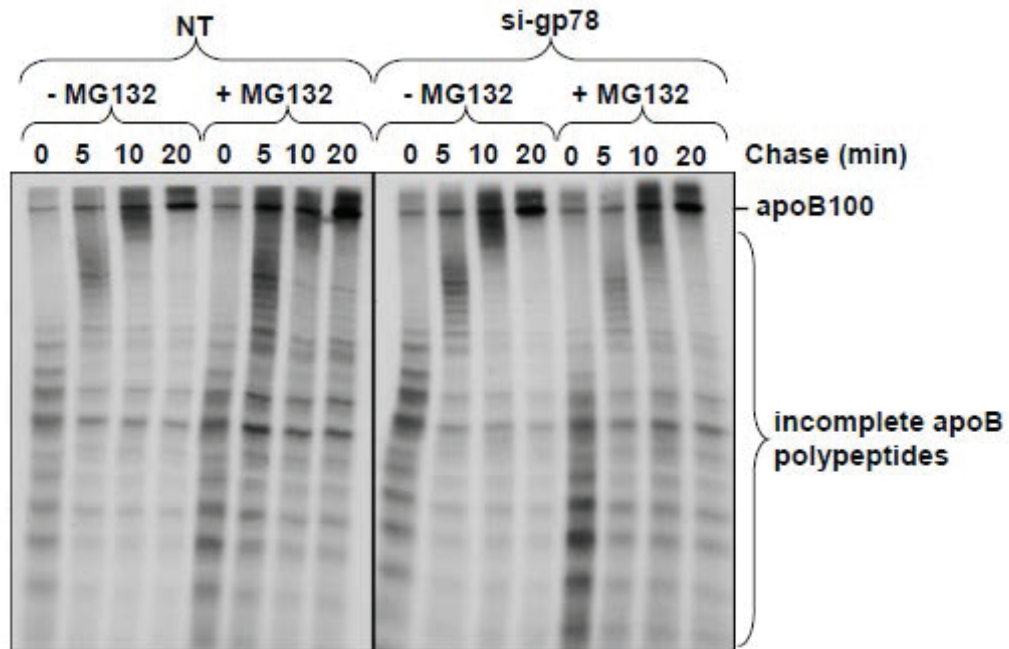
Figure 4.2. Gp78 knockdown reduces the accumulation of radiolabelled apoB-100 synthesized during MG132 treatment in puromycin-synchronized HepG2 cells. Seventy-two hours following transfection with either NT or gp78-targeting siRNA, HepG2 cells were treated with 10 μM puromycin for 5 minutes and then washed for 3 x 10 minutes on ice. Cells were immediately placed in 37ºC media containing [^{35}S] methionine/cysteine for 5 minutes and then chased for up to 20 minutes. Where indicated, 25 μM MG132 was included in the pulse and chase medium. ApoB was recovered from the cells and visualized by autoradiography.

were then collected after a 2 hour chase and analyzed for levels of radiolabelled apoB-100 and apoAI. In the gp78-reduced cells apoB-100 secretion was increased by nearly 30% (Figure 4.3A) over the NT-transfected cells but apoB-100 stability was not increased by gp78 knockdown. Secretion of apoAI was not impaired by the gp78-knockdown (Figure 4.3B), indicating that the secretory pathway was not compromised.

We hypothesized that the increase in apoB-100 secretion might reflect the production of small, dense, poorly lipidated lipoproteins that had escaped degradation. To examine the effect of gp78 knockdown on VLDL assembly, chase medium was fractionated by density gradient ultracentrifugation and radiolabelled apoB-100 was recovered from each fraction. Unexpectedly, we observed a shift in the secretion profile in gp78 knockdown cells compared to NT control cells (Figure 4.4A). Reduced gp78 expression increased the apoB-100 radiolabel in VLDL-sized particles (Figure 4.4B). The unexpected shift in lipoprotein density was also observed with a second siRNA duplex targeting gp78 (Figure 4.4A & 4.4B, si-gp78-A), demonstrating that the enhanced VLDL assembly was not an off-target effect of that particular siRNA.

It appeared that when gp78 expression was reduced, the apoB protein could acquire more lipid than NT control cells, since the decreased density of the secreted lipoproteins is indicative of an increased lipid to protein ratio. [^{3}H]Glycerol labelling revealed that triglyceride secretion was modestly increased by the gp78 knockdown in the presence of oleic acid (Figure 4.4C). Interestingly, triglyceride synthesis from glycerol was reduced in si-gp78 cells (Figure 4.4D), but this did not compromise TG secretion. Notably, gp78 reduction did not alter the levels of several proteins involved in lipid
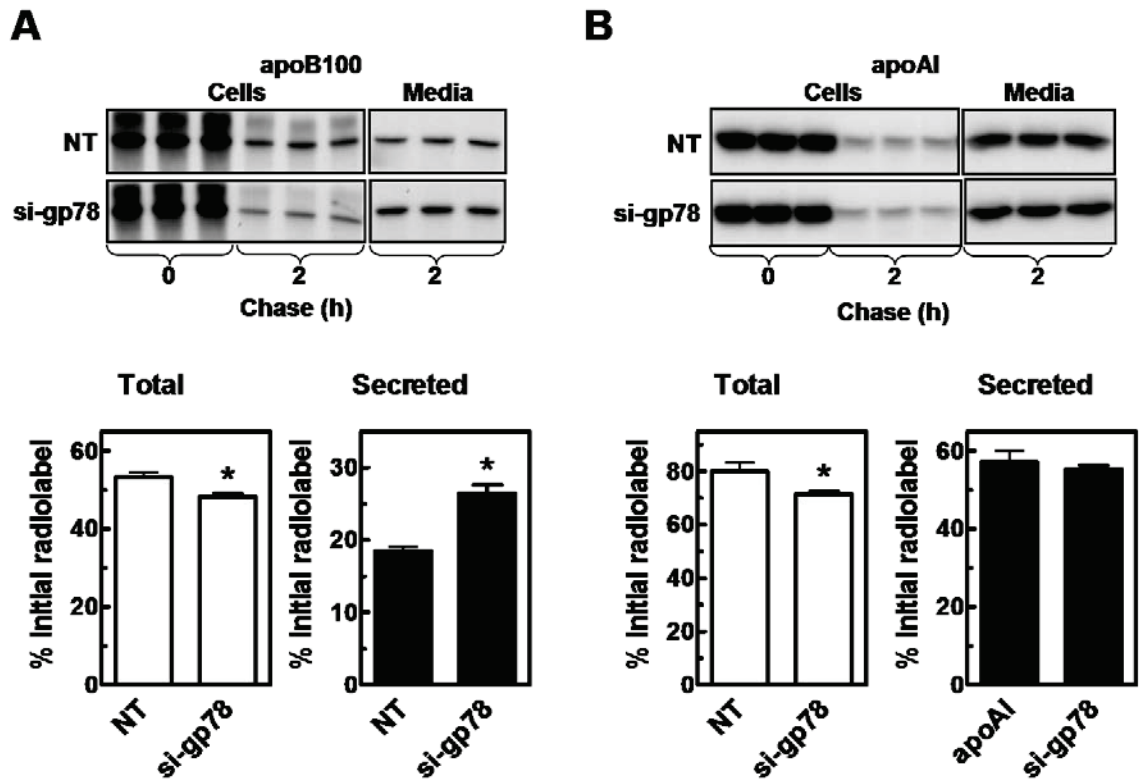
Figure 4.3. siRNA-mediated reduction of gp78 increases apoB-100 secretion. Autoradiographs and quantitation of apoB-100 **(A)** and apoAI **(B)** in cells and medium by pulse-chase analysis. Seventy-two hours following transfection with either non-targeting (NT) or gp78-targeting (si-gp78) siRNA, HepG2 cells were labelled with [^{35}S]cysteine/methionine for 1 hour and then chased for 2 hours as described in Chapter 2. ApoB and apoAI were recovered from cells and media by immunoprecipitation and visualized in SDS-PAGE gels by autoradiography (*top panels*). *Total* (medium plus cells) and *Secreted* radiolabelled proteins are expressed as percent of initial radiolabel. Autoradiographs and quantitation (mean ± S.D.) are derived from triplicate wells from a representative experiment, which was repeated three times. Asterisks denote significant differences (P<0.05) as determined by unpaired t tests.
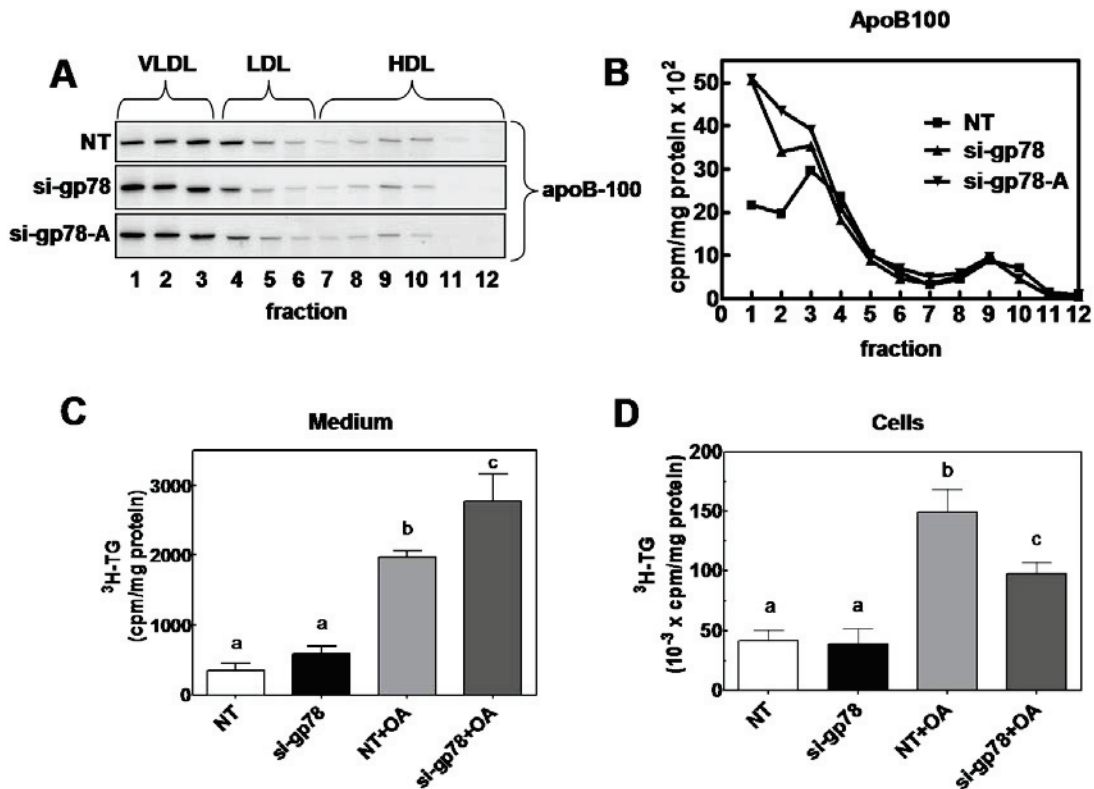
Figure 4.4. siRNA-mediated reduction of cellular gp78 enhances VLDL and triglyceride secretion from HepG2 cells. A. Density gradient ultracentrifugation profiles of secreted apoB-100. Cells were transfected with either NT siRNA, or siRNA duplexes targeting gp78 (si-gp78 or si-gp78-A). Seventy-two hours post-transfection, cells were depleted for one hour in cysteine/methionine-free media and then pulse-labelled for one hour with [^{35}S]cysteine/methionine. Pulse medium was replaced with chase medium for two hours after which medium samples were collected. Samples were subjected to density gradient ultracentrifugation and apoB was immunoprecipitated from each fraction and visualized by SDS-PAGE and autoradiography. **B.** Quantitation of apoB-100. Radiolabelled apoB-100 bands were excised from the gel and quantified by liquid scintillation counting. Results are expressed as cpm per mg cell protein. The data presented is representative of three experiments. **C & D**. Transfected HepG2 cells were labelled for 2 h with [2-^{3}H] glycerol in the presence or absence of 360 μM oleic acid. Lipids were extracted from cells and media in methanol/chloroform and separated by thin layer chromatography. The triglyceride bands were visualized by iodine staining and quantified by liquid scintillation counting. Data are mean ± S.D., n=3. Different letters denote significant differences (P<0.05) as determined by Tukey's Multiple Comparison test.

Figure 4.5. Gp78 siRNA does not alter levels of proteins involved in lipid metabolism. Cells were transfected with NT or si-gp78 and harvested by lysis 72 hours posttransfection. Total cell lysates were resolved by SDS-PAGE and the indicated proteins were visualized by immunoblotting.

metabolism including DGAT1, MTP, HMG CoA reductase, SREBP1a, PPARα and PPARγ (Figure 4.5).

4.2.3 Reduction of Gp78 Alters the Cytosolic Exposure of ApoB-100

It has been shown that a portion of the cellular apoB-100 pool is cytosolically exposed as it progresses through the secretory pathway (Borchardt and Davis, 1987; Macri and Adeli, 1997). The extent of cytosolic exposure of apoB-100 could affect its susceptibility to degradation. We hypothesized that reduced ubiquitination might decrease the cytosolic exposure of apoB-100. To test this, permeabilized NT and si-gp78 cells were trypsin digested to destroy proteins not protected within the microsomal and nuclear membrane compartments. The ER-luminal N-terminus of calnexin was protected against trypsin digestion in both NT and si-gp78 cells (Figure 4.6A, *lower panel*). ApoB-100 was sensitive to trypsin digestion but more apoB-100 was protected in si-gp78 than in NT cells (Figure 4.6A & B). A radiolabeling approach also revealed improved protection of apoB-100 against trypsin digestion with si-gp78 when normalized to apoA-I (Figure 4.7A & B). This suggested that reduced gp78 expression alters the membrane topology of apoB-100.

4.2.4 Inhibition of ERK1/2 Phosphorylation in HepG2 cells Improves VLDL Assembly, Lipid Incorporation and Secretion

As previously reported (Tsai et al., 2007), we found that the MEK inhibitor U0126 shifted the apoB100 density profile in a dose-responsive manner from LDL to VLDL when radiolabelled cell culture medium was examined by gradient
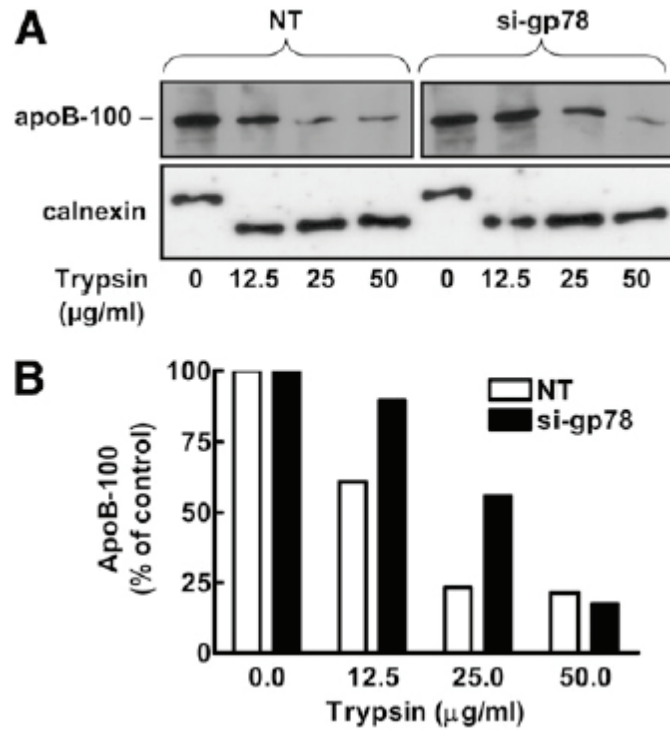
Figure 4.6. Reduced gp78 expression protects apoB-100 from trypsin digestion in digitonin-permeabilized HepG2 cells. A. Cells were transfected with either non-targeting (NT) or gp78-targeting siRNA. Seventy-two hours post-transfection the cells were permeabilized with digitonin and the supernatant was discarded, leaving only the nuclear and microsomal membranes intact. The remaining monolayers were then treated with trypsin at the indicated concentration for 30 minutes on ice. Soybean trypsin inhibitor was added and the monolayers were collected. Calnexin and apoB were visualized in each sample by immunoblot analysis. **B.** ApoB-100 was quantified by scanning densitometry and is expressed as percent of 0 μg/ml trypsin control.
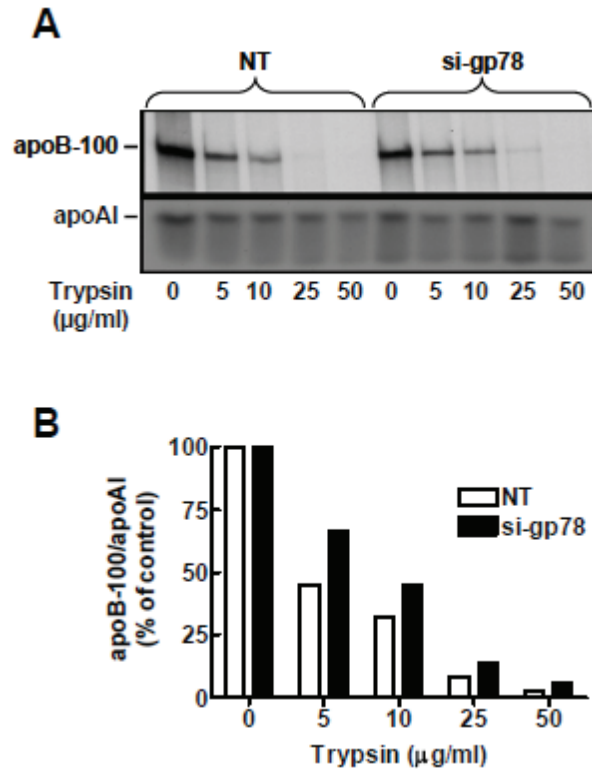
Figure 4.7. Reduced gp78 expression protects radiolabelled apoB-100 from trypsin digestion in digitonin-permeabilized HepG2 cells. A. Cells were transfected with either non-targeting (NT) or gp78-targeting siRNA. Seventy-two hours post-transfection the cells were labelled with [^{35}S]cysteine/methionine for 1 hour. Cells were then permeabilized with digitonin and the supernatant was discarded. The remaining monolayers were then treated with trypsin at the indicated concentration for 30 minutes on ice. Soybean trypsin inhibitor was then added and the monolayers were collected. ApoB-100 and apoAI were recovered from cells by immunoprecipitation and visualized by autoradiography. **B.** ApoB-100 and apoAI bands were excised and quantified by liquid scintillation counting. The ratio of apoB-100 to apoAI is expressed as percent of 0 μg/ml trypsin control (NT and si-gp78) to demonstrate the relative level of digestion.
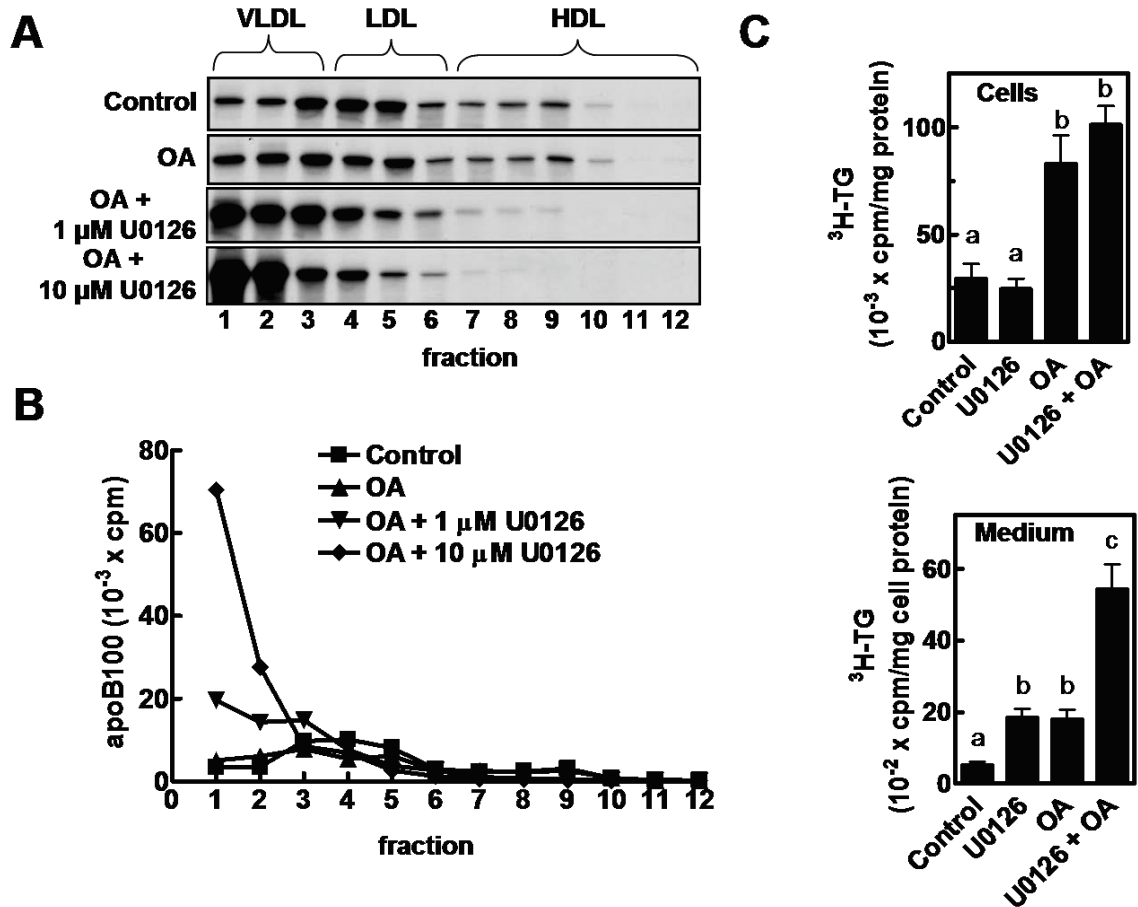
Figure 4.8. U0126 treatment enhances assembly of VLDL in HepG2 cells and increases secretion of radiolabelled triglycerides. HepG2 cells were treated with 1 or 10 μM U0126 for 16 hours. Cells were then incubated in the presence or absence of 360 μM oleic acid and labeled with [^{35}S]cysteine/methionine for 3.5 hours. After labeling, the media were fractionated by sucrose density gradient ultracentrifugation and each fraction was subjected to apoB immunoprecipitation using goat anti-human apoB antibody. **A.** Eluted proteins were resolved on a 5% SDS-PAGE gel, visualized by autoradiography. **B.** The radioactivity in apoB100 was quantified by scintillation counting. **C. & D.** HepG2 cells treated with 10 μM U0126 for 16 hours were labelled for 2 h with [2-^{3}H] glycerol in the presence or absence of 360 μM oleic acid. Lipids were extracted from cells and media **(C)** in methanol/chloroform and separated by thin layer chromatography. The triglyceride bands were visualized by iodine staining and quantified by liquid scintillation counting. Values are mean ± S.D., n=3. Different letters denote significant differences (P<0.05) as determined by Tukey's Multiple Comparison test.

106

ultracentrifugation (Figure 4.8A and 4.8B). To examine the secretion of cellular TG, U0126-treated cells were incubated with [2-^{3}H]glycerol for 2 hours, followed by collection and analysis of [^{3}H]TG from the cells and media. U0126 did not stimulate incorporation of [^{3}H]glycerol into cellular TG, whereas oleic acid induced a large increase in cellular [^{3}H]TG levels (Figure 4.8C). Secretion of [^{3}H]TG into the medium was modestly stimulated by either U0126 or OA, and there was a more than additive effect on [^{3}H]TG secretion when U0126 and oleic acid were added together (Figure 4.8D). Taken together, these observations suggested that the increase in cellular [^{3}H]TG with oleic acid alone did not increase [^{3}H]TG secretion markedly, but the inclusion of U0126 improved the incorporation of [^{3}H]TG into VLDL.

4.2.5 MEK1/2 Inhibition Decreases ApoB-100 Ubiquitination and Diverts ApoB-100 ERAD Substrates into the Secretory Pathway

Based on the similar enhancement of VLDL formation in gp78 knockdown cells and with U0126 treatment, we hypothesized that apoB-100 could escape ubiquitination and degradation in U0126-treated cells because the malfolding that triggers ERAD was reduced. When MG132 and U0126 were included together, less nascent apoB accumulated than with MG132 alone (Figure 4.9A, *left panel*), suggesting that U0126 reduced apoB-100 ERAD substrates. Total apoB-100 secretion was profoundly increased by U0126 but MG132 had no effect on apoB-100 secretion (Figure 4.9A, *right panel*). As shown in Figure 4.9B, U0126 and MG132, alone or together, stabilized apoB-100 during a one hour chase compared to the untreated control. Conversely, U0126 increased apoB-100 secretion whereas MG132 did not (Figure 4.9B, *right panel*). Since U0126 did not
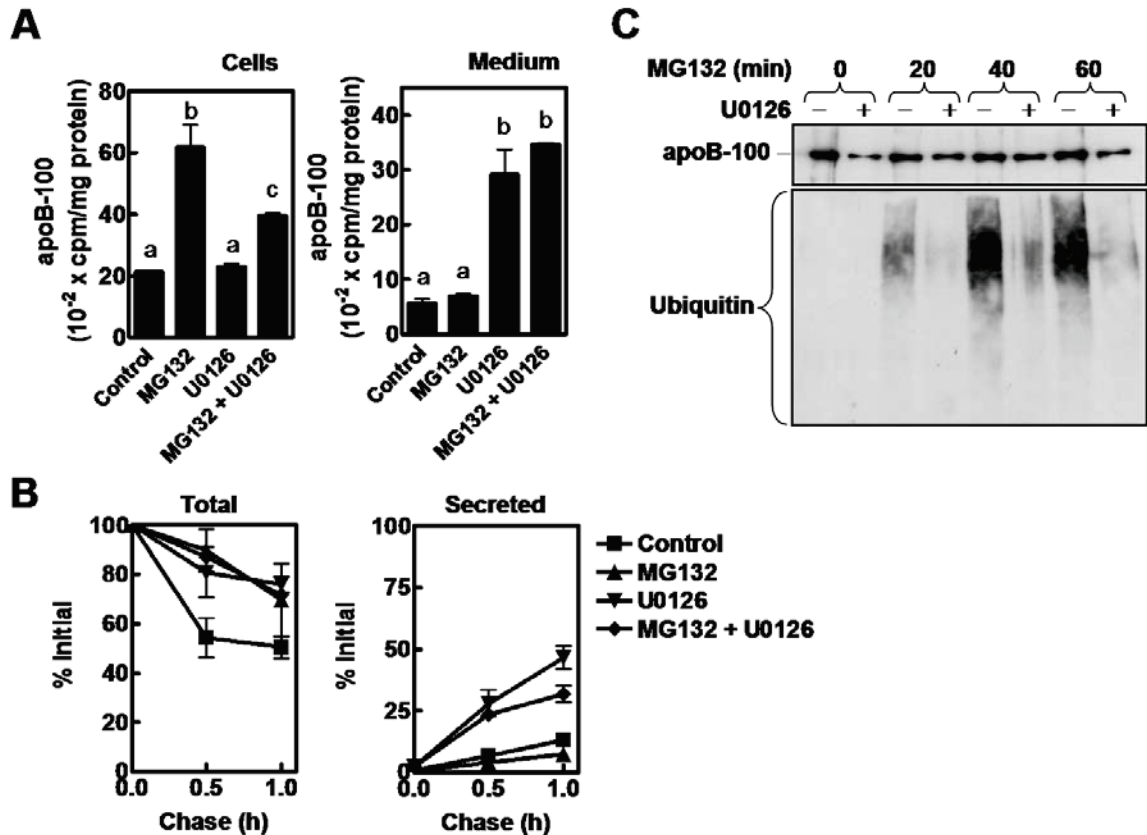
Figure 4.9. U0126 treatment reduces cell apoB-100 ubiquitination and enhances secretion. A. & B. HepG2 cells were treated with U0126 for 16 hours. Cells were then incubated for one hour with 360 μM oleic acid, with or without 25 μM MG132, before a one hour pulse with [^{35}S]cysteine/methionine. Labelled apoB-100 was collected by immunoprecipitation, resolved by SDS-PAGE and quantified by liquid scintillation counting. **A.** Cells and media were collected after the pulse period. Data are mean and range of duplicates. Different letters denote significant differences (P<0.05) as determined by Tukey's Multiple Comparison test. **B.** Medium was removed and replaced with chase medium and cells and media were collected after the indicated chase time. Data are mean ± S.D., n=3. **C.** U0126-treated cells (16 h) were incubated for 1 h with 360 μM oleic acid prior to MG132 treatment for the indicated time period. ApoB immunoprecipitates were collected from cell lysates and analyzed by immunoblotting with for apoB (*top panel*) and ubiquitin (*bottom panel*).

108

increase apoB-100 synthesis (Figure 4.9A, *left panel*), the enhanced secretion appeared to represent apoB-100 that had escaped ERAD during conditions of improved lipid incorporation. Taken together, the reduced cellular apoB-100 accumulation and increased secretion suggested that MEK/ERK inhibition by U0126 reduced the entry of newly synthesized apoB into the ERAD pathway by creating an environment that favoured VLDL assembly.

Immunoblot analysis (Figure 4.9C) showed that U0126-treated cells accumulated much less ubiquitinated apoB following the MG132 treatments. This suggested that in these cells apoB-100 could escape from the ERAD pathway at a step before ubiquitination. The decrease in ubiquitinated apoB was not accompanied by a reduction in global ubiquitination in U0126-treated cells (Figure 4.10A, *left vs right panel*).

4.2.6 Si-gp78 and U0126 Treatment Both Reduce the ApoB-100 Accumulation and BiP Induction Observed in p97-Reduced Cells

p97 facilitates the removal of apoB-100 from the ER into the cytosol for proteasomal degradation (Fisher et al., 2008; Rutledge et al., 2009). Gp78 and p97 are known to associate with one another and coordinate the ubiquitination and retrotranslocation of other ERAD substrates (Ballar and Fang, 2008). Knockdown of p97 delayed the turnover of nascent apoB-100, causing it to accumulate intracellularly (Fisher et al., 2008). We hypothesized that if gp78 and p97 act in the same apoB ERAD pathway, gp78-dependent ubiquitination may occur before p97-mediated retrotranslocation and, if so, gp78 knockdown in p97-reduced cells would reverse the apoB accumulation and enhance secretion. Furthermore, U0126 would reduce apoB accumulation in p97-reduced
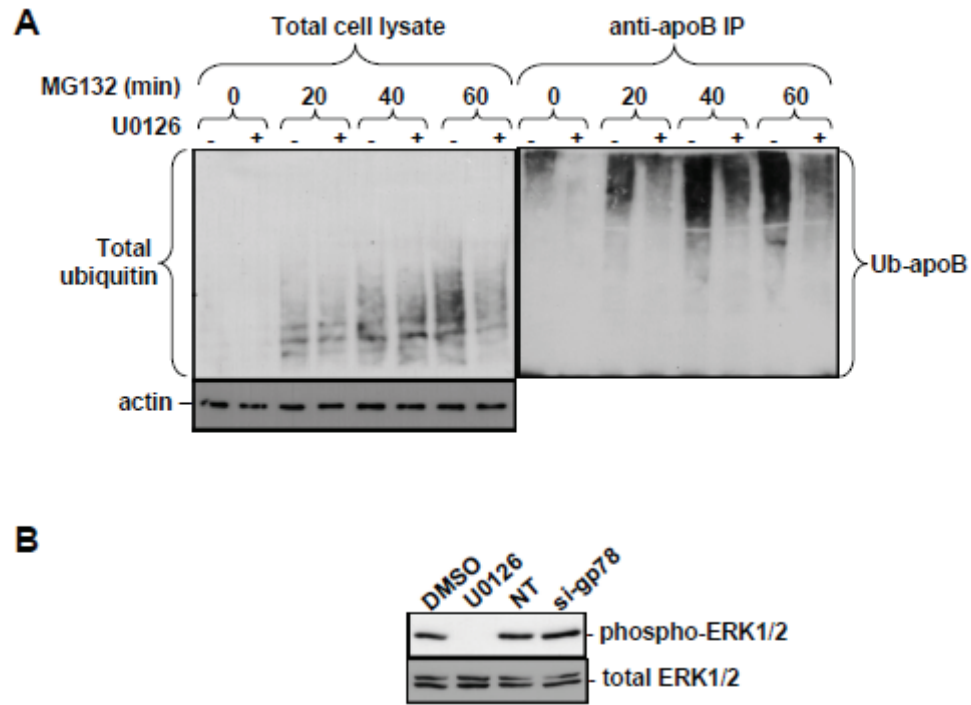
Figure 4.10. U0126 does not affect global ubiquitination during MG132 treatment and si-gp78 does not affect phospho-ERK. A. Cells were pre-treated for 16 hours with either DMSO or 10 μM U0126. Cells were incubated for one hour with 360 μM oleic acid prior to the 25 μM MG132 treatment. From total cell lysates, 6% input was loaded per lane for the total ubiquitin blot (*upper left panel*) and 2% input was loaded for the actin blot (*lower left panel*). ApoB immunoprecipitates (*right panel*) were performed on total cell lysates with a polyclonal anti-apoB and the elutions analyzed by Western blot with anti-ubiquitin antibody. **B.** Cells were harvested 72 hours post-transfection or after 16 h incubation with 10 μM U0126. Total cell lysates were resolved by SDS-PAGE and total ERK and phospho-ERK were visualized by immunoblot analysis.

cells because apoB could be diverted from ERAD before ubiquitination, thus avoiding the p97-dependent step.

Transfected cells were radiolabelled for 3 hours in the presence of oleic acid. While the p97 knockdown caused marked apoB-100 accumulation relative to control cells (NT), the combined knockdown of both p97 and gp78 caused almost no accumulation of nascent apoB-100 (Figure 4.11A, *left panel*). U0126 had the same effect on apoB-100 as gp78 knockdown when superimposed upon the p97 knockdown (Figure 4.11B). Both gp78 knockdown and U0126 were able to enhance apoB-100 secretion from p97 knockdown cells (Figure 4.11A and 4.11B, *right panels*). Unlike U0126, gp78 knockdown did not alter phospho-ERK1/2 levels (Figure 4.10B), suggesting that the effects of gp78 reduction and U0126 treatment are mechanistically distinct.

Our previous study (Fisher et al., 2008) showed an increase in BiP levels with p97 knockdown, consistent with a modest ER stress and this was also observed here (Figure 4.11C and 4.11D). Interestingly, both gp78 knockdown (Figure 4.11C) and U0126 treatment (Figure 4.11D) decreased the elevated BiP levels observed in p97-reduced cells. These observations suggest that either preventing ubiquitination or enhancing assembly can reduce the apoB accumulation and ER stress in p97-reduced cells.

4.3 Discussion

The present work has revealed an expanded role for the ubiquitin ligase gp78 in the metabolism of apoB-100. Our knockdown experiments complement results presented in a gp78 overexpression study (Liang et al., 2003) to indicate that gp78 is a ubiquitin ligase that regulates apoB-100 ERAD. In addition, since decreasing the ubiquitination of
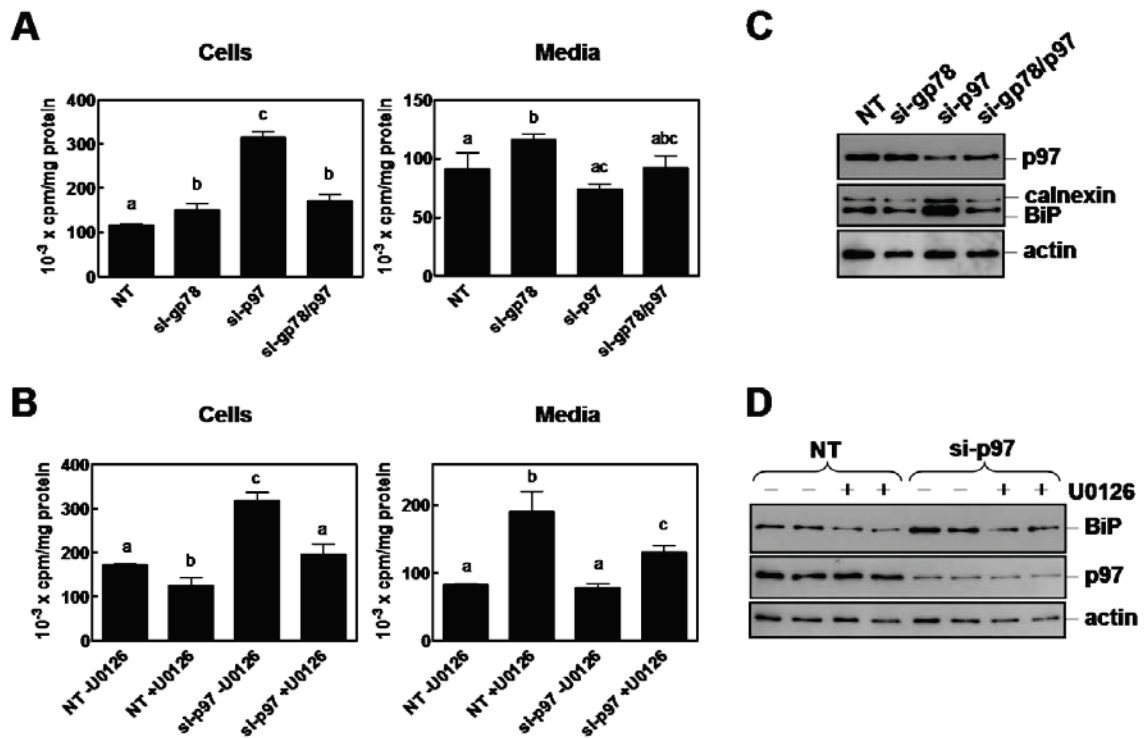
Figure 4.11. gp78 knockdown and U0126 treatment normalize the impaired turnover of apoB-100, and BiP expression, in p97 knockdown cells. A. HepG2 cells were transfected with NT, gp78, p97 siRNA or both gp78 and p97 siRNA. Following a one hour pre-incubation with 360 μM oleic acid in cysteine/methionine free media, cells were labeled with [^{35}S]cysteine/methionine in the presence of oleic acid for 3 h. Cells and media were collected and apoB-100 was recovered by immunoprecipitation, resolved by SDS-PAGE and quantified by liquid scintillation counting. Data points represent mean ± SD (n=3). Different letters denote significant differences (P<0.05) as determined by Tukey's Multiple Comparison test. **B.** Fifty-six hours post-transfection, cells with either NT or p97-targeting siRNA were treated with 10 μM U0126 for 16 hours, then labelled as in panel A in the presence of U0126 (followed by the same analysis). **C. & D.** Immunoblot analysis of cell proteins following siRNA or U0126 treatment.

112

apoB-100 can enhance VLDL assembly, it reveals a new level of complexity in the relationship between apoB secretion and ERAD. Our studies using the MEK/ERK inhibitor U0126 have shown that this compound acts by increasing the efficiency of coupling of new TG synthesis to VLDL assembly in HepG2 cells. Finally, our double knockdown experiments suggest that ubiquitination of apoB100 in HepG2 cells occurs before the involvement of p97 and is the committing step for ERAD. Thus, poorly lipidated or translocation arrested apoB-100 are not ERAD substrates but polyubiquitinated apoB is. These observations lend weight to the new possibility that regulation of VLDL assembly in hepatocytes may be dependent on a functional ERAD pathway.

Our data suggests that a portion of HepG2 apoB-100 that would normally be degraded by the ERAD pathway can continue through the secretory pathway to a different fate when ubiquitination or lipidation is modulated. Decreased ubiquitination (by gp78 knockdown) and improved lipid incorporation (by inhibiting ERK1/2 phosphorylation with U0126) both enhanced the secretion of apoB-100 and lipids without increasing cellular apoB-100 levels. U0126 did not alter global ubiquitination, and gp78 knockdown did not alter ERK1/2 phosphorylation or the expression of proteins known to regulate VLDL secretion and/or lipid metabolism (DGAT1, HMGCoA reductase, MTP, SREBP1a, PPARα and PPARγ). To our knowledge, the only demonstrable similarity between the gp78 knockdown and U0126 are the effects on apoB-100 ubiquitination and VLDL secretion. The ERAD pathway degrades a large portion of nascent apoB and this can increase further when ubiquitination is enhanced (Liang et al., 2003). Since reduction of apoB ubiquitination enhances assembly, apoB substrates could be selected for ERAD

based on folding/assembly kinetics during or after translation and, as a result, prevent assembly at maximum capacity. Taken together these observations suggest that ERAD capacity and VLDL output may be linked.

In gp78 knockdown cells, newly synthesized apoB-100 was less accessible to the cytosol and secretion of both apoB-100 and TG were increased, suggesting that impaired ubiquitination influences both the topology of apoB-100 and lipid recruitment during VLDL biogenesis. If ubiquitin is ligated onto a cytosolic motif of translocation-arrested apoB-100, the branched apoB-ubiquitin conjugate could restrict translocation through the Sec61 channel. Conversely, lack of ubiquitination may allow apoB-100 to avoid prolonged exposure to the cytosol and increase the likelihood of successful translocation and VLDL assembly. The ERAD paradigm posits that recognition of malfolded protein substrates occurs prior to the involvement of ubiquitin ligase enzymes (Nakatsukasa and Brodsky, 2008). U0126 treatment enhances incorporation of TG into VLDL and in so doing may allow apoB to avoid translocation arrest and escape ERAD at the substrate recognition stage. Improved lumenal lipidation and decreased cytosolic exposure (presumably due to increased translocation efficiency) occur together when apoB escapes ERAD. Nevertheless, the location and molecular nature of the recognition event(s) remain(s) unclear. ApoB-100, because of its unique exposure to the cytosol during assembly, may not require the targeting and partial retrotranslocation steps required by most ERAD substrates before their ubiquitination (Vembar and Brodsky, 2008). If poorly lipidated apoB-100 is not ubiquitinated, it appears to be able to re-engage with the factors that support VLDL assembly, possibly displacing ERAD substrate recognition factors.

Our data suggests a regulatory role for ubiquitination in VLDL assembly. During biogenesis, a portion of the nascent apoB-100 may exist in an intermediate, uncommitted state: not fully secretion-competent, yet not terminally malfolded. ApoB-100 contains hydrophobic beta domains that bind strongly to lipids (Wang et al., 2009). Until the quality control surveillance machinery is satisfied with the status of these domains, it appears that apoB-100 must remain accountable to the ERAD pathway. ApoB-100 associates with the membrane during initial stages of assembly and then is released into the lumen during VLDL particle maturation (Adeli et al., 1997b; Dixon et al., 1992), coinciding with conformational changes in apoB in the Golgi (Gusarova et al., 2007). Cytosol-exposed apoB-100 has been observed in post-ER compartments after translation has been completed but perhaps before the final maturation step (Du et al., 1998). Release of apoB-100 into the lumen during particle maturation may release apoB from susceptibility to proteasome-mediated ERAD. Perhaps there exist basal levels of ubiquitination that do not trigger ERAD but can be extended or removed based on temporal quality control surveillance.

When p97 is reduced, apoB-100 proteins become arrested at the ER membrane due to limited retrotranslocation (Fisher et al., 2008). The accumulated apoB-100 apparently cannot re-enter the assembly pathway, since oleic acid supplementation during pulse-chase radiolabelling did not elicit additional apoB-100 secretion from si-p97 cells. However, apoB-100 can become secretion-competent if ERAD is blocked at the recognition or ubiquitination step (U0126 and gp78 knockdown, respectively). Since U0126 and gp78 knockdown normalized cellular apoB-100 turnover in si-p97 cells, our

observations suggest that the gp78-dependent ubiquitination of apoB-100 is the committing step of ERAD and that p97-mediated retrotranslocation occurs thereafter.

Gp78 is an integral membrane protein that can serve as a scaffold for the assembly of protein complexes that coordinate the ERAD of several substrates (Ballar and Fang, 2008). Gp78 can directly bind to and recruit p97 to the surface of the ER membrane (Zhong et al., 2004). It is possible that decreased gp78 expression alters the stoichiometry of dedicated ERAD complexes (containing p97 and other proteins) at the ER bilayer. However, it was recently reported that the expanded polyglutamine tracts of the huntingtin protein bind the Cue domain of gp78 and sterically hinder the gp78/p97 association but do not affect the ability of gp78 to ubiquitinate the huntingtin protein (Yang et al., 2010a). This suggests that the E3 ligase activity of gp78 does not depend on the formation of a p97-associated ERAD complex. Since the gp78 and p97 knockdowns have essentially opposite effects on apoB-100 fate, disrupted ubiquitination of apoB-100 is the probable cause of increased apoB-100 secretion in gp78-reduced cells.

The lack of ER stress in gp78-reduced cells may relate to the modest knockdown efficiency or may indicate that other ubiquitin ligases can partially compensate for decreased gp78 activity. The knockdown of p97 induces BiP expression to varying degrees depending on knockdown efficiency and cell type (Alzayady et al., 2005; Wojcik et al., 2006), indicative of UPR activation (Ron and Walter, 2007). In our system this stress appears to be relatively mild as it does not impair the synthesis or secretion of apoB-100 or apoAI. More severe levels of UPR activation have been shown to compromise the biogenesis of apoB-100 (Ota et al., 2008). When gp78 knockdown or U0126 treatment was superimposed upon si-p97 cells, BiP levels were lower than with

the p97 knockdown alone. Therefore, by modulating apoB-100 metabolism through distinct mechanisms, gp78 knockdown and U0126 are able to improve ER homeostasis in p97-reduced cells. This suggests that delayed apoB-100 turnover may be the major cause of the ER stress in p97 knockdown cells. Indeed, it was recently proposed that overproduction of the apoB-100 protein may be a "molecular link" between lipid-induced ER stress and hepatic insulin resistance (Su et al., 2009).

Hepatic apoB-100 secretion is of emerging relevance in the regulation of plasma LDL (Sniderman et al., 2009). The present study highlights the importance of a functional ERAD pathway in regulating levels of apoB-100 secretion from HepG2 cells. The liver, among other organs, displays an age-related decline in protein quality control, including decreased ability to induce expression of heat shock proteins, including Hsp70 and Hsp90 (Calderwood et al., 2009; Tower, 2009). With aging, compromised quality control and decreased ubiquitination could contribute to the overproduction and secretion of apoB-100. It would be interesting to examine how pathological conditions that arise in the liver affect the capacity to degrade apoB-100 by ERAD.

In conclusion, our work suggests that ubiquitination of apoB-100 has a regulatory role during VLDL assembly in HepG2 cells. Moreover, gp78 acts before and independently of p97 in the same apoB-100 ERAD pathway. Taken together our data implicates ubiquitination as the committing step of apoB-100 to ERAD, without which the nascent protein can proceed to assemble mature VLDL.

4.4 Updated Model

To summarize these findings since their initial publication, a model depicting the dynamic interaction between apoB ubiquitination and VLDL assembly is presented in Figure 4.12. This model was serves to describe the hypotheses that resulted from these studies.
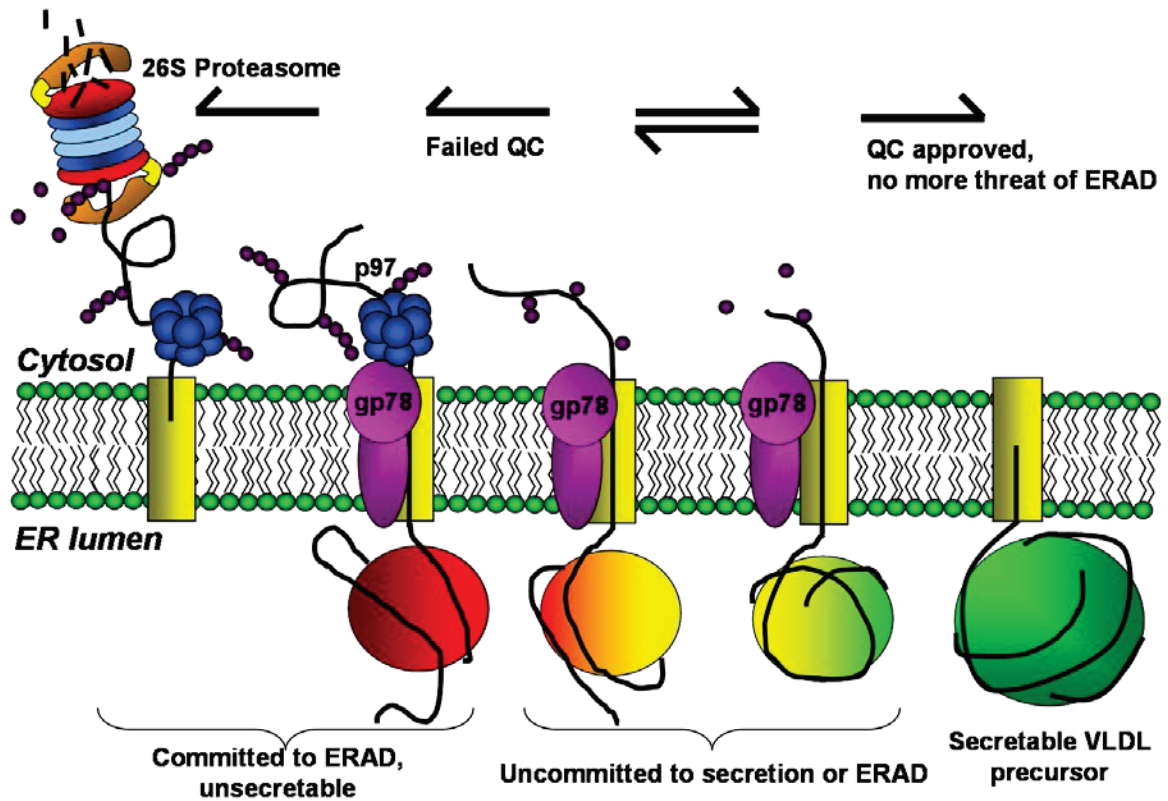
Figure 4.12. Cartoon representation of apoB-100 ERAD. Updated model of apoB-100 degradation based on the results presented in Chapters 3, 4 and 6. For simplicity, many known ERAD components have been omitted. This cartoon illustrates the theory that nascent apoB-100 remains uncommitted to ERAD or secretion for a period of time, while attempting to assembly into a secretion-competent particle. During this time window, apoB-100 is exposed to the cytosol, perhaps to a degree that is inversely proportional to the amount of luminal lipidation that is occurring. ApoB-100 may become ubiquitinated while in juxtaposition to cytosolic ERAD components, but will only provoke retrotranslocation by p97 once chains of at least four ubiquitin moieties form. In this scenario, a balance between ubiquitin ligase and deubiquitinases activity, influenced by apoB-100 lipidation/cytosolic exposure, contributes to ERAD substrate selection or "QC approval", allowing the nascent particle to proceed to downstream checkpoints in the secretory pathway.

CHAPTER 5 – IDENTIFICATION OF NOVEL APOB-INTERACTING PROTEINS BY FUNCTIONAL PROTEOMICS

5.1.1 Introduction

The degradation of apoB-100 is a complex process requiring coordination among machinery that spans several cellular environments. The delivery of secretion-incompetent apoB polypeptides from the ER to the proteasome has been shown to require proteins from the ER lumen, ER membrane, cytosolic lipid droplet, cytosolic proteins and the cytosolic 26S proteasome (together forming the ERAD pathway). Alternatively, lysosomal disposal of apoB can mobilize the autophagy machinery for the regulated removal of apoB from the secretory pathway (PERPP pathway) (Pan et al., 2008). While the proteolytic endpoint of ERAD substrates inside the 20S proteasome core is well documented, our understanding of the entire apoB ERAD pathway is by no means complete. For example, the mechanism of substrate recognition remain particularly mysterious for most ERAD substrates, apoB included. The identity of a putative ER-membrane retrotranslocation channel has proven to be elusive and remains a significant technical and conceptual challenge. And while several known proteins are implicated in the disposal of hydrophobic, misfolded apoB, there are major question marks throughout the apoB degradation pathway(s), and for most ERAD substrates.

With advances in protein purification technologies, mass spectrometry and protein sequence databases (such as SwissProt), functional proteomics has become an increasingly affordable and attractive means by which to identify novel protein-protein interactions. These experiments represent a powerful marriage of techniques that can reveal entire interactomes, using a chosen target protein as bait. Positive "hits" often

serve as a means to an end, in that the protein-protein associations can provide candidates, but must be confirmed by additional methods. Furthermore, a functional relationship is by no means guaranteed simply because two proteins are found in the same place under a specific experimental condition. With these caveats in mind, I set out to identify apoB-associating proteins specific to the ERAD pathway.

ApoB-100 is both a secretory protein and ERAD substrate, with unique properties such as the need for lipid ligands and transient exposure to the cytosol. The quality control process that monitors VLDL assembly maintains a certain portion of cellular apoB in a cytosolically exposed state during early stages of assembly, until the lipoprotein is freed from association with the membrane by release into the lumen of the secretory pathway. ER-associated, ubiquitinated apoB is detectable in low amounts in the absence of proteasome inhibition (Figure 4.1D). This basal level of ubiquitinated apoB may represent the steady state level of not-yet degraded apoB, or alternatively, may signify that ubiquitin is reversibly attached to apoB during transient exposure to the cytosol. Notably, MEK inhibition (by U0126 treatment) enhances VLDL assembly and almost abolishes this Ub-apoB pool. Since apoB ubiquitination, by definition, must occur in the cytosol, identification of target lysines will reveal information about apoB topology during VLDL assembly, an area that remains poorly understood.

The potential existence of reversible, lipid-sensitive apoB ubiquitination begs several questions. What sort of ubiquitination profile does secretion-competent apoB possess? Through what lysines are the ubiquitin chains linked? Is there a deubiquitinating enzyme with a particular affinity for apoB-ubiquitin conjugates? Are the ubiquitinated

lysines identifiable by mass spectrometry? This project was an exercise in application of new technologies and techniques to address these gaps in apoB metabolism.

There are virtually no data describing apoB ubiquitination at any level of detail beyond immunoblot analysis. I have made steps toward establishing a proteomics-based approach to characterize apoB ubiquitination. Proteasome substrates typically possess polyubiquitin chains of at least four lysines linked through lysine 48 (K48). While canonical proteasome substrates are tagged with ubiquitin on specific lysine residues, there are many notable exceptions to this, especially with substrates whose ubiquitination may serve a regulatory purpose (Liu and Walters, 2010). Diversity is found even within one substrate species. The inositol 1,4,5-triphosphate receptor is an ERAD substrate that undergoes regulated degradation in response to changes in cellular calcium (Wojcikiewicz et al., 2009). Ubiquitin linkages through K48 and K63 are found on the receptor, with K48 being necessary for ERAD of the receptor, and the function of K63 being completely unknown (Sliter et al., 2011).

Analysis of protein ubiquitination by mass spectrometry (MS) exploits a unique characteristic of this post-translational modification. MS analyses of proteins are often initiated by proteolytic digestion of sample proteins (usually with trypsin). Trypsin cleaves polypeptides at the carboxyl side of the positively charged amino acids arginine and lysine (unless followed by proline). However, if a lysine has been conjugated with ubiquitin (in the form of an isopeptide bond), trypsin can no longer cleave at this specific lysine. Because of this, tryptic digests of ubiquitinated proteins generate different peptide profiles than their non-ubiquitinated counterparts. In addition, ubiquitin monomers contain an arginine three residues away from the C-terminus that is covalently bound to

122

the target substrate. In between the isopeptide bond and this arginine lie two glycine residues. After trypsin digest, ubiquitination sites that have had their ubiquitin moiety cleaved will possess a diglycine ubiquitin-remnant or "signature". These unique traits have been exploited to identify endogenous ubiquitination sites on many proteins (Xu and Peng, 2006).

5.1.2 Approach

I have demonstrated an ERAD-specific interaction between p97 and apoB (Fisher et al., 2008). This was accomplished by treating HepG2 cells with or without the proteasome inhibitor MG132 for one hour followed by cell harvest in non-denaturing immunoprecipitation (NDIP) buffer. Immunoblot analysis of the subsequent apoB IP revealed the p97-apoB interaction to be MG132-specific, co-IP only occurred when the proteasome was inhibited. Permeabilization of HepG2 cells with digitonin revealed that apoB ERAD substrates accumulated in both the cytosol and ER during the proteasome blockade. I then recognized that staining a gel containing these samples would reveal protein bands unique to the MG132-treated cells. The MG132-specific bands might include apoB-associated proteins that participate in apoB ERAD. Excision of these bands and identification of the proteins by mass spectrometry would have the potential to unveil novel apoB-associating ERAD components. Further, direct analysis by MS of apoB collected from MG132-treated cells may reveal ubiquitination sites.

5.2 Results

5.2.1 Establishing Functional Proteomics as a Means to Identify ERAD-Specific ApoB-associated Proteins

ApoB is removed from the ER by the ERAD machinery and rapidly degraded in the proteasome, such that interactions between apoB and known ERAD components p97 and Hsp70 are barely detectable under steady-state conditions in HepG2 cells. The proteasome inhibitor MG132 was employed under the assumption that a proteasome blockade and the subsequent accumulation of intracellular apoB ERAD substrates would prolong, enhance and preserve the association of apoB with the degradation machinery. MG132 is a reversible, competitive inhibitor of catalytic subunits of the 20S proteasome. A one hour treatment with 25 μM MG132 was optimal for these experiments because it induces large amounts of apoB-100 and ubiquitinated apoB to accumulate (Fisher et al., 2008). The apoB-ubiquitin signal visualized by immunoblot analysis of apoB IP elutions reached a maximum after approximately one hour and gradually declined thereafter (for an example, see Figure 6.4). The later decrease in ubiquitinated apoB may arise for several reasons: the Ub-apoB is degraded by another mechanism, or MG132 loses its efficacy and the proteasome regains activity, or the accumulated apoB pool becomes deubiquitinated. Additionally, longer periods of proteasome inhibition enhance the clearance of accumulated proteasome substrates via autophagy and activates the Heat Shock Response (Bush et al., 1997; Ding et al., 2007; Janen et al., 2010; Liao et al., 2006). Thus, long-term proteasome blockade has the potential to cause protein interactions not specific to the apoB ERAD pathway.

MG132 and DMSO-treated HepG2 cells were collected in a non-denaturing immunoprecipitation buffer (NDIP), followed by an overnight incubation with a polyclonal anti-apoB antibody and protein A Sepharose beads. IP elutions were resolved by 10% acrylamide gel. Gels were then incubated in fixing solution, washed and then placed in staining solution in the presence of the colloidal stain Coomassie Brilliant Blue G250 for 3 days to allow maximum protein staining. Gel staining revealed multiple protein bands that are distinct to the MG132-treated cells (Figure 5.1A). In the initial trial experiment several "bands of interest" were excised from the gel and prepared for analysis by LC-MS/MS at the DalGen Proteomics facility (see sections 2.1.13-17 for methods). Several more analyses were performed on MG132-treated cells using large 5%, 7.5%, 10% and 15% acrylamide gels to resolve proteins across all molecular mass ranges.

Summarized in Figure 5.2 are proteins identified by MS from these experiments. Among the proteins identified were two proteasome subunits, Rpn2 and Rpn3, which are components of the base and lid of the 19S regulatory cap, respectively (Wang et al., 2007). I also identified the cytosolic chaperone Hsc71 and its inducible form Hsp70. These heat shock proteins are known to participate in apoB-100 ERAD (Gusarova et al., 2001; Zhou et al., 1995). The retrieval of 19S proteasome cap subunits and Hsp70 validated this approach to discovery of ERAD-specific apoB-associated proteins. It also suggested that while MG132 blocked proteolytic activity within the 20S proteasome core, at least some apoB protein in the immunoprecipitation may have been delivered to the mouth" of the 20S core.
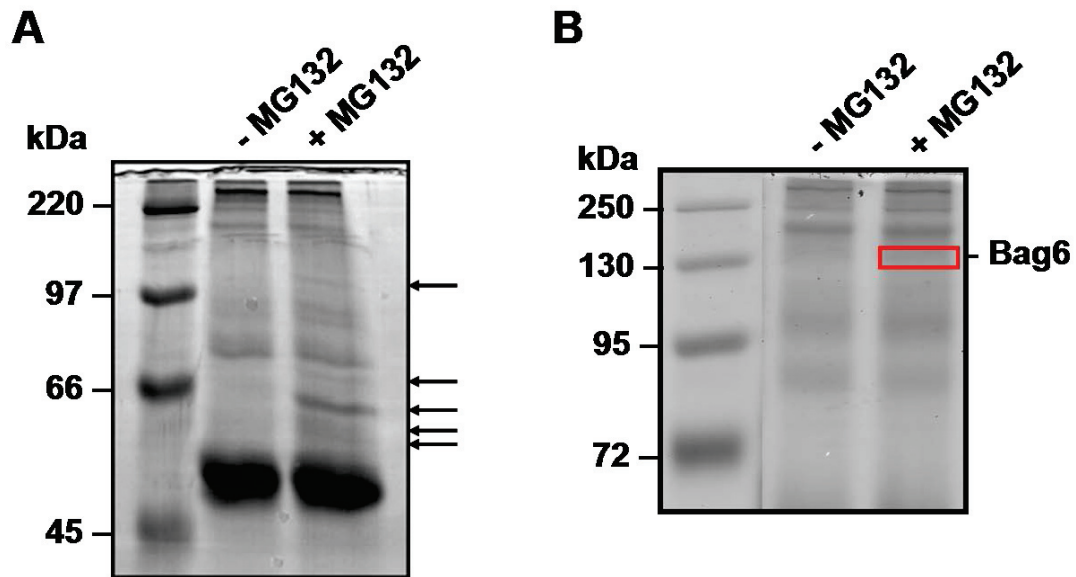
Figure. 5.1. Identification of ERAD-specific apoB-associating proteins by mass spectrometry analysis of excised bands of interest. HepG2 cells grown in 10 cm dishes were treated for 1 h with 25 μM MG132 or DMSO. Cells were harvested under non-denaturing conditions (NDIP buffer). Following the removal of insoluble cell debris by centrifugation, apoB (and any associated protein) was collected by overnight immunoprecipitation. IP elutes were resolved by 10% SDS-PAGE and gels were stained for 3 days using Coomassie Brilliant Blue G 250. Bands that were increased in strength or unique to the MG132-treated were excised under sterile conditions and delivered to the DalGen proteomics facility. Samples were subject to tryptic digest and analysis by LC-MS/MS. Experimental peptides were identified by comparison to protein fragments in the SwissProt database. **A**. Representative image of a stained gel. Bands of interest are highlighted by the black arrow **B**. The gel from which Bag6 was identified (from an excised gel slice, represented by a rectangle in the *+MG132* lane).
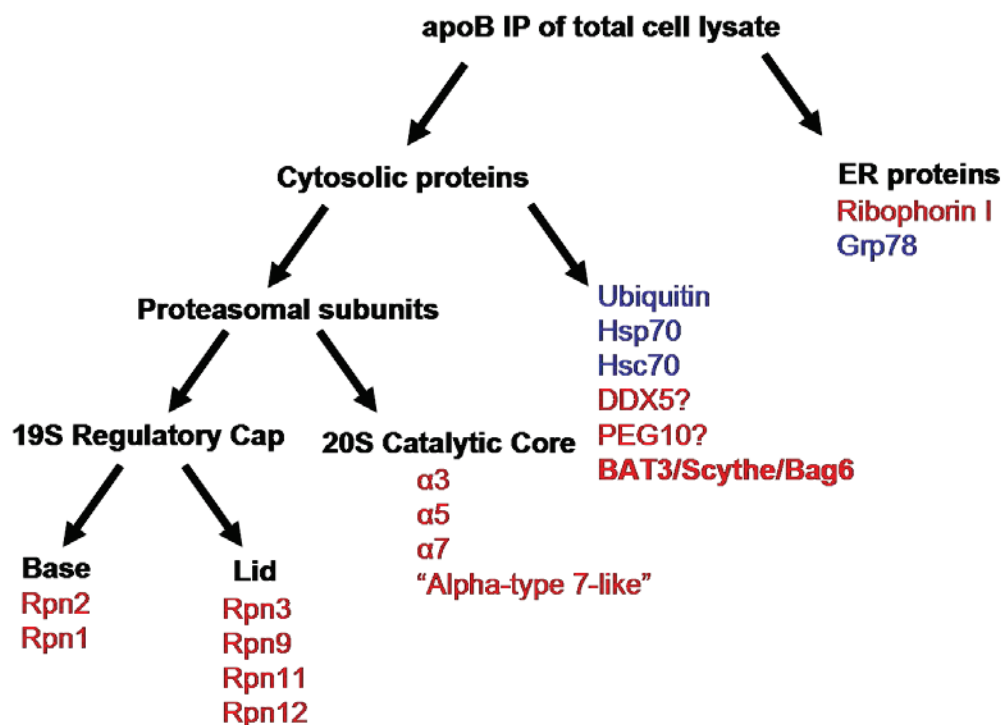
Figure 5.2. Summary of apoB-associating proteins identified from HepG2 cells by mass spectrometry. Listed in this figure are apoB-associating proteins identified from gel slices by LC/MS-MS. The proteins have been separated by subcellular location, and for simplicity, proteasomal subunits separated further into their respective location within the 26S proteasome structure. The proteins listed in blue font have been reported in the literature to associate with apoB. Proteins listed in red front were identified by the functional proteomics experiments as relevant apoB ERAD-specific candidates.

Further exploration of the ERAD-specific apoB interactome revealed not only additional subunits of the 19S cap, but also members from within the 20S core. Not all of these subunits are involved in substrate binding. Therefore, I speculate that the non-denaturing conditions of the IP may be purifying intact, apoB-associated proteasomes. Bag6/BAT3/Scythe, predicted to be 119 kDa, was identified from a gel slice taken near the 130 kDa marker (Figure 5.1B). The functional role of Bag6 in both the ERAD pathway (Claessen and Ploegh, 2011) and trafficking of proteasome substrates (Wang et al., 2011) provoked further investigation of this interaction.

5.2.2 Validation of the Bag6-apoB Association by Immunoblot Analysis

Using a commercial anti-human Bag6 antibody, the association between apoB and Bag6 in HepG2 cells was validated by immunoblot analysis (Figure 5.3). Neither the anti-apoAI IP or the non-immune goat serum control IP displayed any Bag6 signal, indicating that association detected by this technique was apoB-specific. Also, the Bag6.apoB association was detectable only in MG132-treated cells, suggesting the band that appeared in the total gel stain was likely ERAD-specific. Further analysis of the functional relationship between Bag6 and apoB is presented in Chapter 6.

5.2.3 Differential Solubility of Cellular ApoB in Non-ionic and Ionic Detergents

Anti-apoB immunoprecipitation with a polyclonal antibody yields a diverse set of peptide species. The anti-apoB elutions contain full-length apoB-100, smaller sized co-translationally truncated apoB ERAD substrates and partially proteolyzed degradation products. As well, the greater-than full length apoB-100 peptides that are ubiquitin-
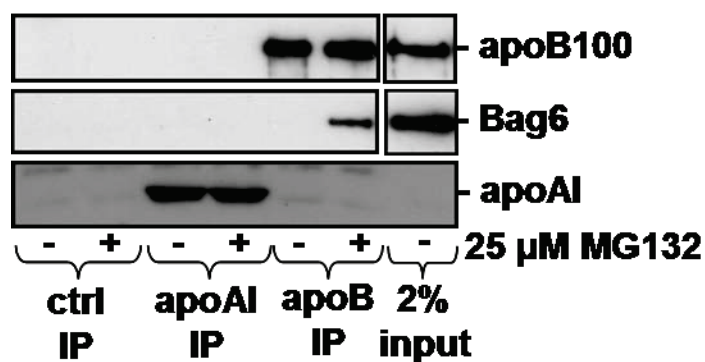
Figure 5.3. Validation of the MS-detected Bag6.apoB association by immunoblot analysis. HepG2 cells grown in 10 cm dishes were treated for 1 h with 25 μM MG132 or DMSO. Cells were harvested under non-denaturing conditions (NDIP buffer). Following the removal of insoluble cell debris by centrifugation, apoB was collected by overnight immunoprecipitation with either non-immune goat serum (*ctrl*), anti-apoAI or anti-apoB antibody. Immunoprecipitate and input samples were resolved by SDS-PAGE and proteins were visualized by immunoblot analysis.

positive likely represent poly-ubiquitinated ERAD substrates (for example, see figure 4.1C and D). I used 2D electrophoresis and MS technology to analyse ubiquitinated apoB. The heterogeneity of apoB peptides warranted testing the relative solubility of apoB in different buffer systems prior to performing 2D electrophoresis and MS experiments.

Ionic detergent-containing samples are not compatible with the isoelectric focusing step (ie- the 1st dimension) because the presence of a charged detergent will interfere with the migration of proteins to their native isoelectric point (pI). Thus, I compared the yield of total apoB and ubiquitin-positive apoB in SDS and an uncharged detergent (Nonidet P-40 (NP-40)) containing buffer. Buffer comparison was performed by harvesting HepG2 cells in either 1% SDS-RIPA buffer or NDIP buffer. Aside from those detergent components, the buffers were similar, with the other difference being that SDS-RIPA additionally contains 1% Triton X-100 and NDIP contains 20% sucrose. Following the IP in either 0.1% SDS-RIPA or NDIP buffer, proteins were released from the protein A Sepharose beads by either boiling the samples in 2x sample buffer containing β-mercaptoethanol or by 30 minute incubation at room temperature in 1.5x isoelectric focusing (IEF) buffer. The 2x sample buffer contains SDS and is used for immunoblotting analysis of fully denatured protein samples. A recipe for 1.5x IEF buffer was adapted from the 1x IEF buffer (the IEF buffer components were not fully soluble at 2x concentrations) to attempt IP elutions into volumes and buffer concentrations suitable for the IEF protocol.

Figure 5.4 is an immunoblot analysis of apoB and ubiquitin from anti-apoB IP samples from cells treated with or without MG132, as well a non-IP input samples. The
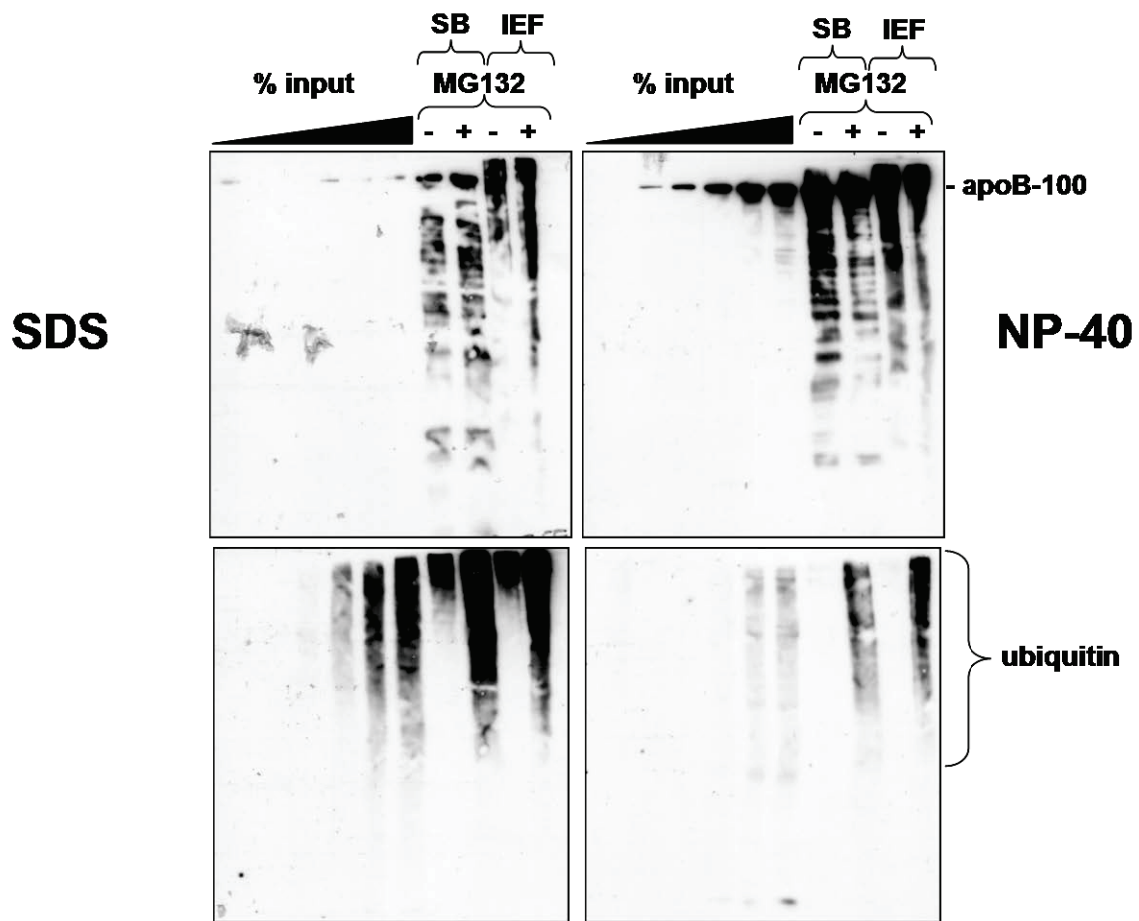
Figure 5.4. Differential solubility of full length apoB-100 and ubiquitinated apoB species between ionic and non-ionic detergents. HepG2 cells were treated for 1 h with 25 μM MG132 or DMSO. Cells were harvested in either SDS (*left panels*) or NP-40-containing buffer (*right panels*). ApoB was immunoprecipitated overnight from the cell lysates and was eluted from the beads with either 2x sample buffer (**SB**) or 1.5x isoelectric focusing (**IEF**) buffer. Separate samples (MG132 treated) were reserved for the "**% input**". Samples were resolved by 5% SDS-PAGE followed by sequential analysis of ubiquitin (*lower panels*) and apoB (*upper panels*) by immunoblotting.

131

chemiluminescence signal from the anti-ubiquitin antibody is orders of magnitude weaker than apoB, therefore the membranes were first probed for ubiquitin and then reprobed for apoB the following day. Inputs from the pre-IP samples were loaded at five percentages ranging from 0.25% to 7.00%. The left and right panels of Figure 5.4 (SDS and NP-40, respectively) were exposed for the same time period, on the same film. Remarkably, the NDIP buffer yields far more full-length apoB-100 than 1% SDS-RIPA samples (top panels), while much more ubiquitinated apoB appears with SDS than without (lower panels). The same trend was observed when the two buffers were used following the apoB IP, regardless of whether sample buffer (SB) or IEF buffer is used to elute the protein. Notably, the resolution of full length apoB-100 is obscured by eluting samples into IEF buffer instead of SB buffer (top panels, SB vs. IEF), suggesting that apoB-100 is not fully denatured by the IEF elution conditions. IEF buffer elution does not seem to affect the anticipated anti-ubiquitin "smear" commonly observed following 1 hour MG132 treatment.

The differential solubility of full length apoB-100 and the heterogeneous ubiquitin-positive apoB pool has been observed repeatedly. SDS-containing buffers were clearly superior at solubilizing ubiquitinated apoB, but they are not compatible with 2D electrophoresis protocol. Thus, I decided to transition from SDS to NP-40 over the course of the IP washes. I harvested the cells and performed the anti-apoB IP in the presence of SDS, and performed the five bead washes in NDIP buffer to remove the SDS. Figure 5.5 demonstrates that transitioning from SDS to NDIP preserved the pool of ubiquitin-positive apoB (Figure 5.5, right panel, SDS vs S→N), while using NDIP buffer throughout yields relatively little ubiquitinated apoB following cell harvest (right panel,
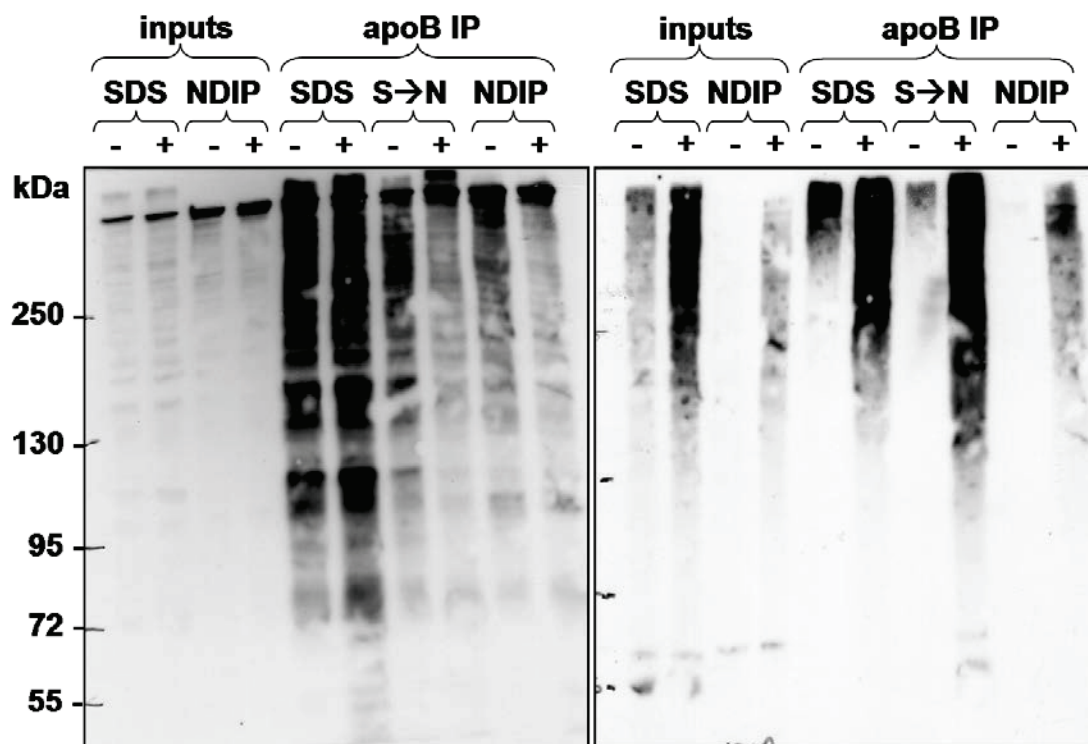
Figure. 5.5. The SDS required at cell harvest may be removed by washing prior to post-IP protein elution without compromising the high yield of ubiquitinated apoB. HepG2 cells were treated for 1 h with 25 µM MG132 or DMSO. Cells were harvested in either 1% SDS-RIPA buffer or NDIP buffer. ApoB was immunoprecipitated overnight from the cell lysates in the presence of the same detergent as the harvest. 5x washes were conducted this way as well except for the S→N samples, which were incubated during the overnight IP in 0.1% SDS-RIPA and then were subject to NDIP buffer during the washes to remove the SDS. Samples were eluted into 2x sample buffer. Separate samples (MG132 treated) were reserved for the "% input" analysis. Samples were resolved by 5% SDS-PAGE followed by sequential analysis of ubiquitin (*right panel*) and apoB (*left panel*) by immunoblotting.

inputs: SDS vs NDIP) and the apoB IP (right panel, apo IP: SDS vs NDIP). Taken together, these data suggest that performing the cell harvest and IP in 1% SDS-RIPA followed by transitioning to NDIP buffer during the washes enables a sufficiently high yield of ubiquitinated apoB that is compatible with the buffer requirements for 2D gel electrophoresis analysis.

5.2.4 Resolution of Ubiquitinated ApoB by 2-dimensional Acrylamide Gel

I learned these 2D gel techniques with the assistance of Craig Steeves, a Masters student at the time in the Bearne lab. A detailed protocol can be found in section 2.1.14. For the isoelectric focussing step (1st dimension), an acrylamide gel strip with a pH gradient of 3-10 was chosen as a starting point. Following the overnight separation of sample proteins by charge, the strip was subjected to stepwise reduction and alkylation and then resolved on a 5% acrylamide gel and then transferred to nitrocellulose membrane for immunoblotting.

Two-dimensional gel analysis reaffirmed that the SDS-containing buffer is superior to NP-40 at yielding ubiquitinated apoB and the MG132-induced species with varying isoelectric points (Figure 5.6 VS 5.7). With the NP-40 samples, MG132 treatment somehow decreased the overall intensity of the apoB signal compared to DMSO alone, in spite of the ubiquitin-positive smear appearing in the lower weight regions (Figure 5.7). An important observation is that the ubiquitin-positive patterns on the blots from the SDS and NP-40-containing samples are almost mutually exclusive (ie-they yield distinct pools of apoB that do not overlap). SDS yields high molecular weight Ub-apoB, while NP-40 reveals lower molecular weight species that are not observed in
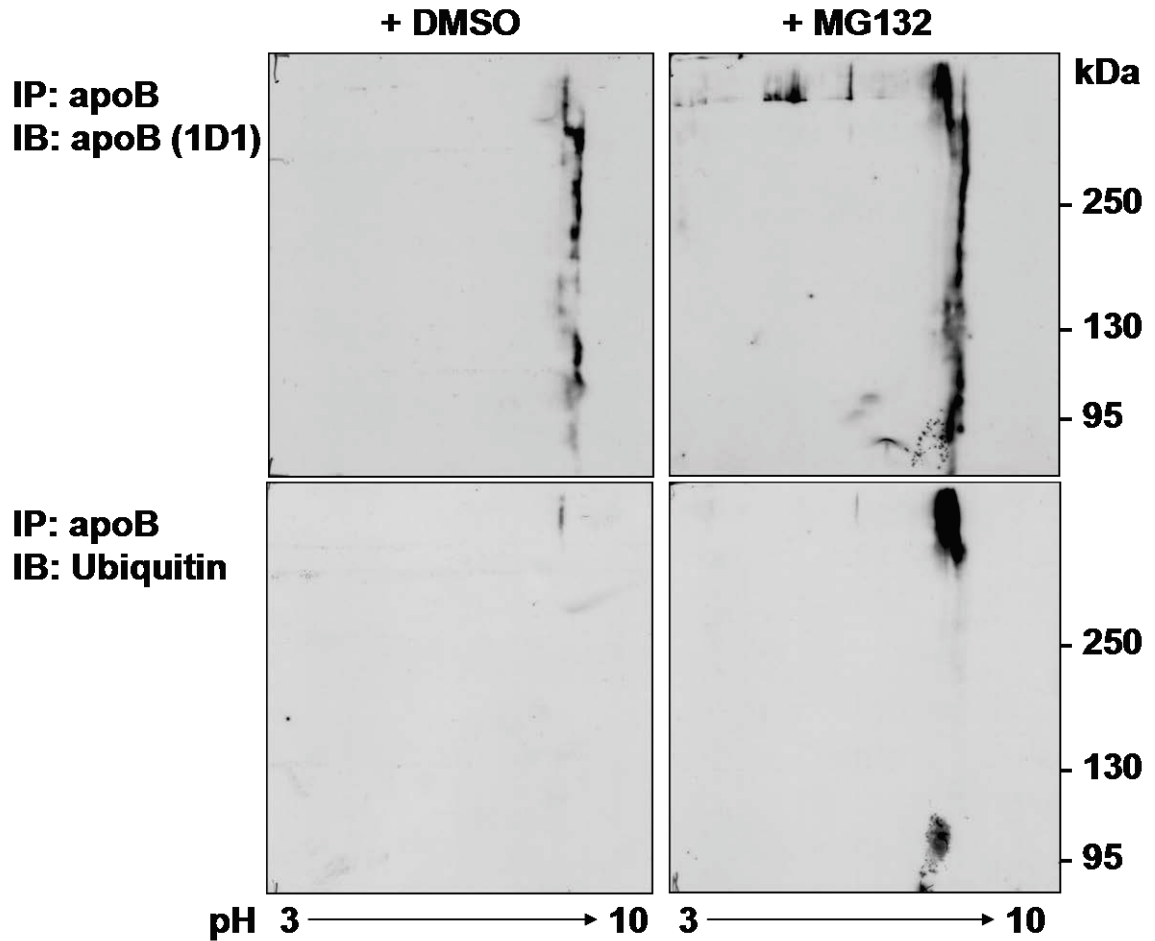
Figure 5.6. ApoB-100 ubiquitination from cells harvest in SDS as seen by 2 dimensional gel electrophoresis. HepG2 cells were treated for 1 h with 25 μM MG132 or DMSO. Cells were harvested in 1% SDS-RIPA, then apoB was collected by IP from the cell lysate in 0.1% SDS-RIPA, but washed in NDIP buffer. ApoB was eluted from the beads with 1.5x isoelectric focusing (IEF) buffer. Samples were resolved by isoelectric focusing on pH 3-10 strip followed by 5% SDS-PAGE. Proteins were then transferred to a nitrocellulose membrane and ubiquitin and apoB were sequentially visualized by immunoblotting.

135
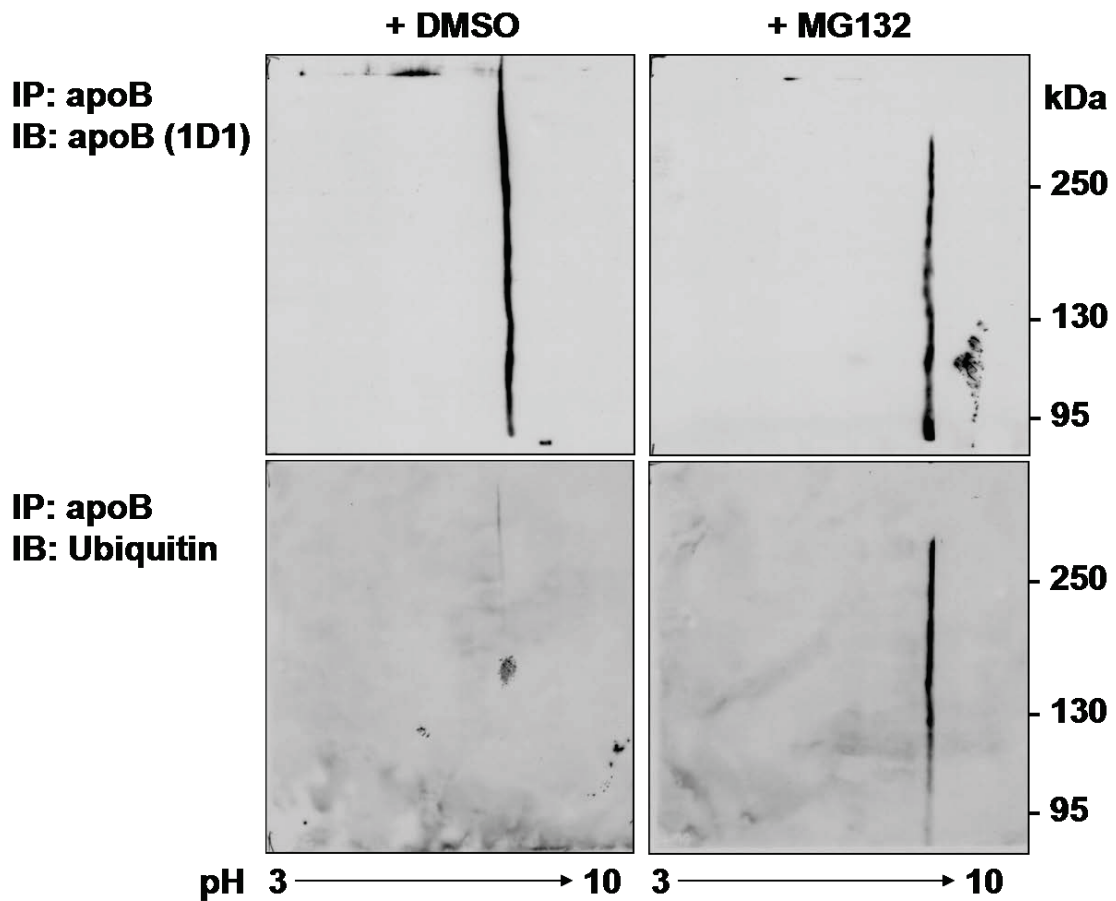
Figure 5.7. ApoB-100 ubiquitination from cells harvest in NP-40 as seen by 2 dimensional gel electrophoresis. HepG2 cells were treated for 1 h with 25 µM MG132 (*right panels*) or DMSO (*left panels*). Cell harvest, apoB IP and washes were performed in NDIP buffer. ApoB was eluted from the beads with 1.5x isoelectric focusing (IEF) buffer. Samples were resolved by isoelectric focusing on pH 3-10 strip followed by 5% SDS-PAGE. Proteins were then transferred to a nitrocellulose membrane and ubiquitin (*lower panels*) and apoB (*upper panels*) were sequentially visualized by immunoblotting.

136

the SDS-containing samples. Neither buffer alone provides a complete picture of intracellular apoB ubiquitin conjugates, which is something to bear in mind when drawing conclusions from these types of studies.

Figure 5.8 displays apoB and ubiquitin blots from an IP with a higher protein yield than in Figure 5.6. Full-length apoB-100 species display a range of isoelectric points. This may represent the effects of various post-translational modifications (PTMs) that influence the net charge of the protein. Notably, the distribution of apoB-100 along the pH range is changed by MG132 treatment (Figure 5.8, top panels, left vs. right). The anti-ubiquitin blots contain a ubiquitin-positive smear in the same region, not unlike that seen with standard 1D SDS-PAGE immunoblots of these samples. Notably, the ubiquitin signals that appear toward the pH 3 side of the gradient overlap with a distinct pattern of apoB at the same place on the membrane, indicating that these are ubiquitinated apoB species also bearing isoelectric points unique to the MG132 treatment (Figure 5.8, lower right panel). Also worth noting is that ubiquitinated apoB is readily detectable even without the proteasome blockade, consistent previous with 1D immunoblots.

5.2.5 Attempts to Detail ApoB Ubiquitination by Mass Spectrometry

To determine whether ubiquitin remnants were detectable on apoB collected from MG132-treated HepG2 cells, sections of 5% acrylamide gels were excised at the MW of apoB-100, as well as above and below the location of the full-length protein. The polypeptides contained in the excised gel slices were subject to trypsin digest, followed by analysis by LC-MS/MS. One sample had 23% sequence coverage of full length apoB-100, with sequence coverage scattered throughout the entire apoB-100 protein sequence.
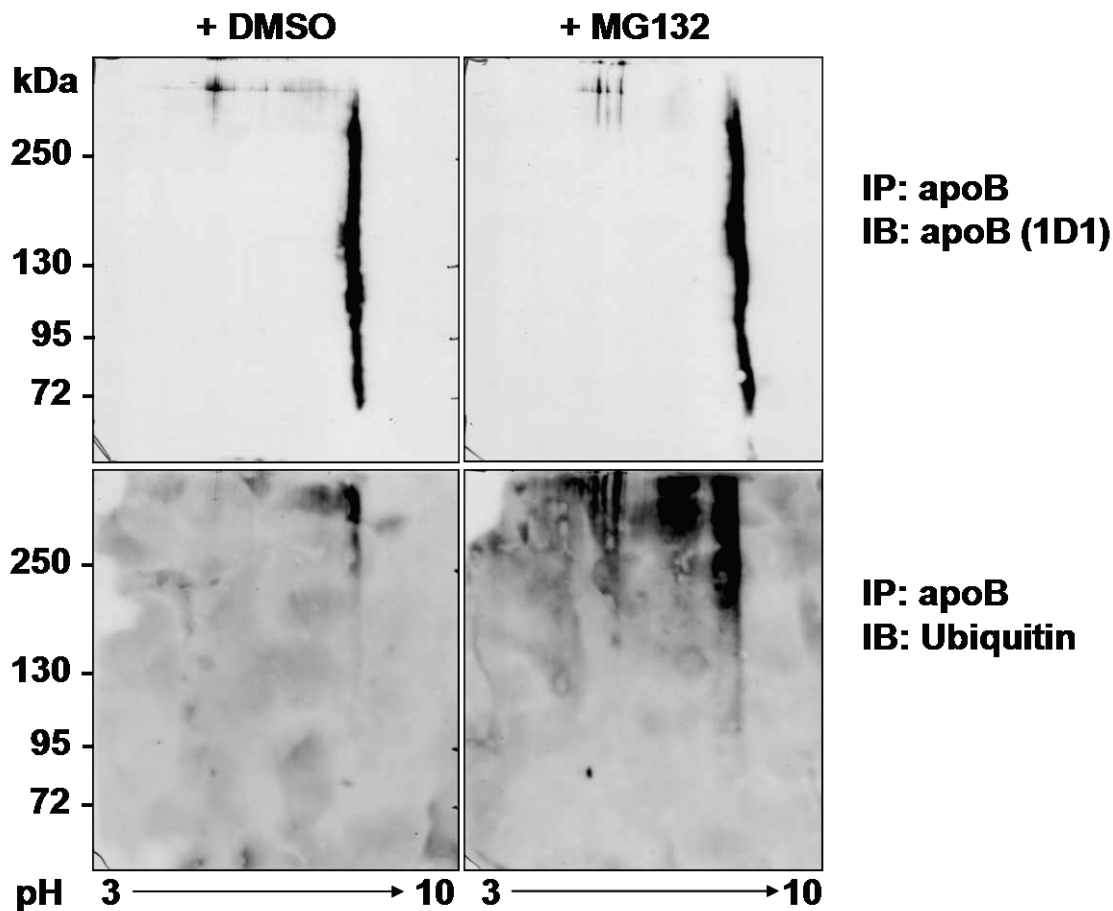
Figure 5.8. ApoB-100 ubiquitination profiles viewed by 2 dimensional gel electrophoresis. HepG2 cells were treated for 1 h with 25 µM MG132 (*right panels*) or DMSO (*left panels*). Cells were harvested in 1% SDS-RIPA, then apoB was collected by IP from the cell lysate in 0.1% SDS-RIPA, but washed in NDIP buffer. ApoB was eluted from the beads with 1.5x isoelectric focusing (IEF) buffer. Samples were resolved by isoelectric focusing on pH 3-10 strip followed by 5% SDS-PAGE. Proteins were then transferred to a nitrocellulose membrane and ubiquitin (*lower panels*) and apoB (*upper panels*) were sequentially visualized by immunoblotting.

Interestingly, the apoB from residues 1800-2400 was very well represented in the sequence coverage, relative to other regions. Unfortunately, no 114.1 Da diglycine ubiquitin remnants, or skipped cleavage sites, were found on any fragments. Future efforts may be more fruitful, in light of the significantly more powerful MS instrument now in use at the DalGen proteomics facility. Increased resolution will likely yield increased numbers of discreet, unique peptides that could not be resolved by the previous generation of MS instruments. As well, exploring alternative means of purifying apoB-ubiquitin conjugates may increase the representation of Ub-apoB in samples.

5.3 Discussion

The incorporation of proteomics techniques has been a rewarding learning experience. Many known ERAD components and chaperones were found to associate with apoB during proteasome inhibition. Since detecting its association with apoB, Bag6 has emerged to play a novel role in HepG2 production of apoB-100 (presented in Chapter 6). These methods may now be expanded and adapted to test new hypotheses. The importance of detergent choice during protein isolation has been highlighted by my efforts to develop 2 D electrophoretic apoB profiles. Although I was unable to discover detailed information on apoB ubiquitination, I am confident that improvements to sample preparation conditions, and technological advancements in mass spectrometry, will yield these data in the future.

It is important to note that this project sought to identify novel participants in apoB ERAD via mass spectrometry without placing significant weight on the sequence coverage or score of the positive hits. A more comprehensive proteomics project would

rely on stringent criteria to accept or reject the validity of the MS results, whereas I was specifically looking for novel protein interactions. The goal was to identify novel targets and determine the functional relevance of these protein-protein associations with further experiments. The intention to validate the results by other methods diminished the need to put statistical weight on the sequence coverage and scores of the identified proteins.

It is worth noting that preliminary MS results contained significant amounts of β-keratin type proteins, implying that I was contaminating the samples. Under the guidance of the MS technician Elden Rowland, I successfully reduced β-keratin levels in my samples by adopting a stringent protocol to collect gel slices under sterile conditions (section 2.2.16). However, some of the MS results are likely false positives based on their function documented in the literature (proteins localized to the nucleus, for example). This suggests that my protocol for sample purification could be further optimized as well. As well, the singular pI of the heterogeneous apoB species seen in the 2D gels immunoblots is a sign that the IEF is unable to resolve these heterogeneous peptides to their native pI. Future efforts could employ partial trypsin digest of cell lysates to generate smaller, more soluble apoB fragments. A similar approach has been used prior to 2D gel analysis of conformation changes in apoB-100 collected from HepG2 medium (Manocha et al., 2009).

Regarding the MS analysis of ubiquitination, several methods may be used to further these studies. For example, reagents such as Tandem Ubiquitin Binding Entities (TUBEs) may yield higher amounts of purified, ubiquitinated apoB than the IP alone (Balut et al., 2011). In combination with the enhanced resolution of the new mass spectrometers, the likelihood of finding target lysines is higher with improved sample

preparation techniques. Ubiquitin chain linkages can be measured by Absolute quantification (AQUA) (Kirkpatrick et al., 2005), which uses stable isotope-labelled peptides of all seven possible –GG ubiquitin remnants as internal standards (Kirkpatrick et al., 2006). These peptides behave the same chemically as those ubiquitin remnants in the experimental samples, but are slightly heavier due to the presence of stable isotopes, thus shifting the mass/charge ratio slightly and allowing one to discriminate between the two species. Levels of each unknown lysine linkage can then be quantified against the known labelleed, internal standard. One can perform MS analysis with selected reaction monitoring (SRM) to enhance detection sensitivity. As alluded to in Chapter 1, all 7 possible linkages have been found *in vivo*, yet functional relevance of most of these is poorly understood. Ubiquitin chain remodelling and recognition by ubiquitin-binding proteins are rapidly expanding research areas. The regulatory functions of this post-translational modifier (and also ubiquitin-like proteins) continue to be revealed. When a detailed, dynamic view of apoB-100 ubiquitination is established, it will inform us more precisely of the role ubiquitin plays in apoB-100 quality control.

CHAPTER 6 – BAG6 ASSOCIATES WITH APOB IN HEPG2 CELLS AND FACILITATES EFFICIENT DEGRADATION AND SECRETION OF APOB

6.1 Introduction

Bag6, also known as BAT3 and Scythe, is found in the cytosol and nucleus of mammalian cells. Bag6 has become known as an ATP-neutral "chaperone holdase" that can maintain proteasome substrates in a soluble state (Wang et al., 2011). Bag6 demonstrates an affinity for substrates with relatively long exposed tracts of hydrophobic residues (Mariappan et al., 2010). Bag6 activity may allow cells to stabilize hydrophobic tracts and prevent energy-dependent chaperones such as Hsp70 from needlessly re-folding substrates already bound for degradation (Hessa et al., 2011; Wang et al., 2011). In the cytosol, Bag6 forms a trimeric complex with Ubl4A and Trc35 which together participate in promoting membrane integration of tail-anchored proteins (Leznicki et al., 2010; Mariappan et al., 2010). Bag6 also sequesters "mislocalized" ribosome-associated nascent polypeptides that do not properly engage the translocation apparatus at the ER membrane (Hessa et al., 2011). Another study showed that Bag6 substrates include newly synthesized defective ribosomal products, termed DRiPs (Minami et al., 2010). Trc35 is required to mask the nuclear localization signal of Bag6 such that it remains in the cytosol (Wang et al., 2011). Analysis of Bag6 function using overexpression is difficult because excess Bag6 traffics to the nucleus due the limiting amount of Trc35. Bag6 is recruited to the site of retrotranslocation of misfolded glycoproteins from the ER and appears to help prevent polypeptide aggregation prior to their degradation (Claessen and Ploegh, 2011). With these studies in mind, I investigated the potential functional relevance of Bag6 in the apoB-100 ERAD pathway.

Bag6 was identified by mass spectrometry and immunoblot analysis to be an apoB-associated protein following proteasome inhibition in HepG2 cells (see section 5.2.2). Further analysis revealed that Bag6 was associated with cytosolic apoB ERAD substrates. Reduced cellular Bag6 levels disrupted apoB metabolism in several ways, causing decreased apoB secretion efficiency, altered proteolysis of apoB, and prevention of improved apoB secretion efficiency after promoting VLDL assembly pharmacologically. These data highlight a possible role of Bag6 in the regulation of apoB at the protein quality control level. This chapter presents the results garnered from exploring the functional relationship between Bag6 and intracellular apoB-100 metabolism in HepG2 cells, discusses their significance and speculates on future studies that could delineate the role of Bag6 in VLDL production.

6.2 Results

6.2.1 Bag6 Associates with Cytosolic ApoB During Proteasome Inhibition

Immunoprecipitation analysis revealed that apoB and Bag6 associate almost exclusively during proteasome inhibition (Figure 5.3). To distinguish between the binding of Bag6 to cytosolic apoB or ER-associated apoB, cells were treated with MG132 and permeabilized with digitonin (which creates pores in cholesterol-rich membranes). Analysis of the cytosolic contents and membrane compartments revealed that Bag6 associated primarily with cytosolic apoB (Figure 6.1). This indicated that Bag6 associated with apoB that had been fully extracted from the ER.

In order to preserve transient protein-protein associations, a non-denaturing buffer was used to harvest the cells. The absence of ionic detergent in this harvest buffer renders
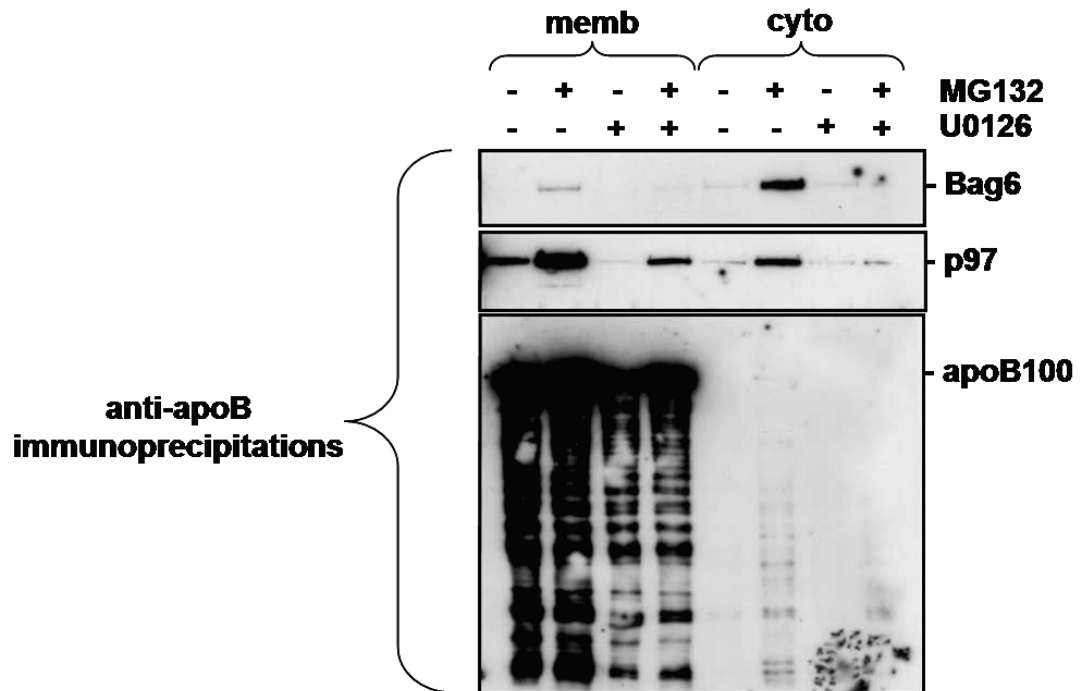
Figure 6.1. Bag6 associates with apoB in HepG2, particularly during proteasome inhibition. HepG2 cells were incubated with or without 25 µM MG132 for 1 h and then lysed into non-denaturing immunoprecipitation (NDIP) buffer. Where indicated, cells were pre-treated for 16 h with U0126. Cells were permeabilized with digitonin prior to harvest to allow separate analysis of cytosol (**cyto**) and membrane-bound contents (**memb**). Following clearance by centrifugation lysates were subjected to immunoprecipitation (IP) with an anti-apoB polyclonal antibody. IP elutions and lysate inputs were resolved by SDS-PAGE, transferred to nitrocellulose and visualized by immunoblotting.

a portion of ubiquitinated apoB insoluble (See Chapter 5 for details). Therefore a subset of ubiquitinated apoB is underrepresented in this type of this experiment compared to the yield with SDS-containing harvest buffers. Despite the relatively small amount of apoB in the cytosol generated during MG132 treatment, this pool associated with Bag6 to a much greater extent than membrane-associated apoB. Cytosolic apoB is spread across molecular weight ranges that are less than full-length apoB. These apoB species are likely comprised of truncated apoB polypeptides generated by cotranslational interruption of synthesis, rather than degradation products originating from the breakdown of full length apoB-100 or experimental artefacts.

Treatment of HepG2 cells with the MEK/ERK inhibitor U0126 enhances lipidation of apoB and allows for more efficient assembly of VLDL (Tsai et al., 2007). Normally HepG2 cells can secrete only LDL-sized particles, but U0126 treatment allows these cells to secrete VLDL-sized particles, similar to hepatocytes *in vivo*. It follows that there are fewer apoB ERAD substrates in U0126-treated HepG2 cells due to the improved efficiency of apoB secretion. The U0126-induced evasion of apoB-ERAD prevents its ubiquitination and in turn reduces the association between apoB and the retro-translocation mediator p97 (Figure 6.1). Similarly, Bag6-apoB association during proteasome inhibition is almost abolished by U0126 treatment (Figure 6.1). Notably, the majority of apoB-associated p97 is in the membrane fraction, whereas Bag6 associates with the cytosolic fraction. This suggests that Bag6 could participate in apoB ERAD downstream of the retrotranslocation step performed by p97.

6.2.2   Temporal Analysis of the Bag6-apoB Association by Puromycin-synchronization

To investigate the timing of the Bag6-apoB association I employed puromycin synchronization to directly monitor co-translational progress of apoB synthesis over short time intervals. Puromycin experiments have been used to monitor the growth of nascent, radiolabelled apoB peptides (Benoist and Grand-Perret, 1997). Figure 6.2 (left panels) demonstrates that this method allows detection of protein-protein associations between newly synthesized apoB and proteins of the ERAD machinery. As expected, Bag6 interacts with apoB only in the presence of MG132 (Figure 6.2, +MG132 vs –MG132). Only after 20 minutes does Bag6 detectably associate with apoB in this system. The cytosolic proteins Hsp70 and p97 associate with apoB 10 minutes after re-initiation of translation, with p97 requiring the proteasome inhibition to detectably associate with apoB throughout the hour. This is consistent with previous conclusions regarding the role of p97 during degradation of co-translationally generated apoB ERAD substrates (Fisher et al., 2008; Rutledge et al., 2009). In contrast, the ER resident chaperone BiP associates with apoB at every timepoint, regardless of MG132 inclusion. Interestingly, the pattern of the Hsp70-apoB association is also similar between –MG132 and +MG132 cells. Hsp70 has been proposed to facilitate both apoB secretion and degradation by way of maintaining the solubility of cytosolically exposed regions of apoB, which is believed to occur in both instances. However, it is worth noting that although Hsp70 associates with apoB in the non-puromycin treated cells in response to MG132, there is no increased co-translational binding during MG132 treatment in synchronized cells compared to control cells.
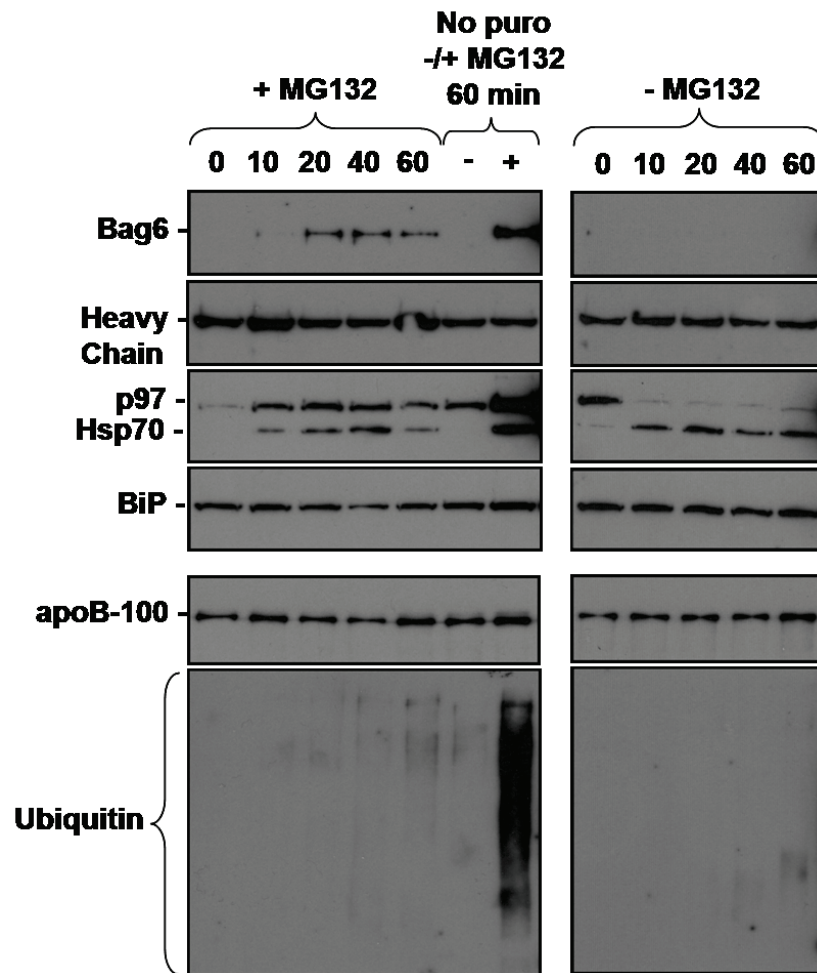
Figure 6.2. The Bag6-apoB association is time-dependent and is preceded by the p97-apoB association. HepG2 cells treated with puromycin for 10 minutes and then washed three times on ice for 10 minutes with fresh, puromycin-free media. Cells were then immediately brought to 37ºC in media containing either 25 µM MG132 or DMSO for up to 1 h and then lysed into non-denaturing immunoprecipitation (NDIP) buffer. Following clearance by centrifugation lysates were subjected to IP with an anti-apoB polyclonal antibody. IP elutions and lysate inputs were resolved by SDS-PAGE, transferred to nitrocellulose and visualized by immunoblotting. Samples treated with MG132 or DMSO and no puromycin were included to demonstrate the difference in the protein associations.

147

6.2.3 Cytosolic Turnover of Radiolabelled ApoB ERAD Substrates in Puromycin-Synchronized Cells

In the previous section, I presented blots depicting the temporal Bag6-apoB association in synchronized cells. The following section does not directly involve Bag6, but presents data that is relevant regarding the exact apoB pool with which Bag6 appears to associate. In past experiments, I have analysed co-translational apoB peptide elongation at time points up to 20 minutes (when apoB reaches full length apoB-100). Figure 6.3 presents an experiment examining the fate of nascent apoB peptides in the cytosol during the post-translational time period following a 10 minute synchronized pulse-labelling period (>20 minutes, up to 2 hours). Cells were permeabilized with digitonin to separate the cytosol from the luminal/membrane-bound contents. At the outset of this experiment, it was not known whether the brief 10 minute pulse would create a detectable cytosolic pool of radiolabelled apoB.

MG132 was included in during the pulse and chase, where indicated. As a result of the proteasome blockade full-length apoB-100 accumulated in the membrane contents and cytosol, with its highest levels found at the 20 minute chase point. The turnover, or clearance, of apoB-100 is markedly delayed by MG132 (Figure 6.3, +MG132 time points compared to –MG132, both cells + cytosol). Interestingly, full-length apoB-100, as well as a heterogeneous "smear" of smaller apoB fragments, were visible in the cytosol in the absence of MG132. The smear fades over time, most likely due to proteasomal degradation, since the smear is more pronounced in the cytosol of MG132-treated cells (Figure 6.3, right panel, -MG132).
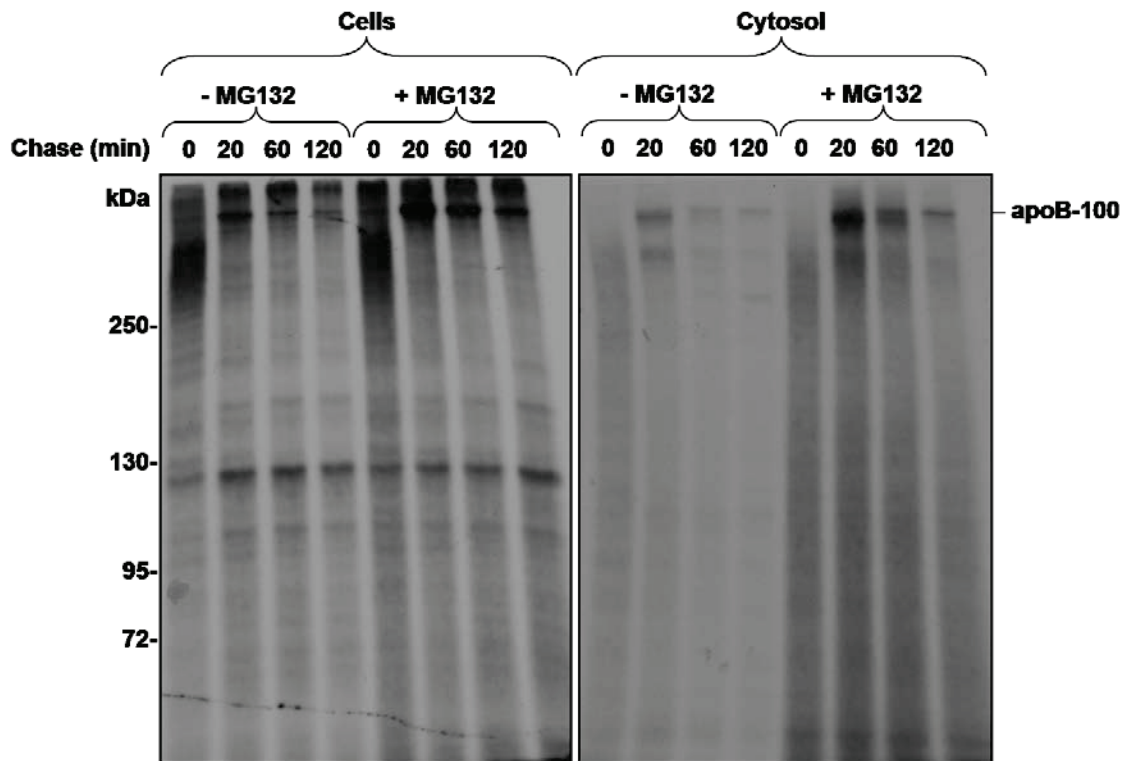
Figure 6.3. Detection of delayed cytosolic turnover of newly synthesized apoB in puromycin-synchronized HepG2 cells. Cells were depleted of cysteine/methionine and then subjected to puromycin treatment. After three washes on ice, cells were placed immediately at 37C in [^{35}S]cysteine/methionine containing media, with or without 25 M MG132. Media was then replaced with chase media containing an excess of unlabelled cysteine/methionine, also with or without MG132. At the indicated chase time points, cells were permeabilized with digitonin to collect the cytosol contents. The remaining monolayers were harvested in 1% SDS-RIPA. ApoB was collected by IP from the cell and cytosol samples, resolved by 5% SDS-PAGE and visualized by autoradiography.

The co-translationally generated apoB smear most likely represents the polyubiquitinated pool that is detected in the cytosol of MG132-treated cells. The full length apoB-100 in the cytosol disappears rapidly, relative to the MG132-induced lower molecular weight smear of apoB-positive signal (Figure 6.3, right panel, 20 min vs 60 min). This suggests that these ERAD substrates are processed differently, or alternatively that full-length apoB-100 is disposed of by a compensatory degradation mechanism more readily than smaller, partially translated apoB fragments.

The Bag6 association begins 10-20 minutes after synthesis has begun (or re-started) (Figure 6.2) and is almost exclusive to cytosolic apoB. Therefore, according to figure 6.3, Bag6 may only associate with full length apoB-100 since at the 0 and 20 minute chase time (MG132 treated), the cytosolic LMW smear does not increase, but both Bag6 binding and full-length apoB-100 increase substantially (Figure 6.3).

This experiment demonstrates a successful merging of techniques for the direct tracking of various newly-synthesized apoB species in multiple cellular compartments. Clearly, this method should be applied to the siRNA-mediated Bag6 knockdown cells (presented in the next section) to assess the role of Bag6 in the turnover of cytosolic apoB ERAD substrates. This protocol can now be applied to test subsequent hypotheses concerning treatments or genetic manipulations that are thought to modulate intracellular apoB degradation.

6.2.4 Effect of the Bag6 Knockdown on ApoB Ubiquitination

The established role of Bag6 in stabilizing proteasome substrates led me to hypothesize that the knockdown of Bag6 may disrupt the proteasomal degradation of

apoB ERAD substrates. While the 19S proteasome cap performs unfolding of polypeptides directly as they enter the 20S core, the "tail end" of large protein substrates, such as apoB, probably associates with chaperones like Hsp70 and Bag6 while degradation of the other end has already begun in the core. Indeed, efficient ERAD is dependent on substrate stability (linearization, or solubization, of large hydrophobic regions freely in the cytosol) which in turn relies on chaperone activity.

To explore the role of Bag6 in apoB metabolism, siRNA-mediated knockdown of Bag6 was conducted in HepG2 cells. 72 hours following transfection with non-targeting (NT) or Bag6-targeting siRNA, cells were harvested and analyzed for knockdown efficiency at the protein level. Figure 6.4 shows a robust knockdown of Bag6 (siBag6 versus NT cells). The Bag6 knockdown does not appear to restrict cell growth according to protein mass. Hsp70 is sometimes modestly increased, as is BiP (Figure 6.4A), which likely correlates with knockdown efficiency. This suggests that Bag6 depletion may cause a mild, chronic stress response in HepG2 cells.

To determine whether apoB ubiquitination was affected by reduction of Bag6 protein, Bag6 knockdown and NT cells were subjected to MG132 or ALLN treatment (a proteasome inhibitor with broad specificity for other proteases as well). ApoB was collected by IP and analysed by immunoblot for the presence of ubiquitin conjugation. Since these are IPs and not immunoblots with corresponding loading controls, differences in total protein mass between NT and siBag6 cannot be accounted for by protein assay. In this regard, analysis should be responsibly limited to observing ubiquitination patterns independently *within* each cell/treatment type rather than looking at differences in "absolute" amounts between NT and siBag6 cells.
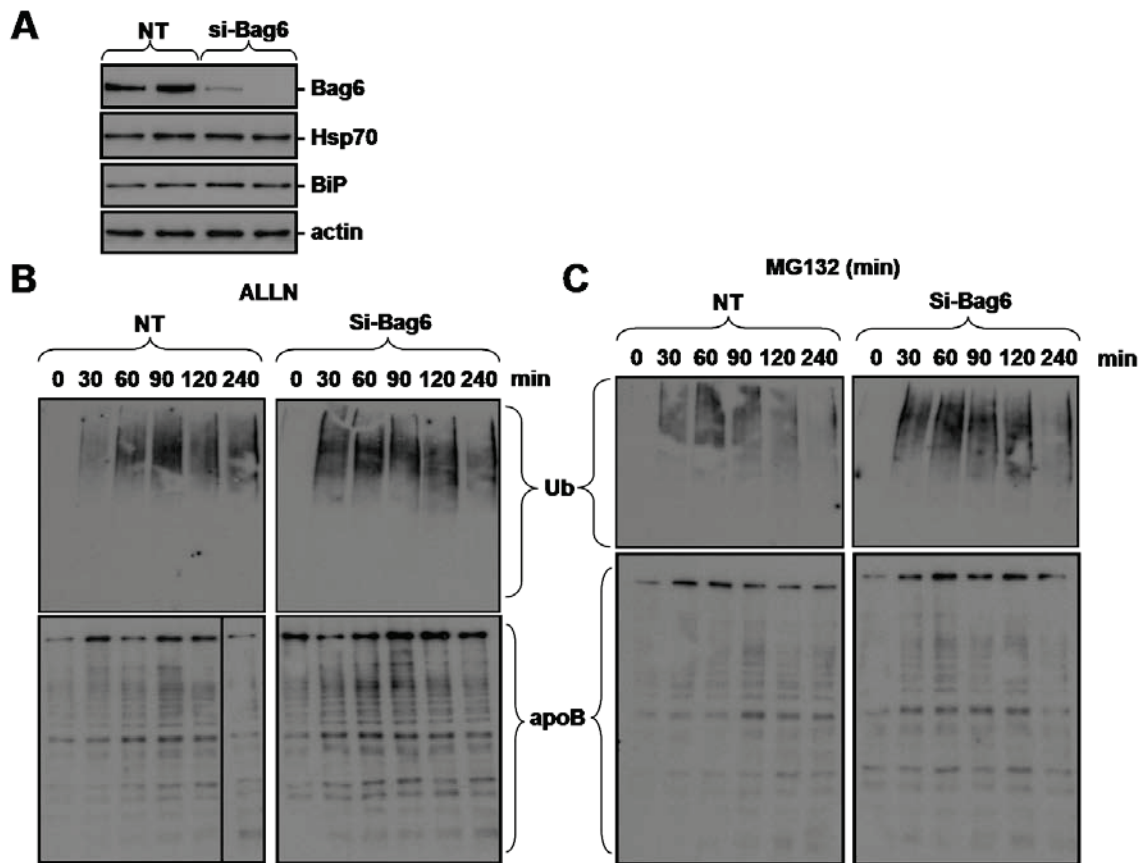
Figure 6.4. Effect of Bag6 knockdown on apoB ubiquitination during proteasome inhibition. A. Immunoblot analysis of HepG2 protein levels. Seventy-two hours following transfection with either NT or Bag6-targeting siRNA. Cells were harvested in 1% SDS-RIPA buffer, resolved by SDS-PAGE followed by visualization of Bag6, Hsp70, BiP and actin by immunoblot analysis. Cells were treated with **(B)** 40 μg/ml ALLN or **(C)** 25 μM MG132 for 30 min, up to 4 h. Cells were harvested in 1% SDS-RIPA and apoB was recovered by IP from diluted lysates (0.1% SDS-RIPA). Approx. 80% of the IP elutions, in sample buffer, were used for the anti-ubiquitin immunoblot (*upper panels*, B & C) and the remaining 20% used for the anti-apoB immunoblots (*lower* panels, B & C).

Figure 6.4 displays the pattern of apoB-ubiquitin conjugates over a 4 hour period. In MG132 and ALLN-treated siBag6 cells, apoB-ubiquitin conjugates appear to reach their highest level, faster than in NT cells. Later during the MG132 treatment, the apoB-ubiquitin conjugates are cleared from the NT cells between 60 and 120 to a much greater extent than those in the siBag6 cells. This ubiquitin analysis shows that cells with lower Bag6 generate apoB-ubiquitin conjugates at an increased rate, possibly due to delays in substrate turnover.

6.2.5 Reduction of Bag6 Decreases ApoB Secretion Efficiency Without Increasing Proteasomal Degradation

To determine whether the secretion of apoB-containing lipoproteins in HepG2 cells was affected by reduction of Bag6 protein, siRNA-mediated knockdown of Bag6 was performed, followed by metabolic radiolabelling. After a one hour incubation in radiolabelled cysteine/methionine, cells were placed in fresh media for two hours and then both media and cells were collected. The Bag6 knockdown did not have a significant effect on apoB production by the cells during the one hour labelling period (Figure 6.5C, cells). However, the secretion efficiency of apoB is reduced in si-Bag6 cells by approximately 45%. Given that the effect on secretion is likely dependent on knockdown efficiency, the data cannot be used to derive a mean value between experiments. The Bag6 knockdown reduces apoB secretion efficiency in the range of 20-50%.

The loss of this apoB pool from the secretory pathway was not accounted for by a corresponding intracellular accumulation of apoB during the chase period (Figure 6.5C,
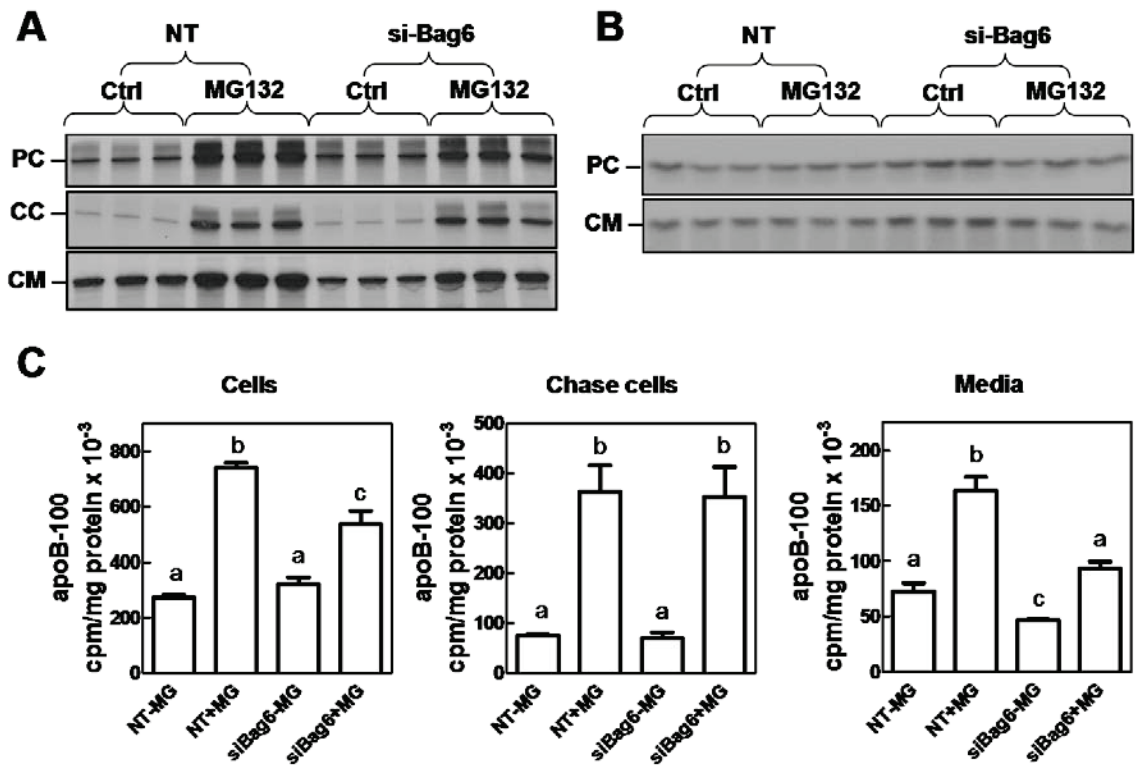
Figure 6.5. siRNA-mediated Bag6 knockdown reduces the secretion efficiency of apoB-100. HepG2 cells were transfected with non-targeting (NT) or Bag6-targeting siRNA (si-Bag6). Transfected cells were labelled with [^{35}S]cysteine/methionine for 1 hour and then chased for 2 hours. ApoB (**A**) and apoAI (**B**) were recovered from cells and media by IP and visualized in SDS-PAGE gels by autoradiography. Pulse cells (*PC*), chase cells (*CC*) and chase medium (*CM*). **C.** Quantitation of apoB-100 in cells and medium by pulse-chase analysis. Each bar represents mean ± S.D. Different letters denote significant differences ($P<0.05$) as determined by Tukey's Multiple Comparison test.

middle graph). The decreased secretion is not accompanied by an increase in proteasomal degradation of full-length apoB-100, as shown by MG132 treatment during the pulse and chase. This suggests that a portion of the apoB pool labelled during the pulse failed to attain "secretion-competence" during the chase and was degraded intracellularly before the end of the chase.

During proteasome inhibition a considerable amount of apoB-100 is secreted from control cells that would have otherwise been an ERAD substrate, in the absence of MG132. This suggests that in NT cells apoB can escape ERAD and become secretion-competent during a proteasome blockade. Reduction of Bag6 prevented the rescue of apoB secretion to the same extent as control cells in response to MG132. The Bag6 knockdown appears to cause a defect in apoB production that results in reduced apoB secretion competence and eventual removal of that apoB from the secretory pool.

When pulse labelling is performed in Bag6 cells the amount of isotope incorporation into nascent apoB is similar to control cells. Between experiments, the level of apoB synthesis in siBag6 cells relative to control is sometimes slightly elevated, or decreased. This is either normal experimental variation or an effect of knockdown efficiency. The knockdown efficiency is typically greater than 90%, or in other words, so efficient that it is difficult to detect Bag6 in KD cells without over-exposing the corresponding Bag6 signal from the NT cells. After the two hour chase period, the cells display no difference in the amount of cellular apoB that remains from the pulse. This indicates that the rates of synthesis and turnover are unaltered by the Bag6 knockdown.

The level of cellular apoB-100 remaining after the chase in MG132-treated cells is similar between knockdown and control (Figure 6.5C, middle graph). Over the time-

scale of the chase the stability, or half-life, of apoB-100 proteasome substrates is unaltered. The depletion of Bag6 appears to affect the cytosolic processing of apoB ERAD substrates, while also triggering the loss of apoB-100 posttranslationally to a non-proteasomal mechanism.

Panel B of Figure 6.5 shows that apoAI synthesis, the non-proteasome substrate secretory protein that serves as a control, is decreased in siBag6 cells treated with MG132 compared to untreated siBag6 cells. Thus this result may also be related to reduced protein synthesis in siBag6 cells in reaction to the proteasome blockade. A more detailed kinetic analysis of apoB proteasome substrate turnover must be performed to determine the exact effect of reduced Bag6 levels on apoB proteasomal targeting.

6.2.6 Synthesis of ApoB is Unaltered by Bag6 Knockdown

To monitor the effect of reduced Bag6 on apoB polypeptide growth, puromycin synchronization radiolabelling of apoB was performed. Complete translation of the apoB-100 protein requires approximately 20 minutes. The rate and amount of apoB synthesis was unaltered by the Bag6 knockdown, as observed in Figure 6.6. While the Bag6 KD does not create any obvious abnormalities during this time-frame, more subtle events might occur regarding assembly kinetics that could preclude the eventual secretion of successfully translated apoB-100.
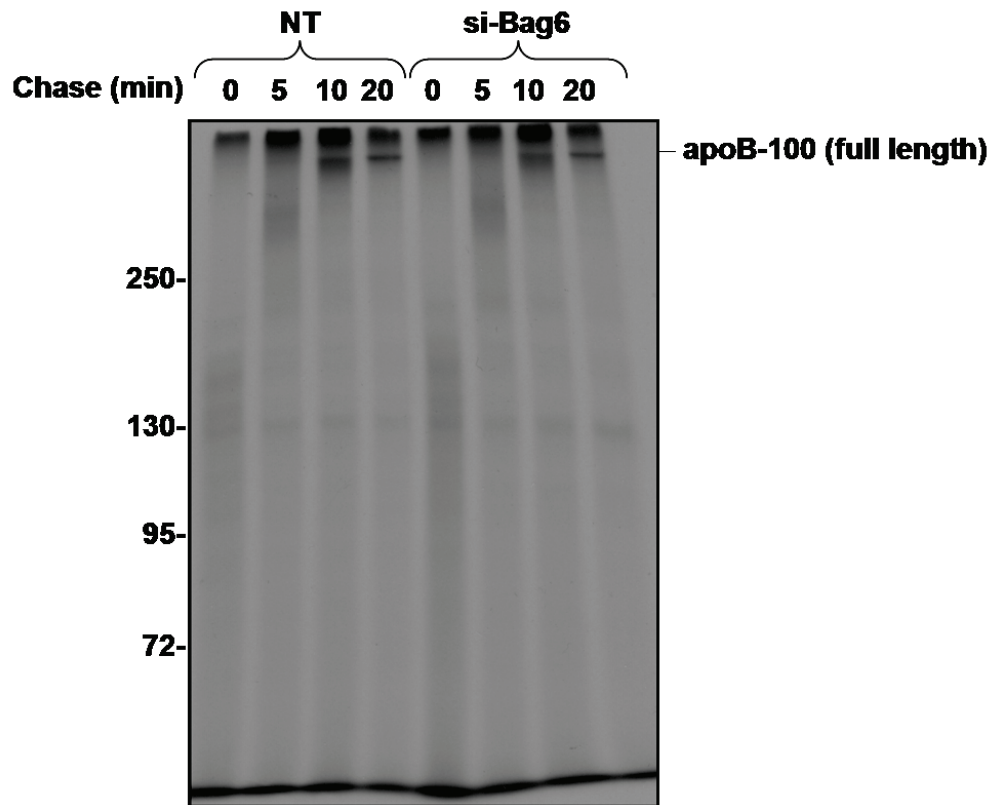
Figure 6.6. Reduced Bag6 levels do not alter apoB synthesis in puromycin-synchronized cells. Seventy-two hours following transfection with either NT or Bag6-targeting siRNA, HepG2 cells were treated with 10 μM puromycin for 5 minutes and then washed for 3 x 10 minutes on ice. Cells were immediately placed in 37ºC media containing [^{35}S] methionine/cysteine for 5 minutes and then chased for up to 20 minutes. ApoB was recovered from the cells and visualized by autoradiography.

6.2.7 Bag6 is Required for ApoB Secretion Independently of the U0126-induced Increase in Lipid Availability

As a result of U0126 treatment, apoB secretion is increased and apoB ERAD is decreased at a step prior to ubiquitination. This effect is probably accounted for by enhanced mobilization of newly synthesized triglycerides and phospholipids by U0126 (Fisher et al., 2011). Thus, apoB is able to assemble into full-sized VLDL particles. The Bag6 knockdown rendered HepG2 cells less able to respond to U0126, at least with regards to apoB-100 secretion. Figure 6.7A & B demonstrate that in Bag6 knockdown cells apoB secretion is restored by U0126 only to the same level as untreated control cells. The percent increase in apoB secretion elicited by U0126 is similar between control and knockdown cells. However, the absolute levels of apoB secretion are unable to be rescued by U0126.

Density gradients of apoB-containing lipoproteins secreted from U0126-treated HepG2 cells display a remarkable shift toward VLDL particle buoyancy, away from LDL-type particles with smaller lipid cores (Tsai et al., 2007). To examine whether Bag6-depleted cells were able to form full-sized VLDL particles, or whether this action of U0126 is impaired by the knockdown, density gradient analysis of labelled apoB was performed (Figure 6.7C). First, the data revealed that the decreased apoB secretion from siBag6 cells is accounted for in the first three, lightest-buoyancy fractions of the gradient (Figure 6.7D). Second, the response by siBag6 cells to U0126 is robust with respect to improved VLDL formation, but with less amplitude than control cells. The U0126-dependent increase in lipid supply is able to enhance the assembly and secretion of a
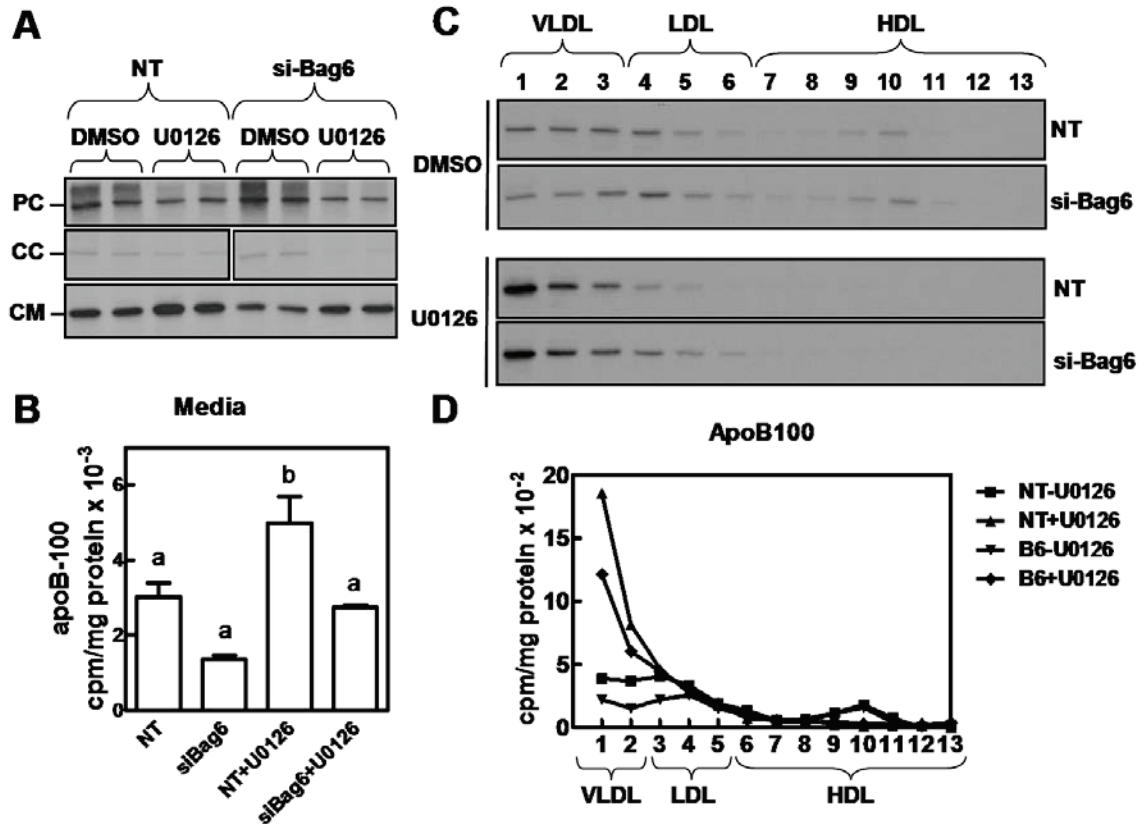
Figure 6.7. siRNA-mediated reduction of cellular Bag6 impairs rescue of total apoB-100 secretion and VLDL assembly by U0126 treatment. A. Cells were transfected with either NT siRNA or siRNA duplex targeting Bag6. Seventy-two hours post-transfection, cells were depleted for one hour in cysteine/methionine-free media and then pulse-labelled for one hour with [^{35}S]cysteine/methionine. Pulse medium was discarded, followed by addition of chase medium for two hours. Media was collected after which apoB was immunoprecipitated and visualized by SDS-PAGE and autoradiography. Pulse cells (*PC*), chase cells (*CC*) and chase medium (*CM*). **B.** Scintillation counting from excised apoB-100 bands shown in panel A., expressed as cpm/mg protein. Data are presented as means ± SD. Different letters denote significant differences (P<0.05) as determined by Tukey's Multiple Comparison test. **C.** Density gradient ultracentrifugation profiles of secreted apoB-100. Cell were treated as in described panel A. Media was collected and subjected to density gradient ultracentrifugation after which apoB was immunoprecipitated from each fraction. ApoB-100 was visualized by SDS-PAGE and autoradiography. **D.** Quantitation of apoB-100. Radiolabelled apoB-100 bands were excised from the gel and quantified by liquid scintillation counting. Results are expressed as cpm per mg cell protein.

comparable proportion of the total apoB pool in both cell treatments indicating that the effects of reduced Bag6 on apoB-100 secretion are independent of U0126-sensitive pathways and are perhaps not lipid-ligand related. It follows that the Bag6 knockdown and U0126 affect independent processes that both influence apoB production, and do not directly antagonize each other. Following Bag6 depletion there may simply be fewer competent apoB proteins available for VLDL production, regardless of the increased lipid supply and ability to produce full-sized VLDL.

6.3 Discussion

The current study began with probing for novel apoB protein-protein associations within the ERAD pathway. We identified Bag6 via mass spectrometry and immunoblot analysis to associate with apoB following proteasome inhibition. Bag6 primarily associates with apoB ERAD substrates in the cytosol that are likely (poly)ubiquitinated. Knockdown of Bag6 levels by siRNA typically reduces the secretion efficiency of apoB-100 by 20-50%. Furthermore, pharmacologic conditions that enhance apoB lipidation (U0126 treatment) or increase apoB secretion via blocking its proteasomal degradation (MG132 treatment) are unable to completely rescue secretion or the loss of apoB in cells with reduced Bag6 levels. Bag6 expression seems to support apoB production in a manner that is independent of lipid supply. When faced with an inadequate level of Bag6, a portion of apoB appears to be targeted rapidly by cellular proteolytic activity during the posttranslational period of VLDL assembly. Inhibitors of autophagy, cathepsin and calpain protease activity revealed no striking differences in apoB turnover by these mechanisms in Bag6-reduced cells. Interestingly, the synthesis of apoB and its stability

within the cells was unaffected by the Bag6 depletion, despite the loss of apoB from the secretory pathway. These data present a scenario where an endogenous ERAD substrate is degraded by an unidentified, atypical mechanism upon depletion of Bag6, a cytosolic chaperone holdase (summarized in Figure 6.8). At present it is unclear whether or not apoB loses secretion competence and is then targeted for degradation, or whether apoB is vulnerable to proteolysis in the midst of assembling into a functional lipoprotein. In other words, is this a quality control-dependent mechanism at work, or is this a circumvention of quality control processes?

The secretion efficiency of apoB-100 is reduced in Bag6 knockdown cells, while the intracellular stability is unaltered. The depletion of Bag6 may cause a disturbance in quality control processes, leading to the loss of apoB-100 to an unknown degradative mechanism. Autophagy is known to deliver apoB to the lysosome during post-ER, pre-secretory proteolyis (PERPP) of nascent lipoproteins (Pan et al., 2008). Inhibitors of the proteasome (MG132, ALLN), and lysosome (3-methyl adenine, E64d) did not rescue any of the apoB lost from the secretory pathway. ALLN also inhibits calpain and cathepsin proteases. A screen of calpain protease inhibitors revealed no significant changes in apoB in siBag6 cells. ALLN appears to be marginally better than MG132 at rescuing apoB secretion, but neither garnered a response anywhere similar to that seen in control cells. Also, blots of ALLN-treated Bag6 knockdown cells revealed an increased abundance of LMW apoB fragments that are absent from the MG132-treated cells. Considering that MG132 and ALLN provoke the same level of ubiquitinated apoB-accumulation, ALLN may affect additional degradative process independent of proteasomal degradation.
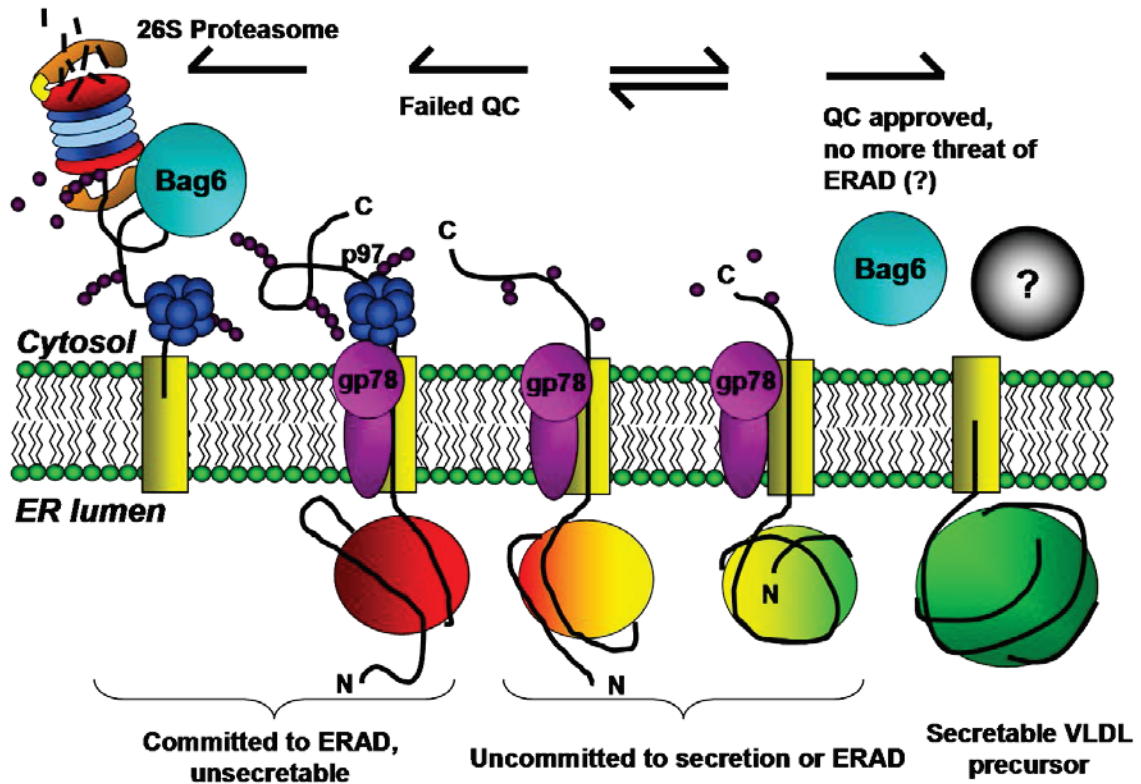
Figure 6.8 Working model of the role Bag6 in apoB metabolism. Updated cartoon representation of apoB ERAD model first presented in figure 4.12. This working model now includes Bag6. Bag6 is found in association with newly synthesized, freely cytosolic apoB that may be committed to ERAD. Bag6 may facilitate the efficient degradation of ubiquitinated apoB species. However, depletion of Bag6 in HepG2 cells removes a substantial amount of newly synthesized apoB from the secretory pool. The precise mechanism is unclear, yet the data indicate a possible role for Bag6 in the quality control of apoB in HepG2 cells.

However, since MG132 and ALLN elicit equivalent amounts of full length apoB-100 accumulation, it follows that the majority of ALLN-sensitive apoB-100 degradation in siBag6 cells is proteasomal.

If the loss of newly synthesized apoB from the secretory pathway cannot be readily accounted for by inhibitors of the proteasome, lysosome or calpain proteases, then what others mechanisms might be at work in Bag6-depleted cells? The ER resident protease/chaperone ER-60 associates with apoB-100 (Adeli et al., 1997a), and when overexpressed, facilitates the non-proteasomal degradation of apoB in the microsome lumen (Qiu et al., 2004). The increased apoB-100 proteolysis observed is ALLN-insensitive, but was blocked by the protease inhibitor *p*-chloromercuribenzoate (*p*CMB) (Qiu et al., 2004). Treatment of primary hamster hepatocytes with *p*CMB effectively rescued apoB-100 secretion. Interestingly, ER-60 levels are low in fructose-fed hamsters, coinciding with increased VLDL production (Taghibiglou et al., 2002). It would be worthwhile to determine whether ER-60-dependent proteolysis is occurring in siBag6 cells.

The ER membrane-resident rhomboid protease RHBDL4 was recently shown to cleave a variety of transmembrane ERAD substrates that also rely on p97 for dislocation from the ER (Fleig et al., 2012). This opens the possibility of intramembrane cleavage of apoB-100 in Bag6-depleted cells. Such a process could remove apoB-100 from the secretory pool while it is still membrane-associated, during the particle maturation process. This cleavage would also prevent apoB-100 from persisting in the cell until the end of the chase period, effectively making it undetectable during the analysis. Rhomboid transmembrane proteins possess an irregular shape that alters the local bilayer structure

such that "membrane thinning" is observed. This has implications for the stability of nearby ERAD substrates and their possible exposure to cytosolic ERAD components (Bondar et al., 2009). The juxtaposition of the E3 ligase active sites and cytosolically exposed substrate residues may be particularly important in governing the rate of substrate turnover by ERAD. Intramembrane proteolysis is an emerging area in ERAD, still in its infancy, and could turn out to be the cause of decreased secretion in siBag6 cells.

When secretion of apoB is enhanced by U0126 treatment, the Bag6-apoB association is all but abolished, as is apoB ubiquitination and the appearance of apoB in the cytosol during proteasome blockade. The Bag6.apoB association appears to also be one of the downstream events that is avoided under lipid-rich conditions. Following U0126 treatment, the same characteristic shift from LDL to VLDL is evident in Bag6 knockdown cells, however with less amplitude than control cells. The ability of U0126-treated Bag6 knockdown cells to form VLDL suggests that Bag6 is not involved in lipid recruitment or assembly *per se*. However, it does appear that reduced Bag6 levels may enable an otherwise dormant degradative mechanism to target apoB, in spite the improved lipid availability in the VLDL assembly pathway following U0126 treatment. The extra apoB-100 degradation is not likely due to poor assembly kinetics typically associated with lipid-deficient conditions in HepG2 cells. However, future studies should include measurement of proteins directly involved in creating the lipid supply for apoB (such as MTP, HMGCoA reductase, SREBP1a) in Bag6-reduced cells.

Could Bag6 be required during the retrotranslocation of apoB-100? This was the case for T-cell receptor α (TCRα) (Claessen and Ploegh, 2011). Unlike TCRα, apoB-100

does not accumulate in the cells in the absence of a proteasome inhibitor when Bag6 is depleted. Pulse-chase labelling revealed that synthesis and stability of apoB-100 was unaltered by Bag6 depletion, even though secretion of apoB-100 was decreased substantially. Perhaps the observed differences are substrate and/or cell-type specific.

Wang *et al* showed that Bag6 associates with the MHC class I HC equally at the ER and in the cytosol. In contrast, Bag6 associates strongly with cytosolic apoB and sparingly with membrane-associated apoB. This indicates that Bag6 may have substrate-specific roles during ERAD. The HC "dislocation intermediate" may require Bag6 binding prior to engagement with p97, while apoB may only need Bag6 once *en route* to the proteasome, after complete removal from the ER.

Claessen and Ploegh speculate that Bag6 could be involved in ERAD before *and* after p97-dependent retrotranslocation (Claessen and Ploegh, 2011). Given that poly-ubiquitination is required for p97 to act upon substrates, and that the ubiquitin machinery lies within the cytosol, ERAD substrates emerging from the ER membrane may require temporary stabilization of their exposed hydrophobic (misfolded) regions. In addition, Bag6 associates with the proteasome (Minami et al., 2010), hinting at the prospect of Bag6-mediated substrate delivery to the proteasome.

p97 associates with apoB approximately 10 minutes from the beginning of translation when MG132 is included. The p97-apoB association is predominantly at the membrane while Bag6 associates almost exclusively with cytosolic apoB. The association between Bag6 and apoB occurs minutes after the p97 association. The data suggest that Bag6 binds ERAD substrates in a post-retrotranslocation step. The MG132-enhanced Bag6-apoB association suggests that apoB is not necessarily directly

transferred from p97 to the proteasome cap. Taken together, these data suggest that Bag6 may act downstream in the same ERAD pathway as p97 (and by extension, potentially gp78 also, since ubiquitination by gp78 precedes p97-dependent retrotranslocation).

The post-translational delivery of apoB-100 to cytosolic lipid droplets is reported to be the convergence of proteasomal and autophagic degradation pathways (Ohsaki et al., 2006). Intriguingly, it appears as though p97 is involved in not only extracting apoB from the ER, but also from these "apoB crescents" found on the surface of ER-associated cytosolic lipid droplets (Suzuki et al., 2012). This revelation came as a surprise since it was generally assumed that the apoB crescents were insoluble apoB deposits awaiting digestion by the lysosome. It is remarkable that the apoB peptides residing in these structures can still be extracted and delivered to the proteasome efficiently.

These apoB-100 ERAD substrates only form when MTP activity is intact, suggesting an exit point toward ERAD from the secretory pathway at a post-translational, well-lipidated stage of the assembly pathway. Suzuki *et al* found that the protein Ubxd8 plays a major role in recruiting p97 to the cytosolic surface of ER-associated lipid droplets. Ubxd8 regulates lipid droplet homeostasis in general (Wang and Lee, 2012), possibly by way of it being a sensor for unsaturated fatty acids and a regulator of triglyceride synthesis (Lee et al., 2010b). Interestingly, Derlin-1, a candidate for the elusive ERAD retrotranslocation channel, is required for movement of apoB from the ER to the surface of the CLD (Suzuki et al., 2012). Derlin-1 and Ubxd8 associate "near" lipid droplets, in an ER membrane region that is supposedly continuous with the CLD, providing support for a model of ER exit site of lipidated apoB-100 at the ER-CLD juncture.

It is possible, if not likely, that Bag6 solubilizes apoB-100 after its extraction by p97 from ER-associated lipid droplets, thus enabling delivery of linearized apoB-100 to the proteasome. This is supported by the observation that only freely cytosolic apoB associates with Bag6, and not until approximately 20 minutes after translation is re-initiated. Full-length apoB-100 does not accumulate in the cell upon Bag6 depletion, but that does not preclude the involvement of Bag6 in its disposal, as apoB-100 appears to be diverted into a compensatory mechanism of degradation. Perhaps a compensatory lipid-based escape hatch (Ploegh, 2007) (and/or intramembrane cleavage?) is somehow facilitating the sequestration of secretion-competent apoB into a destructive micro-environment in the absence of Bag6.

The digitonin permeabilization may leave CLD-associated apoB "crescents" intact and in the cell, rather than in the cytosol supernatant fraction. If this is the case, the cytosolic, ERAD-committed apoB pool would appear as luminal. Where is this organelle situated following permeabilization? This must be addressed in future studies. Furthermore, what is the rate of movement through the CLD-mediated arm of the ERAD pathway? The kinetics of apoB-100 movement through this post-translational, CLD-dependent ERAD pathway are unclear at this time.

HMG CoA reductase is delivered to lipid droplets after it is dislocated from the ER membrane, and before it is degraded in the proteasome (Hartman et al., 2010). The reductase shares many of the same ERAD machinery requirements as apoB ERAD substrates, and could very well require Bag6 as well to stabilize its membrane spanning regions during proteasome delivery, en route from the CLD.

Although Bag6 interacts with polyubiquitinated substrates in cells (Minami et al., 2010) Bag6 does not possess the ability to bind ubiquitin. Ubiquitin-shuttling proteins such as ataxin-3 and Rad23 can facilitate the transfer of ubiquitinated ERAD substrates from p97 to the proteasome (Doss-Pepe et al., 2003). One possible scenario is that Bag6 can act in concert with ubiquitin-binding proteins during the processing of cytosolic apoB. Alternatively, the increase in cytosolic apoB caused by proteasome inhibition may provoke the sudden, previously unnecessary need for apoB stabilization by Bag6.

Bag6 expression is another component of hepatic quality control upon which apoB depends for stable assembly and secretion. It is unclear whether reduced Bag6 causes a greater proportion of apoB to misfold or whether the observed loss of apoB secretion is folding-state independent. It should be noted that this is the first time, to my knowledge, that Bag6 levels have influenced the net output of a secretory protein, rather than simply delaying the turnover of ERAD substrates. More specifically, Bag6 is the first cytosolic chaperone shown to influence apoB secretion that is not a Heat shock protein.

Bag6 has been referred to as a chaperone holdase (Wang et al., 2011). This aptly describes the ability of Bag6 to preferentially bind exposed hydrophobic regions of its substrates and hold them in a soluble state without expending ATP. Attempts to refold ERAD substrates doomed to degradation are unnecessary, even deleterious to the cell. Bag6 can stabilize terminally misfolded proteins in an energy-neutral manner, thus avoiding costly and unnecessary ATP-dependent substrate binding cycles by Hsp70 and Hsp90. Bag6 may be an energy-saving tool for the cell. It binds poorly folded

hydrophobic regions on substrates that are bound for degradation. However, it appears that a significant amount of apoB-100 requires Bag6 to attain secretion competence.

The size of lesions on cytosolic apoB may govern the binding affinity of Bag6, relative to other chaperones with which Bag6 competes. Binding assays show that Bag6 out-competes Hsp70 for binding to long hydrophobic tracts of residues, even when it is present in lower abundance than Hsp70 (Wang et al., 2011). Longer tracts of hydrophobic residues attract strong Bag6 binding, whereas shorter lesions recruit Heat Shock proteins.

Hsc70/Hsp70 has a dual role in CFTR metabolism in folding functional receptors and binding CFTR ERAD substrates (Matsumura et al., 2011). ApoB-100 biogenesis also requires Hsp70, however an overabundance of the chaperone favours apoB-100 degradation rather than secretion. It appears that Hsp70 levels are modestly increased in response to the Bag6 knockdown. Depletion of Bag6 levels could allow more of the Hsp70 pool to bind apoB in a pro-degradative manner, if Bag6 binds secretion competent (or undecided) apoB at all. When Hsp70 is increased in HepG2 cells by Herbimycin A treatment, apoB ubiquitination was increased, with a corresponding decrease in secretion(Gusarova et al., 2001). The exaggerated degradation of apoB induced by Herbimycin A was mediated by the proteasome. Proteasome inhibition in siBag6 cells saw increased levels of apoB ubiquitination compared to control cells. However, there is no additional accumulation of radiolabelled apoB-100 to accompany the decrease in secretion when MG132 is inclu□. Notably, Bag6 has been shown to inhibit Hsp70 activity *in vitro* (Thress et al., 2001), which opens the possibility that Hsp70 activity could be augmented by the loss of Bag6.

An observation that requires reconciliation is that the Bag6 knockdown reduced apoB secretion, without detectably binding to apoB without proteasome inhibition. It is possible that Bag6 and apoB interact in a weak and transient manner that is not preserved during the apoB pull-down. However, the loss of secretion competence in Bag6-depleted cells appears to be an indirect effect of the knockdown, since Bag6 only associates with cytosolic apoB ERAD substrates and not apoB in the assembly pathway. Regardless, there may be multiple points (or perhaps more accurately, windows, of time and space) during apoB metabolism that are partly Bag6-dependent. It will be intriguing to determine the underlying mechanisms behind these effects of the knockdown. It would also be fascinating to profile the "chaperone load" on an individual apoB protein and how the balance/ratio between chaperones such as Bag6, Hsp70 and Hsp90 might impact the net rates of apoB turnover and secretion.

SGTA (Small glutamine-rich tetratricopetide repeat-containing protein α) associates with hydrophobic polypeptides (including tail-anchored proteins) (Leznicki et al., 2010) and is a Bag6-interacting protein (Winnefeld et al., 2006). SGTA was found to counteract the activity of the Bag6 complex, resulting in reduced ubiquitination of mislocalized peptides (Leznicki and High, 2012). It appears that increased SGTA expression results in the deubiquitination of Bag6 complex client peptides. Interestingly, the tetratricopeptide repeat region of SGTA facilitates interaction with Hsp70 and Hsp90 proteins. The authors speculate that SGTA may assist nascent tail-anchored proteins by allowing them to escape "premature" poly-ubiquitination and giving them more time to adopt their native conformation without being degraded. A Bag6/SGTA cycle of substrate binding might serve as a quality control mechanism for tail-anchored proteins,

analogous to the calnexin system in the ER lumen (Leznicki and High, 2012). A separate study revealed that SGTA associates with and enhances the Bag6 complex in binding aggregate-prone ERAD substrates (Xu et al., 2012), a clear departure from the antagonizing role of SGTA in nascent, mislocalized proteins.

Depletion of Bag6 reduces the ubiquitination of nascent, mislocalized proteins targeting to the ER inefficiently (Hessa et al., 2011). In contrast, apoB ubiquitination is similar, if not increased, depending on the time-point, and more long-lived. This suggests that ERAD substrates and nascent mislocalized proteins respond differently to Bag6 depletion. In Bag6-knockdown cells, ubiquitinated Bag6 clients from the ERAD pathway may reside "in limbo" after their retrotranslocation and prior to Bag6-dependent delivery to the proteasome. There may not exist an efficient deubiquitination mechanism for ERAD substrates that accumulate in Bag6 knockdown cells, compared to the SGTA-mediated removal of ubiquitin from mislocalized Bag6 client proteins (Leznicki and High, 2012). SGTA allows mislocalized tail-anchored proteins more time to reach their native state by impeding their Bag6-dependent shunting toward proteasomal degradation. In contrast, the role of SGTA in ERAD appears to be pro-degradative. It is entirely possible that SGTA enhances the loading of apoB ERAD substrates onto the Bag6 complex.

The direct role of Bag6 in apoB metabolism may be limited to solubilizing cytosolic apoB ERAD substrates en route to the proteasome. While it is tempting to speculate that Bag6 could stabilize exposed residues of secretion-competent apoB, the data does not support such a model. The loss of efficient proteasome substrate disposal in si-Bag6 cells may activate compensatory degradative mechanisms to overcome the Bag6

knockdown. In this regard, destruction of otherwise-secretable of apoB-100 may be collateral damage.

Production of secretion-competent apoB-100 in HepG2 cells relies partially on Bag6 expression. While my work has characterized the role of Bag6 in apoB metabolism in part, further experiments are required to determine the mechanism behind the decreased apoB-100 output from Bag6-depleted cells. Characterizing the Bag6-depleted HepG2 cells with immunofluorescent microscopy may shed light on the matter. Specifically, do apoB ERAD substrates accumulate (localize) differently when Bag6 is reduced? Are any ER or Golgi structures altered? If treatment with the chemical chaperone 4-phenyl butyric acid (4-PBA) were to rescue apoB-100 secretion, misfolding of the apoB protein in the absence of Bag6 would become the prime suspect. However, if 4-PBA does not rescue secretion in si-Bag6 cells (as has been shown during ER stress), the continued overzealous removal of apoB would be considered folding-state independent, and possibly represent an example of extra-judicial destruction of an ER client protein.

CHAPTER 7 – DISCUSSION

7.1 Overview

The studies presented herein have focused on the components and events of the apoB-100 ERAD pathway. Using the human hepatoma HepG2 cell line, I have learned much about the relationship between lipoprotein assembly and hepatic quality control processes. The influence of quality control machinery and the Unfolded Protein Response on VLDL output is a fascinating and evolving story. Several metabolic diseases are associated with VLDL overproduction, especially type 2 diabetes and familial combined hyperlipidemia. The protein folding environment for apoB-100 in the hepatic ER is heavily influenced by disruptions in metabolic and signalling pathways. In this Discussion, I will present a model focusing on apoB-100 protein production. I will outline the basic biological processes that serve to enable or limit apoB-100 secretion and offer my insights into the interconnections between these processes that allow for their deterioration in parallel with disease. In addition, I will discuss pertinent new literature that has emerged since the initial publication of my enclosed manuscripts.

7.2 Diverse Mechanisms Affecting Hepatic ApoB-100 Production

Based on my studies in protein quality control and apoB-100 metabolism, I provide a Venn diagram presenting the major contributing factors to the net amount of VLDL particles released from the liver (Figure 7.1). It should be noted that while whole body metabolism, hepatic lipid metabolism, protein folding and degradation capacity are listed separately, some factors can be placed in several, if not all, of these categories.

Factors influencing the net output of VLDL

Hepatic Lipid Metabolism

Protein Folding Capacity

VLDL secretion

Whole Body Metabolism

Degradative Capacity
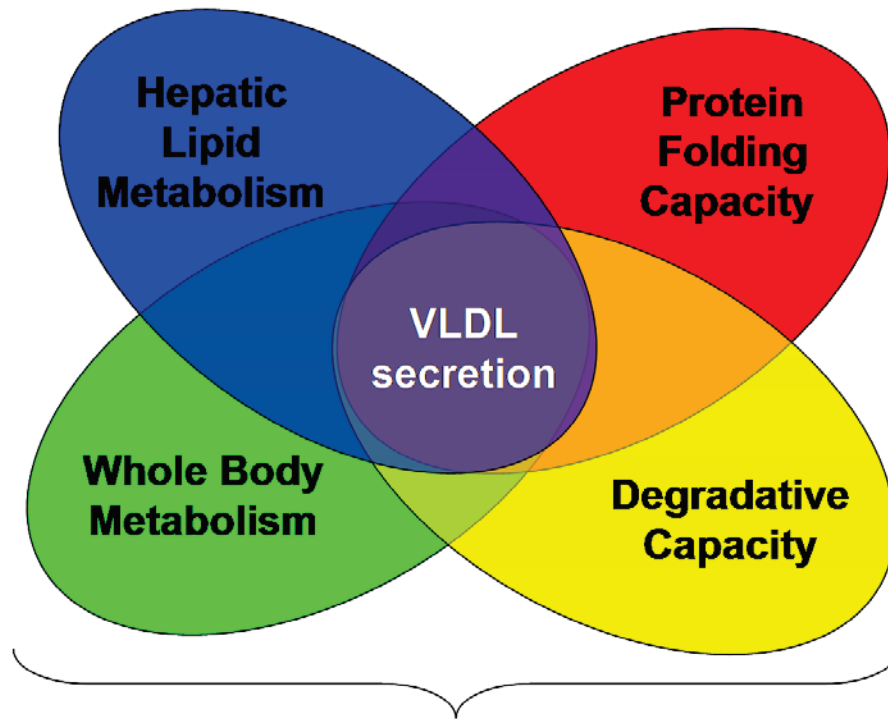
Physiological UPR Activation, Pathological ER stress, Inflammation, Insulin Resistance, Hepatic Steatosis, Chronic and Acute Positive Energy Balance

Figure 7.1. Venn diagram representation of the determinants of net VLDL secretion. This diagram illustrates the distinct, yet related, processes that contribute to the rate of VLDL output. The size and position of the shapes have no significance regarding the relative input of each process; the figure is meant as a qualitative schematic to envision factors that influence the quality control and regulatory decisions during VLDL assembly. These can all impact the fate of each nascent apoB-100 protein. Listed below the diagram are several scenarios where one, or several, of the processes become dysregulated and in turn augment VLDL output.

For example, hepatic IRE1α is a canonical pathway of the UPR (folding and degradation). It also regulates *de novo* lipogenesis and participates in regulating post-prandial metabolism (whole body). A pro-inflammatory milieu exerted from extra-hepatic sources (adipose tissue, for example) can influence hepatic lipid metabolism and ER homeostasis. Inflammation, hepatic steatosis and ER stress are often pathological bedfellows, after all. Conversely, apoB-100 production can reciprocally alter the status of the very factors that determine net VLDL output. The image serves as a qualitative summary of the factors affecting VLDL production.

The VLDL particle, as it is made by the human liver *in vivo*, is produced at a rate determined by innumerable metabolic and signalling inputs. Net apoB-100 production is nominally controlled by its stability, which is in turn determined not only by net lipid ligand availability and folding capacity in the ER, but also by cytosolic chaperoning capacity (Zhou et al., 1995), ERAD (Fisher et al., 2011) and PERPP capacity (Brodsky and Fisher, 2008). Amazingly, the functional properties and metabolic outcome of a particular apoB-100-containing particle are even partly governed by the type and quantity of its lipid cargo (such as acyl chain length and their degree of unsaturation). An extreme example of this is the destruction of damaged, nascent apoB-100 when lipid peroxides are incorporated into the lipoprotein (Pan et al., 2004). Poorly-formed VLDL particles are rapidly removed from the hepatocyte, a process that depends on proper regulation of ER homeostasis and the secretory pathway.

7.3 ApoB-100 Degradation: Update and Perspective

How does apoB traffic from the translocon to the proteasome? Following synthesis, how does apoB topology change over time while maintaining membrane association? It is tempting to speculate that the "hydrophobicity" threshold of the hydrophobic core in the Sec61 channel may play a role in apoB quality control (Junne et al., 2010). This attribute of the Sec61 core was described in the context of determining nascent transmembrane domain integration into the bilayer. As apoB undergoes translocation arrest, its densely hydrophobic epitopes could trigger a similar process, resulting in the lateral movement of apoB into the ER bilayer. The topology of cytosolically exposed, membrane-bound apoB is poorly understood. Cotranslational apoB ERAD substrates may traverse laterally out of the Sec61 channel into an ERAD-specific channel/complex as an immediate prelude to p97-mediated retrotranslocation.

A recent report detailed the liver-specific ablation of the ubiquitin ligase gp78 in mice (Liu et al., 2012). The hepatic gp78-deficient mice were protected from glucose intolerance and age/diet-induced obesity. The improvement of metabolic parameters was attributed to the stabilization of Insig-1/-2, a gp78 substrate. In turn, Insig retained SREBP at the ER, which downregulated lipid synthesis. Curiously, the gp78$^{-/-}$ livers produced more FGF21, which provoked energy expenditure in brown adipose tissue.

It is unclear how a key component of the mammalian ERAD machinery is dispensable, serving as yet another remarkable example of the plasticity of the cellular quality control system. My use of RNAi to decrease gp78 is on a much shorter time-scale than the liver-specific gp78-deficient mice, which were analyzed at 8 weeks of age. Perhaps short-term depletion of gp78 mainly alters apoB ubiquitination and VLDL

assembly, while in the long-term, gp78 deficiency causes metabolic re-programming of hepatic lipid metabolism and secondary effects on whole body metabolism. I reported no change in SREBP1a protein mass, while gp78$^{-/-}$ mouse livers had a 50% decrease in SREBP1a mRNA. These findings are intriguing, yet I am hesitant to agree that gp78 represents a viable therapeutic target (Liu et al., 2012). Partial, transient inhibition of gp78 may not provide the same metabolic benefits as the ablated livers. Further, pharmacological inhibition of gp78 may have unwanted extra-hepatic effects, potentially related to any number of the non-ERAD functions of the ligase. It would be interesting, however, to examine the effects of short-term gp78 depletion *in vivo*, perhaps with a lentivirus-mediated delivery of short hairpin RNA (shRNA).

Since the initial publication of the p97 manuscript (Fisher et al., 2008) several new discoveries have come light regarding the role of p97 in mammalian cells. p97 has been implicated in the extraction of apoB from lipid droplets for proteasomal degradation (Suzuki et al., 2012). The authors found that lipidated apoB-100 ERAD substrates localize to apoB-crescents on cytosolic lipid droplets, and that this was preserved by knocking down Ubxd8 expression. The role of p97 in apoB ERAD now appears to be twofold: retrotranslocation of poorly-lipidated apoB from the ER and extraction of partially-lipidated apoB ERAD substrates from lipid droplets. These are two distinct subclasses of apoB ERAD substrates that now share some, but not all, ERAD component requirements.

The membrane-spanning ERAD component Derlin-1 appeared to interact with apoB "near LDs," but is likely excluded physically from entering the LD phospholipid monolayer due to its membrane-spanning topology (Suzuki et al., 2012). If the bulk

addition of lipid to apoB during the second step of assembly is inefficient, the membrane associated apoB may be trafficked to the cytosol via Derlin-1 at the ER-associated lipid droplet. In turn, Ubxd8 may bridge the gap by recruiting p97 to the CLD. Gp78 has been found on CLD (Hartman et al., 2010), but it is unclear whether it remains functional or is simply *en route* to the proteasome itself.

Interestingly, mutations that disrupt p97 function revealed p97 to be essential for the maturation of ubiquitin-containing autophagosomes (Ballar et al., 2007; Ju et al., 2009; Tresse et al., 2010). Small p97/VCP-interacting protein (SVIP) was initially characterized as an endogenous inhibitor of p97-dependent ERAD (Ballar et al., 2007), but its function has now been expanded to include a regulatory role in autophagy (Wang et al., 2011). p97 could also be involved in apoB clearance by autophagy. However, the observations that the PERPP pathway is not normally active in HepG2 cells (Qiu et al., 2011) and that p97 depletion in HepG2 cells has an immediate, co-translational effect on apoB accumulation suggests that impaired p97-dependent autophagy is not driving changes to apoB metabolism in this model system (Fisher et al., 2008).

7.4 The Close Relationship Between ApoB-100, Lipid Droplets and Autophagy

In addition to serving as sinks for excess fatty acids and cholesterol, which are stored as triglycerides and cholesterol esters (Martin and Parton, 2006), lipid droplets are protein storage depots (Cermelli et al., 2006). CLD appear to be a sink for proteasome substrates. These organelles have emerged in recent years as an intersection of lipid metabolism and protein quality control, not just for apoB, but other ERAD and proteasome substrates as well. Ancient ubiquitous protein 1 (AUP1) may facilitate the

delivery of ERAD substrates to lipid droplets en route to the proteasome (Klemm et al., 2011). HMG CoA reductase is delivered to lipid droplets after it is dislocated from the ER membrane, and before it is degraded in the proteasome (Hartman et al., 2010). Furthermore, Ubxd8-depleted Huh7 cells accumulate many different ubiquitinated proteins in addition to apoB (Suzuki et al., 2012).

Ubxd8 has also been shown to regulate lipid droplet homeostasis in general (Wang and Lee, 2012). Unsaturated fatty acids cause Ubxd8 to dissociate from ubiquitinated Insig-1 and polymerize, which in turn increases Insig-1 levels at the ER and prevents the activation of SREBP. Saturated fats do not provoke this response, however, resulting in inadequate regulation of lipids. The inability of Ubxd8 to "sense" saturated fats has been proposed as a means for hepatic metabolism to become dysregulated in the face of a Western-style diet (Ye, 2012). Additionally, the Scap/SREBP proteins are essential for the progression of diabetic fatty liver (Moon et al., 2012). It would be fascinating to know whether Ubxd8 modulates neutral lipid availability for apoB-100 production while also facilitating its movement through the CLD compartment during ERAD, and whether these processes are directly related.

How the biogenesis of lipid droplets is organized to support both assembly and degradation of apoB-100 is unclear. How do the pro-secretion formation of LLD and the ERAD-enabling formation of CLD relate to one another? Are these biochemically similar processes somehow regulated reciprocally, or co-regulated? It is fascinating that apoB-100 that has failed to assemble into VLDL particle is stabilized by an organelle with similar characteristics as VLDL, the cytosolic lipid droplet. Researchers studying the proteasomal degradation of apoB have long been faced with the question of "where does

the lipid go?" At some point between substrate recognition and degradation, non-exchangeable apoB polypeptides must be stripped of their lipid ligands, which, *in vitro,* bind irreversibly to sequences in the β1 domain (Wang et al., 2009). The answer to this question may emerge from studies of lipid droplet metabolism.

Autophagy has emerged to play an integrated role in lipid metabolism and the disposal of lipoproteins and lipid droplets. Glucosamine induces a PERK-dependent decrease in translation and an increase in autophagic and proteasomal degradation to clear apoB-100 (Qiu et al., 2006; Qiu et al., 2009; Qiu et al., 2011). Defective hepatic autophagy has been suggested to promote ER stress and insulin resistance (Yang et al., 2010b), while the omega-3 fatty acid DHA has been shown to induce hepatic autophagy of apoB-100 (Pan et al., 2008). CLD appear to form an intersection of proteasomal and autophagic degradation of apoB. As such, the two distinct degradation pathways may share numerous cellular components such as ubiquitin machinery, p97 and other proteins residing in supra-molecular complexes at the microsomal membrane. As with ERAD, the mechanism of substrate selection is unknown in the apoB autophagy (PERPP) pathway. The p62 protein binds LC3, a critical protein component of autophagosome formation, possesses an ubiquitin associated (UBA) domain and is involved in ubiquitin-dependent substrate selection for autophagy (Komatsu et al., 2012). Interestingly, ubiquitin- and p62-positive aggregates are observed in multiple human disorders, including neurological diseases, steatohepatitis and several forms of cancer (Zatloukal et al., 2002). p62 is involved in the regulated removal of large protein complexes from the ER by selective autophagy, illustrating a mechanism of bulk ER-to-cytosol protein transport by non-COPII vesicles, independent of other putative retrotranslocation mechanisms (Le Fourn

et al., 2013). Binding of p62 to polyubiquitin chains at the ER membrane could conceivably allow the regulated removal of apoB-containing lipoproteins from the secretory pathway.

Insulin resistance is associated with impaired hepatic autophagy. Autophagy, in turn, appears to reciprocally affect lipid metabolism. Defective clearance of apoB-100 by autophagy, combined with substrate abundance for VLDL assembly, could greatly increase the net burden that apoB-100 production imposes on hepatocytes. Can apoB-100-dependent ER stress affect hepatic steatosis by improper clearance via autophagy? It should be noted that the overproduction of VLDL may still occur in this scenario, alongside disrupted apoB degradation. This type of dysregulation in lipoprotein metabolism may contribute to the concomitant emergence of an atherogenic plasma lipid profile and hepatic steatosis.

7.5 Effects of ER Stressors and the Unfolded Protein Response on ApoB-100

ER stress and activation of the UPR are observed in many diverse disease states. However, it is not always clear whether the ER stress and resulting cellular response is a cause, or an effect, of the disease. Complicating matters is the emerging distinction between physiological and pathological ER stress (Rutkowski and Hegde, 2010; Walter and Ron, 2011). The UPR pathways are highly integrated into energy metabolism. Crosstalk between the UPR and inflammatory pathways seems particularly relevant in several human diseases (Garg et al., 2012; Rath and Haller, 2011). In the diabetic liver, dysregulated lipid metabolism (Kumashiro et al., 2011) and the bifurcation of insulin sensitivity (Li et al., 2010) can combine with ER stress and inflammation to chronically

disrupt energy homeostasis. The following studies provide insight into how apoB-100 production proceeds in this pathological setting.

The UPR signalling arm of IRE1α has a role in regulating hepatic lipid homeostasis, particularly through modulating insulin-mediated *de novo* lipogenesis (Ning et al., 2011). Overactivation of IRE1α may provide excess lipids to support VLDL assembly. Activation of the UPR, generally speaking, curtails the synthesis of new proteins and increases the degradation of ER luminal and transmembrane ERAD substrates with the goal of restoring ER homeostasis. Thus, during ER stress the protein folding environment for apoB-100 *in vivo* is dynamic and complex, with simultaneous activation of processes that are known to independently either support or limit VLDL assembly. Understanding the precise characteristics of individual ER stressors is essential to properly interpreting the net effect on ER homeostasis.

There are some discrepancies in the literature regarding apoB-100 production within the stressed hepatic ER. On one hand, apoB-100 secretion is observed to decrease in the presence of a variety of ER stressors, both artificial and physiological. While on the other hand, diabetic dyslipidemia and NAFLD (Higuchi et al., 2011) can simultaneously display activation of ER stress markers and increased VLDL output. The widely-employed pharmacologic ER stressors dithiothreitol (DTT) and tunicamycin directly and immediately disrupt disulfide bond formation and O-linked glycosylation, respectively. DTT and tunicamycin induce ER stress and curtail VLDL assembly *in vitro*. ApoB misfolds and is rapidly rendered secretion-incompetent by these compounds. Because the folding capacity of apoB-100 is obliterated immediately by these compounds and the response to ER stress happens in parallel, it cannot be concluded that ER stress

itself caused VLDL production to decrease. Similarly, pharmacologically-induced ER stress in ATF6 knockout mice results in hepatic steatosis and lipid droplet formation, in part by direct interference with apoB-100 protein synthesis and folding. Intracellular lipid accumulation occurs in lieu of decreased hepatic lipid output via lipoprotein secretion (Yamamoto et al., 2010). Again, this model does not prove that an ER stress-dependent decrease in VLDL production is a causative mechanism of hepatic steatosis *in vivo*.

Another group injected tunicamycin into mice to analyze the progression of hepatic steatosis during pharmacologically-induced ER stress (Lee et al., 2012). Along with a litany of hepatic lipogenic gene upregulation, there was a rapid decrease in plasma LDL and HDL, and increased hepatic TG. The authors concluded that pharmacologic ER stress is a strong "hit" that triggers NASH. In reality, their experimental results in the context of apoB-100 literature suggest their tunicamycin injection immediately destroyed the secretion competence of nascent apoB-100, in addition to activation of the UPR. Thus, the design of this study confounds any mechanistic conclusions about ER stress-induced steatosis in relation to VLDL production.

The most physiological hepatic ER stressors are no doubt free fatty acids. A widely cited example of reduced VLDL output in the face of FFA-induced ER stress (Ota et al., 2008) is also, sadly, the most misinterpreted in review articles. Severe ER stress does indeed curtail VLDL production in their animal and cell models, yet the authors emphasized that apoB-100 demonstrates a dose- and time-dependent parabolic response to FFA treatments. At low to medium levels of ER stress, apoB-100 secretion is substantially increased, perhaps at a point where lipid availability is able to outstrip the decline in protein folding capacity at the ER. And since fatty acids do not pose an

immediate threat to apoB-100 folding, unlike chemical ER stressors, VLDL production responds in kind to the boost in lipid ligand availability. The studies mentioned above are too often cited as evidence suggesting that ER stress-induced reduction of VLDL secretion is a causative mechanism in steatosis (Cnop et al., 2012; Kammoun et al., 2009; Ozcan, 2012; Pagliassotti, 2012). Several studies discussed below suggest the situation *in vivo* is quite different.

Recent studies have found connections between the hepatic IRE1α arm of the UPR and VLDL output. IRE1α -XBP1s induced PDI expression, which in turn increased MTP activity and apoB-100 secretion (Wang et al., 2012). Notably, the catalytic activity of PDI is dispensable for this particular function in lipoprotein assembly. IRE1α is known to carry out regulated IRE-dependent mRNA decay (RIDD) of ER-associated mRNAs during the UPR, and is thus thought to be one manner by which the cell lessens the protein folding burden on the ER (Hollien and Weissman, 2006). Ablation of murine hepatic XBP1, the transcription factor induced directly downstream of IRE1α, caused a feedback activation of IRE1α RIDD activity. Microarray analysis of the liver revealed that RIDD silences genes involved in lipid metabolism, resulting in decreased plasma lipids in the XBP1-deficient livers of these mice (So et al., 2012). Amazingly, a model of liver-specific, inducible XBP1 revealed that XBP1 expression alone is sufficient to trigger a switch into the postprandial state, even in the absence of any caloric intake (Deng et al., 2013). These data show how the UPR is fully integrated into hepatic energy metabolism and lipoprotein production.

Protein synthesis and energy/nutrient levels are elegantly coordinated by mTORC1; moderate reduction of protein folding chaperones enhances mTORC1

signalling, while severe depletion of chaperone capacity deactivates mTORC1 (Qian et al., 2010). This presents a mechanism by which protein misfolding is coupled to metabolic disruptions in the diseased state. Sortilin-1 is a protein capable of facilitating the regulated removal of apoB-100 from the secretory pathway via degradation by PERPP. Sortilin-1 levels are suppressed in the livers of obese mice, a result of the chronic ER stress and mTORC1 signalling (Ai et al., 2012). Interestingly, sortilin-1 was repressed in diet-induced and genetic models of mouse obesity. The authors delineated a mechanism by which the mTOR inhibitor rapamycin decreased ER stress, relieved Atf3-driven suppression of sortilin-1 levels and ameliorated VLDL overproduction. In this model, VLDL overproduction persisted despite obesity-induced ER stress. In fact, one might say the VLDL overproduction occurring in this model is not in spite of, but *because* of the ER stress. The authors speculate that in this environment of chronic lipid overabundance it may be necessary to expel lipid from the liver to stave off hepatic steatosis at the expense of an atherogenic plasma lipid profile (Ai et al., 2012).

One report elegantly demonstrated the difference between excess *de novo* lipogenesis (high fructose feeding) and exogenous lipid oversupply (high fat feeding) in rats (Ren et al., 2012). Both diets caused steatosis and blunted insulin sensitivity within days. Interestingly, ER stress was induced in the fructose-fed animals and not in the high fat-fed animals, suggesting that the stress was associated with the lipogenesis, and was not an immediate component of the early fatty liver disease or insulin resistance induced by a high fat diet (Ren et al., 2012). Additionally, increased mRNA expression of both MTP and apoB-100 was observed in NAFLD patients (Higuchi et al., 2011). However, patients in this study with the most severe insulin resistance displayed reduced MTP,

suggesting that as the liver disease worsens this compensatory mechanism is lost. These data imply that VLDL secretion persists during pathological hepatic ER stress and NAFLD, perhaps until progressive liver damage dampens the capacity of the secretory pathway to assemble and secretion VLDL.

Insulin-mediated suppression of VLDL output thus coincides with physiological activation of the UPR. Yet insulin resistance is also associated with hepatic ER stress, chronic UPR upregulation and increased VLDL. These studies underscore the fact that important differences exist regarding the outcome of physiological and pathological UPR activation. Given that proper quality control of ER proteins is heavily reliant on ER folding and degradative capacity, whose levels are in turn controlled by the UPR transcription factors that help elicit the feeding response, it is a novel yet unsurprising finding that some UPR signals have significant impact on hepatic VLDL output and the metabolic status of the liver.

While evidence does not support an ER stress-dependent decrease in VLDL as a causative mechanism of fatty liver, perturbed apoB protein quality control during the progression of insulin resistance and NAFLD may have unique, deleterious consequences. Overexpression of apoB itself induces ER stress (Su et al., 2009). I have also observed the opposite scenario, where pharmalogic enhancement of apoB lipidation can decrease levels of the ER stress marker Grp78/BiP (Fisher et al., 2011). These data imply that augmenting the protein folding burden posed by apoB is sufficient to either worsen or improve ER homeostasis. Loss of insulin-dependent suppression of hepatic apoB-100 levels may confer an additional metabolic burden on hepatocytes, on top of that already posed by chronic overnutrition. Indeed, apoB-100 is proposed to be

molecular link between insulin resistance and chronic ER stress (Su et al., 2009). These are two pathologies associated with metabolic disorders, of which VLDL overproduction can be an important component. One may now speculate that successful moderation of apoB-100 production is dependent on ER homeostasis, while conversely, hepatic ER homeostasis is dependent on the unimpeded export of lipidated apoB-100.

I propose that apoB-100 production inflicts a constant, unique metabolic burden on hepatocytes, relative to cell-types not charged with this task. To cease VLDL output means to accumulate neutral lipid and its affiliated, cytotoxic by-products like diacylglycerol (DAG) and ceramide. The continuous, proper production of hepatic apoB-100 may be more important to the liver than it is for the periphery to receive fats. Combined with β-oxidation, VLDL output serves as a means to consume and partition energy resources within hepatocytes such that lipotoxic intermediary metabolites do not accumulate. In this respect, apoB-100 is perhaps a molecular "steatosis suppressor," to borrow some semantics from cancer researchers.

Lipoprotein secretion and lipogenic and UPR pathways appear to be directly linked. The chaperoning component of ER homeostasis is a precisely regulated "double-edged sword" where too much or too little can be dangerous (Fu et al., 2012). The enhancement of chaperone function is an intriguing therapeutic avenue for many human diseases, especially given the well-documented age-related decline in chaperone regulation (Calderwood et al., 2009; Morimoto, 2011). The chemical chaperone 4-phenyl butyric acid (PBA) was able to normalize ER homeostasis and VLDL secretion under conditions of chronic oleate exposure (Ota et al., 2008). Interestingly, PBA may improve insulin signalling and β-cell function in humans with lipid-induced insulin resistance

(Xiao et al., 2011). Treatment of humans with tauro-ursodeoxycholic acid (TUDCA) may improve insulin sensitivity in the liver and skeletal muscle (Kars et al., 2010). Improved protein folding may represent an accessible point at which persistant vicious cycles of ER stress, inflammation and insulin-resistance might be interrupted (Imrie and Sadler, 2012). Perhaps normalization of ER homeostasis in parallel with increased insulin sensitivity will someday emerge as a therapeutic approach.

Therapeutic targeting of the UPR is an exciting and promising avenue toward treatment of several diseases for which effective interventions are lacking. Often the observed increase in ER stress markers are just that--biomarkers of a disease, rather than a cause of the pathology itself. Thus, augmenting ER homeostasis without addressing the underlying mechanism or original source of the *in vivo* stressor may not provide the desired outcome. I do believe, however, that the age-related decline in chaperone regulation and loss in fidelity of protein production are drivers of age-dependent metabolic and neurological disease. In general, I am optimistic that therapeutics that improve or maintain protein quality control will become integrated into healthcare practices in the future.

BIBLIOGRAPHY

Adams, J. (2004). The development of proteasome inhibitors as anticancer drugs. Cancer. Cell. *5,* 417-421.

Adeli, K., Macri, J., Mohammadi, A., Kito, M., Urade, R., and Cavallo, D. (1997a). Apolipoprotein B is intracellularly associated with an ER-60 protease homologue in HepG2 cells. J. Biol. Chem. *272,* 22489-22494.

Adeli, K., Wettesten, M., Asp, L., Mohammadi, A., Macri, J., and Olofsson, S.O. (1997b). Intracellular assembly and degradation of apolipoprotein B-100-containing lipoproteins in digitonin-permeabilized HEP G2 cells. J. Biol. Chem. *272,* 5031-5039.

Adiels, M., Olofsson, S.O., Taskinen, M.R., and Boren, J. (2008). Overproduction of very low-density lipoproteins is the hallmark of the dyslipidemia in the metabolic syndrome. Arterioscler. Thromb. Vasc. Biol. *28,* 1225-1236.

Ai, D., Baez, J.M., Jiang, H., Conlon, D.M., Hernandez-Ono, A., Frank-Kamenetsky, M., Milstein, S., Fitzgerald, K., Murphy, A.J., Woo, C.W.*, et al.* (2012). Activation of ER stress and mTORC1 suppresses hepatic sortilin-1 levels in obese mice. J. Clin. Invest. *122,* 1677-1687.

Alder, N.N., Shen, Y., Brodsky, J.L., Hendershot, L.M., and Johnson, A.E. (2005). The molecular mechanisms underlying BiP-mediated gating of the Sec61 translocon of the endoplasmic reticulum. J. Cell Biol. *168,* 389-399.

Alexandru, G., Graumann, J., Smith, G.T., Kolawa, N.J., Fang, R., and Deshaies, R.J. (2008). UBXD7 Binds Multiple Ubiquitin Ligases and Implicates p97 in HIF1α Turnover. Cell *134,* 804-816.

Alzayady, K.J., Panning, M.M., Kelley, G.G., and Wojcikiewicz, R.J. (2005). Involvement of the p97-Ufd1-Npl4 complex in the regulated endoplasmic reticulum-associated degradation of inositol 1,4,5-trisphosphate receptors. J. Biol. Chem. *280,* 34530-34537.

Anderson, T.A., Levitt, D.G., and Banaszak, L.J. (1998). The structural basis of lipid interactions in lipovitellin, a soluble lipoprotein. Structure *6,* 895-909.

Ason, B., Castro-Perez, J., Tep, S., Stefanni, A., Tadin-Strapps, M., Roddy, T., Hankemeier, T., Hubbard, B., Sachs, A.B., Michael Flanagan, W., Kuklin, N.A., and Mitnaul, L.J. (2011). ApoB siRNA-induced liver steatosis is resistant to clearance by the loss of fatty acid transport protein 5 (Fatp5). Lipids *46,* 991-1003.

Babin, P.J., Bogerd, J., Kooiman, F.P., Van Marrewijk, W.J., and Van der Horst, D.J. (1999). Apolipophorin II/I, apolipoprotein B, vitellogenin, and microsomal triglyceride transfer protein genes are derived from a common ancestor. J. Mol. Evol. *49,* 150-160.

Baker, B.M., and Tortorella, D. (2007). Dislocation of an endoplasmic reticulum membrane glycoprotein involves the formation of partially dislocated ubiquitinated polypeptides. J. Biol. Chem. *282,* 26845-26856.

Ballar, P., Shen, Y., Yang, H., and Fang, S. (2006). The role of a novel p97/valosin-containing protein-interacting motif of gp78 in endoplasmic reticulum-associated degradation. J. Biol. Chem. *281,* 35359-35368.

Ballar, P., Zhong, Y., Nagahama, M., Tagaya, M., Shen, Y., and Fang, S. (2007). Identification of SVIP as an endogenous inhibitor of endoplasmic reticulum-associated degradation. J. Biol. Chem. *282,* 33908-33914.

Ballar, P., and Fang, S. (2008). Regulation of ER-associated degradation via p97/VCP-interacting motif. Biochem. Soc. Trans. *036,* 818-822.

Ballar, P., Pabuccuoglu, A., and Kose, F.A. (2011). Different p97/VCP complexes function in retrotranslocation step of mammalian Er-associated degradation (ERAD). Int. J. Biochem. Cell Biol. *43,* 613-621.

Balut, C.M., Loch, C.M., and Devor, D.C. (2011). Role of ubiquitylation and USP8-dependent deubiquitylation in the endocytosis and lysosomal targeting of plasma membrane KCa3.1. FASEB J. *25,* 3938-3948.

Bays, N.W., and Hampton, R.Y. (2002). Cdc48-Ufd1-Npl4: stuck in the middle with Ub. Curr. Biol. *12,* R366-71.

Bech-Otschir, D., Helfrich, A., Enenkel, C., Consiglieri, G., Seeger, M., Holzhutter, H.G., Dahlmann, B., and Kloetzel, P.M. (2009). Polyubiquitin substrates allosterically activate their own degradation by the 26S proteasome. Nat. Struct. Mol. Biol. *16,* 219-225.

Bedford, L., Paine, S., Sheppard, P.W., Mayer, R.J., and Roelofs, J. (2010). Assembly, structure, and function of the 26S proteasome. Trends Cell Biol. *20,* 391-401.

Behrends, C., and Harper, J.W. (2011). Constructing and decoding unconventional ubiquitin chains. Nat. Struct. Mol. Biol. *18,* 520-528.

Bengtson, M.H., and Joazeiro, C.A. (2010). Role of a ribosome-associated E3 ubiquitin ligase in protein quality control. Nature *467,* 470-473.

Benoist, F., and Grand-Perret, T. (1997). Co-translational degradation of apolipoprotein B100 by the proteasome is prevented by microsomal triglyceride transfer protein. Synchronized translation studies on HepG2 cells treated with an inhibitor of microsomal triglyceride transfer protein. J. Biol. Chem. *272,* 20435-20442.

Bohn, S., Beck, F., Sakata, E., Walzthoeni, T., Beck, M., Aebersold, R., Forster, F., Baumeister, W., and Nickell, S. (2010). Structure of the 26S proteasome from Schizosaccharomyces pombe at subnanomer resolution. Proc. Natl. Acad. Sci. U. S. A. *107,* 20992-20997.

Bondar, A.N., del Val, C., and White, S.H. (2009). Rhomboid protease dynamics and lipid interactions. Structure *17,* 395-405.

Borchardt, R.A., and Davis, R.A. (1987). Intrahepatic assembly of very low density lipoproteins. Rate of transport out of the endoplasmic reticulum determines rate of secretion. J. Biol. Chem. *262,* 16394-16402.

Boren, J., Rustaeus, S., and Olofsson, S.O. (1994). Studies on the assembly of apolipoprotein B-100- and B-48-containing very low density lipoproteins in McA-RH7777 cells. J. Biol. Chem. *269,* 25879-25888.

Boren, J., Rustaeus, S., Wettesten, M., Andersson, M., Wiklund, A., and Olofsson, S.O. (1993). Influence of triacylglycerol biosynthesis rate on the assembly of apoB-100-containing lipoproteins in Hep G2 cells. Arterioscler. Thromb. *13,* 1743-1754.

Borradaile, N.M., de Dreu, L.E., Barrett, P.H., and Huff, M.W. (2002). Inhibition of hepatocyte apoB secretion by naringenin: enhanced rapid intracellular degradation independent of reduced microsomal cholesteryl esters. J. Lipid Res. *43,* 1544-1554.

Bou Khalil, M., Sundaram, M., Zhang, H.Y., Links, P.H., Raven, J.F., Manmontri, B., Sariahmetoglu, M., Tran, K., Reue, K., Brindley, D.N., and Yao, Z. (2009). The level and compartmentalization of phosphatidate phosphatase-1 (lipin-1) control the assembly and secretion of hepatic VLDL. J. Lipid Res. *50,* 47-58.

Brandman, O., Stewart-Ornstein, J., Wong, D., Larson, A., Williams, C.C., Li, G.W., Zhou, S., King, D., Shen, P.S., Weibezahn, J.*, et al.* (2012). A ribosome-bound quality control complex triggers degradation of nascent peptides and signals translation stress. Cell *151,* 1042-1054.

Braun, S., Matuschewski, K., Rape, M., Thoms, S., and Jentsch, S. (2002). Role of the ubiquitin-selective CDC48 UFD1/NPL4 chaperone (segregase) in ERAD of OLE1 and other substrates. EMBO J. *21,* 615-621.

Brodsky, J.L., and Fisher, E.A. (2008). The many intersecting pathways underlying apolipoprotein B secretion and degradation. Trends Endocrinol. Metab. *19,* 254-259.

Brown, M.S., and Goldstein, J.L. (1980). Multivalent feedback regulation of HMG CoA reductase, a control mechanism coordinating isoprenoid synthesis and cell growth. J. Lipid Res. *21,* 505-517.

Burnett, B., Li, F., and Pittman, R.N. (2003). The polyglutamine neurodegenerative protein ataxin-3 binds polyubiquitylated proteins and has ubiquitin protease activity. Hum. Mol. Genet. *12,* 3195-3205.

Bush, K.T., Goldberg, A.L., and Nigam, S.K. (1997). Proteasome inhibition leads to a heat-shock response, induction of endoplasmic reticulum chaperones, and thermotolerance. J. Biol. Chem. *272,* 9086-9092.

Cabibbo, A., Pagani, M., Fabbri, M., Rocchi, M., Farmery, M.R., Bulleid, N.J., and Sitia, R. (2000). ERO1-L, a human protein that favors disulfide bond formation in the endoplasmic reticulum. J. Biol. Chem. *275,* 4827-4833.

Calderwood, S.K., Murshid, A., and Prince, T. (2009). The shock of aging: molecular chaperones and the heat shock response in longevity and aging--a mini-review. Gerontology *55,* 550-558.

Cao, J., Wang, J., Qi, W., Miao, H.H., Wang, J., Ge, L., DeBose-Boyd, R.A., Tang, J.J., Li, B.L., and Song, B.L. (2007). Ufd1 is a cofactor of gp78 and plays a key role in cholesterol metabolism by regulating the stability of HMG-CoA reductase. Cell Metab. *6,* 115-128.

Carman, G.M., and Han, G.S. (2006). Roles of phosphatidate phosphatase enzymes in lipid metabolism. Trends Biochem. Sci. *31,* 694-699.

Carvalho, P., Stanley, A.M., and Rapoport, T.A. (2010). Retrotranslocation of a Misfolded Luminal ER Protein by the Ubiquitin-Ligase Hrd1p. Cell *143,* 579-591.

Cases, S., Stone, S.J., Zhou, P., Yen, E., Tow, B., Lardizabal, K.D., Voelker, T., and Farese, R.V.,Jr. (2001). Cloning of DGAT2, a second mammalian diacylglycerol acyltransferase, and related family members. J. Biol. Chem. *276,* 38870-38876.

Cavallo, D., McLeod, R.S., Rudy, D., Aiton, A., Yao, Z., and Adeli, K. (1998). Intracellular Translocation and Stability of Apolipoprotein B Are Inversely Proportional to the Length of the Nascent Polypeptide. J. Biol. Chem. *273,* 33397-33405.

Cermelli, S., Guo, Y., Gross, S.P., and Welte, M.A. (2006). The lipid-droplet proteome reveals that droplets are a protein-storage depot. Curr. Biol. *16,* 1783-1795.

Chen, L., and Madura, K. (2002). Rad23 promotes the targeting of proteolytic substrates to the proteasome. Mol. Cell. Biol. *22,* 4902-4913.

Chen, Y., Le Caherec, F., and Chuck, S.L. (1998). Calnexin and other factors that alter translocation affect the rapid binding of ubiquitin to apoB in the Sec61 complex. J. Biol. Chem. *273,* 11887-11894.

Chen, Z., Gropler, M.C., Norris, J., Lawrence, J.C.,Jr, Harris, T.E., and Finck, B.N. (2008). Alterations in hepatic metabolism in fld mice reveal a role for lipin 1 in regulating VLDL-triacylglyceride secretion. Arterioscler. Thromb. Vasc. Biol. *28,* 1738-1744.

Chuck, S.L., and Lingappa, V.R. (1992). Pause transfer: a topogenic sequence in apolipoprotein B mediates stopping and restarting of translocation. Cell *68,* 9-21.

Chung, K.T., Shen, Y., and Hendershot, L.M. (2002). BAP, a mammalian BiP-associated protein, is a nucleotide exchange factor that regulates the ATPase activity of BiP. J. Biol. Chem. *277,* 47557-47563.

Claessen, J.H., and Ploegh, H.L. (2011). BAT3 guides misfolded glycoproteins out of the endoplasmic reticulum. PLoS One *6,* e28542.

Cnop, M., Foufelle, F., and Velloso, L.A. (2012). Endoplasmic reticulum stress, obesity and diabetes. Trends Mol. Med. *18,* 59-68.

Cole, L.K., Vance, J.E., and Vance, D.E. (2012). Phosphatidylcholine biosynthesis and lipoprotein metabolism. Biochim. Biophys. Acta *1821,* 754-761.

Colland, F. (2010). The therapeutic potential of deubiquitinating enzyme inhibitors. Biochem. Soc. Trans. *38,* 137-143.

Crosas, B., Hanna, J., Kirkpatrick, D.S., Zhang, D.P., Tone, Y., Hathaway, N.A., Buecker, C., Leggett, D.S., Schmidt, M., King, R.W., Gygi, S.P., and Finley, D. (2006). Ubiquitin chains are remodeled at the proteasome by opposing ubiquitin ligase and deubiquitinating activities. Cell *127,* 1401-1413.

Dashti, N., Manchekar, M., Liu, Y., Sun, Z., and Segrest, J.P. (2007). Microsomal triglyceride transfer protein activity is not required for the initiation of apolipoprotein B-containing lipoprotein assembly in McA-RH7777 cells. J. Biol. Chem. *282,* 28597-28608.

Davis, R.A., McNeal, M.M., and Moses, R.L. (1982). Intrahepatic assembly of very low density lipoprotein. Competition by cholesterol esters for the hydrophobic core. J. Biol. Chem. *257,* 2634-2640.

De Lemos-Chiarandini, C., Ivessa, N.E., Black, V.H., Tsao, Y.S., Gumper, I., and Kreibich, G. (1992). A Golgi-related structure remains after the brefeldin A-induced formation of an ER-Golgi hybrid compartment. Eur. J. Cell Biol. *58,* 187-201.

Deng, Y., Wang, Z.V., Tao, C., Gao, N., Holland, W.L., Ferdous, A., Repa, J.J., Liang, G., Ye, J., Lehrman, M.A.*, et al.* (2013). The Xbp1s/GalE axis links ER stress to postprandial hepatic metabolism. J. Clin. Invest. *123,* 455-468.

Devaraneni, P.K., Conti, B., Matsumura, Y., Yang, Z., Johnson, A.E., and Skach, W.R. (2011). Stepwise insertion and inversion of a type II signal anchor sequence in the ribosome-Sec61 translocon complex. Cell *146,* 134-147.

Deveraux, Q., Jensen, C., and Rechsteiner, M. (1995). Molecular cloning and expression of a 26 S protease subunit enriched in dileucine repeats. J. Biol. Chem. *270,* 23726-23729.

Dietschy, J.M. (1998). Dietary fatty acids and the regulation of plasma low density lipoprotein cholesterol concentrations. J. Nutr. *128,* 444S-448S.

Ding, W.X., Ni, H.M., Gao, W., Yoshimori, T., Stolz, D.B., Ron, D., and Yin, X.M. (2007). Linking of autophagy to ubiquitin-proteasome system is important for the regulation of endoplasmic reticulum stress and cell viability. Am. J. Pathol. *171,* 513-524.

Dixon, J.L., Chattapadhyay, R., Huima, T., Redman, C.M., and Banerjee, D. (1992). Biosynthesis of lipoprotein: location of nascent apoAI and apoB in the rough endoplasmic reticulum of chicken hepatocytes. J. Cell Biol. *117,* 1161-1169.

Dixon, J.L., Furukawa, S., and Ginsberg, H.N. (1991). Oleate stimulates secretion of apolipoprotein B-containing lipoproteins from Hep G2 cells by inhibiting early intracellular degradation of apolipoprotein B. J. Biol. Chem. *266,* 5080-5086.

Dong, M., Bridges, J.P., Apsley, K., Xu, Y., and Weaver, T.E. (2008). ERdj4 and ERdj5 are required for endoplasmic reticulum-associated protein degradation of misfolded surfactant protein C. Mol. Biol. Cell *19,* 2620-2630.

Doss-Pepe, E.W., Stenroos, E.S., Johnson, W.G., and Madura, K. (2003). Ataxin-3 interactions with rad23 and valosin-containing protein and its associations with ubiquitin chains and the proteasome are consistent with a role in ubiquitin-mediated proteolysis. Mol. Cell. Biol. *23,* 6469-6483.

Dougan, S.K., Hu, C.C., Paquet, M.E., Greenblatt, M.B., Kim, J., Lilley, B.N., Watson, N., and Ploegh, H.L. (2011). Derlin-2-deficient mice reveal an essential role for protein dislocation in chondrocytes. Mol. Cell. Biol. *31,* 1145-1159.

Du, E.Z., Kurth, J., Wang, S.L., Humiston, P., and Davis, R.A. (1994). Proteolysis-coupled secretion of the N terminus of apolipoprotein B. Characterization of a transient, translocation arrested intermediate. J. Biol. Chem. *269,* 24169-24176.

Du, X., Stoops, J.D., Mertz, J.R., Stanley, C.M., and Dixon, J.L. (1998). Identification of two regions in apolipoprotein B100 that are exposed on the cytosolic side of the endoplasmic reticulum membrane. J. Cell Biol. *141,* 585-599.

Erion, D.M., and Shulman, G.I. (2010). Diacylglycerol-mediated insulin resistance. Nat. Med. *16,* 400-402.

Ernst, R., Mueller, B., Ploegh, H.L., and Schlieker, C. (2009). The otubain YOD1 is a deubiquitinating enzyme that associates with p97 to facilitate protein dislocation from the ER. Mol. Cell *36,* 28-38.

Fairbank, M., St Pierre, P., and Nabi, I.R. (2009). The complex biology of autocrine motility factor/phosphoglucose isomerase (AMF/PGI) and its receptor, the gp78/AMFR E3 ubiquitin ligase. Mol. Biosyst. *5,* 793-801.

Fang, S., Ferrone, M., Yang, C., Jensen, J.P., Tiwari, S., and Weissman, A.M. (2001). The tumor autocrine motility factor receptor, gp78, is a ubiquitin protein ligase implicated in degradation from the endoplasmic reticulum. Proc. Natl. Acad. Sci. U. S. A. *98,* 14422-14427.

Fei, W., Wang, H., Fu, X., Bielby, C., and Yang, H. (2009). Conditions of endoplasmic reticulum stress stimulate lipid droplet formation in Saccharomyces cerevisiae. Biochem. J. *424,* 61-67.

Finck, B.N., Gropler, M.C., Chen, Z., Leone, T.C., Croce, M.A., Harris, T.E., Lawrence, J.C.,Jr, and Kelly, D.P. (2006). Lipin 1 is an inducible amplifier of the hepatic PGC-1alpha/PPARalpha regulatory pathway. Cell. Metab. *4,* 199-210.

Fisher, E.A., and Ginsberg, H.N. (2002). Complexity in the secretory pathway: the assembly and secretion of apolipoprotein B-containing lipoproteins. J. Biol. Chem. *277,* 17377-17380.

Fisher, E.A., Khanna, N.K., and McLeod, R.S. (2011). Ubiquitination regulates the assembly of very low density lipoprotein in HepG2 cells and is the committing step of the apoB100 ERAD pathway.

Fisher, E.A., Lapierre, L.R., Junkins, R.D., and McLeod, R.S. (2008). The AAA-ATPase p97 facilitates degradation of apolipoprotein B by the ubiquitin-proteasome pathway. J. Lipid Res. *49,* 2149-2160.

Fleig, L., Bergbold, N., Sahasrabudhe, P., Geiger, B., Kaltak, L., and Lemberg, M. (2012). Ubiquitin-Dependent Intramembrane Rhomboid Protease Promotes ERAD of Membrane Proteins. Mol. Cell *47,* 558-569.

Flierman, D., Ye, Y., Dai, M., Chau, V., and Rapoport, T.A. (2003). Polyubiquitin serves as a recognition signal, rather than a ratcheting molecule, during retrotranslocation of proteins across the endoplasmic reticulum membrane. J. Biol. Chem. *278,* 34774-34782.

Fox, C.S., Evans, J.C., Larson, M.G., Kannel, W.B., and Levy, D. (2004). Temporal trends in coronary heart disease mortality and sudden cardiac death from 1950 to 1999: the Framingham Heart Study. Circulation *110,* 522-527.

Fu, S., Watkins, S.M., and Hotamisligil, G.S. (2012). The role of endoplasmic reticulum in hepatic lipid homeostasis and stress signaling. Cell. Metab. *15,* 623-634.

Garg, A.D., Kaczmarek, A., Krysko, O., Vandenabeele, P., Krysko, D.V., and Agostinis, P. (2012). ER stress-induced inflammation: does it aid or impede disease progression? Trends Mol. Med.

Garza, R.M., Sato, B.K., and Hampton, R.Y. (2009). In vitro analysis of Hrd1p-mediated retrotranslocation of its multispanning membrane substrate 3-hydroxy-3-methylglutaryl (HMG)-CoA reductase. J. Biol. Chem. *284,* 14710-14722.

Gastaminza, P., Cheng, G., Wieland, S., Zhong, J., Liao, W., and Chisari, F.V. (2008). Cellular determinants of hepatitis C virus assembly, maturation, degradation, and secretion. J. Virol. *82,* 2120-2129.

Glatz, J.F., and van der Vusse, G.J. (1996). Cellular fatty acid-binding proteins: their function and physiological significance. Prog. Lipid Res. *35,* 243-282.

Goldstein, J.L., and Brown, M.S. (1990). Regulation of the mevalonate pathway. Nature *343,* 425-430.

Gordon, D.A., and Jamil, H. (2000). Progress towards understanding the role of microsomal triglyceride transfer protein in apolipoprotein-B lipoprotein assembly. Biochim. Biophys. Acta *1486,* 72-83.

Greenblatt, E.J., Olzmann, J.A., and Kopito, R.R. (2011). Derlin-1 is a rhomboid pseudoprotease required for the dislocation of mutant alpha-1 antitrypsin from the endoplasmic reticulum. Nat. Struct. Mol. Biol. *18,* 1147-1152.

Gretch, D.G., Sturley, S.L., Wang, L., Lipton, B.A., Dunning, A., Grunwald, K.A., Wetterau, J.R., Yao, Z., Talmud, P., and Attie, A.D. (1996). The amino terminus of apolipoprotein B is necessary but not sufficient for microsomal triglyceride transfer protein responsiveness. J. Biol. Chem. *271,* 8682-8691.

Groll, M., Ditzel, L., Lowe, J., Stock, D., Bochtler, M., Bartunik, H.D., and Huber, R. (1997). Structure of 20S proteasome from yeast at 2.4 A resolution. Nature *386,* 463-471.

Guerrero, C., Milenkovic, T., Przulj, N., Kaiser, P., and Huang, L. (2008). Characterization of the proteasome interaction network using a QTAX-based tag-team strategy and protein interaction network analysis. Proc. Natl. Acad. Sci. U. S. A. *105,* 13333-13338.

Gusarova, V., Brodsky, J.L., and Fisher, E.A. (2003). Apolipoprotein B100 exit from the endoplasmic reticulum (ER) is COPII-dependent, and its lipidation to very low density lipoprotein occurs post-ER. J. Biol. Chem. *278,* 48051-48058.

Gusarova, V., Caplan, A.J., Brodsky, J.L., and Fisher, E.A. (2001). Apoprotein B degradation is promoted by the molecular chaperones hsp90 and hsp70. J. Biol. Chem. *276,* 24891-24900.

Gusarova, V., Seo, J., Sullivan, M.L., Watkins, S.C., Brodsky, J.L., and Fisher, E.A. (2007). Golgi-associated maturation of very low density lipoproteins involves conformational changes in apolipoprotein B, but is not dependent on apolipoprotein E. J. Biol. Chem. *282,* 19453-19462.

Hampton, R.Y., and Sommer, T. (2012). Finding the will and the way of ERAD substrate retrotranslocation. Curr. Opin. Cell Biol.

Hanna, J., and Finley, D. (2007). A proteasome for all occasions. FEBS Lett. *581,* 2854-2861.

Hanna, J., Hathaway, N.A., Tone, Y., Crosas, B., Elsasser, S., Kirkpatrick, D.S., Leggett, D.S., Gygi, S.P., King, R.W., and Finley, D. (2006). Deubiquitinating enzyme Ubp6 functions noncatalytically to delay proteasomal degradation. Cell *127,* 99-111.

Hartman, I.Z., Liu, P., Zehmer, J.K., Luby-Phelps, K., Jo, Y., Anderson, R.G.W., and DeBose-Boyd, R.A. (2010). Sterol-induced dislocation of 3-Hydroxy-3-methylglutaryl coenzyme a reductase from endoplasmic reticulum membranes into the cytosol through a subcellular compartment resembling lipid droplets. J. Biol. Chem. *285,* 19288-19298.

Hartmann-Petersen, R., and Gordon, C. (2004). Integral UBL domain proteins: a family of proteasome interacting proteins. Semin. Cell Dev. Biol. *15,* 247-259.

Hassink, G.C., Zhao, B., Sompallae, R., Altun, M., Gastaldello, S., Zinin, N.V., Masucci, M.G., and Lindsten, K. (2009). The ER-resident ubiquitin-specific protease 19 participates in the UPR and rescues ERAD substrates. EMBO Rep. *10,* 755-761.

Hayashi, T., Hayashi, E., Fujimoto, M., Sprong, H., and Su, T.P. (2012). The lifetime of UDP-galactose:ceramide galactosyltransferase is controlled by a distinct endoplasmic reticulum-associated degradation (ERAD) regulated by sigma-1 receptor chaperones. J. Biol. Chem.

Hebbachi, A., and Gibbons, G.F. (1999). Inactivation of microsomal triglyceride transfer protein impairs the normal redistribution but not the turnover of newly synthesized glycerolipid in the cytosol, endoplasmic reticulum and Golgi of primary rat hepatocytes. Biochim. Biophys. Acta *1441,* 36-50.

Helenius, A., and Aebi, M. (2004). Roles of N-linked glycans in the endoplasmic reticulum. Annu. Rev. Biochem. *73,* 1019-1049.

Hessa, T., Sharma, A., Mariappan, M., Eshleman, H.D., Gutierrez, E., and Hegde, R.S. (2011). Protein targeting and degradation are coupled for elimination of mislocalized proteins. Nature *475,* 394-397.

Higa, A., and Chevet, E. (2012). Redox signaling loops in the unfolded protein response. Cell. Signal. *24,* 1548-1555.

Higo, T., Hattori, M., Nakamura, T., Natsume, T., Michikawa, T., and Mikoshiba, K. (2005). Subtype-specific and ER lumenal environment-dependent regulation of inositol 1,4,5-trisphosphate receptor type 1 by ERp44. Cell *120,* 85-98.

Higuchi, N., Kato, M., Tanaka, M., Miyazaki, M., Takao, S., Kohjima, M., Kotoh, K., Enjoji, M., Nakamuta, M., and Takayanagi, R. (2011). Effects of insulin resistance and hepatic lipid accumulation on hepatic mRNA expression levels of apoB, MTP and L-FABP in non-alcoholic fatty liver disease. Exp. Ther. Med. *2,* 1077-1081.

Hiller, M.M., Finger, A., Schweiger, M., and Wolf, D.H. (1996). ER degradation of a misfolded luminal protein by the cytosolic ubiquitin-proteasome pathway. Science *273,* 1725-1728.

Hochstrasser, M. (2009). Origin and function of ubiquitin-like proteins. Nature *458,* 422-429.

Hollien, J., and Weissman, J.S. (2006). Decay of endoplasmic reticulum-localized mRNAs during the unfolded protein response. Science *313,* 104-107.

Horn, S.C., Hanna, J., Hirsch, C., Volkwein, C., Schütz, A., Heinemann, U., Sommer, T., and Jarosch, E. (2009). Usa1 Functions as a Scaffold of the HRD-Ubiquitin Ligase. Mol. Cell *36,* 782-793.

Huang, X.F., and Shelness, G.S. (1997). Identification of cysteine pairs within the amino-terminal 5% of apolipoprotein B essential for hepatic lipoprotein assembly and secretion. J. Biol. Chem. *272,* 31872-31876.

Hussain, M.M., Bakillah, A., Nayak, N., and Shelness, G.S. (1998). Amino acids 430-570 in apolipoprotein B are critical for its binding to microsomal triglyceride transfer protein. J. Biol. Chem. *273,* 25612-25615.

Hwang, C., Sinskey, A.J., and Lodish, H.F. (1992). Oxidized redox state of glutathione in the endoplasmic reticulum. Science *257,* 1496-1502.

Imai, Y., Soda, M., Hatakeyama, S., Akagi, T., Hashikawa, T., Nakayama, K.I., and Takahashi, R. (2002). CHIP is associated with Parkin, a gene responsible for familial Parkinson's disease, and enhances its ubiquitin ligase activity. Mol. Cell *10,* 55-67.

Imrie, D., and Sadler, K.C. (2012). Stress management: How the unfolded protein response impacts fatty liver disease. J. Hepatol. *57,* 1147-1151.

Ingram, M.F., and Shelness, G.S. (1996). Apolipoprotein B-100 destined for lipoprotein assembly and intracellular degradation undergoes efficient translocation across the endoplasmic reticulum membrane. J. Lipid Res. *37,* 2202-2214.

Jacobs, R.L., Devlin, C., Tabas, I., and Vance, D.E. (2004). Targeted deletion of hepatic CTP:phosphocholine cytidylyltransferase alpha in mice decreases plasma high density and very low density lipoproteins. J. Biol. Chem. *279,* 47402-47410.

Jacobs, R.L., Lingrell, S., Zhao, Y., Francis, G.A., and Vance, D.E. (2008). Hepatic CTP:phosphocholine cytidylyltransferase-alpha is a critical predictor of plasma high density lipoprotein and very low density lipoprotein. J. Biol. Chem. *283,* 2147-2155.

Jamil, H., Dickson, J.K.,Jr, Chu, C.H., Lago, M.W., Rinehart, J.K., Biller, S.A., Gregg, R.E., and Wetterau, J.R. (1995). Microsomal triglyceride transfer protein. Specificity of lipid binding and transport. J. Biol. Chem. *270,* 6549-6554.

Jamsa, E., Simonen, M., and Makarow, M. (1994). Selective retention of secretory proteins in the yeast endoplasmic reticulum by treatment of cells with a reducing agent. Yeast *10,* 355-370.

Janen, S.B., Chaachouay, H., and Richter-Landsberg, C. (2010). Autophagy is activated by proteasomal inhibition and involved in aggresome clearance in cultured astrocytes. Glia *58,* 1766-1774.

Jensen, T.J., Loo, M.A., Pind, S., Williams, D.B., Goldberg, A.L., and Riordan, J.R. (1995). Multiple proteolytic systems, including the proteasome, contribute to CFTR processing. Cell *83,* 129-135.

Jo, Y., and De Bose-Boyd, R.A. (2010). Control of cholesterol synthesis through regulated ER-associated degradation of HMG CoA reductase. Crit. Rev. Biochem. Mol. Biol. *45,* 185-198.

Jo, Y., Lee, P.C., Sguigna, P.V., and DeBose-Boyd, R.A. (2011). Sterol-induced degradation of HMG CoA reductase depends on interplay of two Insigs and two ubiquitin ligases, gp78 and Trc8. Proc. Natl. Acad. Sci. U. S. A. *108,* 20503-20508.

Johs, A., Hammel, M., Waldner, I., May, R.P., Laggner, P., and Prassl, R. (2006). Modular structure of solubilized human apolipoprotein B-100. Low resolution model revealed by small angle neutron scattering. J. Biol. Chem. *281,* 19732-19739.

Joyce, C.W., Shelness, G.S., Davis, M.A., Lee, R.G., Skinner, K., Anderson, R.A., and Rudel, L.L. (2000). ACAT1 and ACAT2 membrane topology segregates a serine residue essential for activity to opposite sides of the endoplasmic reticulum membrane. Mol. Biol. Cell *11,* 3675-3687.

Ju, J.S., Fuentealba, R.A., Miller, S.E., Jackson, E., Piwnica-Worms, D., Baloh, R.H., and Weihl, C.C. (2009). Valosin-containing protein (VCP) is required for autophagy and is disrupted in VCP disease. J. Cell Biol. *187,* 875-888.

Junne, T., Kocik, L., and Spiess, M. (2010). The hydrophobic core of the Sec61 translocon defines the hydrophobicity threshold for membrane integration. Mol. Biol. Cell *21,* 1662-1670.

Kammoun, H.L., Hainault, I., Ferre, P., and Foufelle, F. (2009). Nutritional related liver disease: targeting the endoplasmic reticulum stress. Curr. Opin. Clin. Nutr. Metab. Care *12,* 575-582.

Karimian Pour, N., and Adeli, K. (2011). Insulin silences apolipoprotein B mRNA translation by inducing intracellular traffic into cytoplasmic RNA granules. Biochemistry *50,* 6942-6950.

Kars, M., Yang, L., Gregor, M.F., Mohammed, B.S., Pietka, T.A., Finck, B.N., Patterson, B.W., Horton, J.D., Mittendorfer, B., Hotamisligil, G.S., and Klein, S. (2010). Tauroursodeoxycholic Acid may improve liver and muscle but not adipose tissue insulin sensitivity in obese men and women. Diabetes *59,* 1899-1905.

Khan, B.V., Fungwe, T.V., Wilcox, H.G., and Heimberg, M. (1990). Cholesterol is required for the secretion of the very-low-density lipoprotein: in vivo studies. Biochim. Biophys. Acta *1044,* 297-304.

Kim, I., Ahn, J., Liu, C., Tanabe, K., Apodaca, J., Suzuki, T., and Rao, H. (2006). The Png1-Rad23 complex regulates glycoprotein turnover. J. Cell Biol. *172,* 211-219.

Kirkpatrick, D.S., Gerber, S.A., and Gygi, S.P. (2005). The absolute quantification strategy: a general procedure for the quantification of proteins and post-translational modifications. Methods *35,* 265-273.

Kirkpatrick, D.S., Hathaway, N.A., Hanna, J., Elsasser, S., Rush, J., Finley, D., King, R.W., and Gygi, S.P. (2006). Quantitative analysis of in vitro ubiquitinated cyclin B1 reveals complex chain topology. Nat. Cell Biol. *8,* 700-710.

Klemm, E.J., Spooner, E., and Ploegh, H.L. (2011). Dual role of ancient ubiquitous protein 1 (AUP1) in lipid droplet accumulation and endoplasmic reticulum (ER) protein quality control. J. Biol. Chem. *286,* 37602-37614.

Koegl, M., Hoppe, T., Schlenker, S., Ulrich, H.D., Mayer, T.U., and Jentsch, S. (1999). A novel ubiquitination factor, E4, is involved in multiubiquitin chain assembly. Cell *96,* 635-644.

Komatsu, M., Kageyama, S., and Ichimura, Y. (2012). p62/SQSTM1/A170: physiology and pathology. Pharmacol. Res. *66,* 457-462.

Kumashiro, N., Erion, D.M., Zhang, D., Kahn, M., Beddow, S.A., Chu, X., Still, C.D., Gerhard, G.S., Han, X., Dziura, J.*, et al.* (2011). Cellular mechanism of insulin resistance in nonalcoholic fatty liver disease. Proc. Natl. Acad. Sci. U. S. A. *108,* 16381-16385.

Laco, M.N., Cortes, L., Travis, S.M., Paulson, H.L., and Rego, A.C. (2012). Valosin-containing protein (VCP/p97) is an activator of wild-type ataxin-3. PLoS One *7,* e43563.

Lam, Y.A., Xu, W., DeMartino, G.N., and Cohen, R.E. (1997). Editing of ubiquitin conjugates by an isopeptidase in the 26S proteasome. Nature *385,* 737-740.

Lapierre, L.R., Currie, D.L., Yao, Z., Wang, J., and McLeod, R.S. (2004). Amino acid sequences within the beta1 domain of human apolipoprotein B can mediate rapid intracellular degradation. J. Lipid Res. *45,* 366-377.

Le Fourn, V., Park, S., Jang, I., Gaplovska-Kysela, K., Guhl, B., Lee, Y., Cho, J.W., Zuber, C., and Roth, J. (2013). Large protein complexes retained in the ER are dislocated by non-COPII vesicles and degraded by selective autophagy. Cell Mol. Life Sci.

Lee, B.H., Lee, M.J., Park, S., Oh, D.C., Elsasser, S., Chen, P.C., Gartner, C., Dimova, N., Hanna, J., Gygi, S.P.*, et al.* (2010a). Enhancement of proteasome activity by a small-molecule inhibitor of USP14. Nature *467,* 179-184.

Lee, J.N., Kim, H., Yao, H., Chen, Y., Weng, K., and Ye, J. (2010b). Identification of Ubxd8 protein as a sensor for unsaturated fatty acids and regulator of triglyceride synthesis. Proc. Natl. Acad. Sci. U. S. A. *107,* 21424-21429.

Lee, J.S., Zheng, Z., Mendez, R., Ha, S.W., Xie, Y., and Zhang, K. (2012). Pharmacologic ER stress induces non-alcoholic steatohepatitis in an animal model. Toxicol. Lett. *211,* 29-38.

Lee, M.J., Lee, B.H., Hanna, J., King, R.W., and Finley, D. (2011). Trimming of ubiquitin chains by proteasome-associated deubiquitinating enzymes. Mol. Cell. Proteomics *10,* R110.003871.

Lee, R.J., Liu, C.W., Harty, C., McCracken, A.A., Latterich, M., Romisch, K., DeMartino, G.N., Thomas, P.J., and Brodsky, J.L. (2004). Uncoupling retro-translocation and degradation in the ER-associated degradation of a soluble protein. EMBO J. *23,* 2206-2215.

Leznicki, P., Clancy, A., Schwappach, B., and High, S. (2010). Bat3 promotes the membrane integration of tail-anchored proteins. J. Cell. Sci. *123,* 2170-2178.

Leznicki, P., and High, S. (2012). SGTA antagonizes BAG6-mediated protein triage. Proc. Natl. Acad. Sci. U. S. A. *109,* 19214-19219.

Li, S., Brown, M.S., and Goldstein, J.L. (2010). Bifurcation of insulin signaling pathway in rat liver: mTORC1 required for stimulation of lipogenesis, but not inhibition of gluconeogenesis. Proc. Natl. Acad. Sci. U. S. A. *107,* 3441-3446.

Li, W., Tu, D., Brunger, A.T., and Ye, Y. (2007). A ubiquitin ligase transfers preformed polyubiquitin chains from a conjugating enzyme to a substrate. Nature *446,* 333-337.

Li, X., Ye, J., Zhou, L., Gu, W., Fisher, E.A., and Li, P. (2012). Opposing roles of cell death-inducing DFF45-like effector B and perilipin 2 in controlling hepatic VLDL lipidation. J. Lipid Res. *53,* 1877-1889.

Liang, J., Wu, X., Jiang, H., Zhou, M., Yang, H., Angkeow, P., Huang, L.S., Sturley, S.L., and Ginsberg, H. (1998). Translocation efficiency, susceptibility to proteasomal degradation, and lipid responsiveness of apolipoprotein B are determined by the presence of beta sheet domains. J. Biol. Chem. *273,* 35216-35221.

Liang, J.J., Oelkers, P., Guo, C., Chu, P.C., Dixon, J.L., Ginsberg, H.N., and Sturley, S.L. (2004). Overexpression of human diacylglycerol acyltransferase 1, acyl-coa:cholesterol acyltransferase 1, or acyl-CoA:cholesterol acyltransferase 2 stimulates secretion of apolipoprotein B-containing lipoproteins in McA-RH7777 cells. J. Biol. Chem. *279,* 44938-44944.

Liang, J.S., Kim, T., Fang, S., Yamaguchi, J., Weissman, A.M., Fisher, E.A., and Ginsberg, H.N. (2003). Overexpression of the tumor autocrine motility factor receptor Gp78, a ubiquitin protein ligase, results in increased ubiquitinylation and decreased secretion of apolipoprotein B100 in HepG2 cells. J. Biol. Chem. *278,* 23984-23988.

Liang, S., Wu, X., Fisher, E.A., and Ginsberg, H.N. (2000). The amino-terminal domain of apolipoprotein B does not undergo retrograde translocation from the endoplasmic reticulum to the cytosol. Proteasomal degradation of nascent apolipoprotein B begins at the carboxyl terminus of the protein, while apolipoprotein B is still in its original translocon. J. Biol. Chem. *275,* 32003-32010.

Liao, W., Chang, B.H., Mancini, M., and Chan, L. (2003). Ubiquitin-dependent and -independent proteasomal degradation of apoB associated with endoplasmic reticulum and Golgi apparatus, respectively, in HepG2 cells. J. Cell. Biochem. *89,* 1019-1029.

Liao, W., Li, X., Mancini, M., and Chan, L. (2006). Proteasome inhibition induces differential heat shock protein response but not unfolded protein response in HepG2 cells. J. Cell. Biochem. *99,* 1085-1095.

Lilley, B.N., and Ploegh, H.L. (2004). A membrane protein required for dislocation of misfolded proteins from the ER. Nature *429,* 834-840.

Linnik, K.M., and Herscovitz, H. (1998). Multiple molecular chaperones interact with apolipoprotein B during its maturation. The network of endoplasmic reticulum-resident chaperones (ERp72, GRP94, calreticulin, and BiP) interacts with apolipoprotein b regardless of its lipidation state. J. Biol. Chem. *273,* 21368-21373.

Lippincott-Schwartz, J., Bonifacino, J.S., Yuan, L.C., and Klausner, R.D. (1988). Degradation from the endoplasmic reticulum: disposing of newly synthesized proteins. Cell *54,* 209-220.

Liu, F., and Walters, K.J. (2010). Multitasking with ubiquitin through multivalent interactions. Trends Biochem. Sci. *35,* 352-360.

Liu, T.F., Tang, J.J., Li, P.S., Shen, Y., Li, J.G., Miao, H.H., Li, B.L., and Song, B.L. (2012). Ablation of gp78 in Liver Improves Hyperlipidemia and Insulin Resistance by Inhibiting SREBP to Decrease Lipid Biosynthesis. Cell. Metab.

Liu, Y., Millar, J.S., Cromley, D.A., Graham, M., Crooke, R., Billheimer, J.T., and Rader, D.J. (2008). Knockdown of acyl-CoA:diacylglycerol acyltransferase 2 with antisense oligonucleotide reduces VLDL TG and ApoB secretion in mice. Biochim. Biophys. Acta *1781,* 97-104.

Lord, J.M., Roberts, L.M., and Lencer, W.I. (2005). Entry of protein toxins into mammalian cells by crossing the endoplasmic reticulum membrane: co-opting basic mechanisms of endoplasmic reticulum-associated degradation. Curr. Top. Microbiol. Immunol. *300,* 149-168.

Maattanen, P., Gehring, K., Bergeron, J.J., and Thomas, D.Y. (2010). Protein quality control in the ER: the recognition of misfolded proteins. Semin. Cell Dev. Biol. *21,* 500-511.

Macri, J., and Adeli, K. (1997). Conformational changes in apolipoprotein B modulate intracellular assembly and degradation of ApoB-containing lipoprotein particles in HepG2 cells. Arterioscler. Thromb. Vasc. Biol. *17,* 2982-2994.

Madsen, L., Seeger, M., Semple, C.A., and Hartmann-Petersen, R. (2009). New ATPase regulators—p97 goes to the PUB. Int. J. Biochem. Cell Biol. *41,* 2380-2388.

Manmontri, B., Sariahmetoglu, M., Donkor, J., Bou Khalil, M., Sundaram, M., Yao, Z., Reue, K., Lehner, R., and Brindley, D.N. (2008). Glucocorticoids and cyclic AMP selectively increase hepatic lipin-1 expression, and insulin acts antagonistically. J. Lipid Res. *49,* 1056-1067.

Mann, C.J., Anderson, T.A., Read, J., Chester, S.A., Harrison, G.B., Kochl, S., Ritchie, P.J., Bradbury, P., Hussain, F.S., Amey, J.*, et al.* (1999). The structure of vitellogenin provides a molecular model for the assembly and secretion of atherogenic lipoproteins. J. Mol. Biol. *285,* 391-408.

Manocha, M., Malinowski, P., Li, K., and Macri, J. (2009). Development of a 2-D apoB peptide profile to detect conformational changes associated with apoB-containing lipoproteins. Electrophoresis *30,* 2227-2233.

Mantzaris, M.D., Tsianos, E.V., and Galaris, D. (2011). Interruption of triacylglycerol synthesis in the endoplasmic reticulum is the initiating event for saturated fatty acid-induced lipotoxicity in liver cells. FEBS J. *278,* 519-530.

Mariappan, M., Li, X., Stefanovic, S., Sharma, A., Mateja, A., Keenan, R.J., and Hegde, R.S. (2010). A ribosome-associating factor chaperones tail-anchored membrane proteins. Nature *466,* 1120-1124.

Martin, S., and Parton, R.G. (2006). Lipid droplets: a unified view of a dynamic organelle. Nat. Rev. Mol. Cell Biol. *7,* 373-378.

Matsumura, Y., David, L.L., and Skach, W.R. (2011). Role of Hsc70 binding cycle in CFTR folding and endoplasmic reticulum-associated degradation. Mol. Biol. Cell *22,* 2797-2809.

Mayer, T.U., Braun, T., and Jentsch, S. (1998). Role of the proteasome in membrane extraction of a short-lived ER-transmembrane protein. EMBO J. *17,* 3251-3257.

McLeod, R.S., Zhao, Y., Selby, S.L., Westerlund, J., and Yao, Z. (1994). Carboxyl-terminal truncation impairs lipid recruitment by apolipoprotein B100 but does not affect secretion of the truncated apolipoprotein B-containing lipoproteins. J. Biol. Chem. *269,* 2852-2862.

McLeod, R.S., Wang, Y., Wang, S., Rusi+ ol, A., Links, P., and Yao, Z. (1996). Apolipoprotein B Sequence Requirements for Hepatic Very Low Density Lipoprotein Assembly. J. Biol. Chem. *271,* 18445-18455.

Mehnert, M., Sommer, T., and Jarosch, E. (2010). ERAD ubiquitin ligases: multifunctional tools for protein quality control and waste disposal in the endoplasmic reticulum. Bioessays *32,* 905-913.

Meister, S., Schubert, U., Neubert, K., Herrmann, K., Burger, R., Gramatzki, M., Hahn, S., Schreiber, S., Wilhelm, S., Herrmann, M., Jack, H.M., and Voll, R.E. (2007). Extensive immunoglobulin production sensitizes myeloma cells for proteasome inhibition. Cancer Res. *67,* 1783-1792.

Millar, J.S., Stone, S.J., Tietge, U.J., Tow, B., Billheimer, J.T., Wong, J.S., Hamilton, R.L., Farese, R.V.,Jr, and Rader, D.J. (2006). Short-term overexpression of DGAT1 or DGAT2 increases hepatic triglyceride but not VLDL triglyceride or apoB production. J. Lipid Res. *47,* 2297-2305.

Minami, R., Hayakawa, A., Kagawa, H., Yanagi, Y., Yokosawa, H., and Kawahara, H. (2010). BAG-6 is essential for selective elimination of defective proteasomal substrates. J. Cell Biol. *190,* 637-650.

Mitchell, D.M., Zhou, M., Pariyarath, R., Wang, H., Aitchison, J.D., Ginsberg, H.N., and Fisher, E.A. (1998). Apoprotein B100 has a prolonged interaction with the translocon during which its lipidation and translocation change from dependence on the microsomal triglyceride transfer protein to independence. Proc. Natl. Acad. Sci. U. S. A. *95,* 14733-14738.

Miyanari, Y., Atsuzawa, K., Usuda, N., Watashi, K., Hishiki, T., Zayas, M., Bartenschlager, R., Wakita, T., Hijikata, M., and Shimotohno, K. (2007). The lipid droplet is an important organelle for hepatitis C virus production. Nat. Cell Biol. *9,* 1089-1097.

Moon, Y.A., Liang, G., Xie, X., Frank-Kamenetsky, M., Fitzgerald, K., Koteliansky, V., Brown, M.S., Goldstein, J.L., and Horton, J.D. (2012). The Scap/SREBP pathway is essential for developing diabetic fatty liver and carbohydrate-induced hypertriglyceridemia in animals. Cell. Metab. *15,* 240-246.

Moore, P., Bernardi, K.M., and Tsai, B. (2010). The Ero1alpha-PDI redox cycle regulates retro-translocation of cholera toxin. Mol. Biol. Cell *21,* 1305-1313.

Morimoto, R.I. (2011). The heat shock response: systems biology of proteotoxic stress in aging and disease. Cold Spring Harb. Symp. Quant. Biol. *76,* 91-99.

Morito, D., Hirao, K., Oda, Y., Hosokawa, N., Tokunaga, F., Cyr, D.M., Tanaka, K., Iwai, K., and Nagata, K. (2008). Gp78 cooperates with RMA1 in endoplasmic reticulum-associated degradation of CFTRDeltaF508. Mol. Biol. Cell *19,* 1328-1336.

Mullick, A.E., Fu, W., Graham, M.J., Lee, R.G., Witchell, D., Bell, T.A., Whipple, C.P., and Crooke, R.M. (2011). Antisense oligonucleotide reduction of apoB-ameliorated atherosclerosis in LDL receptor-deficient mice. J. Lipid Res. *52,* 885-896.

Nag, D.K., and Finley, D. (2012). A small-molecule inhibitor of deubiquitinating enzyme USP14 inhibits Dengue virus replication. Virus Res. *165,* 103-106.

Nahmias, Y., Goldwasser, J., Casali, M., van Poll, D., Wakita, T., Chung, R.T., and Yarmush, M.L. (2008). Apolipoprotein B-dependent hepatitis C virus secretion is inhibited by the grapefruit flavonoid naringenin. Hepatology *47,* 1437-1445.

Nakatsukasa, K., and Brodsky, J.L. (2008). The recognition and retrotranslocation of misfolded proteins from the endoplasmic reticulum. Traffic *9,* 861-870.

Neuber, O., Jarosch, E., Volkwein, C., Walter, J., and Sommer, T. (2005). Ubx2 links the Cdc48 complex to ER-associated protein degradation. Nat. Cell Biol. *7,* 993-998.

Nicodeme, E., Benoist, F., McLeod, R., Yao, Z., Scott, J., Shoulders, C.C., and Grand-Perret, T. (1999). Identification of domains in apolipoprotein B100 that confer a high requirement for the microsomal triglyceride transfer protein. J. Biol. Chem. *274,* 1986-1993.

Ning, J., Hong, T., Ward, A., Pi, J., Liu, Z., Liu, H.Y., and Cao, W. (2011). Constitutive role for IRE1alpha-XBP1 signaling pathway in the insulin-mediated hepatic lipogenic program. Endocrinology *152,* 2247-2255.

Nissila, E., Ohsaki, Y., Weber-Boyvat, M., Perttila, J., Ikonen, E., and Olkkonen, V.M. (2012). ORP10, a cholesterol binding protein associated with microtubules, regulates apolipoprotein B-100 secretion. Biochim. Biophys. Acta *1821,* 1472-1484.

Obeng, E.A., Carlson, L.M., Gutman, D.M., Harrington, W.J.,Jr, Lee, K.P., and Boise, L.H. (2006). Proteasome inhibitors induce a terminal unfolded protein response in multiple myeloma cells. Blood *107,* 4907-4916.

Oberdorf, J., Carlson, E.J., and Skach, W.R. (2006). Uncoupling proteasome peptidase and ATPase activities results in cytosolic release of an ER polytopic protein. J. Cell. Sci. *119,* 303-313.

Ohsaki, Y., Cheng, J., Fujita, A., Tokumoto, T., and Fujimoto, T. (2006). Cytoplasmic lipid droplets are sites of convergence of proteasomal and autophagic degradation of apolipoprotein B. Mol. Biol. Cell *17,* 2674-2683.

Ohsaki, Y., Cheng, J., Suzuki, M., Fujita, A., and Fujimoto, T. (2008). Lipid droplets are arrested in the ER membrane by tight binding of lipidated apolipoprotein B-100. J. Cell. Sci. *121,* 2415-2422.

Ota, T., Gayet, C., and Ginsberg, H.N. (2008). Inhibition of apolipoprotein B100 secretion by lipid-induced hepatic endoplasmic reticulum stress in rodents. J. Clin. Invest. *118,* 316-332.

Otero, J.H., Lizak, B., and Hendershot, L.M. (2010). Life and death of a BiP substrate. Semin. Cell Dev. Biol. *21,* 472-478.

Owen, M.R., Corstorphine, C.C., and Zammit, V.A. (1997). Overt and latent activities of diacylglycerol acytransferase in rat liver microsomes: possible roles in very-low-density lipoprotein triacylglycerol secretion. Biochem. J. *323 (Pt 1),* 17-21.

Oyadomari, S., Yun, C., Fisher, E.A., Kreglinger, N., Kreibich, G., Oyadomari, M., Harding, H.P., Goodman, A.G., Harant, H., Garrison, J.L.*, et al.* (2006). Cotranslocational degradation protects the stressed endoplasmic reticulum from protein overload. Cell *126,* 727-739.

Ozcan, L. (2012). Endoplasmic Reticulum Stress in Cardiometabolic Disorders. Curr. Atheroscler. Rep.

Pagani, M., Fabbri, M., Benedetti, C., Fassio, A., Pilati, S., Bulleid, N.J., Cabibbo, A., and Sitia, R. (2000). Endoplasmic reticulum oxidoreductin 1-lbeta (ERO1-Lbeta), a human gene induced in the course of the unfolded protein response. J. Biol. Chem. *275,* 23685-23692.

Pagliassotti, M.J. (2012). Endoplasmic reticulum stress in nonalcoholic Fatty liver disease. Annu. Rev. Nutr. *32,* 17-33.

Pan, M., Cederbaum, A.I., Zhang, Y.L., Ginsberg, H.N., Williams, K.J., and Fisher, E.A. (2004). Lipid peroxidation and oxidant stress regulate hepatic apolipoprotein B degradation and VLDL production. J. Clin. Invest. *113,* 1277-1287.

Pan, M., Liang Js, J.S., Fisher, E.A., and Ginsberg, H.N. (2002). The late addition of core lipids to nascent apolipoprotein B100, resulting in the assembly and secretion of triglyceride-rich lipoproteins, is independent of both microsomal triglyceride transfer protein activity and new triglyceride synthesis. J. Biol. Chem. *277,* 4413-4421.

Pan, M., Maitin, V., Parathath, S., Andreo, U., Lin, S.X., St Germain, C., Yao, Z., Maxfield, F.R., Williams, K.J., and Fisher, E.A. (2008). Presecretory oxidation, aggregation, and autophagic destruction of apoprotein-B: a pathway for late-stage quality control. Proc. Natl. Acad. Sci. U. S. A. *105,* 5862-5867.

Pariyarath, R., Wang, H., Aitchison, J.D., Ginsberg, H.N., Welch, W.J., Johnson, A.E., and Fisher, E.A. (2001). Co-translational interactions of apoprotein B with the ribosome and translocon during lipoprotein assembly or targeting to the proteasome. J. Biol. Chem. *276,* 541-550.

Park, S., Isaacson, R., Kim, H.T., Silver, P.A., and Wagner, G. (2005). Ufd1 exhibits the AAA-ATPase fold with two distinct ubiquitin interaction sites. Structure *13,* 995-1005.

Parker, R.A., Flint, O.P., Mulvey, R., Elosua, C., Wang, F., Fenderson, W., Wang, S., Yang, W.P., and Noor, M.A. (2005). Endoplasmic reticulum stress links dyslipidemia to inhibition of proteasome activity and glucose transport by HIV protease inhibitors. Mol. Pharmacol. *67,* 1909-1919.

Phung, T.L., Roncone, A., Jensen, K.L., Sparks, C.E., and Sparks, J.D. (1997). Phosphoinositide 3-kinase activity is necessary for insulin-dependent inhibition of apolipoprotein B secretion by rat hepatocytes and localizes to the endoplasmic reticulum. J. Biol. Chem. *272,* 30693-30702.

Pickart, C.M. (2000). Ubiquitin in chains. Trends Biochem. Sci. *25,* 544-548.

Ploegh, H.L. (2007). A lipid-based model for the creation of an escape hatch from the endoplasmic reticulum. Nature *448,* 435-438.

Prakash, S., Tian, L., Ratliff, K.S., Lehotzky, R.E., and Matouschek, A. (2004). An unstructured initiation site is required for efficient proteasome-mediated degradation. Nat. Struct. Mol. Biol. *11,* 830-837.

Qi, J., Lang, W., Geisler, J.G., Wang, P., Petrounia, I., Mai, S., Smith, C., Askari, H., Struble, G.T., Williams, R.*, et al.* (2012). The use of stable isotope-labeled glycerol and oleic acid to differentiate the hepatic functions of DGAT1 and -2. J. Lipid Res. *53,* 1106-1116.

Qian, S.B., Zhang, X., Sun, J., Bennink, J.R., Yewdell, J.W., and Patterson, C. (2010). mTORC1 links protein quality and quantity control by sensing chaperone availability. J. Biol. Chem. *285,* 27385-27395.

Qin, W., Sundaram, M., Wang, Y., Zhou, H., Zhong, S., Chang, C.C., Manhas, S., Yao, E.F., Parks, R.J., McFie, P.J.*, et al.* (2011). Missense mutation in APOC3 within the C-terminal lipid binding domain of human ApoC-III results in impaired assembly and secretion of triacylglycerol-rich very low density lipoproteins: evidence that ApoC-III plays a major role in the formation of lipid precursors within the microsomal lumen. J. Biol. Chem. *286,* 27769-27780.

Qiu, W., Avramoglu, R.K., Rutledge, A.C., Tsai, J., and Adeli, K. (2006). Mechanisms of glucosamine-induced suppression of the hepatic assembly and secretion of apolipoprotein B-100-containing lipoproteins. J. Lipid Res. *47,* 1749-1761.

Qiu, W., Kohen-Avramoglu, R., Mhapsekar, S., Tsai, J., Austin, R.C., and Adeli, K. (2005). Glucosamine-induced endoplasmic reticulum stress promotes ApoB100 degradation: evidence for Grp78-mediated targeting to proteasomal degradation. Arterioscler. Thromb. Vasc. Biol. *25,* 571-577.

Qiu, W., Kohen-Avramoglu, R., Rashid-Kolvear, F., Au, C.S., Chong, T.M., Lewis, G.F., Trinh, D.K., Austin, R.C., Urade, R., and Adeli, K. (2004). Overexpression of the endoplasmic reticulum 60 protein ER-60 downregulates apoB100 secretion by inducing its intracellular degradation via a nonproteasomal pathway: evidence for an ER-60-mediated and pCMB-sensitive intracellular degradative pathway. Biochemistry *43,* 4819-4831.

Qiu, W., Su, Q., Rutledge, A.C., Zhang, J., and Adeli, K. (2009). Glucosamine-induced endoplasmic reticulum stress attenuates apolipoprotein B100 synthesis via PERK signaling. J. Lipid Res. *50,* 1814-1823.

Qiu, W., Zhang, J., Dekker, M.J., Wang, H., Huang, J., Brumell, J.H., and Adeli, K. (2011). Hepatic autophagy mediates endoplasmic reticulum stress-induced degradation of misfolded apolipoprotein B. Hepatology *53,* 1515-1525.

Raabe, M., Veniant, M.M., Sullivan, M.A., Zlot, C.H., Bjorkegren, J., Nielsen, L.B., Wong, J.S., Hamilton, R.L., and Young, S.G. (1999). Analysis of the role of microsomal triglyceride transfer protein in the liver of tissue-specific knockout mice. J. Clin. Invest. *103,* 1287-1298.

Rath, E., and Haller, D. (2011). Inflammation and cellular stress: a mechanistic link between immune-mediated and metabolically driven pathologies. Eur. J. Nutr. *50,* 219-233.

Rava, P., Ojakian, G.K., Shelness, G.S., and Hussain, M.M. (2006). Phospholipid transfer activity of microsomal triacylglycerol transfer protein is sufficient for the assembly and secretion of apolipoprotein B lipoproteins. J. Biol. Chem. *281,* 11019-11027.

Ren, L.P., Chan, S.M., Zeng, X.Y., Laybutt, D.R., Iseli, T.J., Sun, R.Q., Kraegen, E.W., Cooney, G.J., Turner, N., and Ye, J.M. (2012). Differing endoplasmic reticulum stress response to excess lipogenesis versus lipid oversupply in relation to hepatic steatosis and insulin resistance. PLoS One *7,* e30816.

Richardson, P.E., Manchekar, M., Dashti, N., Jones, M.K., Beigneux, A., Young, S.G., Harvey, S.C., and Segrest, J.P. (2005). Assembly of lipoprotein particles containing apolipoprotein-B: structural model for the nascent lipoprotein particle. Biophys. J. *88,* 2789-2800.

Richly, H., Rape, M., Braun, S., Rumpf, S., Hoege, C., and Jentsch, S. (2005). A series of ubiquitin binding factors connects CDC48/p97 to substrate multiubiquitylation and proteasomal targeting. Cell *120,* 73-84.

Riddle, T.M., Schildmeyer, N.M., Phan, C., Fichtenbaum, C.J., and Hui, D.Y. (2002). The HIV protease inhibitor ritonavir increases lipoprotein production and has no effect on lipoprotein clearance in mice. J. Lipid Res. *43,* 1458-1463.

Riess, O., Rub, U., Pastore, A., Bauer, P., and Schols, L. (2008). SCA3: neurological features, pathogenesis and animal models. Cerebellum *7,* 125-137.

Rizzo, M., and Wierzbicki, A.S. (2011). New lipid modulating drugs: the role of microsomal transport protein inhibitors. Curr. Pharm. Des. *17,* 943-949.

Ron, D., and Walter, P. (2007). Signal integration in the endoplasmic reticulum unfolded protein response. Nat. Rev. Mol. Cell Biol. *8,* 519-529.

Rumpf, S., and Jentsch, S. (2006). Functional division of substrate processing cofactors of the ubiquitin-selective Cdc48 chaperone. Mol. Cell *21,* 261-269.

Ruschak, A.M., Religa, T.L., Breuer, S., Witt, S., and Kay, L.E. (2010). The proteasome antechamber maintains substrates in an unfolded state. Nature *467,* 868-871.

Rusinol, A., Verkade, H., and Vance, J.E. (1993). Assembly of rat hepatic very low density lipoproteins in the endoplasmic reticulum. J. Biol. Chem. *268,* 3555-3562.

Rustaeus, S., Stillemark, P., Lindberg, K., Gordon, D., and Olofsson, S.O. (1998). The microsomal triglyceride transfer protein catalyzes the post-translational assembly of apolipoprotein B-100 very low density lipoprotein in McA-RH7777 cells. J. Biol. Chem. *273,* 5196-5203.

Rutkowski, D.T., and Hegde, R.S. (2010). Regulation of basal cellular physiology by the homeostatic unfolded protein response. J. Cell Biol. *189,* 783-794.

Rutkowski, D.T., Kang, S.W., Goodman, A.G., Garrison, J.L., Taunton, J., Katze, M.G., Kaufman, R.J., and Hegde, R.S. (2007). The role of p58IPK in protecting the stressed endoplasmic reticulum. Mol. Biol. Cell *18,* 3681-3691.

Rutledge, A.C., Qiu, W., Zhang, R., Kohen-Avramoglu, R., Nemat-Gorgani, N., and Adeli, K. (2009). Mechanisms targeting apolipoprotein B100 to proteasomal degradation: evidence that degradation is initiated by BiP binding at the N terminus and the formation of a p97 complex at the C terminus. Arterioscler. Thromb. Vasc. Biol. *29,* 579-585.

Rutledge, A.C., Su, Q., and Adeli, K. (2010). Apolipoprotein B100 biogenesis: a complex array of intracellular mechanisms regulating folding, stability, and lipoprotein assembly. Biochem. Cell Biol. *88,* 251-267.

Sacchettini, J.C., and Gordon, J.I. (1993). Rat intestinal fatty acid binding protein. A model system for analyzing the forces that can bind fatty acids to proteins. J. Biol. Chem. *268,* 18399-18402.

Saeki, Y., and Tanaka, K. (2012). Assembly and function of the proteasome. Methods Mol. Biol. *832,* 315-337.

Sakata, N., Stoops, J.D., and Dixon, J.L. (1999). Cytosolic components are required for proteasomal degradation of newly synthesized apolipoprotein B in permeabilized HepG2 cells. J. Biol. Chem. *274,* 17068-17074.

Sakata, N., Wu, X., Dixon, J.L., and Ginsberg, H.N. (1993). Proteolysis and lipid-facilitated translocation are distinct but competitive processes that regulate secretion of apolipoprotein B in Hep G2 cells. J. Biol. Chem. *268,* 22967-22970.

Sato, K., Cho, Y., Tachibana, S., Chiba, T., Schneider, W.J., and Akiba, Y. (2005). Impairment of VLDL secretion by medium-chain fatty acids in chicken primary hepatocytes is affected by the chain length. J. Nutr. *135,* 1636-1641.

Scapin, G., Gordon, J.I., and Sacchettini, J.C. (1992). Refinement of the structure of recombinant rat intestinal fatty acid-binding apoprotein at 1.2-A resolution. J. Biol. Chem. *267,* 4253-4269.

Schafer, A., and Wolf, D.H. (2009). Sec61p is part of the endoplasmic reticulum-associated degradation machinery. EMBO J. *28,* 2874-2884.

Schonfeld, G., Lin, X., and Yue, P. (2005). Familial hypobetalipoproteinemia: genetics and metabolism. Cell Mol. Life Sci. *62,* 1372-1378.

Schubert, U., Anton, L.C., Gibbs, J., Norbury, C.C., Yewdell, J.W., and Bennink, J.R. (2000). Rapid degradation of a large fraction of newly synthesized proteins by proteasomes. Nature *404,* 770-774.

Schuberth, C., and Buchberger, A. (2008). UBX domain proteins: major regulators of the AAA ATPase Cdc48/p97. Cell Mol. Life Sci. *65,* 2360-2371.

Schuberth, C., and Buchberger, A. (2005). Membrane-bound Ubx2 recruits Cdc48 to ubiquitin ligases and their substrates to ensure efficient ER-associated protein degradation. Nat. Cell Biol. *7,* 999-1006.

Schumaker, V.N., Phillips, M.L., and Chatterton, J.E. (1994). Apolipoprotein B and low-density lipoprotein structure: implications for biosynthesis of triglyceride-rich lipoproteins. Adv. Protein Chem. *45,* 205-248.

Segrest, J.P., Jones, M.K., and Dashti, N. (1999). N-terminal domain of apolipoprotein B has structural homology to lipovitellin and microsomal triglyceride transfer protein: a "lipid pocket" model for self-assembly of apob-containing lipoprotein particles. J. Lipid Res. *40,* 1401-1416.

Segrest, J.P., Jones, M.K., De Loof, H., and Dashti, N. (2001). Structure of apolipoprotein B-100 in low density lipoproteins. J. Lipid Res. *42,* 1346-1367.

Sevier, C.S., and Kaiser, C.A. (2008). Ero1 and redox homeostasis in the endoplasmic reticulum. Biochim. Biophys. Acta *1783,* 549-556.

Shabek, N., Herman-Bachinsky, Y., Buchsbaum, S., Lewinson, O., Haj-Yahya, M., Hejjaoui, M., Lashuel, H.A., Sommer, T., Brik, A., and Ciechanover, A. (2012). The size of the proteasomal substrate determines whether its degradation will be mediated by mono- or polyubiquitylation. Mol. Cell *48,* 87-97.

Shelness, G.S., Hou, L., Ledford, A.S., Parks, J.S., and Weinberg, R.B. (2003). Identification of the lipoprotein initiating domain of apolipoprotein B. J. Biol. Chem. *278,* 44702-44707.

Shimizu, Y., Okuda-Shimizu, Y., and Hendershot, L.M. (2010). Ubiquitylation of an ERAD substrate occurs on multiple types of amino acids. Mol. Cell *40,* 917-926.

Sidiropoulos, K.G., Pontrelli, L., and Adeli, K. (2005). Insulin-mediated suppression of apolipoprotein B mRNA translation requires the 5' UTR and is characterized by decreased binding of an insulin-sensitive 110-kDa 5' UTR RNA-binding protein. Biochemistry *44,* 12572-12581.

Sidiropoulos, K.G., Zastepa, A., and Adeli, K. (2007). Translational control of apolipoprotein B mRNA via insulin and the protein kinase C signaling cascades: evidence for modulation of RNA-protein interactions at the 5'UTR. Arch. Biochem. Biophys. *459,* 10-19.

Sliter, D.A., Aguiar, M., Gygi, S.P., and Wojcikiewicz, R.J. (2011). Activated inositol 1,4,5-trisphosphate receptors are modified by homogeneous Lys-48- and Lys-63-linked ubiquitin chains, but only Lys-48-linked chains are required for degradation. J. Biol. Chem. *286,* 1074-1082.

Sniderman, A., Couture, P., and De Graaf, J. (2010). Diagnosis and treatment of apolipoprotein B dyslipoproteinemias. Nat. Rev. Endocrinol. *6,* 335-346.

Sniderman, A.D., De Graaf, J., Couture, P., Williams, K., Kiss, R.S., and Watts, G.F. (2009). Regulation of plasma LDL: the apoB paradigm. Clin. Sci. (Lond). *118,* 333-339.

So, J., Hur, K., Tarrio, M., Ruda, V., Frank-Kamenetsky, M., Fitzgerald, K., Koteliansky, V., Lichtman, A., Iwawaki, T., Glimcher, L., and Lee, A. (2012). Silencing of Lipid Metabolism Genes through IRE1α-Mediated mRNA Decay Lowers Plasma Lipids in Mice. Cell Metabolism *16,* 487-499.

Sommer, T., and Jentsch, S. (1993). A protein translocation defect linked to ubiquitin conjugation at the endoplasmic reticulum. Nature *365,* 176-179.

Song, B.L., Sever, N., and DeBose-Boyd, R.A. (2005). Gp78, a membrane-anchored ubiquitin ligase, associates with Insig-1 and couples sterol-regulated ubiquitination to degradation of HMG CoA reductase. Mol. Cell *19,* 829-840.

Sorensen, L.P., Sondergaard, E., Nellemann, B., Christiansen, J.S., Gormsen, L.C., and Nielsen, S. (2011). Increased VLDL-triglyceride secretion precedes impaired control of endogenous glucose production in obese, normoglycemic men. Diabetes *60,* 2257-2264.

Sowa, M.E., Bennett, E.J., Gygi, S.P., and Harper, J.W. (2009). Defining the human deubiquitinating enzyme interaction landscape. Cell *138,* 389-403.

Sparks, J.D., Phung, T.L., Bolognino, M., and Sparks, C.E. (1996). Insulin-mediated inhibition of apolipoprotein B secretion requires an intracellular trafficking event and phosphatidylinositol 3-kinase activation: studies with brefeldin A and wortmannin in primary cultures of rat hepatocytes. Biochem. J. *313 (Pt 2),* 567-574.

Sparks, J.D., and Sparks, C.E. (1994). Obese Zucker (fa/fa) rats are resistant to insulin's inhibitory effect on hepatic apo B secretion. Biochem. Biophys. Res. Commun. *205,* 417-422.

Sparks, J.D., and Sparks, C.E. (1990). Insulin modulation of hepatic synthesis and secretion of apolipoprotein B by rat hepatocytes. J. Biol. Chem. *265,* 8854-8862.

Sparks, J.D., Sparks, C.E., and Adeli, K. (2012). Selective hepatic insulin resistance, VLDL overproduction, and hypertriglyceridemia. Arterioscler. Thromb. Vasc. Biol. *32,* 2104-2112.

Spring, D.J., Chen-Liu, L.W., Chatterton, J.E., Elovson, J., and Schumaker, V.N. (1992). Lipoprotein assembly. Apolipoprotein B size determines lipoprotein core circumference. J. Biol. Chem. *267,* 14839-14845.

Stanley, A.M., Carvalho, P., and Rapoport, T. (2011). Recognition of an ERAD-L substrate analyzed by site-specific in vivo photocrosslinking. FEBS Lett. *585,* 1281-1286.

Stone, S.J., Myers, H.M., Watkins, S.M., Brown, B.E., Feingold, K.R., Elias, P.M., and Farese, R.V.,Jr. (2004). Lipopenia and skin barrier abnormalities in DGAT2-deficient mice. J. Biol. Chem. *279,* 11767-11776.

Su, Q., Tsai, J., Xu, E., Qiu, W., Bereczki, E., Santha, M., and Adeli, K. (2009). Apolipoprotein B100 acts as a molecular link between lipid-induced endoplasmic reticulum stress and hepatic insulin resistance. Hepatology *50,* 77-84.

Sundaram, M., and Yao, Z. (2010). Recent progress in understanding protein and lipid factors affecting hepatic VLDL assembly and secretion. Nutr. Metab. (Lond) *7,* 35.

Sundaram, M., Zhong, S., Bou Khalil, M., Zhou, H., Jiang, Z.G., Zhao, Y., Iqbal, J., Hussain, M.M., Figeys, D., Wang, Y., and Yao, Z. (2010). Functional analysis of the missense APOC3 mutation Ala23Thr associated with human hypotriglyceridemia. J. Lipid Res. *51,* 1524-1534.

Suzuki, M., Otsuka, T., Ohsaki, Y., Cheng, J., Taniguchi, T., Hashimoto, H., Taniguchi, H., and Fujimoto, T. (2012). Derlin-1 and UBXD8 are engaged in dislocation and degradation of lipidated ApoB-100 at lipid droplets. Mol. Biol. Cell *23,* 800-810.

Swift, L.L. (1995). Assembly of very low density lipoproteins in rat liver: a study of nascent particles recovered from the rough endoplasmic reticulum. J. Lipid Res. *36,* 395-406.

Swift, L.L., Zhu, M.Y., Kakkad, B., Jovanovska, A., Neely, M.D., Valyi-Nagy, K., Roberts, R.L., Ong, D.E., and Jerome, W.G. (2003). Subcellular localization of microsomal triglyceride transfer protein. J. Lipid Res. *44,* 1841-1849.

Tachibana, S., Sato, K., Cho, Y., Chiba, T., Schneider, W.J., and Akiba, Y. (2005). Octanoate reduces very low-density lipoprotein secretion by decreasing the synthesis of apolipoprotein B in primary cultures of chicken hepatocytes. Biochim. Biophys. Acta *1737,* 36-43.

Taghibiglou, C., Rashid-Kolvear, F., Van Iderstine, S.C., Le-Tien, H., Fantus, I.G., Lewis, G.F., and Adeli, K. (2002). Hepatic very low density lipoprotein-ApoB overproduction is associated with attenuated hepatic insulin signaling and overexpression of protein-tyrosine phosphatase 1B in a fructose-fed hamster model of insulin resistance. J. Biol. Chem. *277,* 793-803.

Taniguchi, T., Ishikawa, Y., Tsunemitsu, M., and Fukuzaki, H. (1989). The structures of the asparagine-linked sugar chains of human apolipoprotein B-100. Arch. Biochem. Biophys. *273,* 197-205.

Tcherpakov, M., Broday, L., Delaunay, A., Kadoya, T., Khurana, A., Erdjument-Bromage, H., Tempst, P., Qiu, X.B., DeMartino, G.N., and Ronai, Z. (2008). JAMP optimizes ERAD to protect cells from unfolded proteins. Mol. Biol. Cell *19,* 5019-5028.

Temel, R.E., Hou, L., Rudel, L.L., and Shelness, G.S. (2007). ACAT2 stimulates cholesteryl ester secretion in apoB-containing lipoproteins. J. Lipid Res. *48,* 1618-1627.

Tennyson, G.E., Sabatos, C.A., Higuchi, K., Meglin, N., and Brewer, H.B.,Jr. (1989). Expression of apolipoprotein B mRNAs encoding higher- and lower-molecular weight isoproteins in rat liver and intestine. Proc. Natl. Acad. Sci. U. S. A. *86,* 500-504.

Tep, S., Mihaila, R., Freeman, A., Pickering, V., Huyhn, F., Tadin-Strapps, M., Stracks, A., Hubbard, B., Caldwell, J., Flanagan, W.M., Kuklin, N.A., and Ason, B. (2012). Rescue of Mtp siRNA-induced hepatic steatosis by DGAT2 siRNA silencing. J. Lipid Res. *53,* 859-867.

Thress, K., Song, J., Morimoto, R.I., and Kornbluth, S. (2001). Reversible inhibition of Hsp70 chaperone function by Scythe and Reaper. EMBO J. *20,* 1033-1041.

Tirosh, B., Furman, M.H., Tortorella, D., and Ploegh, H.L. (2003). Protein unfolding is not a prerequisite for endoplasmic reticulum-to-cytosol dislocation. J. Biol. Chem. *278,* 6664-6672.

Tower, J. (2009). Hsps and aging. Trends Endocrinol. Metab. *20,* 216-222.

Tran, K., Boren, J., Macri, J., Wang, Y., McLeod, R., Avramoglu, R.K., Adeli, K., and Yao, Z. (1998). Functional analysis of disulfide linkages clustered within the amino terminus of human apolipoprotein B. J. Biol. Chem. *273,* 7244-7251.

Tran, K., Sun, F., Cui, Z., Thorne-Tjomsland, G., St Germain, C., Lapierre, L.R., McLeod, R.S., Jamieson, J.C., and Yao, Z. (2006). Attenuated secretion of very low density lipoproteins from McA-RH7777 cells treated with eicosapentaenoic acid is associated with impaired utilization of triacylglycerol synthesized via phospholipid remodeling. Biochim. Biophys. Acta *1761,* 463-473.

Tran, K., Thorne-Tjomsland, G., DeLong, C.J., Cui, Z., Shan, J., Burton, L., Jamieson, J.C., and Yao, Z. (2002). Intracellular assembly of very low density lipoproteins containing apolipoprotein B100 in rat hepatoma McA-RH7777 cells. J. Biol. Chem. *277,* 31187-31200.

Tresse, E., Salomons, F.A., Vesa, J., Bott, L.C., Kimonis, V., Yao, T.P., Dantuma, N.P., and Taylor, J.P. (2010). VCP/p97 is essential for maturation of ubiquitin-containing autophagosomes and this function is impaired by mutations that cause IBMPFD. Autophagy *6,* 217-227.

Tsai, J., Qiu, W., Kohen-Avramoglu, R., and Adeli, K. (2007). MEK-ERK inhibition corrects the defect in VLDL assembly in HepG2 cells: potential role of ERK in VLDL-ApoB100 particle assembly. Arterioscler. Thromb. Vasc. Biol. *27,* 211-218.

Tsai, Y.C., Leichner, G.S., Pearce, M.M., Wilson, G.L., Wojcikiewicz, R.J., Roitelman, J., and Weissman, A.M. (2012). Differential regulation of HMG-CoA reductase and Insig-1 by enzymes of the ubiquitin-proteasome system. Mol. Biol. Cell *23,* 4484-4494.

Tsai, Y.C., Mendoza, A., Mariano, J.M., Zhou, M., Kostova, Z., Chen, B., Veenstra, T., Hewitt, S.M., Helman, L.J., Khanna, C., and Weissman, A.M. (2007). The ubiquitin ligase gp78 promotes sarcoma metastasis by targeting KAI1 for degradation. Nat. Med. *13,* 1504-1509.

Ushioda, R., Hoseki, J., Araki, K., Jansen, G., Thomas, D.Y., and Nagata, K. (2008). ERdj5 is required as a disulfide reductase for degradation of misfolded proteins in the ER. Science *321,* 569-572.

Van den Berg, B., Clemons, W.M.,Jr, Collinson, I., Modis, Y., Hartmann, E., Harrison, S.C., and Rapoport, T.A. (2004). X-ray structure of a protein-conducting channel. Nature *427,* 36-44.

VanSlyke, J.K., and Musil, L.S. (2002). Dislocation and degradation from the ER are regulated by cytosolic stress. J. Cell Biol. *157,* 381-394.

Vembar, S.S., and Brodsky, J.L. (2008). One step at a time: endoplasmic reticulum-associated degradation. Nat. Rev. Mol. Cell Biol. *9,* 944-957.

Verges, B. (2010). Abnormal hepatic apolipoprotein B metabolism in type 2 diabetes. Atherosclerosis *211,* 353-360.

Vukmirica, J., Nishimaki-Mogami, T., Tran, K., Shan, J., McLeod, R.S., Yuan, J., and Yao, Z. (2002). The N-linked oligosaccharides at the amino terminus of human apoB are important for the assembly and secretion of VLDL. J. Lipid Res. *43,* 1496-1507.

Walkey, C.J., Donohue, L.R., Bronson, R., Agellon, L.B., and Vance, D.E. (1997). Disruption of the murine gene encoding phosphatidylethanolamine N-methyltransferase. Proc. Natl. Acad. Sci. U. S. A. *94,* 12880-12885.

Walter, P., and Ron, D. (2011). The unfolded protein response: from stress pathway to homeostatic regulation. Science *334,* 1081-1086.

Wang, C.W., and Lee, S.C. (2012). The ubiquitin-like (UBX)-domain-containing protein Ubx2/Ubxd8 regulates lipid droplet homeostasis. J. Cell. Sci. *125,* 2930-2939.

Wang, H., Gilham, D., and Lehner, R. (2007). Proteomic and lipid characterization of apolipoprotein B-free luminal lipid droplets from mouse liver microsomes: implications for very low density lipoprotein assembly. J. Biol. Chem. *282,* 33218-33226.

Wang, L., Fast, D.G., and Attie, A.D. (1997). The enzymatic and non-enzymatic roles of protein-disulfide isomerase in apolipoprotein B secretion. J. Biol. Chem. *272,* 27644-27651.

Wang, L., Martin, D.D., Genter, E., Wang, J., McLeod, R.S., and Small, D.M. (2009). Surface study of apoB1694-1880, a sequence that can anchor apoB to lipoproteins and make it nonexchangeable. J. Lipid Res. *50,* 1340-1352.

Wang, L., Walsh, M.T., and Small, D.M. (2006a). Apolipoprotein B is conformationally flexible but anchored at a triolein/water interface: a possible model for lipoprotein surfaces. Proc. Natl. Acad. Sci. U. S. A. *103,* 6871-6876.

Wang, Q., Li, L., and Ye, Y. (2006b). Regulation of retrotranslocation by p97-associated deubiquitinating enzyme ataxin-3. J. Cell Biol. *174,* 963-971.

Wang, Q., Liu, Y., Soetandyo, N., Baek, K., Hegde, R., and Ye, Y. (2011). A ubiquitin ligase-associated chaperone holdase maintains polypeptides in soluble states for proteasome degradation. Mol. Cell *42,* 758-770.

Wang, S., McLeod, R.S., Gordon, D.A., and Yao, Z. (1996). The microsomal triglyceride transfer protein facilitates assembly and secretion of apolipoprotein B-containing lipoproteins and decreases cotranslational degradation of apolipoprotein B in transfected COS-7 cells. J. Biol. Chem. *271,* 14124-14133.

Wang, S., Chen, Z., Lam, V., Han, J., Hassler, J., Finck, B., Davidson, N., and Kaufman, R. (2012). IRE1α-XBP1s Induces PDI Expression to Increase MTP Activity for Hepatic VLDL Assembly and Lipid Homeostasis. Cell Metabolism *16,* 473-486.

Wang, X., Chen, C.F., Baker, P.R., Chen, P.L., Kaiser, P., and Huang, L. (2007). Mass spectrometric characterization of the affinity-purified human 26S proteasome complex. Biochemistry *46,* 3553-3565.

Wang, Y., Ballar, P., Zhong, Y., Zhang, X., Liu, C., Zhang, Y.J., Monteiro, M.J., Li, J., and Fang, S. (2011). SVIP induces localization of p97/VCP to the plasma and lysosomal membranes and regulates autophagy. PLoS One *6,* e24478.

Wang, Y., McLeod, R.S., and Yao, Z. (1997). Normal activity of microsomal triglyceride transfer protein is required for the oleate-induced secretion of very low density lipoproteins containing apolipoprotein B from McA-RH7777 cells. J. Biol. Chem. *272,* 12272-12278.

Wang, Y., Tran, K., and Yao, Z. (1999). The activity of microsomal triglyceride transfer protein is essential for accumulation of triglyceride within microsomes in McA-RH7777 cells. A unified model for the assembly of very low density lipoproteins. J. Biol. Chem. *274,* 27793-27800.

Ward, C.L., Omura, S., and Kopito, R.R. (1995). Degradation of CFTR by the ubiquitin-proteasome pathway. Cell *83,* 121-127.

Werner, A., Havinga, R., Bos, T., Bloks, V.W., Kuipers, F., and Verkade, H.J. (2005). Essential fatty acid deficiency in mice is associated with hepatic steatosis and secretion of large VLDL particles. Am. J. Physiol. Gastrointest. Liver Physiol. *288,* G1150-8.

Wetterau, J.R., Aggerbeck, L.P., Bouma, M.E., Eisenberg, C., Munck, A., Hermier, M., Schmitz, J., Gay, G., Rader, D.J., and Gregg, R.E. (1992). Absence of microsomal triglyceride transfer protein in individuals with abetalipoproteinemia. Science *258,* 999-1001.

Wetterau, J.R., Combs, K.A., Spinner, S.N., and Joiner, B.J. (1990). Protein disulfide isomerase is a component of the microsomal triglyceride transfer protein complex. J. Biol. Chem. *265,* 9800-9807.

Wiegman, C.H., Bandsma, R.H., Ouwens, M., van der Sluijs, F.H., Havinga, R., Boer, T., Reijngoud, D.J., Romijn, J.A., and Kuipers, F. (2003). Hepatic VLDL production in ob/ob mice is not stimulated by massive de novo lipogenesis but is less sensitive to the suppressive effects of insulin. Diabetes *52,* 1081-1089.

Wiertz, E.J., Tortorella, D., Bogyo, M., Yu, J., Mothes, W., Jones, T.R., Rapoport, T.A., and Ploegh, H.L. (1996). Sec61-mediated transfer of a membrane protein from the endoplasmic reticulum to the proteasome for destruction. Nature *384,* 432-438.

Wiggins, D., and Gibbons, G.F. (1992). The lipolysis/esterification cycle of hepatic triacylglycerol. Its role in the secretion of very-low-density lipoprotein and its response to hormones and sulphonylureas. Biochem. J. *284 (Pt 2),* 457-462.

Winnefeld, M., Grewenig, A., Schnolzer, M., Spring, H., Knoch, T.A., Gan, E.C., Rommelaere, J., and Cziepluch, C. (2006). Human SGT interacts with Bag-6/Bat-3/Scythe and cells with reduced levels of either protein display persistence of few misaligned chromosomes and mitotic arrest. Exp. Cell Res. *312,* 2500-2514.

Wojcik, C., Rowicka, M., Kudlicki, A., Nowis, D., McConnell, E., Kujawa, M., and DeMartino, G.N. (2006). Valosin-containing protein (p97) is a regulator of endoplasmic reticulum stress and of the degradation of N-end rule and ubiquitin-fusion degradation pathway substrates in mammalian cells. Mol. Biol. Cell *17,* 4606-4618.

Wojcikiewicz, R.J., Pearce, M.M., Sliter, D.A., and Wang, Y. (2009). When worlds collide: IP(3) receptors and the ERAD pathway. Cell Calcium *46,* 147-153.

Wonderlin, W.F. (2009). Constitutive, translation-independent opening of the protein-conducting channel in the endoplasmic reticulum. Pflugers Arch. *457,* 917-930.

Wurie, H.R., Buckett, L., and Zammit, V.A. (2011). Evidence that diacylglycerol acyltransferase 1 (DGAT1) has dual membrane topology in the endoplasmic reticulum of HepG2 cells. J. Biol. Chem. *286,* 36238-36247.

Xiao, C., Giacca, A., and Lewis, G.F. (2011). Sodium phenylbutyrate, a drug with known capacity to reduce endoplasmic reticulum stress, partially alleviates lipid-induced insulin resistance and beta-cell dysfunction in humans. Diabetes *60,* 918-924.

Xu, P., Duong, D.M., Seyfried, N.T., Cheng, D., Xie, Y., Robert, J., Rush, J., Hochstrasser, M., Finley, D., and Peng, J. (2009). Quantitative proteomics reveals the function of unconventional ubiquitin chains in proteasomal degradation. Cell *137,* 133-145.

Xu, P., and Peng, J. (2006). Dissecting the ubiquitin pathway by mass spectrometry. Biochim. Biophys. Acta *1764,* 1940-1947.

Xu, Y., Cai, M., Yang, Y., Huang, L., and Ye, Y. (2012). SGTA Recognizes a Noncanonical Ubiquitin-like Domain in the Bag6-Ubl4A-Trc35 Complex to Promote Endoplasmic Reticulum-Associated Degradation. Cell. Rep. *2,* 1633-1644.

Yamaguchi, J., Gamble, M.V., Conlon, D., Liang, J.S., and Ginsberg, H.N. (2003). The conversion of apoB100 low density lipoprotein/high density lipoprotein particles to apoB100 very low density lipoproteins in response to oleic acid occurs in the endoplasmic reticulum and not in the Golgi in McA RH7777 cells. J. Biol. Chem. *278,* 42643-42651.

Yamamoto, K., Takahara, K., Oyadomari, S., Okada, T., Sato, T., Harada, A., and Mori, K. (2010). Induction of liver steatosis and lipid droplet formation in ATF6alpha-knockout mice burdened with pharmacological endoplasmic reticulum stress. Mol. Biol. Cell *21,* 2975-2986.

Yamazaki, T., Sasaki, E., Kakinuma, C., Yano, T., Miura, S., and Ezaki, O. (2005). Increased very low density lipoprotein secretion and gonadal fat mass in mice overexpressing liver DGAT1. J. Biol. Chem. *280,* 21506-21514.

Yan, A.T., Yan, R.T., Tan, M., Hackam, D.G., Leblanc, K.L., Kertland, H., Tsang, J.L., Jaffer, S., Kates, M.L., Leiter, L.A*., et al.* (2006). Contemporary management of dyslipidemia in high-risk patients: targets still not met. Am. J. Med. *119,* 676-683.

Yang, H., Liu, C., Zhong, Y., Luo, S., Monteiro, M.J., and Fang, S. (2010a). Huntingtin interacts with the cue domain of gp78 and inhibits gp78 binding to ubiquitin and p97/VCP. PLoS. One. *5,* e8905.

Yang, L., Li, P., Fu, S., Calay, E.S., and Hotamisligil, G.S. (2010b). Defective hepatic autophagy in obesity promotes ER stress and causes insulin resistance. Cell. Metab. *11,* 467-478.

Yao, Z., and Wang, Y. (2012). Apolipoprotein C-III and hepatic triglyceride-rich lipoprotein production. Curr. Opin. Lipidol. *23,* 206-212.

Yao, Z., Zhou, H., Figeys, D., Wang, Y., and Sundaram, M. (2012). Microsome-associated lumenal lipid droplets in the regulation of lipoprotein secretion. Curr. Opin. Lipidol.

Ye, J. (2012). Cellular responses to unsaturated fatty acids mediated by their sensor Ubxd8. Frontiers in Biology *7,* 397-403.

Ye, J., Li, J.Z., Liu, Y., Li, X., Yang, T., Ma, X., Li, Q., Yao, Z., and Li, P. (2009). Cideb, an ER- and lipid droplet-associated protein, mediates VLDL lipidation and maturation by interacting with apolipoprotein B. Cell. Metab. *9,* 177-190.

Ye, Y., Meyer, H.H., and Rapoport, T.A. (2003). Function of the p97-Ufd1-Npl4 complex in retrotranslocation from the ER to the cytosol: dual recognition of nonubiquitinated polypeptide segments and polyubiquitin chains. J. Cell Biol. *162,* 71-84.

Ye, Y., Meyer, H.H., and Rapoport, T.A. (2001). The AAA ATPase Cdc48/p97 and its partners transport proteins from the ER into the cytosol. Nature *414,* 652-656.

Ye, Y., Shibata, Y., Yun, C., Ron, D., and Rapoport, T.A. (2004). A membrane protein complex mediates retro-translocation from the ER lumen into the cytosol. Nature *429,* 841-847.

Yen, C.L., Stone, S.J., Koliwad, S., Harris, C., and Farese, R.V.,Jr. (2008). Thematic review series: glycerolipids. DGAT enzymes and triacylglycerol biosynthesis. J. Lipid Res. *49,* 2283-2301.

Yoshida, Y., Chiba, T., Tokunaga, F., Kawasaki, H., Iwai, K., Suzuki, T., Ito, Y., Matsuoka, K., Yoshida, M., Tanaka, K., and Tai, T. (2002). E3 ubiquitin ligase that recognizes sugar chains. Nature *418,* 438-442.

Yu, H., Kaung, G., Kobayashi, S., and Kopito, R.R. (1997). Cytosolic degradation of T-cell receptor alpha chains by the proteasome. J. Biol. Chem. *272,* 20800-20804.

Yu, X.X., Murray, S.F., Pandey, S.K., Booten, S.L., Bao, D., Song, X.Z., Kelly, S., Chen, S., McKay, R., Monia, B.P., and Bhanot, S. (2005). Antisense oligonucleotide reduction of DGAT2 expression improves hepatic steatosis and hyperlipidemia in obese mice. Hepatology *42,* 362-371.

Zatloukal, K., Stumptner, C., Fuchsbichler, A., Heid, H., Schnoelzer, M., Kenner, L., Kleinert, R., Prinz, M., Aguzzi, A., and Denk, H. (2002). p62 Is a common component of cytoplasmic inclusions in protein aggregation diseases. Am. J. Pathol. *160,* 255-263.

Zhang, J., and Herscovitz, H. (2003). Nascent lipidated apolipoprotein B is transported to the Golgi as an incompletely folded intermediate as probed by its association with network of endoplasmic reticulum molecular chaperones, GRP94, ERp72, BiP, calreticulin, and cyclophilin B. J. Biol. Chem. *278,* 7459-7468.

Zhang, K., and Kaufman, R.J. (2008). From endoplasmic-reticulum stress to the inflammatory response. Nature *454,* 455-462.

Zhong, S., Magnolo, A.L., Sundaram, M., Zhou, H., Yao, E.F., Di Leo, E., Loria, P., Wang, S., Bamji-Mirza, M., Wang, L.*, et al.* (2010). Nonsynonymous mutations within APOB in human familial hypobetalipoproteinemia: evidence for feedback inhibition of lipogenesis and postendoplasmic reticulum degradation of apolipoprotein B. J. Biol. Chem. *285,* 6453-6464.

Zhong, X., Shen, Y., Ballar, P., Apostolou, A., Agami, R., and Fang, S. (2004). AAA ATPase p97/valosin-containing protein interacts with gp78, a ubiquitin ligase for endoplasmic reticulum-associated degradation. J. Biol. Chem. *279,* 45676-45684.

Zhou, M., Fisher, E.A., and Ginsberg, H.N. (1998). Regulated Co-translational ubiquitination of apolipoprotein B100. A new paradigm for proteasomal degradation of a secretory protein. J. Biol. Chem. *273,* 24649-24653.

Zhou, M., Wu, X., Huang, L.S., and Ginsberg, H.N. (1995). Apoprotein B100, an inefficiently translocated secretory protein, is bound to the cytosolic chaperone, heat shock protein 70. J. Biol. Chem. *270,* 25220-25224.